

Volume 5

Peshdar Plain Project Publications

The Dinka Settlement Complex 2019

Further Archaeological and Geophysical Work on
Qalat-i Dinka and in the Lower Town

edited by

Karen Radner, F. Janoscha Kreppner and Andrea Squitieri



PEWE-VERLAG

PESH DAR PLAIN PROJECT PUBLICATIONS
VOLUME 5

Peshdar Plain Project Publications

edited by

Karen Radner

**The Dinka Settlement Complex 2019
Further Archaeological and Geophysical Work on
Qalat-i Dinka and in the Lower Town**

edited by

Karen Radner, F. Janoscha Kreppner and Andrea Squitieri



PEWE-VERLAG
2020

Gedruckt mit Unterstützung der Alexander von Humboldt-Stiftung

Bibliografische Information der Deutschen Nationalbibliothek

Die Deutsche Nationalbibliothek verzeichnet diese Publikation in der Deutschen Nationalbibliografie; detaillierte bibliografische Daten sind im Internet über <http://dnb.dnb.de> abrufbar.

© PeWe-Verlag – Gladbeck 2020

Alle Rechte, insbesondere das Recht der Vervielfältigung und Verbreitung sowie der Übersetzung, vorbehalten. Kein Teil des Werkes darf in irgendeiner Form durch Fotokopie, Mikrofilm usw. ohne schriftliche Genehmigung des Verlages reproduziert oder unter Verwendung elektronischer Systeme verarbeitet, vervielfältigt oder verbreitet werden.

Layout und Prepress: PeWe-Verlag, Gladbeck

Umschlaggestaltung: PeWe-Verlag, Gladbeck

Umschlagabbildung: The western slope of Qalat-i Dinka with the Lower Zab. Taken with a DJI Phantom 4 drone by Louise König in September 2019.

Gedruckt auf alterungsbeständigem Papier

Printed in Germany

ISBN: 978-3-935012-45-4

Table of contents

Preface	11
A. The Peshdar Plain Project in its fifth year: the 2019 work programme (<i>Karen Radner</i>)	13
A1. The 2019 activities of the Peshdar Plain Project	14
A1.1 Exploring the palaeo-environment and the Chalcolithic settlement in the Bora Plain in spring 2019	19
A1.2 The third excavation campaign on Qalat-i Dinka in autumn 2019	20
A2. The scope of this volume	21
B. Remote sensing and sediment analysis in the Bora Plain, 2019 ..	24
B1. The 2019 Electrical Resistivity Tomography (ERT) survey (<i>Mandana Parsi & Jörg W. E. Fassbinder</i>)	24
B1.1 Investigating the <i>qanat</i> system in the Bora Plain	25
B1.1.1 ERT surveying in the southeastern part of the Bora Plain	27
B1.1.2 ERT surveying near the Lower Town of the Dinka Settlement Complex	28
B1.2 Investigating the Dinka Settlement Complex	30
B1.2.1 ERT surveying in the Lower Town	30
B1.2.2 ERT surveying on Qalat-i Dinka	35
B1.3 Conclusions	35
B2. Soils and sediments in the Dinka Settlement Complex and the surrounding Bora Plain: sampling and new data from 2019 (<i>Eileen Eckmeier</i>)	37
B2.1 Testing ancient <i>qanat</i> locations	41
B2.2 Adding data for the understanding of the Lower and Upper Terrace	41
B2.3 Testing the location of ancient roads	42
C. Excavating the Upper Town of the Dinka Settlement Complex: the 2019 excavation campaign at Qalat-i Dinka	44
C1. Previous work on Qalat-i Dinka and the methodology employed in 2019 (<i>Andrea Squitieri</i>)	44
C2. Absolute chronology and relative stratigraphy	48
C2.1 The radiocarbon dates (<i>Andrea Squitieri</i>)	48
C2.2 The relative stratigraphy and the stratigraphic table (<i>F. Janoscha Kreppner</i>)	48
C3. The trench in Square 181908 (<i>Jens Rohde & Laura Tretow</i>)	52
C3.1 Introduction	52
C3.2 Virgin soil	52
C3.3 Walls and floor levels older than the Main Occupation Period	53
C3.4 Wall LGR:0329 of Building P and the Outdoor Area 70 of the Main Occupation Period	57

C3.5	Graves 102 and 105	61
C3.6	The modern looting pits and the topsoil	62
C3.7	Conclusions	64
C4.	The trench in Square 182908 (<i>Jana Richter & Hero Salih Ahmed</i>)	64
C4.1	Virgin soil	64
C4.2	A stone structure older than the Main Occupation Period ...	64
C4.3	Structures and features of the Main Occupation Period	65
C4.3.1	The southeastern corner of Building P	65
C4.3.2	Outdoor Area 71	65
C4.4	Deposits of the Post-Main Occupation Period	67
C4.5	Grave 103	67
C4.6	The modern looting pits and the topsoil	67
C4.7	Conclusions	69
C5.	The trench in Square 182909 (<i>Jean-Jacques Herr & Louise König</i>)	69
C5.1	Virgin soil	69
C5.2	Features of the Main Occupation Period	69
C5.2.1	Room 59 of Building P	69
C5.2.2	The walls of Room 59	70
C5.2.3	The large stone slab and the floor of Room 59	70
C5.2.4	Outdoor Area 71	71
C5.3	Graves 101, 109 and 110	72
C5.3.1	Grave 101	72
C5.3.2	Grave 109	75
C5.3.3	Grave 110	76
C5.4	The modern looting pits and the topsoil	77
C5.4.1	The fill of Room 59	77
C5.4.2	Outdoor Area 71	77
C5.5	Conclusions	78
C6.	The trench in Square 181909 (<i>Alessio Palmisano & Sophie Pietsch</i>)	78
C6.1	The Main Occupation Period	78
C6.1.1	The northern portion of Building P	78
C6.1.2	Outdoor Area 60	81
C6.2	The Graves 106, 107 and 108	81
C6.2.1	Grave 107	83
C6.2.2	Grave 106	83
C6.2.3	Grave 108	83
C6.3	Skull Locus:181909:084 from a looting pit: evidence for Early Iron Age burials	83
C6.4	The modern looting pits and the topsoil	84
C6.5	Conclusions	84
C7.	Preliminary assessment of the 2019 excavations at QID1 (<i>F. Janoscha Kreppner & Andrea Squitieri</i>)	84
D.	Pottery studies	86
D1.	The 2019 pottery from Qalat-i Dinka (QID1) (<i>Jean-Jacques Herr</i>)	86
D1.1	Pottery from DSC's Main Occupation Period	86
D1.1.1	Outdoor Area 60	86
D1.1.2	Outdoor Area 71	87
D1.2	Graves	87
D1.2.1	Grave 106	87

D1.2.2	Grave 101	87
D1.2.3	Grave 109	89
D1.3	Glazed pottery	89
D1.4	Middle Islamic Period pottery	89
D1.5	Conclusions: putting the QID ₁ pottery in its wider context ..	91
D2.	Petrographic analysis on Iron Age pottery from Graves 101 and 109 (<i>Silvia Amicone</i>)	93
E.	Small finds from the Dinka Settlement Complex, 2015-2019	95
E1.	The 2019 small finds from Qalat-i Dinka (QID ₁) (<i>Andrea Squitieri</i>) ..	95
E1.1	Introduction	95
E1.2	The small finds from graves (Group 1)	96
E1.2.1	Grave 101	96
E1.2.2	Grave 109	98
E1.2.3	Grave 102	98
E1.2.4	Grave 103	99
E1.2.5	Grave 105	99
E1.2.6	Grave 106	99
E1.2.7	Grave 110	102
E1.2.8	General considerations on the grave goods (Group 1)	103
E1.3	Small finds from looted fills and the topsoil (Group 2)	103
E1.3.1	Stone tools	103
E1.3.2	A complete bronze bowl	105
E1.3.3	Metal rods and studs	106
E1.3.4	Metal pieces of personal ornamentation	107
E1.3.5	Carnelian beads	108
E1.3.6	Blue/white-blue beads	108
E1.3.7	White beads	109
E1.3.8	Shell beads and pendants	109
E1.3.9	Bronze beads	110
E1.3.10	Perforated ivory/bone items	110
E1.3.11	Ceramic discs	110
E1.4	Preliminary assessment of the 2019 small finds from QID ₁ ..	111
E2.	Five fibulae from Qalat-i Dinka (QID ₁), 2019 (<i>Friedhelm Pedde</i>)	112
E2.1	Fibulae from Grave 110	112
E2.2	Fibulae from looting pits	114
E2.3	Conclusions	115
E3.	Three cylinder seals from Qalat-i Dinka (QID ₁), 2019 (<i>Anja Fügert</i>) ..	115
E3.1	A seal depicting a row of animals	115
E3.2	A seal depicting a hunting scene	116
E3.3	A seal depicting a contest scene	116
E3.4	Preliminary conclusions	117
E4.	Iron arrowheads from the Dinka Settlement Complex, 2015-2019 (<i>Anja Hellmuth Kramberger</i>)	117
E4.1	Description of the attested arrowhead types	118
E4.1.1	Variant a	118
E4.1.2	Variant b	118
E4.1.3	Variant c	120
E4.1.4	Variant d	120
E4.1.5	“Bodkin type”	120

E4.1.6	Variant e and “Others”	120
E4.2	Comparisons and dating	121
E4.2.1	Variant a	121
E4.2.2	Variant b	123
E4.2.3	Variant c and Variant d	125
E4.2.4	“Bodkin type”	130
E4.2.5	Variant e and “Others”	130
E4.4	Conclusions	131
E5.	Micro-CT study of the “Bodkin type” arrowhead from Gird-i Bazar (<i>Thilo Rehren, Raouf Jemmali, Silvia Amicone & Cristoph Berthold</i>) ...	132
E6.	Artefacts made of faunal remains from the Dinka Settlement Complex, 2015-2019 (<i>Anja Prust</i>)	134
E6.1	Items made of mammal bones	134
E6.2	Items made of marine species	135
E6.3	Conclusions	135
F. Faunal remains from the Dinka Settlement Complex, 2015-2019 (<i>Anja Prust</i>)		139
F1.	Material	139
F2.	Methods	139
F3.	Taphonomic patterns	146
F4.	Taxonomic diversity	148
F4.1	Domestic mammals	148
F4.2	Wild mammals	151
F4.3	Birds	152
F4.4	Amphibians	152
F4.5	Fish	153
F4.6	Molluscs	153
F4.7	Crustaceans	154
F5.	Modifications	154
F6.	Pathologies	155
F7.	Architectural contexts	155
F7.1	Fill of large well in Gird-i Bazar	155
F7.2	Kiln fills in Gird-i Bazar and DLT ₃	155
F7.3	Buildings and rooms of the Iron Age period	157
F7.4	Fills of the Sasanian period graves at Gird-i Bazar	157
F8.	Animal exploitation in the Dinka Settlement Complex	158
G. Phytoliths from the Dinka Settlement Complex, 2015-2019: first results (<i>Fatemeh Ghaheri</i>)		160
G1.	On-site sampling strategy	160
G2.	Methodology for extracting phytoliths	161
G3.	Preliminary results	162
G3.1	Environments of plants	162
G3.2	Pastoral activities	162
G3.3.	Wheat cultivation	162
G3.4	Crop processing	162

G3.5	Activity areas, architectural evaluation and plant consumption	162
G4.	Preliminary conclusions and future research	163
H. Archaeobotanical remains from the Dinka Settlement Complex, 2015-2018: preliminary results		
	<i>(Melissa S. Rosenzweig & Anne Grasse)</i>	164
H1.	Methods	164
H2.	Assemblage composition	164
H3.	Plant ecologies and land use	178
H4.	On-site plant use	186
I. A Chalcolithic kiln in the Bora Plain <i>(Andrea Squitieri, Mark Altaweel, Silvia Amicone, Jean-Jacques Herr, Sophie Pietsch & Jens Rohde)</i>		
		190
I1.	The discovery of the kiln and the goals of the 2019 excavation <i>(Andrea Squitieri & Mark Altaweel)</i>	190
I2.	2019 excavation results <i>(Jens Rohde & Sophie Pietsch)</i>	193
I3.	The kiln's structure and its parallels <i>(Sophie Pietsch)</i>	196
I4.	The Ubaid/LC1 pottery associated with the kiln <i>(Jean-Jacques Herr & Silvia Amicone)</i>	197
I5.	The kiln's radiocarbon dating and preliminary conclusions <i>(Andrea Squitieri)</i>	200
J. Preliminary report on the archaeological survey of the Iron Age sites in the central part of the Sardasht district, Iran		
	<i>(Salahaddin Ebrahimipour, Kazem Mollazadeh & Ali Binandeh)</i>	202
J1.	The surveyed area	202
J2.	The history of the archaeological exploration of Sardasht	202
J3.	Field survey methodology	203
J4.	2018 fieldwork and identified Iron Age sites	203
J5.	Spatial indicators	208
	J5.1 Spatial analysis of sites with access to the water resources ..	208
	J5.2 Spatial analysis of sites according to the elevation	208
J6.	Conclusions	208
K. Conclusions and perspectives		
	<i>(Karen Radner, F. Janoscha Kreppner & Andrea Squitieri)</i>	222
Bibliography		228

Preface

Karen Radner, F. Janoscha Kreppner & Andrea Squitieri

To Kamal Rasheed Raheem, in admiration and gratitude

The publication of this fifth volume of the series Peshdar Plain Project Publications (4P5) was yet again made possible by the kind support granted by the authorities of the Kurdish Autonomous Region of Iraq: the General Directorate of Antiquities, the Sulaymaniyah Directorate of Antiquities and the Raparin Directorate of Antiquities and their individual staff members, named in Chapter A; the generous sponsorship of the institutions that provided us with funding: the Alexander von Humboldt Foundation, the Gerda Henkel Foundation, the Rust Family Foundation, Ludwig-Maximilians-Universität München (LMU Munich) and Westfälische Wilhelms-Universität Münster; and the hard work and outstanding expertise of our international and interdisciplinary team of specialists: many of these were present in the Peshdar Plain in 2019 (named with their respective areas of responsibility during fieldwork in 2019 in Chapter A of this book) while others took on the analyses of a range of different materials in their labs.

In 2019, we were able to welcome a number of students and staff from Janoscha Kreppner's new academic home at the Westfälische Wilhelms-Universität Münster to the field team, as well as archaeozoologist Anja Prust (Institut für Paläoanatomie, Domestikationsforschung und Geschichte der Tiermedizin, LMU Munich) who presents two detailed studies of the faunal remains excavated from 2015-2019 at the Dinka Settlement Complex. Jörg Fassbinder's geophysics team working at the Dinka Settlement Complex now also includes Mandana Parsi (Department of Earth and Environmental Science, LMU Munich) who specialises in Electrical Resistivity Tomography surveying, which has already proven itself to be a valuable addition to our arsenal of prospecting methods. We are extremely grateful to long-time team members Fatemeh Ghaheri (Department of Anthropology, University of Texas at Austin) and Melissa S. Rosenzweig (joined in the lab by Anne Grasse, both Department of Anthropology, Northwestern University, Evanston, Illinois) for offering reports

on their ongoing analyses of the phytolith samples and the archaeobotanical remains from the Dinka Settlement Complex. We are very pleased to again include reports on petrographic analyses conducted on selected Chalcolithic and Iron Age pottery by Silvia Amicone at the Competence Center Archaeometry Baden-Wuerttemberg (CCA-BW) of Eberhard-Karls-Universität Tübingen, our cooperation partner since 2017, joined for the μ -X-ray computed tomography of an arrowhead by her colleague Christoph Berthold as well as Thilo Rehren of the Cyprus Institute's Science and Technology in Archaeology and Culture Research Center (Nicosia, Cyprus) and by Raouf Jemmali of the German Aerospace Center's, Institute of Structures and Design (Stuttgart, Germany). We were extremely fortunate to persuade Friedhelm Pedde (Assur Project, Berlin) and Anja Fügert (German Archaeological Institute, Berlin) to study the fibulae and cylinder seals excavated on Qalat-i Dinka, and Anja Hellmuth Kramberger (Institutum Studiorum Humanitatis, Fakulteta za podiplomaski humanistični študij, Alma Mater Europaea, Ljubljana, Slovenia) to assess all arrowheads found at the Dinka Settlement Complex since 2015.

It is a special joy to include also a report on the Iron Age settlement survey conducted further upstream on the Lower Zab in the Sardasht district in the Iranian province of West-Azarbaijan, conducted by Salahaddin Ebrahimi-pour, Kazem Mollazadeh and Ali Binandeh of the Department of Archaeology, Bu-Ali Sina University in Hamedan (Iran). This is the direct result of Janoscha Kreppner and Karen Radner's participation in the conference *The Iron Age in Western Iran and Neighbouring Regions* in Sanandaj in November 2019. We are very grateful to the conference's organisers Yousef Hassanzadeh, Ali A. Vahdati and Zahed Karimi for the kind invitation as well as to Jebrael Nokandeh (Director of the National Museum of Iran) and Judith Thomalsky (Director of the Tehran branch of the German Archaeological Institute) for their hospitality and their assistance in facilitating our travel in Iran.

Beyond the individuals mentioned in Chapter A, we are indebted to many colleagues and friends working in the Kurdish Autonomous Region of Iraq for sharing information and expertise, foremost among them our cooperation partner Jessica Giraud, head of the Mission archéologique française du Gouvernement de Soulaïmaniah (MAFGS). We thank Felix Höflmayer (Austrian Academy of Sciences, Institute for Oriental and European Archaeology, Vienna) for preparing the summary charts of the radiocarbon dates across the Dinka Settlement Complex. In Munich, we are immensely grateful to Denise Bolton who made time in her busy schedule to language-edit most of the chapters in this volume. In Gladbeck, our thanks and great appreciation goes – as ever – to our publisher and friend Peter Werner for his careful layout and the well-timed production of another fine-looking volume.

As with the first four volumes of the series Peshdar Plain Project Publications (4P1 = *Exploring the Neo-Assyrian Frontier with Western Iran: The 2015 Season at Gird-i Bazar and Qalat-i Dinka*, edited by Karen Radner, F. Janoscha Kreppner and Andrea Squitieri, Gladbeck 2016; Open Access download: <https://epub.ub.uni-muenchen.de/29236/>; 4P2 = *Unearthing the Dinka Settlement Complex: the 2016 Seasons at Gird-i Bazar and Qalat-i Dinka*, edited by Karen Radner, F. Janoscha Kreppner and Andrea Squitieri, Gladbeck 2017; Open Access download: <https://epub.ub.uni-muenchen.de/40252/>; 4P3 = *The Dinka Settlement Complex 2017: The Final Season at Gird-i Bazar and First Work in the Lower Town*, edited by Karen Radner, F. Janoscha Kreppner and Andrea Squitieri, Gladbeck 2018; Open Access download: <https://epub.ub.uni-muenchen.de/57255/>; and 4P4 = *The Dinka Settlement Complex 2018: Continuing the Excavations at Qalat-i Dinka and the Lower*

Town, Gladbeck 2019; Open Access download: <https://epub.ub.uni-muenchen.de/68561/>), this book is meant to share the results of our fieldwork in a detailed and timely manner. It is deliberately a “work in progress” that represents the current state of our knowledge and interpretation of the Dinka Settlement Complex, and future work and analyses are likely to change some of our views. Whereas in other years we have worked always hard to complete our annual volume in time for it to serve as the basis for the upcoming autumn field campaign, the ongoing COVID-19 pandemic of 2020 and the resultant travel restrictions have rendered excavations in the Peshdar Plain impossible this year.

It is with immense admiration and great affection that we dedicate this volume to our dear friend Kamal Rasheed Raheem, head of the Sulaymaniyah Directorate of Antiquities, without whom there would be no Peshdar Plain Project. Since 2010, Karen Radner and since 2015, also Janoscha Kreppner and Andrea Squitieri have benefited enormously from his knowledge, vision, decisiveness, generosity and unwavering support, also and especially in difficult situations – in addition to having the joy of sampling a great deal of Kurdish culinary delights in Sulaymaniyah and elsewhere.

بۆ هه‌فال و هاوڕێی خوشه‌ویستمان
به‌رێز کاک (که‌مال ره‌شید ره‌حیم) سوپاس بۆ ئه‌و هه‌موو
هاوکاری و یارمه‌تیدانه‌ی که‌ پێشکه‌شت کرد وین
له‌سه‌ره‌تایی کارکردنمان تا‌کو ئێستا، به‌هیوای
به‌رده‌وامی و پیکه‌وه‌ کارکردن له‌سروشته‌ سه‌وز
و شاخه‌ دل‌رفینه‌ کانی کوردستان

Munich and Münster, October 2020

A. The Peshdar Plain Project in its fifth year: the 2019 work programme

Karen Radner

The Peshdar Plain (PPP) was initiated by Karen Radner in 2015 in order to conduct multi-disciplinary fieldwork in the district of Peshdar (also Pishdar or Pizhder) in the province of Sulaymaniyah (Kurdish Autonomous Region of Iraq), with the primary objective to assemble data focused on the early first millennium BC that would allow us to better reconstruct the history of this understudied region on the border with Iran in the shadow of Assyrian imperial power (**Fig. A1**). From the second half of the 9th century BC onwards, the Assyrian Empire controlled the Peshdar Plain, which was situated on its eastern frontier (**Fig. A2**) and formed part of the defensive Border March of the Palace Herald¹. How the transformational processes triggered by proximity to, and later integration into, the Assyrian Empire affected the mountainous regions on the upper reaches of the Lower Zab is still poorly understood, and our fieldwork over the past five years has sought to better address this question by assembling and evaluating a wealth of new data. To this end, PPP has brought together international experts in history, archaeology, bioarchaeology, landscape archaeology, geography, geology, geophysics, material science studies, physical anthropology, GIS, photogrammetry, and 3D modelling who have spent a total of 50 weeks of on-site fieldwork from 2015-2019 in the Peshdar Plain. **Fig. A3** shows the extent of the geophysical surveying and excavations conducted in the past five years – still lots to do!

As its ancient name is unknown, “Dinka Settlement Complex” (DSC) is our provisional designation for the extended urbanised Iron Age settlement of ca. 60 ha that is the focus of our investigation of the Bora Plain, a subunit of the Peshdar Plain that stretches along the northern bank of the Lower Zab in close proximity to the Zagros main ridge, which today forms the border between Iran and the Kurdish Autonomous Region of Iraq in this region. DSC incorporates the previously identified archaeological sites of Gird-i Bazar (UTM 38N 512690 E; 3999300 N) and Qalat-i Dinka (UTM 38N 511920 E; 3999150 N). PPP’s dig

house is located in the district capital of Qaladze while our excavations take place near the village of Nureddin in the Bora Plain. As in previous years, we are very grateful to the people of Qaladze and Nureddin for their hospitality, practical assistance, and interest in our research, which would have been entirely impossible without their support.

Since its inception, PPP’s work has been conducted under the auspices of the Directorate of Antiquities of Sulaymaniyah, headed by Kamal Rasheed Raheem, to whom we gratefully dedicate this volume. We have benefitted from the unfailing support of the General Directorate of Antiquities of the Kurdish Autonomous Region of Iraq (Erbil) under the direction of Kaifi Mustafa Ali and enjoyed the local collaboration with the Raparin Directorate of Antiquities (Raniyah) headed by Barzan Baiz Ismail. As in the past, we are grateful to all three institutions for allowing staff from Sulaymaniyah, Erbil, and Raniyah to join the team as representatives, and excavation and pottery experts and thereby greatly contribute to the success of PPP’s work programme in 2019 by facilitating all sorts of logistical and administrative matters in addition to lending us their archaeological expertise. We are honoured to conduct our work with a formal license issued by the State Board of Antiquities and Heritage of Iraq (Baghdad) on 10 October 2018².

This book presents the results of the last year of fieldwork primarily sponsored by funding received from the Alexander von Humboldt Foundation and LMU Munich as part of the creation of Karen Radner’s Alexander von Humboldt Chair for the Ancient History of the Near and Middle East at LMU in 2015; this extremely generous funding stream, which enabled the conception and realisation of an ambitious fieldwork programme over five years, came to an end in July 2020. Furthermore, we gratefully acknowledge the support of the Gerda Henkel

¹ Radner 2015; 2016.

² We are especially grateful to have been invited to publish a report on our work in its flagship journal *Sumer*: Radner/Kreppner/Squiteri 2019a.

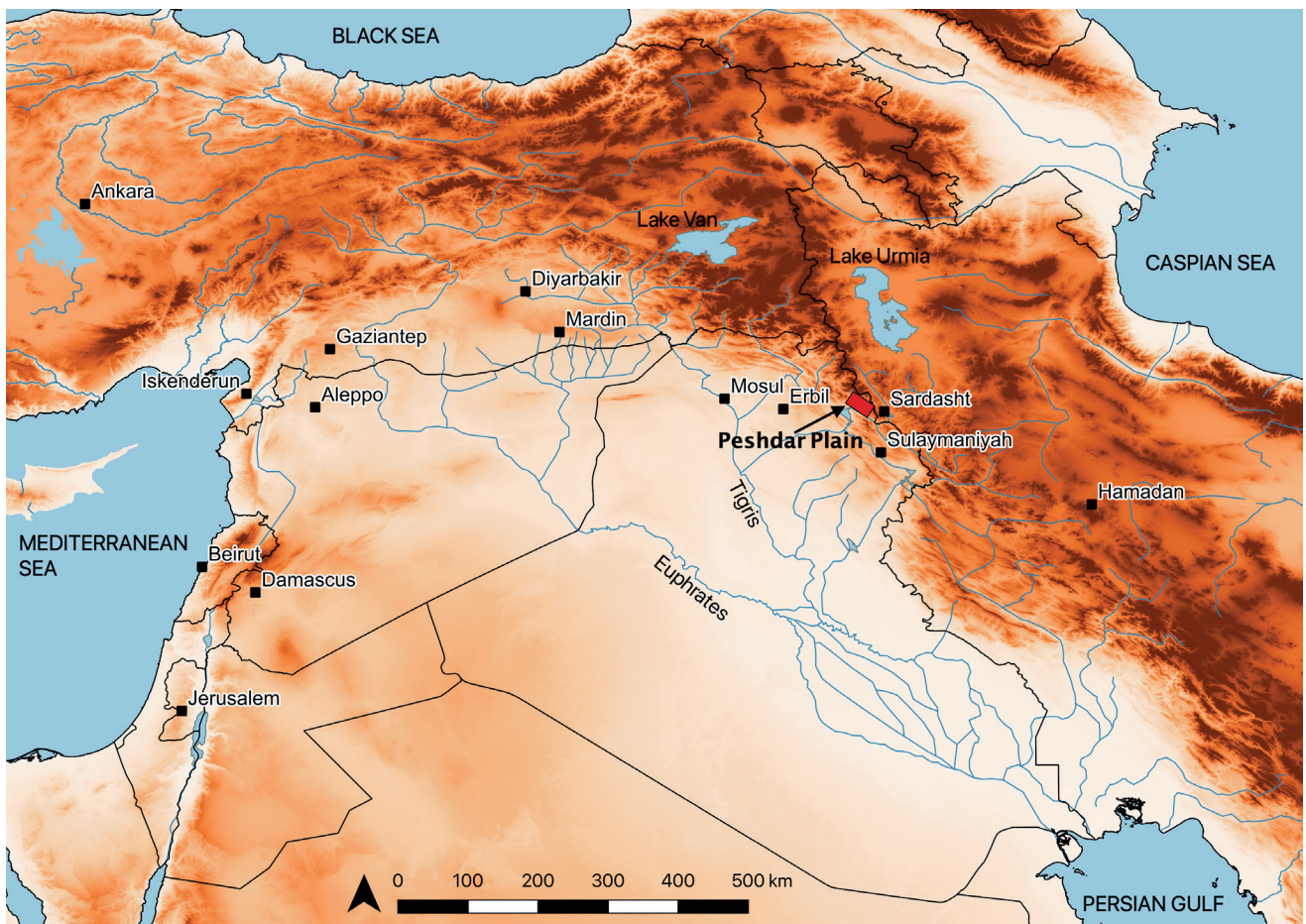


Fig. A1: The position of the Peshdar Plain in the modern Middle East, on the border of the Kurdish Autonomous Region of Iraq with Iran. Prepared by Andrea Squitieri.

Stiftung in the form of two grants awarded to Karen Radner in order to support Christoph Forster's development and refinement of PPP's digital documentation system (AZ 42/V/16), and to Andrea Squitieri and Jean-Jacques Herr (AZ 09/V/19) in order to continue the excavation of the monumental building on Qalat-i Dinka first explored in 2017 and 2018. We are also grateful for the support of the Rust Family Foundation in the form of an archaeology grant awarded to Andrea Squitieri and Mark Altaweel that enabled the fuller investigation of a Chalcolithic kiln discovered in 2018 underneath the Iron Age structures of the DSC. Since his appointment to the professorship in Ancient Near Eastern Archaeology at Westfälische Wilhelms-Universität Münster in October 2018, Karen Radner shares the directorship of the project with F. Janoscha Kreppner (previously PPP's field director) whose new university's starter funding enabled the participation of WWU students and staff in the 2019 autumn campaign.

Due to the rapid spread of the novel coronavirus, the COVID-19 pandemic and the resultant travel restrictions,

a study season planned for spring 2020 could not take place but we are extremely grateful to our colleagues in Sulaymaniyah, most importantly Hero Salih Ahmed, for continuing with some of the scheduled work programme once the Archaeological Museum of Sulaymaniyah, where our finds and materials are stored, was accessible again. We all hope that we will be able to work together again in the Peshdar Plain in 2021.

A1. The 2019 activities of the Peshdar Plain Project

As part of our excavation strategy since 2015, a main focus has been placed on the recovery of charcoal and carbonised seeds from floors and other key contexts in order to procure material for ^{14}C analysis, in addition to suitable human and animal teeth and bones. The effort and cost associated in systematically collecting and testing is considerable but as we are working in a wider

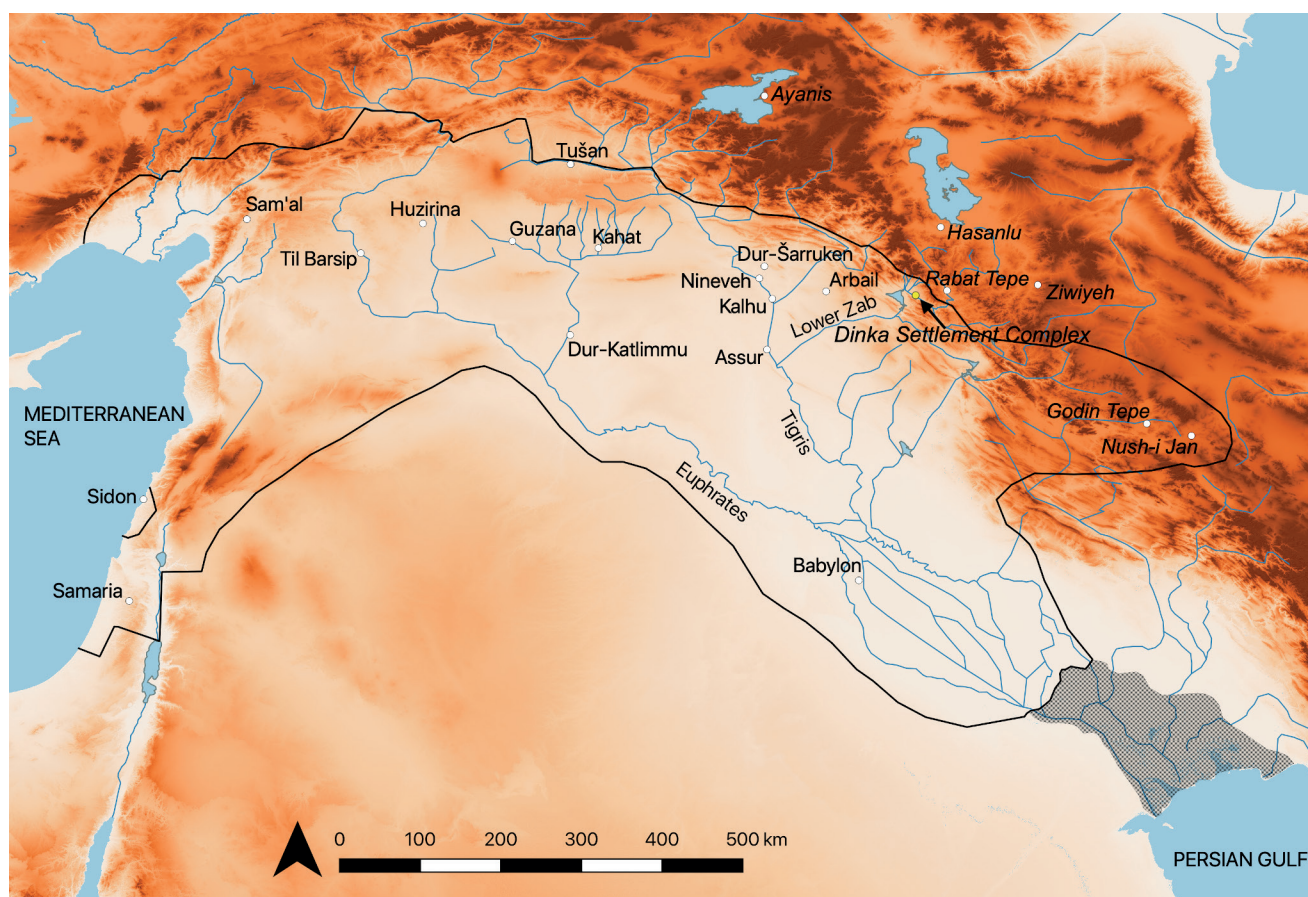


Fig. A2: The position of the Dinka Settlement Complex at the end of the 8th century BC, on the eastern frontier of the Neo-Assyrian Empire. Modern place names in italics. Prepared by Andrea Squitieri.

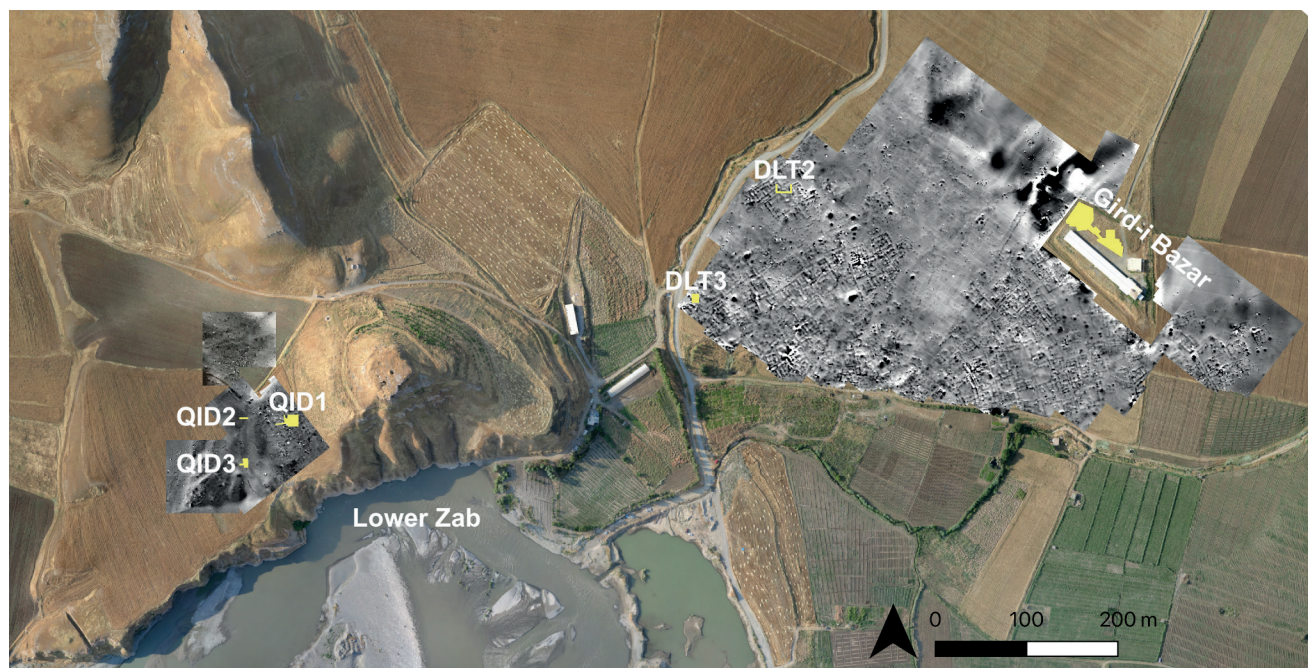


Fig. A3: The Dinka Settlement Complex, overlaid with the magnetograms generated by Jörg Fassbinder and his team since 2015. Marked in yellow, the operations Gird-i Bazar, DLT2, DLT3, QID1, QID2 and QID3. Detail of a drone image created by ICONEM (Paris; <http://iconem.com>), courtesy of Un Film à la Patte (Strasbourg; <http://www.unfilmalapatte.fr>) and Jessica Giraud. Prepared by Andrea Squitieri.



Fig. A4: The positions of the Iron Age ^{14}C samples from the lower town of the Dinka Settlement Complex and the probable calibrated date ranges (calBC). Black dot: charcoal; green dot: carbonised seed; red diamond: human bone; blue triangle: donkey tooth. Detail of a drone image created by ICONEM (Paris; <http://iconem.com>), courtesy of Un Film à la Patte (Strasbourg; <http://www.unfilmalapatte.fr>) and Jessica Giraud. Prepared by Andrea Squitieri.

regional context where there is a pronounced scarcity of Iron Age radiocarbon dates³, we consider it essential to contribute new data. Kathleen Downey (Ohio State University, Columbus, Ohio) and Melissa Rosenzweig (Northwestern University, Evanston, Illinois) have been carefully selecting suitable samples among the human remains and carbonised seeds – during fieldwork and in the lab, respectively. The position and the calibrated date ranges (BC) with the highest probability of the ^{14}C samples from within the Dinka Settlement Complex are shown in **Fig. A4** for the Lower Town (including Gird-i Bazar and the excavation areas DLT2 and DLT3) and in **Fig. A5** for Qalat-i Dinka, differentiating between dates derived from charcoal, human bones and teeth, animal teeth, and car-

bonised seeds. Note that these figures and the accompanying graph (**Fig. A6**) already includes our newest Iron Age radiocarbon date ranges from the excavations on Qalat-i Dinka (presented in **Chapter C**) as well as the new radiocarbon dating from the Chalcolithic kiln excavated underneath the Iron Age layers of DLT3 (presented in **Chapter I**)⁴. In addition, we have two new radiocarbon date ranges derived from our coring activity (presented in **Chapters B1** and **B2**) but as these are not connected to an excavation area, they have been excluded from the maps and the summary graphs (see **Figs. B1.6** and **B1.15**

³ For a first radiocarbon date for one of the burials from the Iron Age cemetery of Sanandaj in the Kurdistan province of Iran, see now Radner/Amelirad/Azizi 2020.

⁴ For the previously obtained ^{14}C results, see Altaweel/Marsh 2016, 27-28 (from the geoarchaeological sounding GA42 = now DLT3); Greenfield 2017, 173-174 (from a burial of the Sasanian-period cemetery in Gird-i Bazar); Kreppner/Radner 2018 (from various contexts in Gird-i Bazar); Radner 2018 (from DLT2); and Radner/Squitieri 2019 (from Qalat-i Dinka).

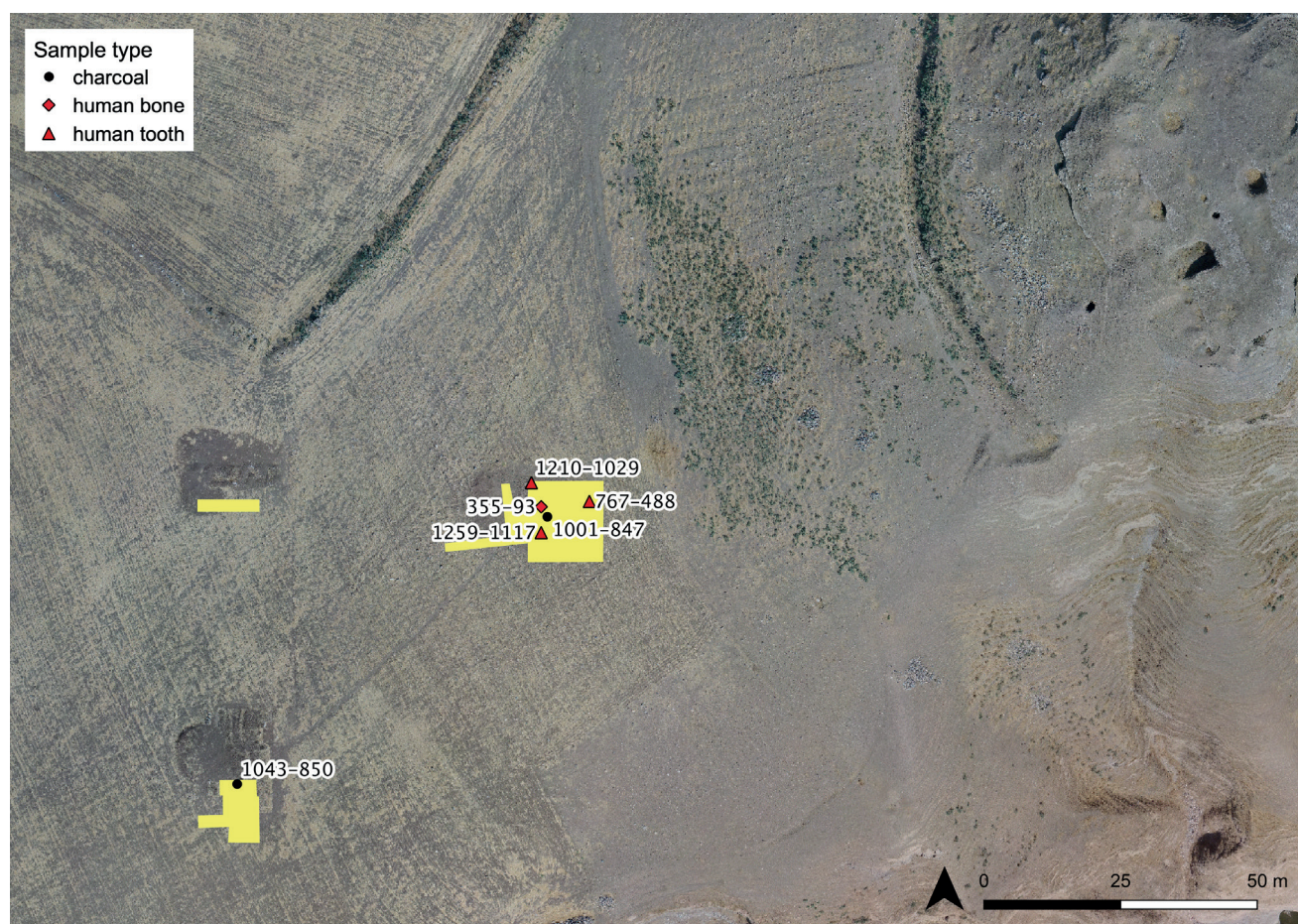


Fig. A5: The positions of the Iron Age ^{14}C samples from Qalat-i Dinka and the probable calibrated date ranges (calBC). Black dot: charcoal; red diamond: human bone; red triangle: human tooth. Orthophoto created by Andrea Squitieri in September 2018. Prepared by Andrea Squitieri.

for the location of Core 36 and its radiocarbon result and **Figs. B2.1** and **B2.4** for the location of Core 26 and its radiocarbon result). However, they are included in **Table A1**, which presents an overview of the key information for all currently available radiocarbon dates from the Dinka Settlement Complex.

In the following, we give a brief overview over the fieldwork undertaken in the Kurdish Autonomous Region of Iraq in 2019, listing the team members on site. As espe-

cially the lineup of the spring campaign demonstrates, the project continues to attract an illustrious range of experienced specialists whose great contribution to the success of PPP is gratefully acknowledged. In addition to the two fieldwork campaigns conducted in the Bora Plain, a range of analyses were conducted in labs and libraries in Austin, Berlin, Evanston, Ljubljana, Munich and Tübingen whose results are presented in **Chapters D, E, F, G** and **H**.

Operation: Gird-i Bazar (GIB)		Material	Context	14C Age (BP)	68.2 %	95.4 %	UTM (38N) Eastings	Northings
Lab ID	Sample reg. n.							
MAMS-32635	PPP 268932:042:001	Seed	Alley 13 floor	2939 ± 22	1207 - 1115 cal BC	1215 - 1055 cal BC	512688.03	3999279.01
MAMS-32638	PPP 268931:041:012	Seed	Courtyard 11 floor	2938 ± 23	1207 - 1114 cal BC	1216 - 1053 cal BC	512683.14	3999310.29
MAMS-33610	PPP 271929:042:004	Donkey tooth	Well in Outdoor Area 7	2797 ± 21	976 - 915 cal BC	1006 - 901 cal BC	512716.87	3999294.25
MAMS-32636	PPP 268932:052:002	Seed	Oven in Courtyard 21	2755 ± 21	921 - 891 cal BC	971 - 834 cal BC	512681.34	3999323.78
UGAMS-23213	PPP 271927:014:008	Charcoal	Room 3 floor	2750 ± 25	916 - 844 cal BC	972 - 829 cal BC	512714.07	3999279.01
MAMS-32637	PPP 268931:032:017	Seed	Room 19 floor	2751 ± 23	916 - 890 cal BC	971 - 831 cal BC	512688.69	3999317.62
MAMS-32639	PPP 272927:020:017	Seed	Room 23 floor	2716 ± 22	894 - 865 cal BC	906 - 816 cal BC	512722.35	3999277.29
MAMS-33609	PPP 267930:037:004	Human bone	Grave 71 in well of Room 49	2439 ± 20	730-431 cal BC	748 - 409 cal BC	512671.95	3999306.56
MAMS-30505	PPP 272927:021:001	Human tooth	Grave 47	1619 ± 19	398 - 429 cal AD	389 - 535 cal AD	512721.39	3999276.84
Operation: DLT2								
Lab ID	Sample reg. n.	Material	Context	14C Age (BP)	68.2 %	95.4 %	UTM (38N) Eastings	Northings
MAMS-34635	PPP 235934:003:001/1	Seed	Fill of vessel Locus:235934:037	2795 ± 24	977 - 911 cal BC	1012 - 856 cal BC	512357.44	3999341.47
MAMS-34636	PPP 235934:003:001/2	Seed	Fill of vessel Locus:235934:037	2740 ± 24	905 - 842 cal BC	930 - 824 cal BC	512357.44	3999341.47
Operation: DLT3								
Lab ID	Sample reg. n.	Material	Context	14C Age (BP)	68.2 %	95.4 %	UTM (38N) Eastings	Northings
MAMS-41835	PPP 225922:049:019	Charcoal	Fill of kiln Locus:225922:056	6170 ± 33	5207 - 5066 cal BC	5218 - 5024 cal BC	512258.34	3999222.74
MAMS-41836	PPP 225922:049:026	Charcoal	Disturbed fill of kiln Locus:225922:056	2966 ± 23	1221 - 1128 cal BC	1262 - 1114 cal BC	512258.82	3999222.43
MAMS-45236	PPP 226922:047:009	Seed	Outdoor Area 63 floor	2787 ± 41	1002 - 897 cal BC	1042 - 833 cal BC	512263.48	3999228.41
UGAMS-23561	/	Charcoal	Geoarchaeological trench GA42	2630 ± 25	813 - 793 cal BC	830 - 789 cal BC	512262.44	3999225.27
Operation: QID1								
Lab ID	Sample reg. n.	Material	Context	14C Age (BP)	68.2 %	95.4 %	UTM (38N) Eastings	Northings
MAMS-36939	PPP 181908:018:016	Human tooth	Grave 99	2963 ± 19	1217 - 1129 cal BC	1259 - 1117 cal BC	511815.09	3999089.66
MAMS-43917	PPP 181909:067:006	Human tooth	Looting pit	2920 ± 24	1189 - 1054 cal BC	1210 - 1029 cal BC	511813.69	3999097.73
MAMS-36674	PPP 181909:038:049	Charcoal	Room 58 floor	2780 ± 22	975 - 899 cal BC	1001 - 847 cal BC	511816.08	3999092.20
MAMS-43915	PPP 182909:067:017	Human tooth	Grave 110	2472 ± 23	751 - 540 cal BC	767 - 488 cal BC	511822.64	3999094.81
MAMS-36938	PPP 181909:031:002	Human tooth	Grave 98	2148 ± 26	347 - 120 cal BC	355 - 93 cal BC	511815.18	3999093.82
Operation: QID3								
Lab ID	Sample reg. n.	Material	Context	14C Age (BP)	68.2 %	95.4 %	UTM (38N) Eastings	Northings
MAMS-36673	PPP 176905:031:004	Charcoal	Floor of open area	2802 ± 32	997 - 917 cal BC	1043 - 850 cal BC	511766.46	3999051.46
Cores								
Lab ID	Core n.	Material	Context	14C Age (BP)	68.2 %	95.4 %	UTM (38N) Eastings	Northings
MAMS-41838	Core C26	Charcoal	Core taken outside the excavated area, near the boundary between the Lower and the Upper Terraces of the Lower Zab.	1428 ± 21	615 - 646 cal AD	592 - 655 cal AD	512480.91	3999078.31
MAMS-41837	Core C36	Charcoal	Core taken within the Lower Town, outside the excavated area, about 180 m west of Gird-i Bazar.	4440 ± 25	3307 - 3022 cal BC	3329 - 2939 cal BC	512458.19	3999271.82

Table A1: Summary table of the radiocarbon dates available from the Dinka Settlement Complex, including also the two new dates derived from sediment cores (see Chapter B). Compiled by Andrea Squitieri and Alessio Palmisano.

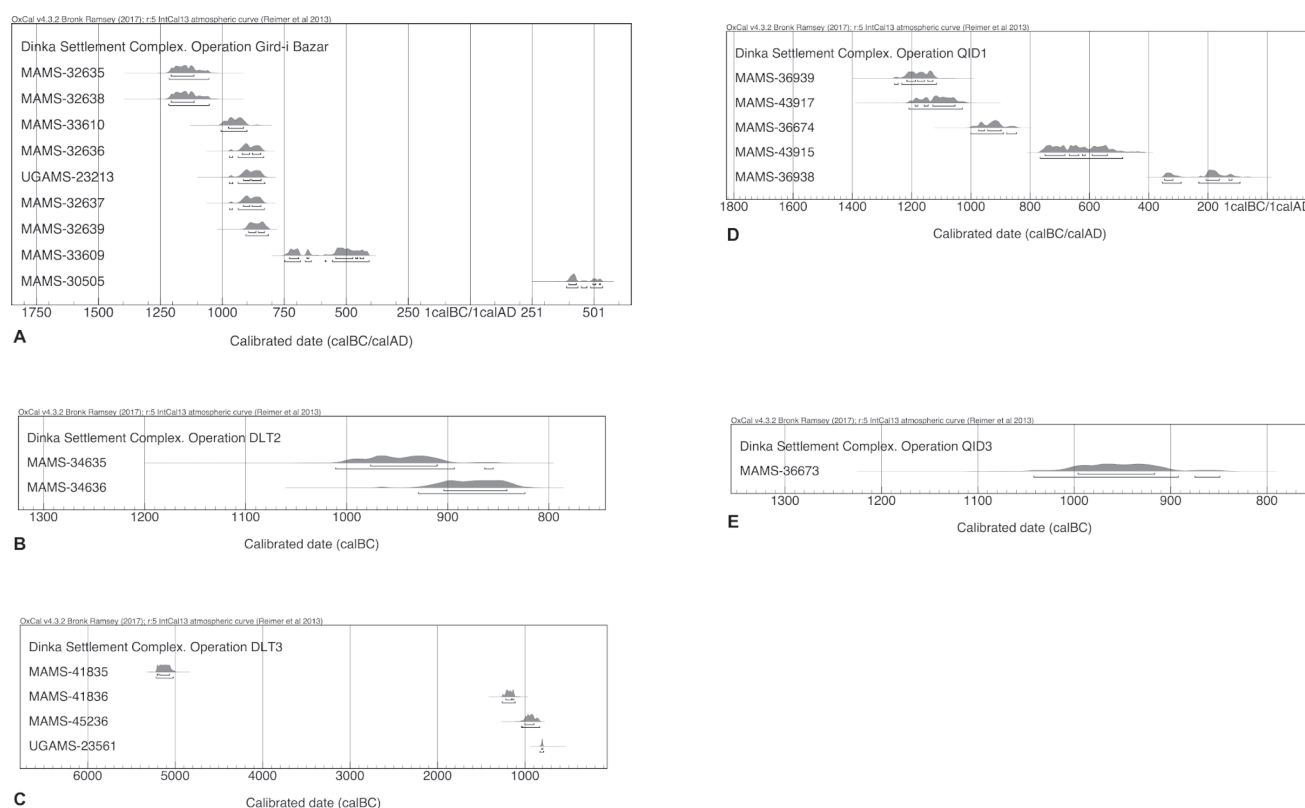


Fig. A6: The range of radiocarbon dates currently available for the different archaeological operations conducted at the Dinka Settlement Complex: in the lower town, Gird-i Bazar = graph A, DLT2 = graph B, DLT3 = graph C; and on Qalat-i Dinka, QID1 = graph D and QID3 = graph E. Calibration OxCal v. 4.3.2 (Bronk Ramsey 2017). Graphs prepared by Felix Höflmayer (Vienna).

A1.1 Exploring the palaeo-environment and the Chalcolithic settlement in the Bora Plain in spring 2019

A spring campaign focusing on procuring further data towards our understanding of the ancient environment of the Bora Plain took place from 19 April to 5 May 2019, with the excavation of a previously identified Chalcolithic kiln conducted on the site thanks to additional funding awarded by the Rust Family Foundation (**Chapter I**). The results from our programme of Electrical Resistivity Tomography (ERT) surveying and sediment coring are presented in **Chapter B**.

Team members (Fig. A7)

Representative of the Sulaymaniyah Directorate of Antiquities:

- Hero Salih Ahmed, also field team.

Representative of the Raparin Directorate of Antiquities:

- Abubakr Qasim, also field team.

Logistics:

- Aziz Sharif, Sulaymaniyah Directorate of Antiquities, driver,
- Ibrahim Manla Issa, Erbil, cook,
- Eimo Mustafa Manla Issa, Erbil, assistant cook and pottery team support.

Field team:

- Andrea Squitieri, LMU Munich, field director, digital documentation and small finds,
- Jens Rohde, LMU Munich, trench supervisor, field photography and 3D stratigraphy,
- Sophie Pietsch, FU Berlin, assistant trench supervisor,
- three workmen from Nuraddin village.

Specialists:

- Mark Altaweel, University College London, geoarchaeology and landscape archaeology,
- Silvia Amicone, University of Tübingen, archaeometry and pyrotechnology,



Fig. A7: The team of the 2019 spring campaign during a trip to the fringes of the Qandil mountain range at the northern edge of the Peshdar Plain (Easter 2019). From left to right: Jean-Jacques Herr, Cajetan Geiger, Mark Altaweel, Andrea Squitieri, Eileen Eckmeier, Hero Salih Ahmed, Jens Rohde, Jörg Fassbinder, Ibrahim Manla Issa, Aziz Sharif, Eimo Mustafa Manla, Abubakr Qasim, Marion Scheiblecker, Silvia Amicone, Sophie Pietsch. Photo by Jean-Jacques Herr (by automatic shutter release).

- Eileen Eckmeier, LMU Munich, geography, landscape archaeology and soil analysis,
- Jörg Fassbinder, Bayerisches Landesamt für Denkmalpflege, Munich & LMU Munich, geophysics,
- Cajetan Geiger, Ruhr-Universität Bochum, geology,
- Jean-Jacques Herr, LMU Munich, pottery,
- Marion Scheiblecker, LMU Munich, geophysics.

A1.2 The third excavation campaign on Qalat-i Dinka in autumn 2019

From 30 August to 7 October 2019, a third excavation campaign on Qalat-i Dinka was dedicated to the further exploration of the monumental Building P. The results of the excavation are presented in **Chapter C** while the pottery is discussed in **Chapter D** and the rich small finds, which include fibulae and cylinder seals from the burials surrounding the building, are analysed in **Chapter E**.

Team members (Fig. A8)

Representative of the Sulaymaniyah Directorate of Antiquities:

- Hero Salih Ahmed, also co-trench supervisor and pottery registration.

Representative of the Raparin Directorate of Antiquities:

- Abubakr Qasim, also field team and pottery drawing.

Logistics:

- Aziz Sharif, Sulaymaniyah Directorate of Antiquities, driver,
- Ibrahim Manla Issa, Erbil, cook,
- Hamrin Ibrahim Manla Issa, Erbil, assistant cook and pottery team support,
- Eimo Mustafa Manla Issa, Erbil, assistant cook and pottery team support.

Field team:

- F. Janoscha Kreppner, WWU Münster, project co-director,



Fig. A8: The team of the 2019 autumn campaign on the roof of the excavation house in Qaladze. From left to right: Aziz Sharif, Sophie Pietsch, Abubakr Qasim, Jamal Jamil Assad, Alessio Palmisano, Jens Rohde, Ibrahim Manla Essa, Janoscha Kreppner, Jana Richter, Hero Salih Ahmed, Laura Tretow, Andrea Squitieri, Luise König, Anja Prust, Mark Altaweel, Hamrin Manla Issa, Jean-Jacques Herr. Photo by Jean-Jacques Herr (by automatic shutter release).

- Andrea Squitieri, LMU Munich, field director, digital documentation and small finds,
- Alessio Palmisano, LMU Munich, trench supervisor and field photography,
- Jana Richter, WWU Münster, co-trench supervisor and heavy fraction analysis,
- Jens Rohde, LMU Munich, trench supervisor, field photography and 3D stratigraphy,
- Louise König, WWU Münster, assistant trench supervisor and small finds registration,
- Sophie Pietsch, WWU Münster, assistant trench supervisor,
- Laura Tretow, WWU Münster, assistant trench supervisor,
- twelve workmen from Nureddin and Qaladze.

Pottery team:

- Jean-Jacques Herr, LMU Munich, lead ceramicist, also trench supervisor,
- Jamal Jamil Assad, General Directorate of Antiquities Erbil, pottery processing and pottery photography.

Specialists:

- Mark Altaweel, University College London, geoarchaeology and landscape archaeology,
- Anja Prust, LMU Munich, archaeozoology.

A2. The scope of this volume

As the four previous volumes of the series *Peshdar Plain Project Publications (4P)* have done for 2015⁵, 2016⁶, 2017⁷ and 2018⁸, this book presents a comprehensive report of the Peshdar Plain Project's fieldwork activities in 2019 and offers results of a range of analyses on materials and data collected in this and earlier years.

Section B presents new data gained with our ongoing programmes of geophysical surveying (since 2015) and sediment analysis (since 2017). Chapter B₁ by Mandana

5 Radner/Kreppner/Squitieri 2016.

6 Radner/Kreppner/Squitieri 2017.

7 Radner/Kreppner/Squitieri 2018.

8 Radner/Kreppner/Squitieri 2019.

Parsi and Jörg Fassbinder discusses the results of the 2019 electric resistivity tomography (ERT) survey, which greatly aid our understanding of the *qanat* system associated with the Dinka Settlement Complex. They also provide new information on some of the Iron Age settlement's architectural features, notably the fortifications on the western slope of Qalat-i Dinka. Eileen Eckmeier's contribution in Chapter B2 presents new results from the systematic sediment analysis programme that has by now collected 60 cores from the Bora Plain. In addition to furthering our understanding of the plain's palaeo-environment, this data is harnessed to help identify the locations of ancient *qanat* structures and roads. Charcoal fragments found in two cores have also yielded additional radiocarbon datings.

In Section C, Jean-Jacques Herr, Louise König, F. Janoscha Kreppner, Alessio Palmisano, Sophie Pietsch, Jana Richter, Jens Rohde, Hero Salih Ahmed, Andrea Squitieri and Laura Tretow detail the results of the 2019 excavations on the western slope of Qalat-i Dinka, which targeted the monumental Building P. This work not only succeeded in completing the unearthing of this badly looted structure but also brought to light more of the cremation and inhumation burials associated with the building, providing also some additional Iron Age radiocarbon dates.

Section D is dedicated to pottery studies. In Chapter D1, Jean-Jacques Herr discusses the pottery recovered during the excavations on Qalat-i Dinka in 2019, especially from the context of the Iron Age cremation burials associated with Building P where several complete or completely reconstructable vessels have been recovered, despite the heavy looting activity that targeted specifically these relatively rich graves. Silvia Amicone supplements this work in Chapter D2 with the results of the petrographic analysis on selected ceramics from Graves 101 and 109, which show that they are made from Fabric C₁ that is typical for the local ceramic production at the Dinka Settlement Complex, using clay from a local source.

Section E consists of six chapters that discuss various categories of small finds found at the Dinka Settlement Complex. In Chapter E1, Andrea Squitieri catalogues and presents a first assessment of all new finds uncovered during the 2019 excavations on Qalat-i Dinka while some of the finds associated with the Iron Age burials around Building P are also the subject of further detailed studies: Friedhelm Pedde discusses the five fibulae in Chapter E2, which can be assigned to the 7th century BC, and Anja Fügert the three cylinder seals in the "Provincial Assyrian Style" in Chapter E3. Anja Hellmuth Kramberger's Chapter E4 surveys all arrowheads found between 2015-2019 at the Dinka Settlement Complex, with most specimens originating from Building P on Qalat-i Dinka; her work

is supplemented in Chapter E5 by the μ -X-ray computed tomography analysis of Thilo Rehren, Raouf Jemmali, Silvia Amicone and Christoph Berthold that elucidates the production processes of the "Bodkin type" arrowhead of unclear date found in 2015 in the topsoil of Gird-i Bazar. In Chapter E6, Anja Prust presents all artifacts made of faunal remains that have been excavated between 2015-2019 at the Dinka Settlement Complex; attested are various objects created from mammal bones and marine species, many of which have only been recently identified due to the fact that Jana Richter has started to analyse in 2019 the heavy fraction assembled routinely from flotation since 2015.

Section F is dedicated to Anja Prust's detailed analysis of the faunal remains recovered from the Dinka Settlement Complex in the years 2015-2019, building on the earlier work of Tina Greenfield on Gird-i Bazar⁹ but integrating now also the evidence from other excavation areas and from the heavy fraction. Across the excavated areas, domestic mammals dominate, and sheep, goat, cattle and pig are by far the most frequent taxa attested. All of these species were exploited for food and presumably also for their secondary products. On the other hand, the exploitation of wildlife (mammals, birds, fish and others) was negligible. While the Iron Age layers have yielded evidence for the consumption of chukar partridge (*Alectoris chukar*), greylag goose (*Anser anser*) and rock dove (*Columba livia*), all attested locally to this day, the number of fish remains is extremely low despite the immediate proximity to the Lower Zab river. Only the remains of an unidentified member of the cyprinid family (*Cyprinidae*) were found in the Iron Age layers, possibly reflecting cultural practices or taboos that rendered fish consumption unusual (at least in secular contexts). Whether the relatively numerous terrestrial snails found in the Iron Age settlement (especially *Helix salomonica*) were consumed as food is possible but uncertain, as there is no clear evidence for shell middens.

Section G presents the first results of Fatemeh Gha-heri's study of the phytolith samples that have been systematically collected during the excavations at the Dinka Settlement Complex by her and others since 2015. The ongoing analysis indicates that the environments where plants were being cultivated and collected were wet and marshy and that pastoral activities took place on the site. In addition, the presence of basketry and floor matting could be demonstrated, as well as the use of reed as a building material.

9 Greenfield 2016; 2017; 2019.

In Section H, Melissa S. Rosenzweig and Anne Grasse discuss the first results of the ongoing archaeobotanical analysis, presenting their analysis and interpretations of 32 samples collected from across all Iron Age excavation areas of the Lower Town of the Dinka Settlement Complex (Gird-i Bazar, DLT2 and DLT3). Already this preliminary dataset demonstrates that the residents of the Lower Town grew and relied on a typical Near Eastern crop package of cereals and pulses supplemented by grapes, figs, and millet. There is also evidence for mixed-cropping (DLT2) and wine-pressing (DLT3), with the solid pomace sieved from the must retained as fertiliser or fuel.

In Section I, Mark Altaweel, Silvia Amicone, Alessio Palmisano, Sophie Pietsch, Jens Rohde and Andrea Squitieri report the results of the excavation of the Chalcolithic kiln first discovered in 2018 underneath the Iron Age structures of DLT3 and present also a first radiocarbon date as well as an assessment of the pottery, whose fabric closely resembles the most frequently used fabric of the Iron Age pottery of the Dinka Settlement Complex (Fabric C1). This indicates that the same local source of clay was exploited over millennia for the production of pottery in the Bora Plain.

Section J does not deal with the Bora Plain, or indeed the Peshdar Plain, but an archaeologically virtually unknown area higher up on the Lower Zab across the border in Iran. Salahaddin Ebrahimipour, Kazem Mollazadeh and Ali Binandeh present first results from their 2018 archaeological surveys in the central part of the Sardasht district in West-Azerbaijan Province and detail the ten Iron Age sites that they identified based on comparison with the material from the important local Iron Age site of Rabat II. We are extremely proud to include their work in this volume. It is the happy result of the participation of Janoscha Kreppner and Karen Radner in the conference *The Iron Age in Western Iran and Neighbouring Regions* in Sanandaj, the capital city of the Iranian Kurdistan Province, in November 2019 where we had been asked to present our work on the Dinka Settlement Complex¹⁰. Survey work on the Iranian stretches of the Lower Zab is immensely important also for the reconstruction of the political geography during the time of the Assyrian Empire.

While 2019 was a productive and eventful year for the PPP, the COVID19 pandemic and the resultant restrictions in travelling made it impossible for the team to return to the Peshdar Plain. We very much hope that fieldwork and study seasons in the Archaeological Museum of Sulaymaniyah will again be possible in 2021.

¹⁰ Published as Radner/Kreppner/Squitieri 2019b.

B. Remote sensing and sediment analysis in the Bora Plain, 2019

B1. The 2019 Electrical Resistivity Tomography (ERT) survey

Mandana Parsi¹¹ & Jörg W. E. Fassbinder¹²

Between 19 April and 5 May 2019, an Electrical Resistivity Tomography (ERT) survey was conducted in the Bora Plain, with two main goals¹³. The first goal was to continue the investigation of the *qanat* system, the underground irrigation system that was first identified on the surface in 2015 and further investigated in 2016-2018¹⁴. The second goal was to investigate at a greater depth the archaeological features of the Dinka Settlement Complex that are visible in the magnetograms generated in 2015-2017 by Jörg Fassbinder and his team¹⁵.

Electrical Resistivity Tomography (ERT) is an effective method for archaeological geophysicists to non-destructively receive detailed information about underground structures, whether they be natural or artificial¹⁶. ERT has become increasingly important for bridging the gap between magnetometry and radar prospecting methods, particularly when wet and clayey soil conditions make GPR prospecting impossible¹⁷. Sophisticated computer programs that trigger multichannel electrodes, combined with inversion and 3D analysis software, allow the tracing of apparent electric resistivity in detail, even in areas located deep under the surface, and the production of multiple 2D- and 3D-modelled images¹⁸.

Different geological parameters or archaeological features affect underground resistivity. Porosity, hydraulic

permeability, moisture content, and soil temperature are additional factors affecting resistivity. The resistivity prospecting method is based on Ohm's law. This law explains the relationship between current, voltage, and resistance. Two different methods are used with the ERT instrument: self-potential (SP) and induced-polarisation (IP). Both methods are suitable for geological purposes. For archaeological purposes, IP is the best method. Electrode configurations are the different arrangements of electrodes which help us to survey more efficiently. The main configurations used for archaeological geophysics are dipole-dipole, Wenner, and occasionally Schlumberger. These arrays require 4 electrodes for each measurement: A and B as emitters, and M and N as receivers.

In the dipole-dipole configuration, emitters are placed on one side of the area being investigated, with an electrode spacing of "a". The receivers are placed on the other side with the separation of "a", while the distance between former and latter equals "n·a". This configuration provides more detailed information about shallow substructures. In the Wenner and Schlumberger configurations, the emitters are the two outer electrodes and receivers are the two inner electrodes. In the Wenner configuration, the electrode spacing between all of the electrodes is "a", and for the Schlumberger configuration only the electrode separation of the receivers is "a" and the remaining are "n·a". The Wenner configuration provides good detail from the deeper areas while the Schlumberger configuration generally supplies information about the geology of the subsurface.

To measure a longer profile with a specific number of electrodes and cables, we use the so-called "roll along" technique. In this method, after measuring the profile, we use the first set of electrodes and cables at the end of the existing profile and then we measure again. We can repeat this process as often as needed to cover the area. Data processing allows us to combine the data to produce a comprehensive profile from our measurements.

For measuring, we use Geosoft software, which gives us the apparent resistivity values of the underground area. Afterwards, for data processing, we use Geotomo's RES-2DINV and RES3DINV software. These programmes calculate the resistivity distribution of the underground area being analysed. Resistivity is a relative value, and therefore each range of resistivity values represents one or more fea-

¹¹ Department of Earth and Environmental Science, LMU Munich.

¹² Department of Earth and Environmental Science, LMU Munich / Bayerisches Landesamt für Denkmalpflege, Munich.

¹³ The authors would like to thank Marion Scheiblecker, Hero Salih Ahmed, Cajetan Geiger, and Andrea Squitieri for their tireless help with the hard work of setting out, hammering in, and removing the ERT electrodes.

¹⁴ Altaweel 2017.

¹⁵ Fassbinder/Ašandulesei 2016; Fassbinder/Ašandulesei/Scheiblecker 2017; 2018; Scheiblecker/Fassbinder 2019.

¹⁶ Schmidt 2013.

¹⁷ Parsi *et al.* 2019.

¹⁸ Loke *et al.* 2013; Schmidt 2013; Tabbagh 2017.

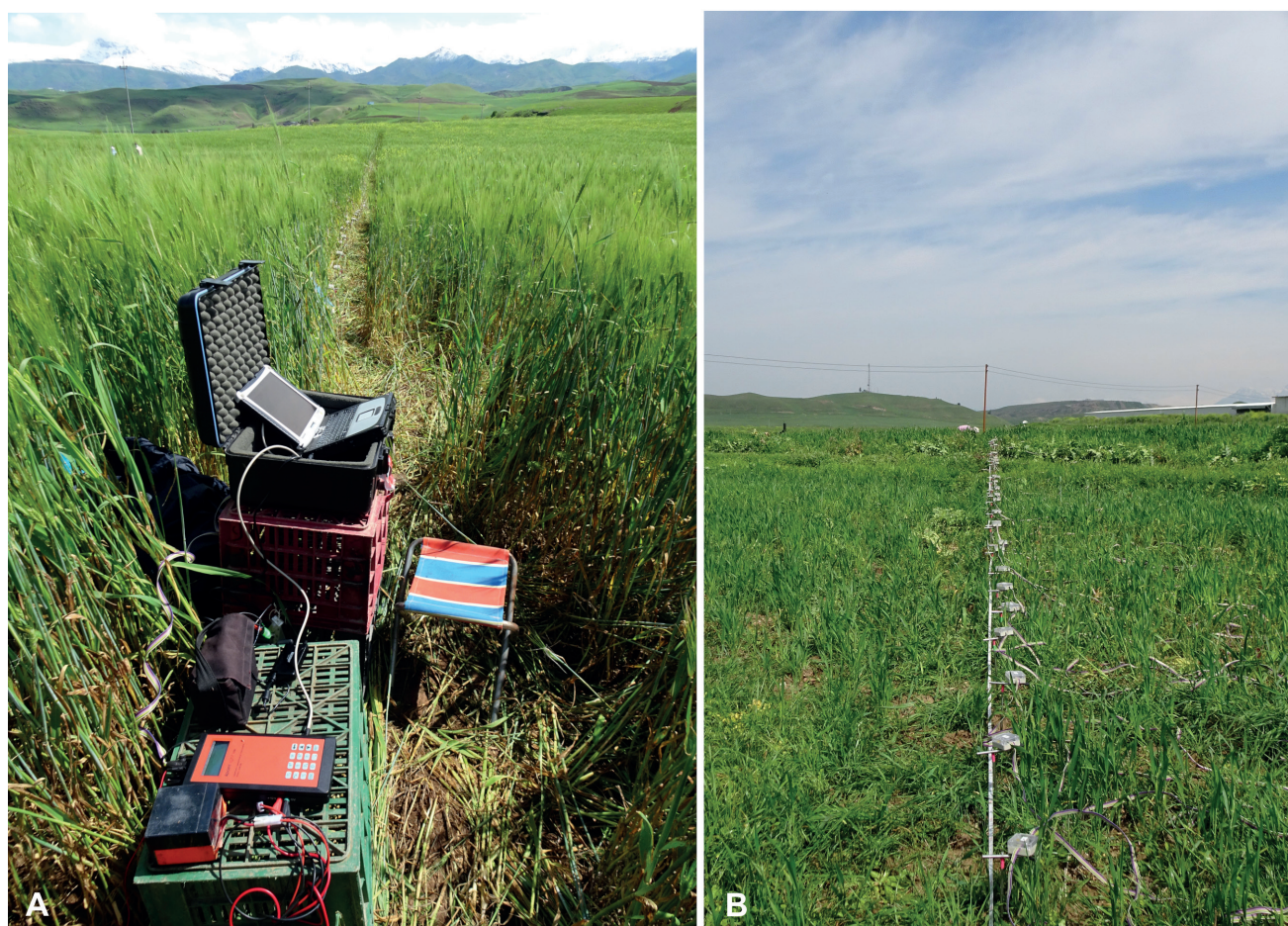


Fig. B1.1: The ERT 4point light 10W instrument (a) and the chain of electrodes (b) used during the 2019 spring campaign. The instrument was developed and designed by Erich Lippmann (Schaufing, Germany; <https://www.l-gm.de/>). Photos by Jörg Fassbinder.

tures. Based on the evidence provided by our results, we can determine what type of features are present in the subsurface and what materials they are composed of.

For the 2019 ERT survey in the Bora Plain, we used the earth resistivity meter 4point light 10W shown in **Fig. B1.1a**, while **Fig. B1.1b** shows the chain of electrodes that were fixed in the ground, with the electric boxes on top of them. **Fig. B1.2** shows the general map of the surveyed area with the positions of the 2019 ERT profiles (marked with yellow lines) and the magnetograms of the Lower Town and the western slope of Qalat-i Dinka.

B1.1 Investigating the *qanat* system in the Bora Plain

After briefly discussing the general characteristics of *qanats* in the Middle East we will present the results of our investigations of the previously identified *qanat* system in the Bora Plain in 2019, gained by ERT survey and by coring.

Qanats occur mainly in the Middle East, but such structures are also known from Nasca (Peru) and likely exist in many other dry areas of the world. They are an irrigation system for agriculture, but they also provide drinking water for humans and animals. *Qanats* are tunnels that draw water from underground aquifers or carry water from other specific sources, usually from a higher elevation (**Fig. B1.3**)¹⁹. In some areas, *qanats* can extend for several kilometres with shafts spaced every 10-20 meters (e.g. Pasargadae in Iran). These shafts were used to construct the tunnels, but then also served as wells and as entrances for cleaning and repairing the *qanats*. Around the shafts the builders deposited the excavated sediment – making these holes easily visible on the surface. Even the shafts that were destroyed or removed are very often still visible on satellite or aerial photographs.

Qanats transport water to a settlement using the power of gravity, and, being subterranean, they prevent the

¹⁹ Lightfoot 1996.



Fig. B1.2: Bing satellite image of the Bora Plain, overlaid by the magnetograms of the Lower Town and Qalat-i Dinka generated by J. Fassbinder and his team. White squares show the zones targeted by the ERT survey, with yellow lines showing ERT profiles. Prepared by Andrea Squitieri.

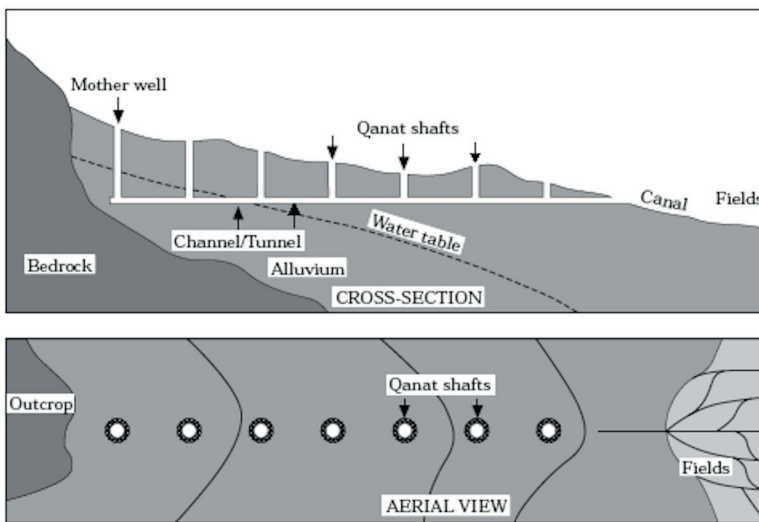


Fig. B1.3: Schematic view of a typical *qanat* system, with the cross section above and the aerial view below. After Lightfoot 1996, Fig. 1.

water from evaporating or becoming polluted. When *qanats* are abandoned, the tunnels and shafts will soon collapse, or become clogged and then refilled by sediments, remaining hidden underground. Detecting such features by ERT is quite challenging, as it is difficult to ascertain whether the tunnels or shafts were dry when they collapsed and refilled, or if water still flows through the stones of the collapsed structure. In the latter case, the ERT data resembles the results for palaeochannels, making a clear identification difficult.



Fig. B1.4: Bing satellite image of the southeastern area of the Bora Plain where the openings of *qanat* shafts are still visible today. The yellow lines show the positions of the ERT profiles (note that Profiles 10-11 and 7-8 were very close to one another so they appear as a single line in the image). The label “fish ponds” shows the location of fish ponds that were created after the satellite image had been taken; they were already in use in 2015 when PPP started work in the region. Prepared by Andrea Squitieri.

B1.1.1 ERT surveying in the southeastern part of the Bora Plain

This section deals with the ERT measurements that were applied to the previously known traces of *qanats* located in the southeastern part of the Bora Plain, about 1.5 km south of the Lower Town of the Dinka Settlement Complex (**Figs. B1.2** and **B1.4**). This *qanat* system was identified by the Peshdar Plain Project team in 2015 through satellite images and ground-truthing as some of the *qanat* shafts’ openings are still visible on the surface today²⁰. Subsequently, ERT measurements were first conducted in this area in autumn 2016 and spring 2017 by a team from the Geology Department of the University of Sulaymaniyah, working under the supervision of Prof. Bakhtiar Qader Azir (University of Sulaymaniyah) and Dr Mark

Altaweel (University College London)²¹. Their results highlighted a possible *qanat* tunnel running almost parallel to the river in a northwest-southeast direction, intersecting another tunnel running in an east-west direction²². Today, fish ponds are located at the point where the two tunnels meet (**Fig. B1.4**, see also **Fig. B2.2** below).

In spring 2019, 10 ERT profiles (**Fig. B1.4**: yellow lines) were measured in this area using the Wenner, Schlumberger and dipole-dipole configurations. For our purpose, the most effective configuration proved to be the dipole-dipole array. **Fig. B1.5** illustrates the ERT result of Profile 8, which is the only profile in this area that yielded significant results. The direction of this profile was southwest-northeast. As the feature was located in a shallow subsurface, we chose the dipole-dipole configuration

²⁰ Altaweel/Marsh 2016.

²¹ Altaweel 2017.

²² Altaweel 2017, 43 Fig. B2.8.

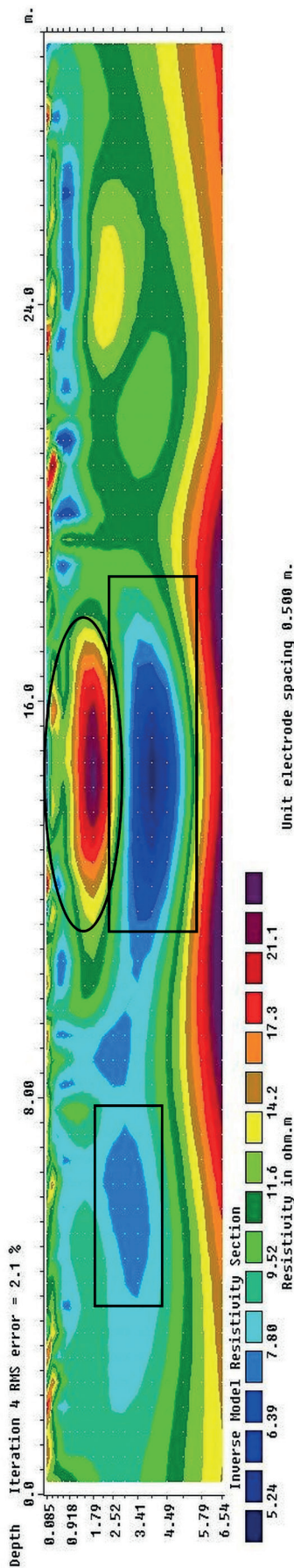


Fig. B1.5: ERT Profile 8. Direction: southwest-northeast. The black circle shows an anomaly that may be the remains of a collapsed qanat shaft at a depth of around 1.7 m. The black rectangle beneath it illustrates the possible active qanat tunnel with water inside of it; while the black rectangle on the left shows traces of a water table at a depth of around 3.5 m. Prepared by Mandana Parsi.

results for our interpretation. The electrode spacing was 0.5 m and the length of the profile was 30 m. In **Fig. B1.5**, the horizontal line shows the x-direction (length of the profile) and the vertical line illustrates the depth of the measurement. Each colour represents a specific resistivity value (the colour scale located at the lower left of the profile describes the correspondence value of each colour). In this profile, we detected two types of anomalies. Ellipsoidal-shaped features that are filled with water (black rectangles in **Fig. B1.5**) and an ellipsoidal-shaped feature filled with materials such as clay, gravel, and sand (black circle in **Fig. B1.5**). The black circle shows an anomaly that may be the remains of a collapsed *qanat* shaft at a depth of around 1.7 m. Other interpretations are possible, however, as this may also be the remains of a refilled palaeochannel. The black rectangle beneath it illustrates the possible active *qanat* tunnel with water inside of it; while the black rectangle on the left shows traces of a water table at a depth of around 3.5 m. On the left side of the profile, towards the top, we detected some features that can be interpreted as small shafts, which may have brought water to the surface. We have to mention that since the spacing of our electrodes was 0.5 m, we were not able to document any features smaller than this size.

We also measured and processed all the other profiles of this area by using a Wenner configuration and an electrode spacing of 0.75 m and 1 m to obtain information from the deeper parts of the subsurface. By increasing the electrode separation, we automatically filtered out any features that were smaller than the spacing. The outcomes, however, did not provide any additional relevant results and therefore are not presented here.

B1.1.2 ERT surveying near the Lower Town of the Dinka Settlement Complex

Moving closer to the Lower Town of the Dinka Settlement Complex, we measured six profiles to the southeast of the Lower Town magnetogram. These are Profiles 1-4 and Profiles 18-19 (**Figs. B1.6** and **B1.7**). The aim was to find traces of *qanats* close to the Lower Town that may have provided water for the settlement or to find further traces indicating that the settlement continued in this direction.

In **Fig. B1.7**, the three parallel Profiles 1, 2, and 3 show the presence of some anomalies. The first two profiles were parallel to each other and ran the same distance, while the third extended further to the west. **Figs. B1.8** and **B1.9** show the results from Profiles 1 and 2, respectively. The distance between the two profiles was 1 m. Both profiles were oriented from west-east, with 0.75 m electrode separation. They had a total length of 45 m, and were measured using a dipole-dipole configuration.

The black circle in **Fig. B1.8** (Profile 1) shows an ellipsoidal-shaped anomaly that first occurs at a depth of around 1.5 m, and extends to a depth of approximately 4 m. The width of this anomaly is hard to estimate, as we do not know how it is oriented within our profile. Further measurements are required to obtain precise information about its true diameter. According to its resistivity values, we suggest that this anomaly represents an artificial structure, possibly a wall. Next to it, the black rectangle shows elongated anomalies which may be the result of the accumulation of coarse gravel; perhaps it represents the remains of a pavement or floor.

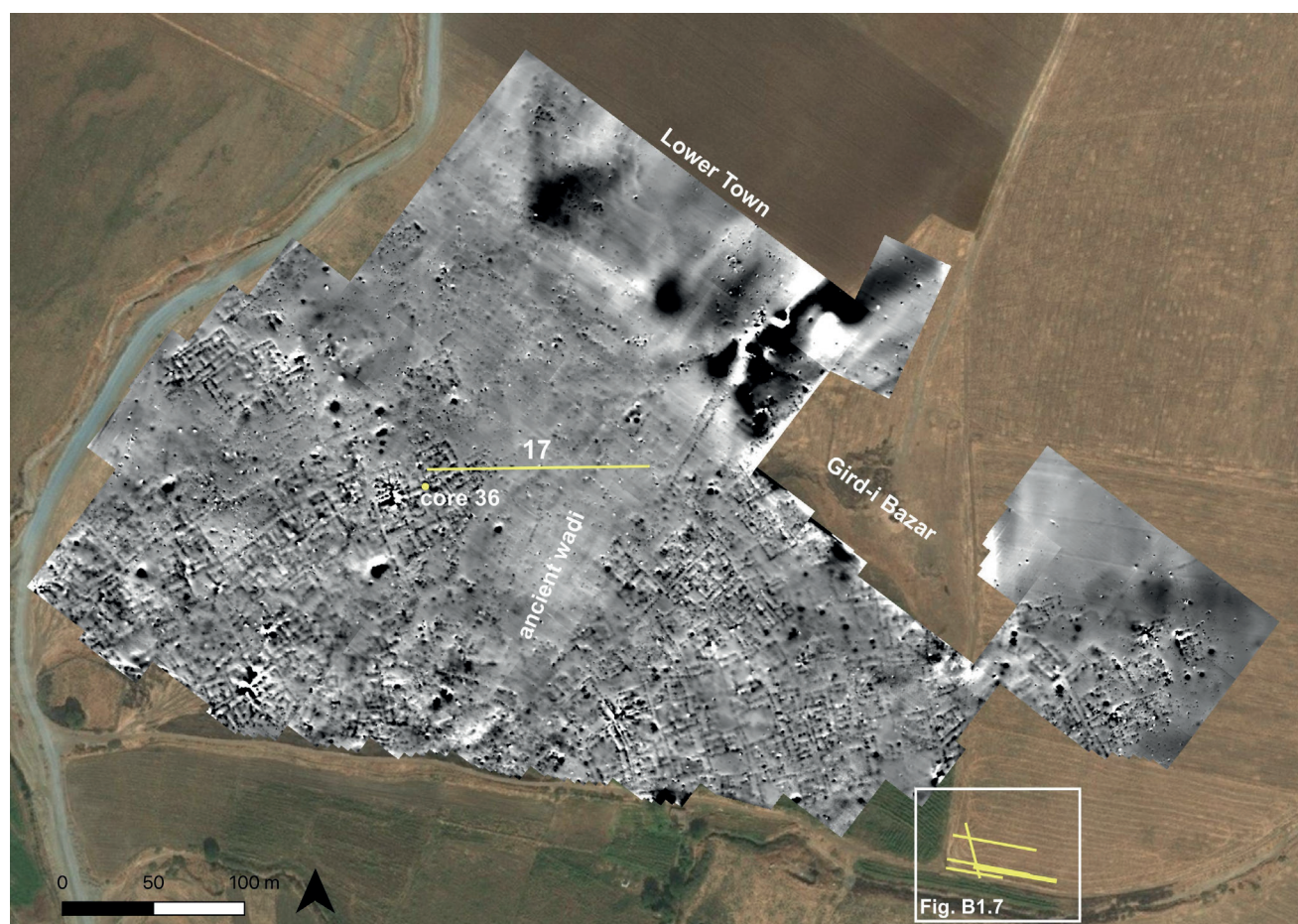


Fig. B1.6: Bing satellite image overlaid by the magnetogram of the Lower Town of the Dinka Settlement Complex showing with yellow lines the locations of the ERT profiles and with a yellow dot the location of Core C36. Note the ancient wadi crossing the settlement. Prepared by Andrea Squitieri.

Due to their elongated shape, it is not clear whether they can be interpreted as buildings. The large anomaly in blue located in the middle of the profile represents a geological formation, perhaps the remains of an alluvium accumulation. Profile 2 (**Fig. B1.9**) yielded the same results as Profile 1. **Fig. B1.10** illustrates the results from Profile 3, which was slightly shifted to the west in comparison to Profiles 1 and 2. It shows the same anomalies visible in the previous profiles, but shifted to the right side of the profile, with the blue alluvium accumulation below them. Profile 4 (**Fig. B1.11**) was oriented in the same direction as Profiles 1-3 but was located c. 15 m north of them. It revealed only geological formations and no anomalies indicating artificial structures. This means that, in this profile, we could not detect any continuation of the features we saw in Profiles 1-3.

To the south of Profile 1, we measured Profile 18, whose results are shown in **Fig. B1.12**. This was a west-east profile, 30 m in length, measured with a dipole-dipole configuration and 0.5 m electrode separation. Three features

were detected; two are indicated with black circles and one with a rectangle. The black circle to the right indicates an anomaly whose width is around 2-2.5 m; the black circle to the left represents an anomaly with a width of approximately 3.5-4 m. The black rectangle designates an elongated anomaly. The depth of all three is around 1.5 m, and the deepest (the middle one) extends down to around 3.5 m. The exact size of these anomalies cannot be estimated, as we need more information about the direction of the ERT profile with respect to them. As with Profiles 1-3, we suggest that these anomalies are not geological formations; the anomalies in the black circles may be artificial structures filled with stones, which may be collapsed palaeochannels but it is not clear. The anomaly in the black rectangle is possibly an accumulation of coarse gravels. As before, it is not clear if the latter can be interpreted as remains of buildings.

The last profile measured in this area was Profile 19, shown in **Fig. B1.13**. This profile was aligned to intersect the previous profiles. It was a northwest-southeast profile



Fig. B1.7: Close-up image showing the location of the ERT Profiles 1-4, 18, and 19 to the south-east of the Lower Town. Prepared by Andrea Squitieri.

with 0.5 electrode spacing, a dipole-dipole configuration, and a total length of 30 m. The black circles show the positions of the artificial features, which are connected to one another and are located at a depth of 1-3 m. They also showed up in Profiles 1 to 3. The black rectangles below them reveal anomalies that, based on their resistivity values, may contain water inside. These anomalies are also interconnected and they are between 3 to 5 m deep. In conclusion, the evidence from Profiles 1-3, 18, and 19 shows the existence of artificial structures that may be interpreted as collapsed structures filled with stones; however, it is not clear whether this can be connected to underground tunnels or palaeochannels. Additional artificial structures, with elongated shapes and made of gravel, were detected, which may belong to floors or pavements.

B1.2 Investigating the Dinka Settlement Complex

The second goal of the 2019 ERT survey was to further investigate the archaeological features of the Dinka Settlement Complex, which can be seen in the magnetograms produced by the surveys conducted by Jörg Fassbinder and his team in 2015-2017²³.

B1.2.1 ERT surveying in the Lower Town

In the Lower Town, a 120 m long profile, called Profile 17, was measured (**Fig. B1.6**). To measure this profile, we used the “roll along” technique suitable for covering a long profile. The electrode spacing was 0.5 m, and the profile used the dipole-dipole configuration. It was oriented from

²³ Fassbinder/Ašandulesei 2016; Fassbinder/Ašandulesei/Scheiblecker 2017; 2018; Scheiblecker/Fassbinder 2019.

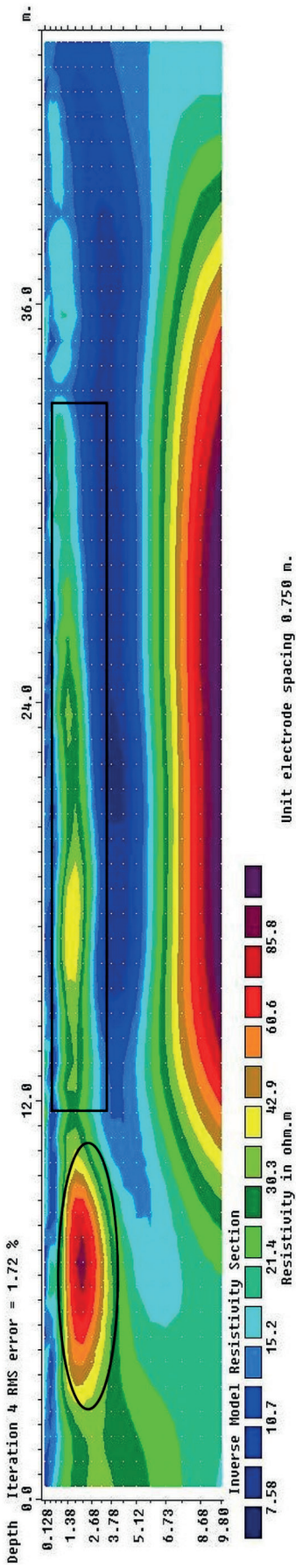


Fig. B1.8: ERT Profile 1. Direction: west-east. The black circle shows the presence of an artificial anomaly; while the black rectangle shows possible accumulations of coarse gravel, perhaps coming from a pavement or a floor. The feature showing in blue is a geological formation. Prepared by Mandana Parsi.

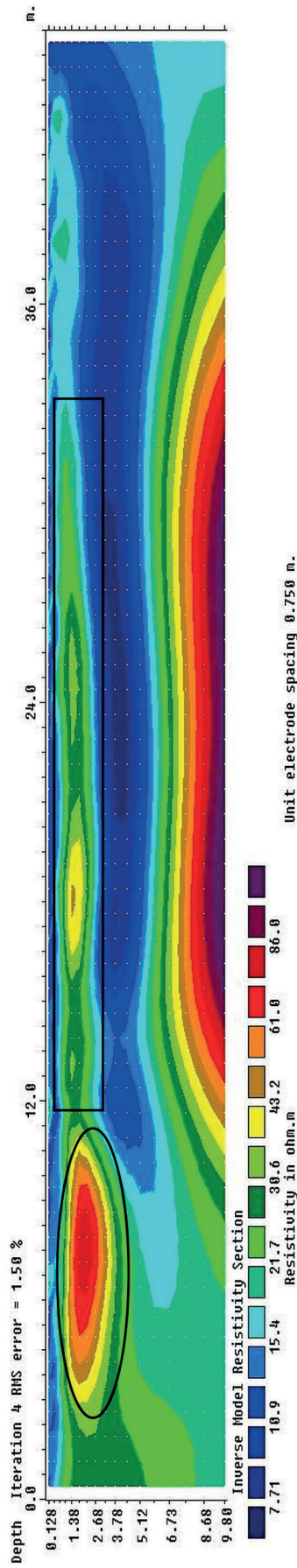


Fig. B1.9: ERT Profile 2. Direction: west-east. This profile shows the same results as Profile 1. Prepared by Mandana Parsi.

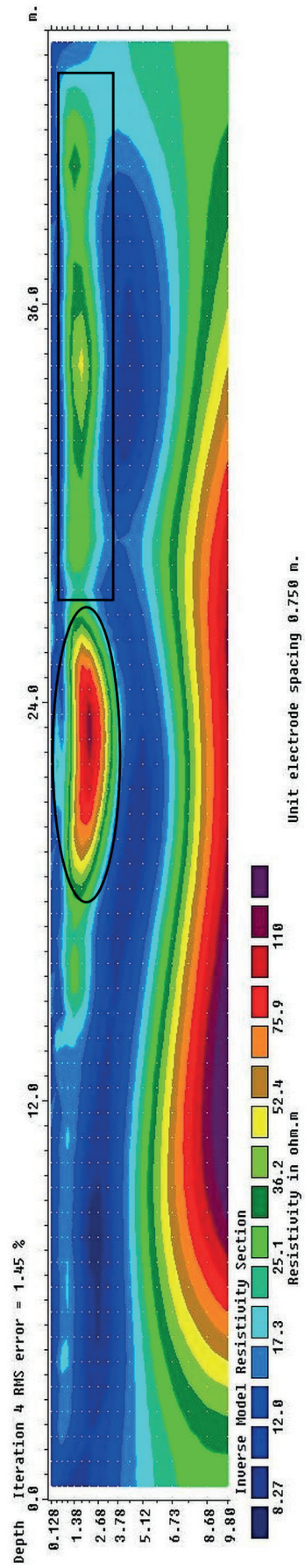


Fig. B1.10: ERT Profile 3. Direction: west-east. This profile shows the same results as Profiles 1 and 2. Prepared by Mandana Parsi.

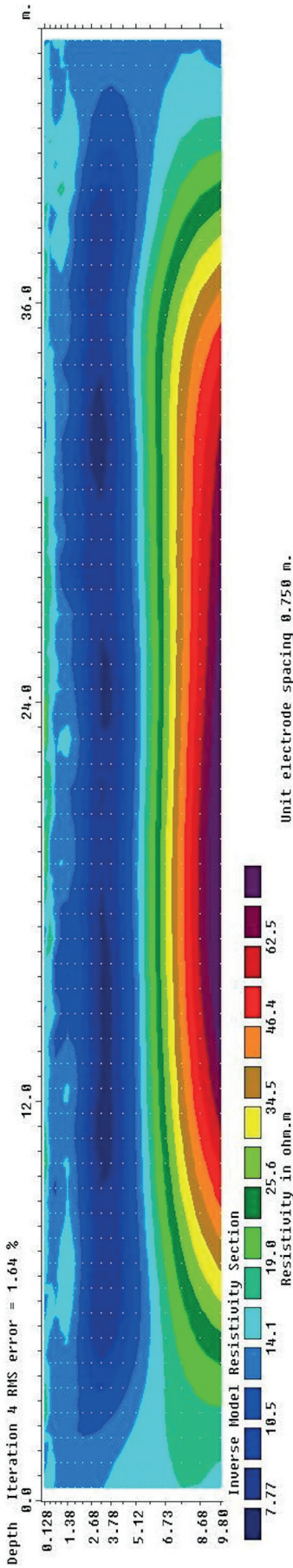


Fig. B1.11: ERT Profile 4. Direction: west-east. This profile shows only geological features. Prepared by Mandana Parsi.

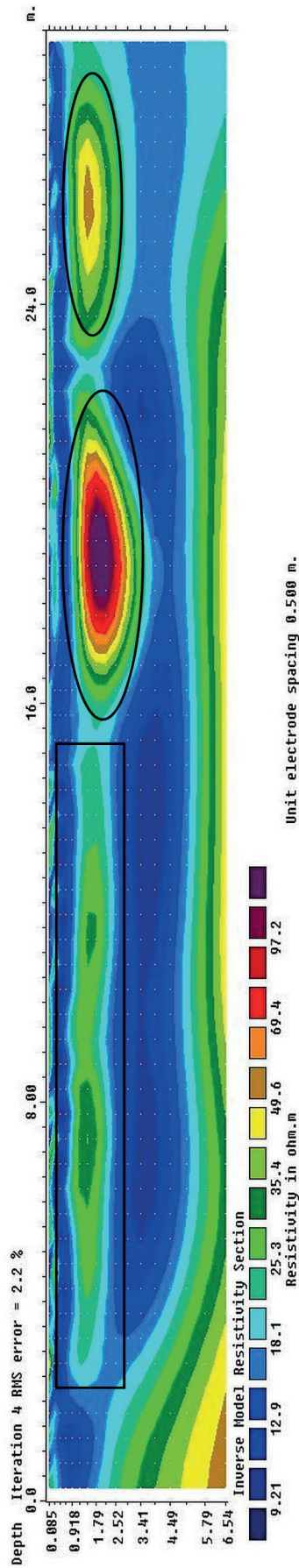


Fig. B1.12: ERT Profile 18. Direction: west-east. Black circles showing the presence and positions of artificial anomalies. The anomaly shown in the rectangle can be a pavement or floor. Prepared by Mandana Parsi.

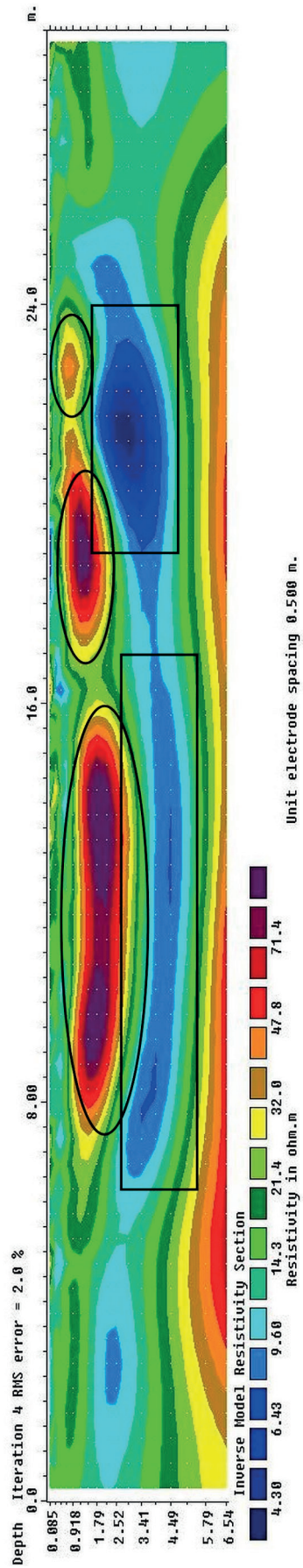


Fig. B1.13: ERT Profile 19. Direction: northwest-southeast. The black circles show the positions of three artificial anomalies while the black squares show features saturated with water. As in previous profiles the anomalies in the circle can be interpreted as a wall. Prepared by Mandana Parsi.

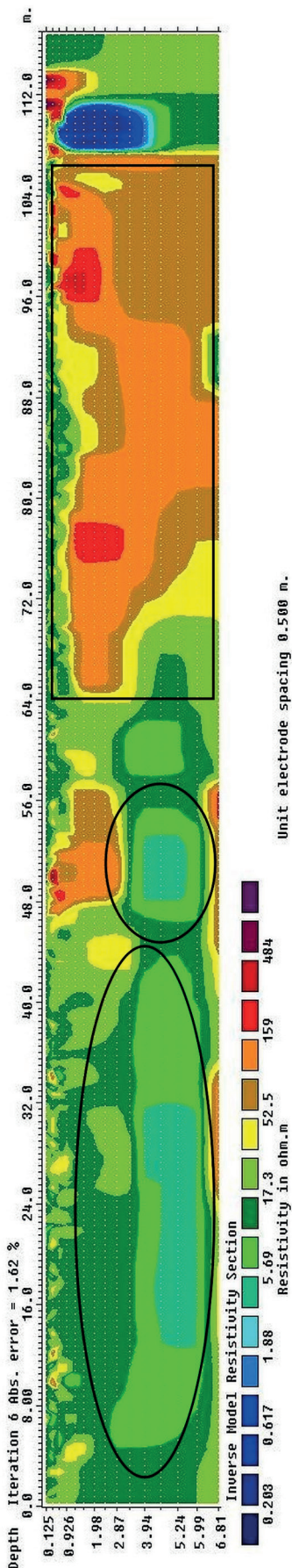


Fig. B1.14: ERT Profile 17. Direction: west-east. On the right, the black rectangle shows the bed of the ancient wadi once crossing the Lower Town; on the left, the two black circles show a possible mudbrick building located below the Iron Age structures which appear as smaller anomalies on the top left. Prepared by Mandana Parsi.

west to east. The results are shown in **Fig. B1.14**. On the right of this figure, the black rectangle shows evidence for the existence of an ancient wadi bed, which is no longer visible on the surface. The existence of this wadi, which in antiquity divided the Lower Town in a roughly north-south direction (**Fig. B1.6**), had originally been suggested by the 2016 magnetometer survey²⁴ and was later confirmed by a hydrological analysis (“Channel Network”) conducted with QGIS-SAGA²⁵. The final proof for its existence came from the 2018 excavation of three geo-archaeological trenches (named GA43, GA44 and GA45) that revealed the fluvial accumulation from the ancient wadi²⁶. The ERT results from Profile 17 represent additional evidence for the existence of this wadi and provide additional information about the depth of its bed, which reached about 7 m.

In the left area of Profile 17, a different situation can be observed. This is where the profile crosses some structures that were visible in the magnetogram. Here the profile shows regular artificial features that appear at a depth of about 3 m, highlighted in black circles in **Fig. B1.14**. In the figure, the black circle on the left shows a linear anomaly that probably runs parallel to the profile. The black circle to the right shows another regular feature that seems to be perpendicular to the profile. The features are approximately 2.5 m high, but their exact width is not clear because we would have to know their exact alignment in relation to the profile to calculate it more precisely. These regular anomalies, which are shown in the black circles of **Fig. B1.14**, do not correspond to the features visible in the magnetogram. This is because the magnetometer prospection was adapted for the purpose of tracing archaeological features no deeper than 2-3 m beneath the ground. Physical laws cause structures from deeper parts of the soil to become blurred and indistinct; moreover, the magnetic intensity is diminished by the factor $1/r^3$ (r = distance from object to magnetometer). On the other hand, the ERT allowed us to reach greater depths. Therefore, the magnetogram shows the archaeological features of the Iron Age period belonging to the Dinka Settlement Complex²⁷, which do not reach depths greater than 2-3 m, while the regular features highlighted in Profile 17 represent older structures located below the Iron Age ones. Based on their regularity and resistivity value, we interpret them to be the remains of mudbrick buildings.

Currently, we have no direct evidence for dating the structures that the ERT profile has revealed, as no excavation has yet been conducted; however, a hint at its dating is provided by a charcoal sample from Core 36 (C36), taken about 10 m south of the western extremity of Profile 17 (**Fig. B1.6**). This core, described in detail below (**Table B2.1**), reached a depth of about 3 m and yielded, among other things, a charcoal sample that was radiocarbon dated to 3329–2939 calBC (95.4 % probability, see **Fig. B1.15**). The charcoal was found at a depth of about 55 cm below the surface, but it could well have travelled there from a much deeper level. Its radiocarbon dating indicates that it must have originated in a structure older than the Iron Age phase. We suggest that the deep mudbrick structure highlighted in Profile 17 may date to the same older phase as the charcoal from Core 36 (C36). Further inves-

24 Fassbinder/Ašandulesei/Scheiblecker 2017, 27–28.

25 Radner/Kreppner/Squitieri 2017a, 178 Fig. H2.

26 Radner 2019c, 16 Fig. A3.

27 Fassbinder/Ašandulesei/Scheiblecker 2017, 27–28.

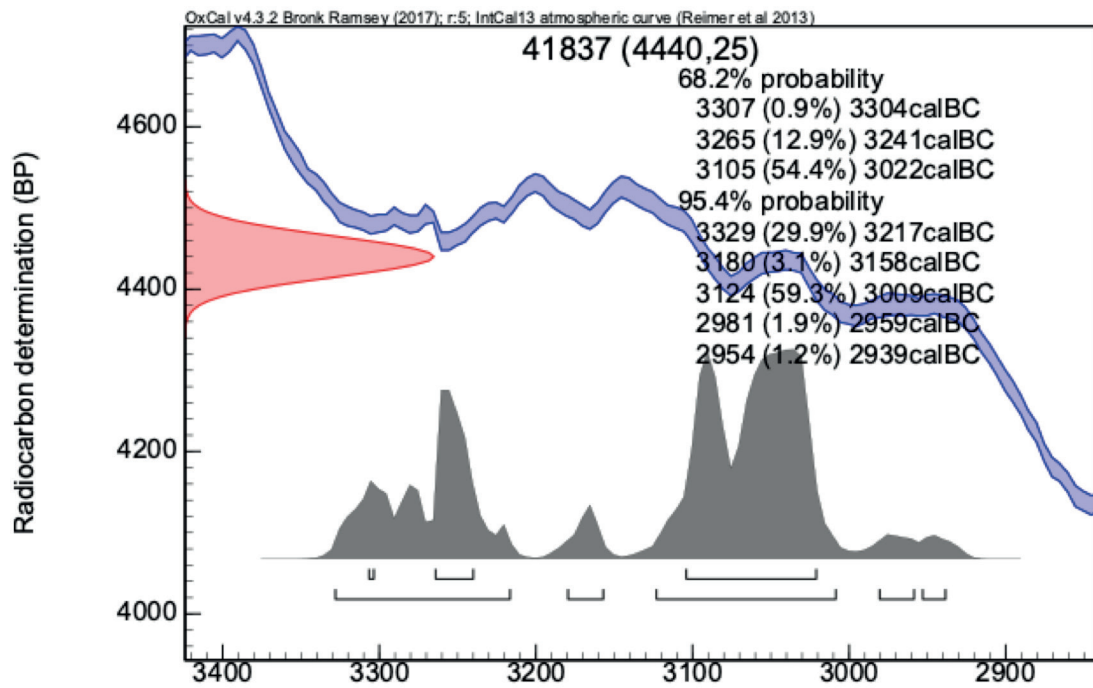


Fig. B1.15: Calibrated radiocarbon dates from the charcoal sample collected at a depth of 55 cm from Core C36, taken in the Lower Town of the Dinka Settlement Complex. Calibration software OxCal v. 4.3.2.

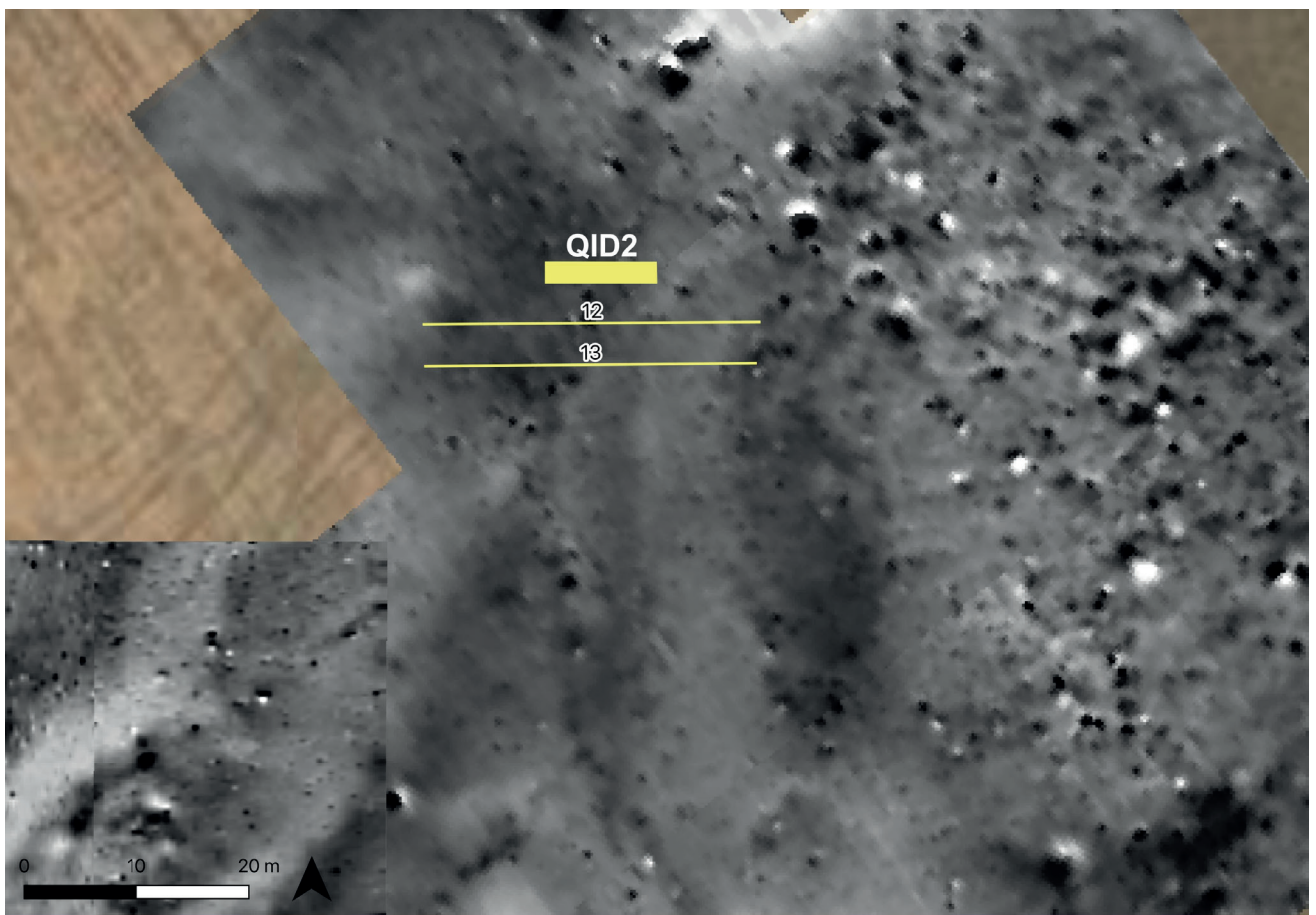


Fig. B1.16: The 2015 magnetogram of the western slope of Qalat-i-Dinka (see Fassbinder/Ašandulesei 2016), overlaid by trench QID2 excavated in 2018 (yellow rectangle) and the two ERT profiles measured in 2019 (yellow lines). Prepared by Andrea Squitieri.

tigations by means of ERT and coring are necessary to further explore this earlier phase of the Dinka Settlement Complex. It should be noted that the existence of archaeological phases considerably older than the Iron Age is also supported by the results of the pottery survey conducted in 2013 by J. Giraud, which identified Late Chalcolithic and Early Bronze Age pottery across the Dinka Settlement Complex²⁸. Also the discovery of a Chalcolithic kiln in the operation DLT₃ (**Chapter I**) supports this.

B1.2.2 ERT surveying on Qalat-i Dinka

Profiles 12 and 13 were measured on the western slope of Qalat-i Dinka, south of the trench QID₂, which was excavated in 2018 (**Figs. B1.2, B1.16**). In this trench, a large stone feature, measuring about 2×7 m and characterised by a 30 % slope, was unearthed and interpreted as a glacis, that is, a sloping structure with defensive purposes²⁹. The aim of Profiles 12 and 13 was to verify whether the glacis continued south of trench QID₂. The two profiles (**Figs. B1.17, B1.18**) were measured from east to west. They were placed parallel to each other at a distance of 1 m, with 0.5 m electrode spacing. Here we present the ERT results of the dipole-dipole configuration.

The total length of each profile was 30 m. At the middle of both profiles (shown by a black circle in each figure), we can see a feature with a width of around 2 m, whose characteristics match those of the glacis excavated in QID₂. In **Fig. B1.17**, the black rectangle to the left, that is, on the east side of the glacis, shows the position of a wall at a depth of around 1 m. We cannot calculate the exact width of the wall, as we need more information about its direction and the angle of the profiles. However, this result shows that a wall may be preserved next to the glacis structure, though this does not show up in Profile 13 (**Fig. B1.18**).

To conclude, Profiles 12-13 support the identification of the structure excavated in QID₂ as a glacis and demonstrate that it continues towards the south for approximately 6.5 m; they also support the suggestion that a wall or palisade was constructed next to the glacis³⁰.

B1.3 Conclusions

The ERT measurement survey carried out in spring 2019 had two aims: first, to investigate the *qanats* of the Bora Plain, and second, to obtain additional information about the archaeological features of the Dinka Settlement Complex.

As to the first objective, we presented in **§B1.1.1** the results from the ERT profiles measured in the southeastern part of the Bora Plain, where the openings of *qanat* shafts are still visible on the ground and one *qanat* tunnel is still used today to supply water to a modern fish farm. The results obtained from Profile 8 revealed the possible presence of closed shafts, at a depth of around 1.7 m. In section **§B1.1.2**, we discussed the results of the ERT profiles measured close to the Lower Town of the Dinka Settlement Complex, where artificial anomalies that may represent remains of archaeological structures were detected, although it is not clear if they belonged to buildings. We suggest that these anomalies represent artificial structures standing next to some elongated features, which could be the accumulation of coarse gravel and can be interpreted as pavement or floor.

In regard to the second objective, we discussed the results of Profile 17 in section **§B1.2.1**. This profile crosses the magnetogram of the Lower Town, supplying additional evidence for the existence of an ancient wadi that once crossed the settlement in a roughly north-south direction. This profile also revealed that below the Iron Age structures of the Lower Town there are older structures, perhaps belonging to the Chalcolithic/Early Bronze Age periods. These will be further investigated in fieldwork scheduled for spring 2021, for which funding from the Gerda Henkel Foundation has already been procured (grant AZ 42/V/20). Finally, we discussed the results from two ERT profiles measured on the western slope of Qalat-i Dinka in **§B1.2.2**. Here, a structure was identified that we interpret as the continuation of the glacis structure unearthed during the 2018 excavations in trench QID₂. The results proved that the structure continues south of QID₂ for at least 6.5 m, and showed the existence of a wall or palisade next to it.

²⁸ Giraud 2016, 33 Fig. B3.4.

²⁹ Hashemi 2019.

³⁰ Radner/Kreppner 2019, 157.

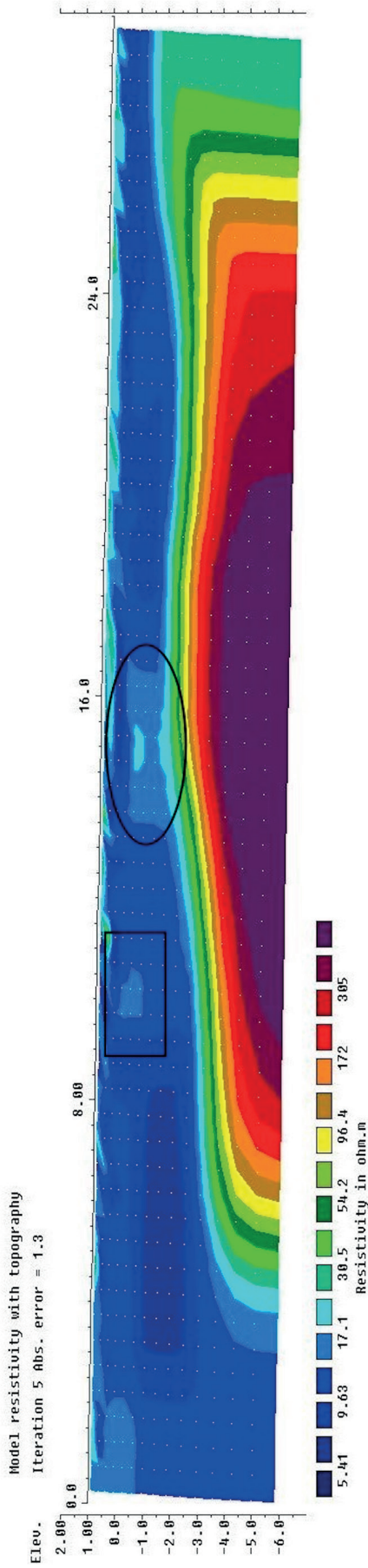


Fig. B1.17: Profile 12, measured in east-west direction with dipole-dipole configuration and 0.5 m spacing. The black circle shows a feature that matches the glacial structure excavated in trench QID2. The black rectangle shows a wall. Prepared by Mandana Parsi.

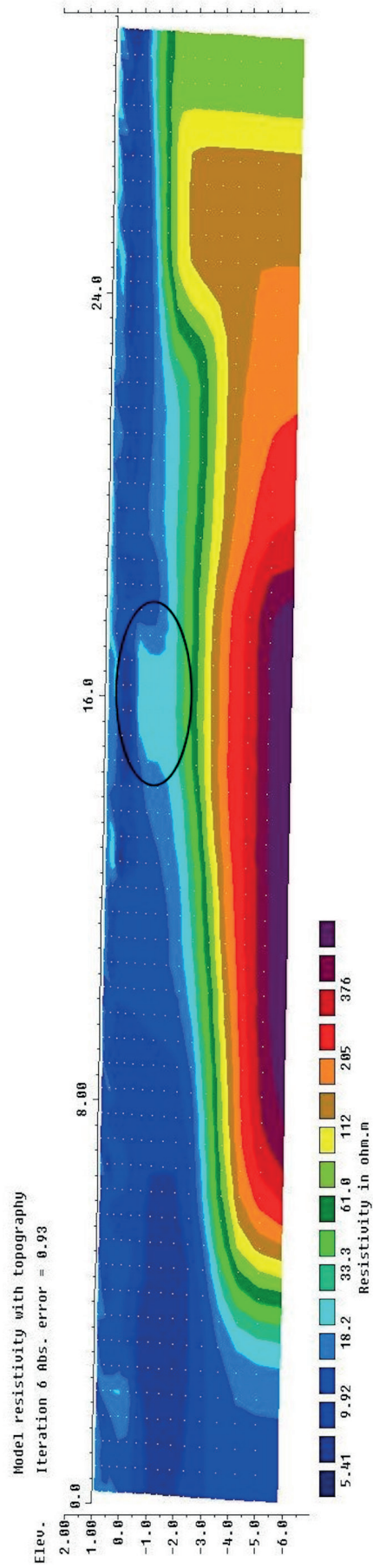


Fig. B1.18: Profile 13, measured in east-west direction, yielding similar results as in Profile 12. Prepared by Mandana Parsi.

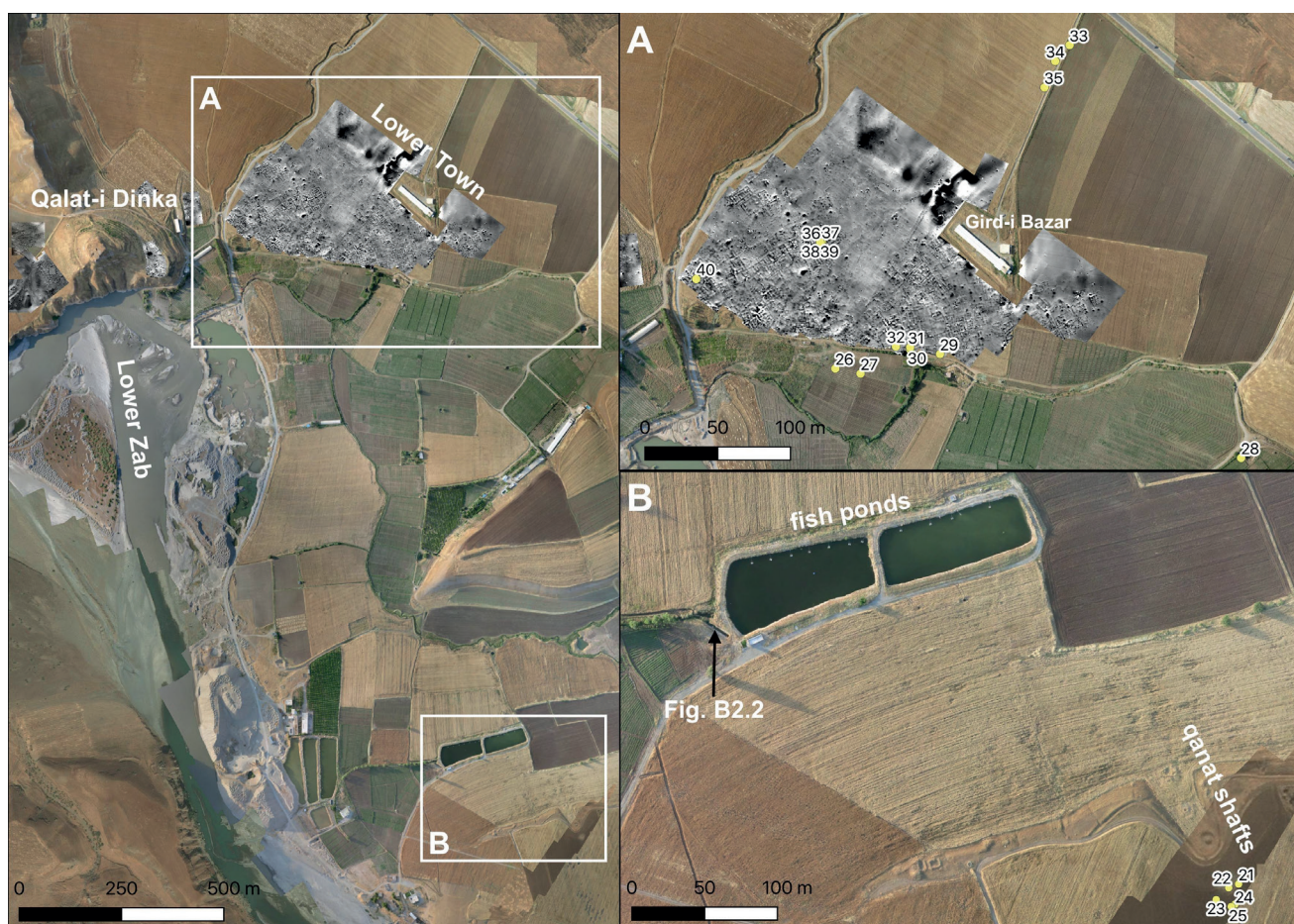


Fig. B2.1: Core locations (marked with yellow dots) of the 2019 spring season. On the left: general map of the Bora Plain, with insets A and B. (A): the Lower Town of the Dinka Settlement Complex with the locations of the cores described in this chapter; (B): the area with the *qanat* system and fish ponds, also shown in Fig. B1.4. Background drone image by ICONEM (courtesy of Jessica Giraud). Magnetograms by Jörg Fassbinder and his team (see Fassbinder/Ašandulesei/Scheiblecker 2018). Prepared by Andrea Squitieri.

B2. Soils and sediments in the Dinka Settlement Complex and the surrounding Bora Plain: sampling and new data from 2019

Eileen Eckmeier³¹

The systematic study of soils and sediments in the Bora Plain, both within and outside the remains of the Dinka Settlement Complex, was begun in 2017³². In 2019, the area under investigation was extended significantly, and new cores were taken to gain a more detailed picture of the sedimentological situation and to identify the alluvial terraces and their evolution (see the map in Fig. B2.1). In addition, coring was used in order to test whether the

sediment material can confirm the presence of ancient *qanats* and ancient streets in the locations suggested by archaeological evidence; an assessment of this evidence is presented below. Cores were also taken to add information to the geophysical ERT measurements (as discussed in §B1.1).

The total number of cores taken in the Bora Plain between 2017 and 2019 has reached 60. Some of these were directly sampled and described in the field, and others were taken in the form of closed cores that can be opened in the laboratory for further analysis. Analyses of the samples from cores C10-20, taken in 2018, is ongoing; the topsoil samples have already been analysed, and their results were published previously³³.

³¹ Geography Department, LMU Munich.

³² Eckmeier/Tolbas/Weidenhiller 2018; Altaweel/Eckmeier 2019.

³³ Eckmeier/Tolbas/Weidenhiller 2018.

During the sampling campaign in April 2019, cores C21-40 were collected. The samples were taken from selected cores in the field and sedimentological analysis was completed in 2020. The descriptions of these cores are presented in **Table B2.1**.

Core	Depth <i>cm</i>	Description	L*	a*	b*	CaCO ₃ %	Clay %	Silt %	Sand %
C21	0-19	fine earth, dark brown (data: 10 cm)	46.0	4.8	16.2	14.6	44	44	12
	19-35	degraded stone and fine earth							
	35-38	stone							
	38-80	fine earth							
	80-100	gravel and fine earth							
	100-110	gravel, stone, fine earth in between							
	> 110	stones							
C22	0-53	gravel and clay, quantity of gravel or stone increases towards bottom							
	53-100	—							
	100-130	gravel, clay lens, stone							
	> 130	stones							
C23	0-35	Fine earth, dark reddish brown							
	35-50	stones							
	> 50	stones							
C24	0-70	fine earth, dark brown, little coarse sand or gravel (data: 10 cm)	47.4	5.5	17.5	5.4	39	58	3
	70-100	—							
	100-123	mixture of clay and gravel							
	123-138	disintegrated stone/gravel, less clay							
	138-155	stones							
	155-159	layer of disintegrated stone/gravel and clay							
	159-180	stones							
C25	0-68	fine earth, dark reddish brown							
	68-100	missing (compacted)							
	100-115	clay, dark brown							
	115-140	clay, few gravel or stones							
	140-100	stone, gravel, partly disintegrated							
C26	0-90	fine earth, brown, scant gravel, very homogeneous (no artefacts in core) (data: 10 cm)	50.3	3.0	17.3	10.0	25	51	23
	100-200	fine earth, brown, charcoal particles, very homogeneous, high moisture content (data: 110 cm)	53.5	3.5	19.6	8.0	38	60	2
	200-300	fine earth, 200-240 charcoal particles, very homogeneous, high moisture content (data: 290 cm)	52.8	2.6	16.9	9.8	33	64	2

Table B2.1: Description of the sampled cores and laboratory data of fine earth samples. Abbreviations used: L* = lightness, a* = redness, b* = yellowness; CaCO₃ = Calcium Carbonate. If a cell is empty no data is available. Prepared by Eileen Eckmeier.

Core	Depth <i>cm</i>	Description	L*	a*	b*	CaCO ₃ %	Clay %	Silt %	Sand %
C27	0-100	a little gravel and stone, lighter towards the bottom, charcoal (no artefacts in core)							
	10		51.4	3.3	17.5	11.1	33	52	15
	22		53.4	3.0	18.0	8.7	39	59	1
	100-200	fine earth, charcoal particles, some red spots (burned clay?), very homogeneous, high moisture content							
C28	0-70	fine earth, gravel, homogeneous (no artefacts in core) (data: 10 cm)	48.9	3.2	18.1	9.9	21	46	34
	100-132	fine earth, gravel							
	132-136	charcoal, small particles							
	136-190	fine earth, no gravel (data: 180 cm)	52.5	3.2	18.8	13.1	27	59	14
	200-257	fine earth, few coarse sand and gravel, scant charcoal (data: 230 cm)	52.1	3.4	19.0	12.6	22	45	33
	257-300	fine earth, scant coarse sand and gravel, more charcoal particles (large piece at 70 cm)							
	300-390	fine earth, brown, homogeneous, scant charcoal, more silt towards bottom, little gravel (data: 320 cm)	53.7	3.3	19.2	15.6	24	49	27
	400-490	fine earth, brown, homogeneous, scant charcoal, little gravel but more at the bottom (data: 410 cm)	53.1	3.3	19.5	14.9	18	45	37
C29	0-26	fine earth, brown, gravel							
	26-48	fine earth, burnt clay/pottery, charcoal							
	48-49	pottery layer, charcoal, road?							
	49-51	pottery pieces, gravel, road?							
	51-85	fine earth, no obvious artefacts							
	100-188	fine earth, small gravel, stone (177 cm)							
	188-198	stones, gravel, partly disintegrated							
	198-200	compacted clay with traces of burnt clay and charcoal							
C30	0-80	fine earth, small particles of burnt clay, very few pieces of gravel, very small piece of pottery at the bottom of the core							
	> 80	stones							
C31	0-100	fine earth, brown, becomes lighter towards bottom, gravel, pottery (32 cm), orange spots, no visible charcoal (data: 20 cm)	50.1	4.5	19.9	0.5	30	49	20
	100-156	fine earth, light brown, gravel, very small pieces of pottery, charcoal							
	156-175	layer of gravel and stone, road?							
	175-200	fine earth, scant coarse sand and gravel (data: 180 cm)	54.5	4.3	20.8	7.6	35	58	8
C32	0-50	fine earth, coarse sand, gravel, pieces of pottery (data: 10 cm)	48.0	5.0	19.8	0.6	28	54	18

Table B2.1 (continued): Description of the sampled cores and laboratory data of fine earth samples. Abbreviations used: L* = lightness, a* = redness, b* = yellowness; CaCO₃ = Calcium Carbonate. If a cell is empty no data is available. Prepared by Eileen Eckmeier.

Core	Depth cm	Description	L*	a*	b*	CaCO ₃ %	Clay %	Silt %	Sand %
	50-68	layer gravel, stone (65 cm), grayish, road?							
	100-115	gravel, greyish							
	115-200	fine earth, light brown, little gravel, up to 50 cm							
C33	0-30	fine earth, dark brown, little coarse sand (data: 10)	46.8	4.9	19.3	0.6	29	51	20
	30-37	more gravel							
	37-80	stones, gravel, coarse sand							
C34	0-24	fine earth, brown							
	24-45	layer of gravel, stone partly disintegrated							
	45-94	fine earth, scant gravel							
	94-100	stone							
	100-110	fine earth, gravel							
	110-130	fine earth, small gravel							
	130-140	coarse gravel							
	140-195	gravel, stone							
C35	0-100	fine earth, little gravel, very homogeneous; only alluvial material!							
	10	—	49.3	4.7	19.8	0.6	31	50	20
	80	—	51.3	4.5	20.3	0.6	29	53	18
	100-200	fine earth, more reddish, less gravel, homogeneous							
	110	—	50.9	5.8	19.6	4.7	45	37	18
	180	—	57.3	5.7	19.7	27.8	41	44	16
	200-300	fine earth, reddish, very dense, scant gravel							
	210	—	55.3	6.3	19.8	15.6	51	40	9
	280	—	53.0	6.5	19.1	11.0	53	41	6
		—							
C36	0-30	fine earth, dark brown, charcoal, burned clay (data: 10)	48.9	4.7	17.6	1.1	29	47	24
	30-50	gravel, more sand, burned clay, lighter (data: 40)	51.4	4.6	18.2	9.9	30	50	20
	50-70	fine earth, charcoal (dated: see Fig. B1.15)	52.3	4.1	19.0	6.3	29	51	20
	70-80	gravel, sand; road?							
	80-100	fine earth, lighter brown							
	100-200	fine earth, coarse sand, no artefacts, white lines (pseudomyceles)							
	110	—	54.0	4.2	19.6	9.0	39	51	10
	180	—	56.1	4.0	19.8	12.4	35	54	12
C37	0-36	fine earth, brown, charcoal							
	36-40	gravel, fine earth							
	40-54	fine earth							
	54-48	burned clay							
	58-68	fine earth							

Table B2.1 (continued): Description of the sampled cores and laboratory data of fine earth samples. Abbreviations used: L* = lightness, a* = redness, b* = yellowness; CaCO₃ = Calcium Carbonate. If a cell is empty no data is available. Prepared by Eileen Eckmeier.

Core	Depth cm	Description	L*	a*	b*	CaCO ₃ %	Clay %	Silt %	Sand %
	68-100	gravel, stones in fine earth; road at 70-80 cm?							
C38	0-20	fine earth, brown							
	20-75	mixture of clay, burnt clay, gravel, charcoal (data: 70 cm)	52.7	3.9	17.9	9.1	35	48	18
	75-80	loose, dark red material; road? (data: 77 cm)	44.2	3.3	13.2	2.7			
	80-100	stone, gravel, smaller particle sizes towards bottom							
C39	0-15	fine earth, brown							
	15-60	fine earth, gravel, burnt clay, charcoal							
	60-75	fine earth, lighter brown, no visible artefacts, less gravel (data: 65 cm)	52.9	4.0	19.0	9.2	29	51	20
	75-86	stone, gravel; road? (data: 80 cm)	53.9	3.4	18.6	6.5	24	36	40
	86-100	fine earth, lighter brown, gravel, no visible artefacts							
C40	0-85	fine earth, brown, coarse sand, little gravel at lower depths, no visible artefacts, stone at 22 cm.							
	85-95	fine earth, darker brown							
	95-100	small piece of pottery, traces of calcite							
	100-165	fine earth, brown, little gravel, coarse sand, a little burnt clay							
	165-175	layer of gravel in fine earth							
	175-200	fine earth, more red, very compact, no gravel, no visible artefacts							

Table B2.1 (continued): Description of the sampled cores and laboratory data of fine earth samples. Abbreviations used: L* = lightness, a* = redness, b* = yellowness; CaCO₃ = Calcium Carbonate. If a cell is empty no data is available. Prepared by Eileen Eckmeier.

B2.1 Testing ancient *qanat* locations

Cores C21-25 were taken where satellite maps and ground-truthing showed the presence of ancient *qanat* systems, and where local farmers are still maintaining *qanats* to feed fish ponds with fresh water³⁴ (**Fig. B2.1B**). The area investigated is located directly at the edge of a small terrace, and the fish ponds sit on the lower level. **Figs. B1.4** and **B2.1B** clearly show a line of *qanat* shafts leading from the edge of the terrace in the direction of the fish ponds. Also, ERT measurements were used to find evidence for their presence (see **§B1.1**). All of the cores reached a stone layer which was too dense to continue the coring; this layer was reached at a variety of depths (110, 130, 50, 180 cm). The material above was a mixture of gravel and fine earth (clay and silt, with little sand). It remains unknown whether this dense stone layer is the top of a manufac-

tured subterranean *qanat* channel or a natural formation; the variations in depth are related to the relative depth from the surface level. Considering its geomorphological position, the stone layer could indicate the natural presence of rocky parent material, which has not eroded, and therefore remains close to the surface. The sediment above the stone layer is layered, and most likely not the result of the anthropogenic deposition of earth material; none of the cores contained archaeological artefacts or any other anthropogenic material. However, an opening to the active *qanat* close to the coring locations revealed uniformly deposited gravel extending from above the channel to the surface, and no fine earth layers or topsoil (**Fig. B2.2**). The surface in the area was most likely also disturbed by the construction of the fish pond.



Fig. B2.2: Sedimented gravel (shown in the lower part) located at the opening of an active *qanat* near the fish pond. See Fig. B2.1 for the location of the area shown in this photo. Photo by Eileen Eckmeier.



Fig. B2.3: Zana Mahmud (left) and Mark Altaweel (right), while taking Core C26 in the Lower Terrace. Photo by Eileen Eckmeier.

B2.2 Adding data for the understanding of the Lower and Upper Terrace

Additional data was collected from the Lower Terrace (**Fig. B2.3**). **Fig. B2.1A** shows the locations of the cores taken in this area. Cores C26 and C27 were positioned close to the previously investigated areas, while C28 was located further to the east. Cores C33-35 were taken north of the chicken farm in Gird-i Bazar, on the Upper Terrace. C26 and 27 were sampled near the boundary between the Lower and the Upper Terraces, marked by a steep gradient with an increase in height of about 2 m. The aim was to find evidence for our hypothesis that the settlement had been eroded by the river. The sediments of C26 and C27 were clearly different from the other cores, as they neither contained any coarser material nor any settlement material, to a depth of 300 cm, with the exception of a few charcoal particles. The fine earth is dominated by

silt (>50 %) and then clay. Sand is prominent only in the topsoil material. This sediment was most likely transported by the river and deposited under slow flowing water conditions, while the sand might have been introduced by more recent irrigation activities. C26 yielded a piece of charcoal at a depth of about 35 cm. This was radiocarbon dated to 592-655 calAD, that is to the late Sasanian/Early Islamic period (**Fig. B2.4**). This date fits with the results of the pottery survey conducted by Jessica Giraud's team, as Core 26 was taken very close to where they had identified a concentration of Sasanian/Early Islamic ceramics³⁵. It is possible that traces of the settlement were removed by erosion, but it is even more likely that the settlement never reached this area because the complete eradication of the larger stone material used for building foundations would require strong erosional forces.

C28, taken about 200 m east of the chicken farm in Gird-i Bazar, is primarily characterised by fine earth sediments, but with a larger proportion of sand throughout the core, to a depth of 500 cm. It contains a few charcoal particles that may have been transported with the sediment. The processes at work here were different than the ones at C26 and C27. The sediments are not well sorted which speaks against an alluvial sediment. It was taken next to a water hole which is currently used as a well, so anthropogenic disturbances are possible. Cores C33-35 are located very close to each other, but their sediments are totally different. None of the cores contained any artefacts or charcoal. Core C33 is composed of fine earth topsoil over a thick layer of gravel and stones. The sediments of C34 are more variable, and layers with higher quantities of fine earth material alternate with more stone-rich layers. Finally, C35 was composed of mainly very heterogeneous, fine earth material to a depth of 300 cm, but showed an increase in both clay (from 31 % at the top to 53 % at the bottom) and carbonate contents towards the lower parts of the profile. This may also be colluvial or alluvial material that was deposited in a sediment trap, e.g. in a former channel. However, it is very likely that this area was outside of the Iron Age settlement's boundary.

B2.3 Testing the location of ancient roads

Cores C29-32 and C36-40 were taken where the geophysical data indicated the possible presence of ancient roads or alleyways that crossed the Lower Town of the Dinka Settlement Complex³⁶. The core's small diameter

³⁵ Giraud 2016, 33 Fig. B3.3a: pottery zone no. 18404.

³⁶ Fassbinder/Aşandulesei/Scheiblecker 2018, Fig. B4.

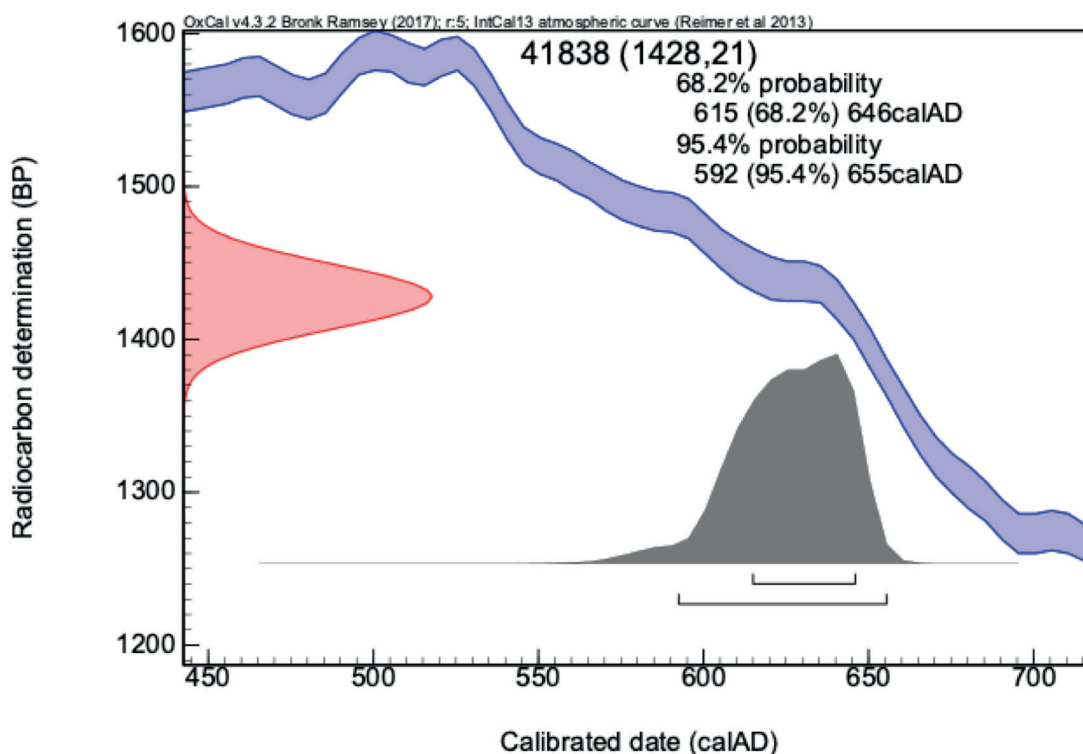


Fig. B2.4: Radiocarbon dating of a charcoal sample obtained from Core C26 on the Lower Terrace. Calibration software OxCal v. 4.3.2.

does not allow us to identify slight variations in such gravel- and stone-rich materials, but some possible traces could be identified. In C29 (Fig. B2.5), C31 and C32, pieces of pottery or charcoal were found above a depth of 50-60 cm, while below only fine earth or coarser material without visible traces of artefacts were found. In C36, C37 and C39, a similar situation occurred at a depth of 70-80 cm, but it is less clear. In C38, a clear boundary was found at a depth of 80 cm (Fig. B2.6), with loose reddish material sitting above a denser layer containing gravel or stone. This might indicate a street level; however, to clearly establish the presence of a road requires a larger-scale investigation of the stratigraphy. Finally, a charcoal sample from Core 36 (about 55 cm below the ground) was radiocarbon dated to 3329-2939 calBC (see Fig. B1.15), hinting at the existence of an even older phase below the Iron Age structures of the Dinka Settlement Complex, as discussed in §B1.2.1.



Fig. B2.5: Core C29. Photo by Eileen Eckmeier.



Fig. B2.6: Core C38. The white arrow shows the 80 cm depth level. Photo by Eileen Eckmeier.

C. Excavating the Upper Town of the Dinka Settlement Complex: the 2019 excavation campaign at Qalat-i Dinka

This chapter presents the results of the excavations, which took place between 29 August and 7 October 2019 in operation QID₁, located on the western slope of Qalat-i Dinka (Fig. C1). The work was funded by the Gerda Henkel Foundation through a project grant awarded to Andrea Squitieri and Jean-Jacques Herr (AZ 09/V/19), with additional financial support provided by the Alexander von Humboldt Foundation (Alexander von Humboldt Professorship 2015 for Karen Radner) and WWU Münster (starter funding for Janoscha F. Kreppner's appointment to the professorship of Near Eastern Archaeology).

C1. Previous work on Qalat-i Dinka and the methodology employed in 2019

Andrea Squitieri

Prompted by the chance discovery of the Neo-Assyrian tablet dated to 725 BC on the western slope of Qalat-i Dinka³⁷, a first magnetometer survey was undertaken on this side of the mount by Jörg Fassbinder and his team in 2015. The resulting magnetogram highlighted several magnetic anomalies that were interpreted as structures, some of which were interpreted to have a possible defensive function³⁸. Already in 2013, an archaeological surface survey had been conducted in this area by Jessica Giraud's team and had yielded a concentration of Iron Age pottery with the same characteristics as those unearthed at Gird-i Bazar, where the Peshdar Plain Project began excavations in 2015³⁹.

Prompted by this combination of data, the decision was made to open a test trench on the western slope of Qalat-i Dinka in the spring of 2016. The trench, extending about 40 m², was dubbed "100000" because, at that time, there was no dGPS available to the team for constructing a square grid system consistent with the one used in Gird-i

Bazar in 2015⁴⁰. Already this test trench yielded important results. First, the same style of pottery as found at Gird-i Bazar was identified on the floors, suggesting contemporaneous occupation; second, a portion of a large stone wall and sections of a paved floor were encountered, which suggested the existence of monumental constructions unparalleled by any of the buildings excavated in the Lower Town; third, a number of decorated ivory or bone objects were collected, along with pieces of jewellery, which were also without parallel among the items unearthed in the Lower Town. On the other hand, the 2016 excavations also brought to light evidence that heavy looting had occurred at the site in recent years: a plastic biscuit wrapper found in one of the looting pits bore a production date of 1999 and an expiry date of 2000, indicating that at least some of the looting activity happened around that time (with the year 1999 as a *post quem* date)⁴¹. Also the subsequent work conducted in this area in 2018 and 2019 revealed further heavy looting, which made it frequently difficult to reconstruct stratigraphic relations.

The archaeological investigations on the western slope of Qalat-i Dinka continued on a larger scope in the spring of 2018, with funding awarded to Andrea Squitieri from the LMUexcellent Junior Researcher Fund. Three trenches were opened (Fig. C2)⁴². The first was called QID₁. It included the 2016 test trench and extended it to the east; its objective was to follow both the large wall and the paved floor that had been partially uncovered in 2016. The trenches QID₂ and QID₃ were opened further down the slope, about 50 m west of QID₁, where a long curved line was visible in the 2015 magnetogram. QID₂ yielded the remains of a wide sloping structure made of stones, which we interpreted as a glacis: a slanted structure commonly used to protect defensive walls. QID₃ yielded the remains

37 Radner 2015.

38 Radner 2016, 17-22; Fassbinder/Ašandulesei 2016, 38-42, Fig. B4.6.

39 Giraud 2016, 29-35; Herr 2016, 80-99.

40 Kreppner/Squitieri 2017a, 44-56, Fig. C5.

41 Kreppner/Squitieri 2017a, 48.

42 Now equipped with a dGPS, the 2018 operations followed our established grid system and were located in Squares 181908 and 181909 (QID₁), Square 176909 (QID₂), and Squares 176904, 176905 and 177905 (QID₃).



Fig. C1: Drone image of the western slope of Qalat-i Dinka taken from the southwest. Gird-i Bazar and the rest of the Lower Town of the Dinka Settlement Complex are visible in the background. Photo taken by Louise König with DJI Phantom 4 Pro drone.

of a linear feature made of loosely set stones that may have been part of a substructure supporting a built fence⁴³.

Important results were obtained from QID₁ where a monumental building was unearthed, designated as Building P. It consists of a large 5×8 m room with a paved floor (Room 58) and a smaller room to the east (Room 59), with which Room 58 is connected by a 1 m wide threshold. The walls of Room 58 are about 1.4-1.5 m wide and made of large cobbles, set in several rows and courses. The inner faces of the northern and southern walls of this room show a series of square stone bases protruding from the walls: three on the northern wall and two on the southern one⁴⁴. These architectural characteristics, as well as its monumentality, set Building P apart from every oth-

er building hitherto uncovered in the Dinka Settlement Complex. Moreover, following the trend observed in 2016, the 2018 campaign again unearthed a rich collection of small finds from Room 58, including several pieces of jewellery and many decorated ivory/bone fragments which have no counterparts in the Lower Town⁴⁵.

These results prompted us to continue the investigation of Building P and its immediate surroundings. In 2019, we expanded on the 2018 operation at QID₁ by opening four contiguous trenches around Building P (**Fig. C3**):

- a 7×5 m trench located to the south of Building P, within Square 181908;
- a 5×5 m trench located to the southeast of Building P, within Square 182908;
- an 8×5 m trench located to the east of Building P, within Square 182909;

43 For QID₁, see Herr 2019, 44-58; for QID₂, see Hashemi 2019, 59-62; and for QID₃, see Wolter 2019, 63-66.

44 Herr 2019, 49-53.

45 Squitieri 2019, 126-132.

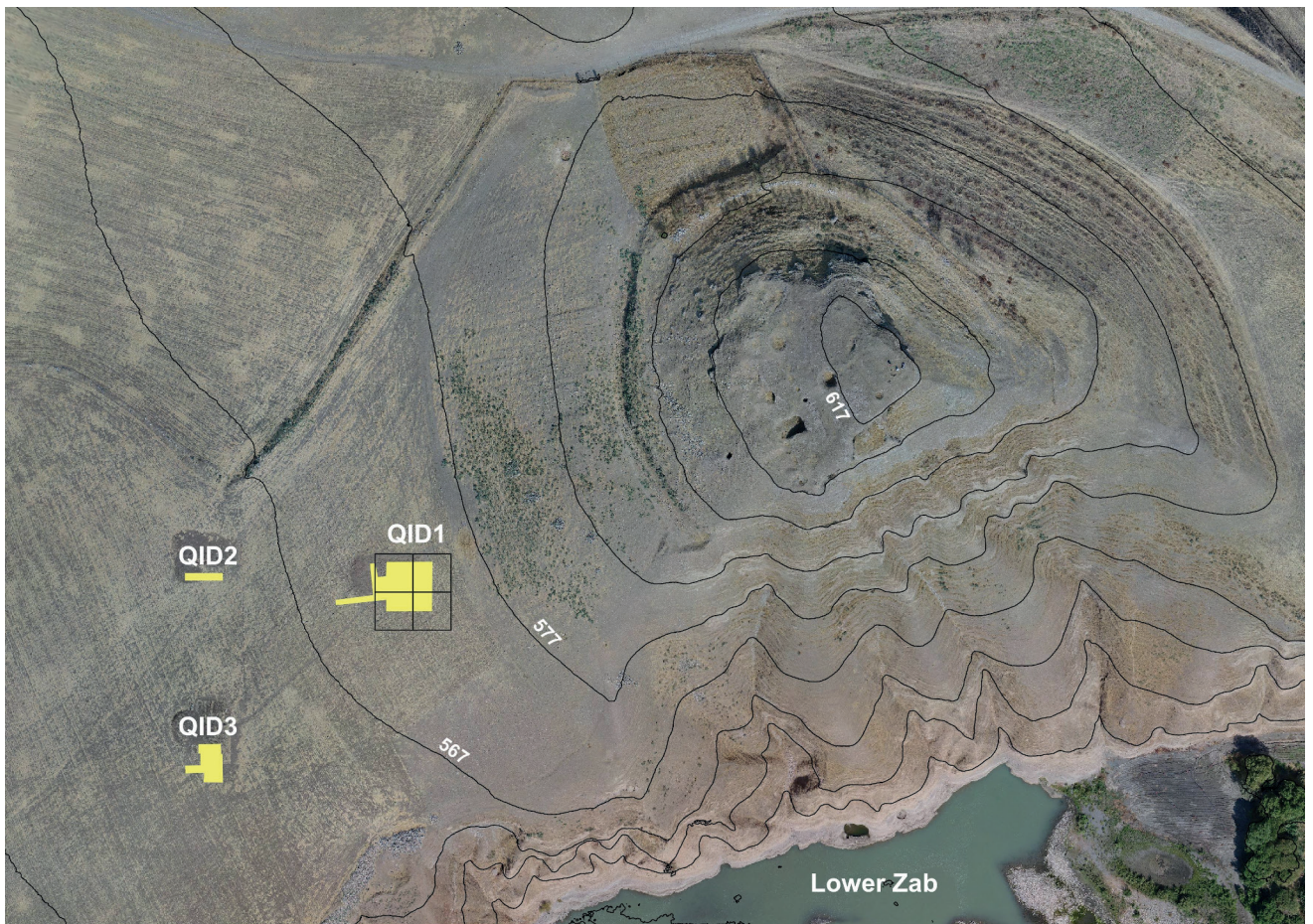


Fig. C2: Orthophoto of the western slope of Qalat-i Dinka, overlaid by contour lines with 10 m elevation intervals. Contour lines' annotations refer to absolute heights in meters a.s.l. In yellow, the three operations QID1, QID2 and QID3. The four black squares on QID1 indicate the 2019 excavation grid. Prepared by Andrea Squitieri.

- a 7×4 m trench located to the north of Building P, within Square 181909.

Squares 181908, 182908, 182909, and 181909 are part of the square grid system that the Peshdar Plain Project has applied since 2015 (with the sole exception of the 2016 test trench on Qalat-i Dinka due to the lack of a dGPS at that time)⁴⁶.

This is a north-oriented, UTM-based grid of 10×10 m squares, each named after the coordinates of their SW corner. So, for example, the SW corner of Square 181908 has the UTM coordinates E: 511810, N: 3999080 (zone 38N), hence the designation as 181908. The square name also appears in the labels assigned to loci (pl. for locus). Loci are defined as stratigraphic units, which can be soil deposits (i.e., fills) or installations (e.g., walls, floors, cuts). Each lo-

cus is assigned a progressive number following the square number in which it lies (e.g., Locus:181908:001). A locus can yield several materials. If the material is in a fragmented state then it is documented as a collection. This commonly occurs with pottery and animal bones. Collections receive a progressive number after the locus number, e.g. Locus:181908:002:001 indicates Collection 001 in Locus 002 in Square 181908. Loci can also yield individual finds. These are given a find number, also following the locus number, though with a slightly different label. An example of a find label is "PPP 181908:029:034". Samples (e.g., charcoals, phytoliths, flotation samples) are labelled like finds. To avoid confusion, the same number is never applied to collections, finds, or samples from the same locus. Finally, there are at least two cases when it is necessary to incorporate two or more loci into a so-called locus group, abbreviated as LGR:

- when two or more loci extend across adjacent squares. In this case, the stratigraphic unit (e.g., a wall) is defined as separate loci in each of the squares it crosses. These loci are then grouped into the same locus group.

⁴⁶ Kreppner/Forster/Squitieri 2016, 43-45; Kreppner/Squitieri 2017b; Kreppner/Squitieri 2018, 31; Squitieri/Rohde 2019.

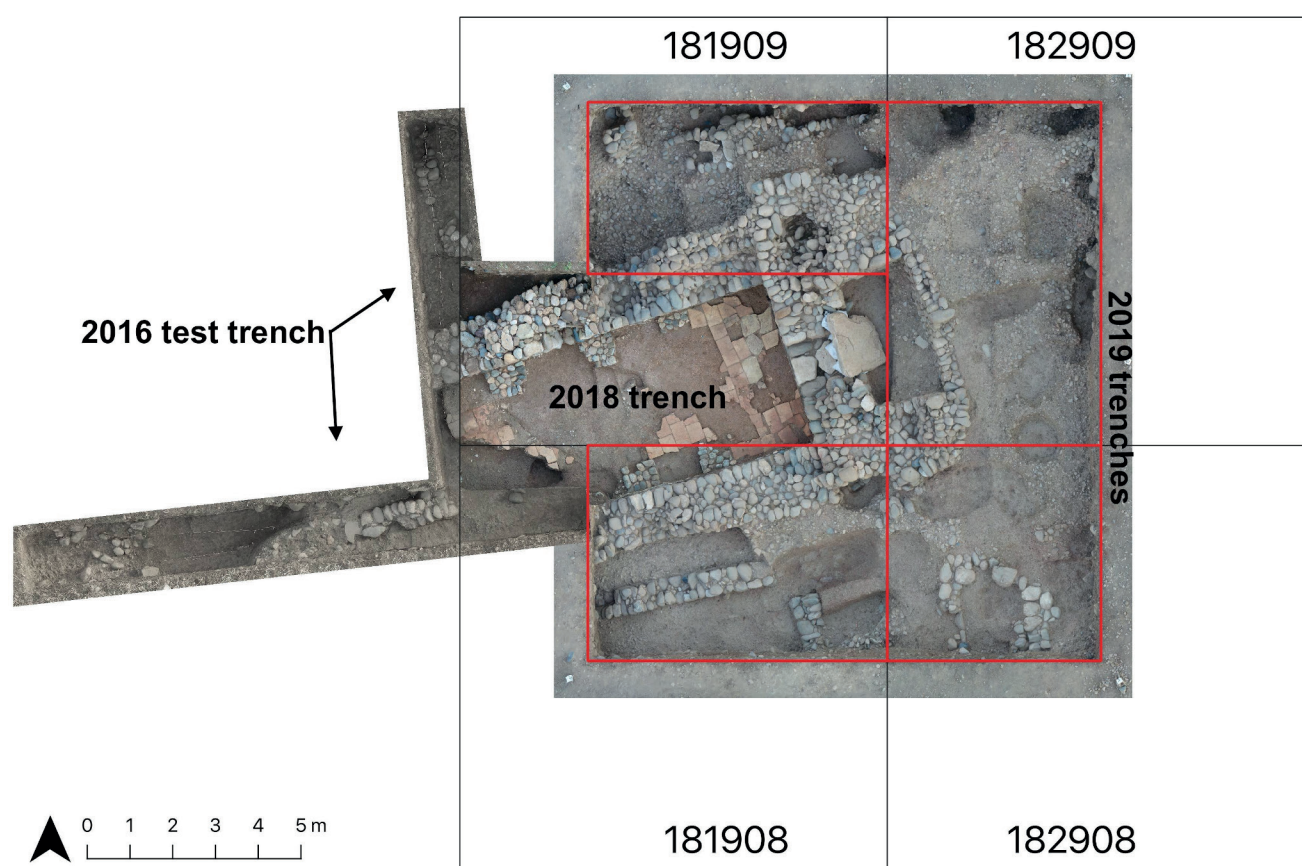


Fig. C3: Combination of the 2016, 2018 and 2019 excavation trenches opened in operation QID1. The red lines show the extensions of the four trenches opened in 2019. The black lines show the square grid. Prepared by Andrea Squitieri.

- when post-excavation analysis revealed that two separately excavated loci actually belong to the same stratigraphic unit.

Locus groups are also given progressive numbers following the label LGR, but unlike the loci, their labels do not provide information about the squares in which they were located. In the discussion below, a frequently used locus group will be LGR:0370⁴⁷, which brings together all the

⁴⁷ Normally, in our system, for two or more loci to be grouped into the same locus group it is necessary that they be contiguous. So, for example, two disconnected parts of what seem to have originally been the same wall would not be grouped into a locus group because they are not in contact. However, we make an exception to this in the case of modern stratigraphic units, such as looting pits, which we group together even when they are not directly in contact with each other. This allows us to flag them when analysing the data. Another exception is represented by the locus group of the virgin soil. Despite this soil being reached in separate places across the excavation, the loci identifying these spots are grouped into the same locus group even though they are not contiguous.

loci (cuts and fills) affected by the many modern looting pits excavated in QID1.

Following the protocol established by the Peshdar Plain Project in 2015, the excavation system adopted in QID1 includes:

- the use of a MySQL-based database to store data, accessible in the field (designed by Cristoph Forster, www.datalino.de);
- the use of a DJI Phantom 4 Pro drone to create daily orthophotos, Digital Elevation Models (DEM), and 3D models of the excavated area by means of the software Agisoft Metashape Pro (replacing earlier versions known as PhotoScan).
- the use of a Leica dGPS “GS18” to allow precise measurements of each feature.
- the creation of a 3D stratigraphy through the visualisation of each deposit in three dimensions within a 3D Photoscan model, by means of Autodesk AutoCad 2018⁴⁸.

⁴⁸ Squitieri/Rohde 2019.

C2. Absolute chronology and relative stratigraphy

C2.1 The radiocarbon dates

Andrea Squitieri

During the 2019 campaign at QID₁ two additional samples were collected for radiocarbon dating, adding to the previously dated samples, which were collected during the 2018 campaign⁴⁹. **Table C1** below sums up all the radiocarbon dates available from operation QID₁, with the graphs shown in **Figs. C4.a-e**.

As **Table C1** shows, the radiocarbon dates from QID₁ span from the Iron Age up to the very late first millennium BC. The contexts of samples PPP 181908:018:016, PPP 181909:038:049, and PPP 181909:031:002 were discussed in the previous volume⁵⁰. The contexts of samples PPP 181909:067:006 (disturbed fill) and PPP 182909:067:017 (Grave 110) are described in detail below (§C6.3 and §C5.3.3). The date ranges of the first three samples (i.e., MAMS 36939, 43917, 36674) very closely match those obtained from the Lower Town. This is the period that in terms of relative stratigraphy we refer to as the “Main Occupation Period”, roughly corresponding to the Iron Age. **Table C1** also shows that the only absolute date associated with architectural features is the one obtained from a charcoal collected in 2018 from the floor of Building P’s Room 58⁵¹ (sample PPP 181909:038:049). This date collocates Building P within the Iron Age horizon. The other dates were obtained from human remains. They show that the area of QID₁ was used for burials across a long span of time from the late second millennium BC until the very late first millennium BC. Whether some burials were constructed during the same period that Building P was in use will be discussed below (§C.7 and §K).

C2.2 The relative stratigraphy and the stratigraphic table

F. Janoscha Kreppner

The relative stratigraphy of operation QID₁ is offered in **Table C2**. This table follows the same principles as previously published stratigraphic tables of the Peshdar Plain Project, and it updates the stratigraphic table of QID₁ referring to the 2018 excavations. Please note the following, when reading this table:

- The rows are ordered chronologically, spanning from the oldest (bottom) to the most recent (top) periods.
- The columns refer to the spaces, such as rooms, courtyards, and outdoor areas. Consequently, roughly contemporary depositional processes and occupation periods that span across various areas of the site can be read in the table horizontally.
- The cells of the table contain a locus number (e.g., Locus:181908:025), a Locus Group number (e.g., LGR:0370) followed by a brief description, or a grave number (e.g., G101).
- The background colours of the cells indicate their interpretation and duration: pink shades are used for top-soil, modern occupation, graves, and virgin soil; brown indicates post-occupation periods (non-use/erosion processes), and yellow is used for occupation periods.
- The table follows the principle of the occupation phases. Occupation phases are defined by floors. The occupation phases can be divided into four sub-phases, to which stratigraphic units from the archaeological record, such as soil deposits, walls, or installations, can be assigned:
 - First, the construction phase which preceded the use phase, including the construction of the walls, floors, and any installations (cell colour: yellow).

Sample registration no.	Lab no. MAMS	Material	Context	Date (calBC, 95% probability)
PPP 181908:018:016	36939	Human tooth	Grave 99	1259-1117
PPP 181909:067:006	43917	Human tooth	Looting pit	1210-1029
PPP 181909:038:049	36674	Charcoal	Floor of Building P Room 58	1001-847
PPP 182909:067:017	43915	Human tooth	Grave 110	767-488
PPP 181909:031:002	36938	Human bone	Grave 98	355-93

Table C1: Radiocarbon dates available from operation QID₁ (campaigns 2018-2019).

⁴⁹ Radner/Squitieri 2019, Fig. D5.

⁵⁰ Radner/Squitieri 2019; Herr 2019.

⁵¹ Herr 2019.

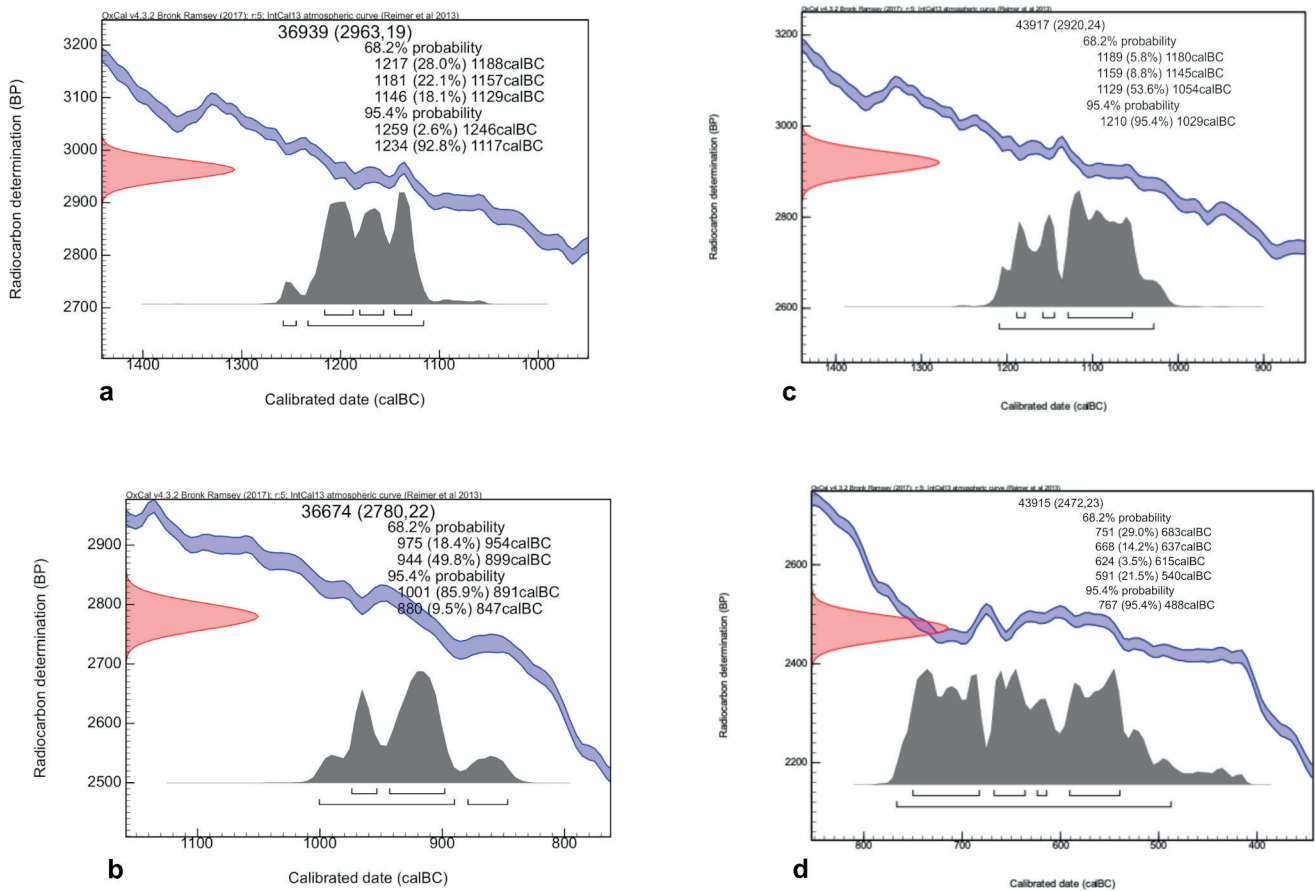


Fig. C4a-d: Radiocarbon dates for samples: (a) PPP 181908:018:016, (b) PPP 181909:038:049, (c) PPP 181909:067:006, (d) PPP 182909:067:017. Calibration software OxCal v. 4.3.2.

- Second, deposits and installations from the period when the floor was in use (cell colour: yellow).
- Third, the end of the occupation period, including deposits that indicate the destruction or abandonment of the floor which cover the finds collected directly on the floor (cell colour: yellow).
- Fourth, the Post-Occupation Period (cell colour: brown) follows each occupation period, representing a period of non-occupation during which erosion phenomena are the main causes for the formation of archaeological deposits.
- These four phases may repeat cyclically if new floors were constructed, which is why yellow and brown rows can alternate in the table. However, not all of these sub-phases are necessarily represented in the archaeological record.
- If a new floor that overlies an earlier one was detected, then a new occupation period is defined. Note that the term “floor” refers to either a purpose-built surface, or a trodden surface created through use, and which is

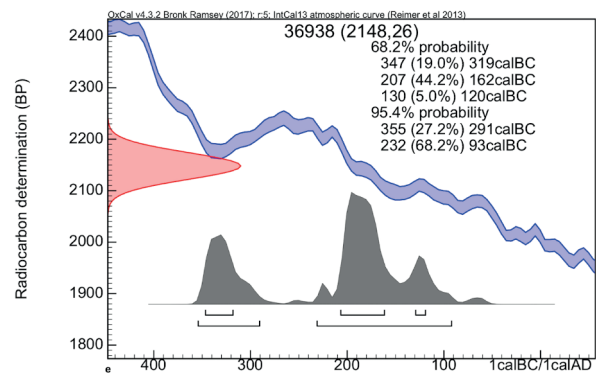


Fig. C4e: Radiocarbon dates for sample PPP 181909:031:002. Calibration software OxCal v. 4.3.2.

assigned a specific locus number. On the other hand, deposits found directly on a floor are given their own locus numbers. This allows us to isolate material found on floors and, at the same time, gain a better understanding of the formation processes of the deposits associated with a use of the floor.

QALAT-I DINKA STRATIGRAPHY QID-1		Building P		
Room (?) 61		Room 58	Room 59	
PRESENT SQUARE SURFACE	Outdoor Area 60	Room 58	Room 59	
Locus:100000-001	Locus:181908-022	Locus:181909-001, Locus:181908-001	Locus:181909-049, Locus:182909-002	
LGR:0368 (Locus:100000-002,	Locus:181909-050, Locus:181909-051, Locus:181909-062	Locus:181908-002, Locus:181909-002	Locus:181909-002, Locus:182909-004, Locus:182909-005	
LGR-0319 looting pit 2016 western trench (Locus:100000-008 stone accumulation, Locus:100000-009 brown loamy soil, Locus:100000-010 stone accumulation, Locus:100000-011, Locus:100000-034 accumulation of large stones)	LGR-0370: Locus:181909-052 and Locus:181909-063 mixed material with dark yellowish brown loamy soil with pebbles, Locus:181909-056 stone accumulation), local pit Locus:181909-057 with fill Locus:181909-058 and Locus:181909-072, local pit cut Locus:181909-059 with fill Locus:181909-060, local pit cut Locus:181909-064 with fill Locus:181909-065, local pit cut Locus:181909-074 with fill Locus:181909-073, local pit cut Locus:181909-079 with fill Locus:181909-078, local pit cut Locus:181909-066 with fill Locus:181909-067 (C14 1188-1054 calBC) and skull Locus:181909-084	LGR-0291 reddish soil (Locus:181908-004, Locus:181909-004), LGR-0290 looting pit central (fill: Locus:181908-006, Locus:181909-006, Locus:100000-007, Locus:100000-012, Locus:100000-013, Locus:100000-027, Locus:100000-031, Locus:100000-032, Locus:181909-018, Locus:181909-020 Locus:181909-024; cut: Locus:100000-017, Locus:181908-005, Locus:181909-005, Locus:181909-014, Locus:181909-036); LGR-0297 stone accumulation (Locus:100000-014, Locus:181908-009, Locus:181909-015), LGR-0299 stone accumulation (Locus:100000-015, Locus:181908-010), Locus 181909-035 accumulation of stone slabs and cobblestones, stones laid down in a row; Locus:181909-017, Locus:181909-019; Locus:181909-021	LGR-0305 looting pit northeast (Locus:181909-012 accumulation of stones; Locus:181909-016, Locus:182909-003, Locus:182909-020 dark brown clayey- silty soil with some pottery and some pebbles, Locus:181909-029, Locus:182909-016 looting pit cut, Locus:181909-026 moved stone slab with hole, looting pit east Locus:181908-012 pit cut)	
MODERN OCCUPATION				
GRAVES	Grave 106 (Locus:181909-068 cut with fill Locus:181909-069 and skeleton Locus:181909-083), Grave 107 (Locus:181909-081 architecture), Grave 108 (Locus:181909-082 architecture)	Grave 97: Locus:100000-021 disturbed skeleton, Grave 98: Locus:181909-031 remains of articulated feet bones and tibia fibula with C14 355-93 cal BC, Grave 99: Locus:181908-018 remains of skeleton with C14 1259-1117 calBC		
POST MAIN OCCUPATION PERIOD				
END MAIN OCCUPATION PERIOD	Locus:181909-055 dark brown moist loose, loamy, poorly sorted soil with common sherd and bone fragments	remnants of deposit on brick floor unfortunately disturbed: LGR-0323 (Locus:181908-014, Locus 181909-038 C14 1001-847 calBC), Locus:100000-019 dark brown clayey-silty soil; Locus 181909-044 and Locus 181909-045 burned mud plaster		
MAIN OCCUPATION PERIOD	Locus:181909-061 and Locus:181909-071 surface of pebble package	LGR-0292 (Locus:181908-008, Locus:181909-011, Locus:100000-020) and LGR-0324 (181908-019, 181909-039) pavement made of baked bricks, Locus:100000-030 beaten mud floor, LGR-0317 (Locus:100000-033, Locus:181908-016), LGR-0320 (Locus:181908-015, Locus:181909-047), Locus 181909-028 and Locus:181909-037, Locus:181909-040 plaster bases (?)	Locus:182909-023 pebble package	
CONSTRUCTION FOR MAIN OCCUPATION PERIOD	Locus:181909-076, Locus 181909-077 pebble package	LGR-0319 (Locus:181909-007, Locus:100000-006, Locus 181909-053, Locus:181909-054) northern wall, LGR-0321 (Locus:181908-021, Locus 181909-023) eastern wall with Locus:181909-022 threshold; LGR-0329 (Locus:100000-016, Locus:181908-007) southern wall, Locus:100000-029 western wall; LGR-0325 (Locus:181909-034, Locus:181908-017), Locus:181908-020, Locus:181909-041, Locus:181909-042 and Locus:181909-043 pebble foundations; Locus:181909-046 burned clay	LGR-0321 (Locus 181909-023, Locus:181908-021) wall with Locus:181909-022 threshold, LGR-0376 massive northeastern corner of Building P (Locus:181909-030, Locus:181909-075, Locus:181909-080, Locus 182909-061, Locus:182909-062), LGR-0381 massive southeastern corner of Building P (Locus:181909-032, Locus:182908-053, Locus:182909-060), Locus:182909-035 walls	
FIRST CONSTRUCTION PHASE FOR MAIN OCCUPATION PERIOD	Locus:100000-028, Locus:100000-029 walls			
older				
VIRGIN	Locus:100000-022	LGR-0322 (Locus:181908-011, Locus 181909-033	Locus:181909-025	

Table C2: QID1 stratigraphy 2019. Prepared by F. Janoscha Kreppner.

QALAT-I DINKA STRATIGRAPHY QID-1	
Outdoor Area 70	Outdoor Area 71
PRESENT SQUARE SURFACE	PRESENT SQUARE SURFACE
Locus:181908:022	Locus:182908:001
TOPSOIL	TOPSOIL
Locus:181908:024, Locus:181908:026, Locus:181908:042	Locus:182908:002, Locus:182908:006, Locus:182908:022
LGR-0370: looting pit deposit dark brown silty soil with pebbles (Locus:181908:025, Locus:181908:027, Locus:181908:028, Locus:181908:029, Locus:181908:039, Locus:181908:043, Locus:181908:044, Locus:181908:045, Locus:181908:046, Locus:181908:050, Locus:181908:054, Locus:181908:056, Locus:181908:057, Locus:181908:058, Locus:181908:059, Locus:181908:060, Locus:181908:061, Locus:181908:062, Locus:181908:067, Locus:181908:068; Locus:181908:030 row of stones set by looters, stone accumulations (Locus:181908:031 and Locus:181908:048, Locus:181908:064), Locus:181908:047 row of stones set by looters, Locus:181908:049 stone accumulation), looted fill of grave 102 (Locus:181908:033, Locus:181908:034, Locus:181908:035, Locus:181908:036, Locus:181908:037, Locus:181908:040, Locus:181908:041), looted fill of Grave 105 (Locus:181908:051, Locus:181908:055), Locus:181908:052 fill of bronze bowl	LGR-0370: mixed material caused by looting activity; Locus:182908:004, Locus:182908:005, Locus:182908:020, Locus:182908:007, Locus:182908:010, Locus:182908:026, Locus:182908:028, Locus:182908:029, Locus:182908:012, Locus:182908:021, Locus:182908:038, Locus:182908:039, Locus:182908:042, Locus:182908:043, Locus:182908:045, Locus:182908:046, Locus:182908:052, Locus:182908:055; Locus:182908:003 and Locus:182908:011 stone concentration, local pit cut Locus:182908:009 with fill (Locus:182908:008, Locus:182908:027, Locus:181908:032), local pit cut Locus:182908:014 with fill Locus:182908:015 and Locus:182908:033, local pit cut Locus:182908:025 with fill Locus:182908:013, local pit cut Locus:182908:016 with fill Locus:182908:017 and Locus:182908:034, local pit cut Locus:182908:023 with fill Locus:182908:024 and Locus:182908:035
GRAVES	GRAVES
Grave 102: Locus:181908:038 architecture, Grave 105: Locus:181908:063 architecture	Grave 103: Locus:182908:018 architecture, Locus:182908:019 fill, Locus:182908:041 skeleton
POST MAIN OCCUPATION PERIOD	POST MAIN OCCUPATION PERIOD
Locus:182908:036, Locus:182908:037, Locus:182908:040 hard dry, silty, poorly sorted yellowish-brown soil with rare pottery and common pebbles	Locus:182908:036, Locus:182908:037, Locus:182908:040 hard dry, silty, poorly sorted yellowish-brown soil with rare pottery and common pebbles
END MAIN OCCUPATION PERIOD	END MAIN OCCUPATION PERIOD
Locus:182908:057 possible surface of pebble package, LGR-0384, stone installation (Locus:181908:053, Locus:182908:050)	Locus:182908:057 possible surface of pebble package, LGR-0384, stone installation (Locus:181908:053, Locus:182908:050)
MAIN OCCUPATION PERIOD	MAIN OCCUPATION PERIOD
Locus:182908:064 and Locus:182909:066, Locus:182909:072 surface of the pebble package	Locus:182909:064 and Locus:182909:066, Locus:182909:072 surface of the pebble package
CONSTRUCTION FOR MAIN OCCUPATION PERIOD	CONSTRUCTION FOR MAIN OCCUPATION PERIOD
Locus:182909:063, Locus:182909:065, Locus:182909:068 package made of pebbles	Locus:182909:063, Locus:182909:065, Locus:182909:068 package made of pebbles
FIRST CONSTRUCTION PHASE FOR MAIN OCCUPATION PERIOD	FIRST CONSTRUCTION PHASE FOR MAIN OCCUPATION PERIOD
Locus:182909:035 wall	LGR-0381 massive south-eastern corner of Building P (Locus:181909:032, Locus:182908:053, Locus:182909:060)
older	Locus:182908:051 stone enclosure with possible floor remains Locus:182908:056
VIRGIN	VIRGIN
Locus:182909:017, Locus:182909:069, Locus:182909:070, Locus:182909:071	Locus:182909:017, Locus:182909:069, Locus:182909:070, Locus:182909:071

Table C2 (continued): QID1 stratigraphy 2019. Prepared by F. Janoscha Kreppner.

Reading **Table C2** from the bottom up, it is possible to identify the following phases:

- Virgin soil. This is a clayey soil, reddish in colour, devoid of any artifacts.
- The oldest phase was identified only in Square 181908. This phase is referred to as “Older than the Main Occupation Period”.
- The “First Construction Phase for the Main Occupation Period” represents the period when the foundations for the Main Occupation Period buildings were laid and the walls erected.
- The “Construction Phase for the Main Occupation Period” represents the construction of the floors and installations, before the floor was used;
- The “Main Occupation Period” indicates the phase when the floors were occupied, resulting in new deposits and installations;
- The “End of Main Occupation Period” is the period from which deposits indicate the destruction or abandonment of the floors. These deposits cover the finds collected directly from the surface of the floor.
- A “Post Main Occupation Period” represents a period of non-occupation during which erosion phenomena resulted in the formation of archaeological deposits.
- “Graves” refers to the phase when graves were cut into the features of the Main Occupation Period. Since the stratigraphic position of the tombs in operation QID-1 cannot always be clearly related to the architecture, due to modern looting, this line also includes graves that may be older or that were built during the Main Occupation Period of Building P.
- “Modern Occupation Period” refers to a recent period of heavy looting which has disturbed almost all the excavated fills and installations, including graves.
- The “Topsoil” represents the even more recent ploughing zone.
- The “Site surface” is the surface of the site from immediately before excavation commenced.

C3. The trench in Square 181908

Jens Rohde & Laura Tretow

C3.1 Introduction

This section presents the results of the trench opened in Square 181908 (**Figs. C3, C5**). This trench includes areas which had been partially excavated in 2016 and 2018⁵². In 2019, we completed the excavation of the southern wall of Building P (LGR:0329), and further enlarged the excavation area to the south of this building. The resulting trench measures 7×5 m⁵³. As elsewhere across QID1, the archaeological features uncovered in this trench had been severely damaged by looting pits opened in modern times (grouped together in LGR:0370). Nevertheless, it has been possible to at least partially reconstruct the stratigraphic sequence of the ancient features, which are described below from the oldest to the youngest.

C3.2 Virgin soil

The virgin soil lying underneath Building P had already been reached in 2018 in several places⁵⁴. It was labelled LGR:0322 and is characterised by a reddish clayey soil, with very few small pebbles embedded in its matrix. In 2019, the virgin soil was reached in the areas approximately 1 m south of wall Locus:181908:065 and 1 m west of wall Locus:181908:066 (**Fig. C5**). Here, it has an elevation of 568.77 m, which matches the elevation of the virgin soil found in 2018 north of wall LGR:0329. Towards the southwest, the virgin soil slopes slightly down to an elevation of 568.71 m, whereas towards the northeast, and immediately west of wall Locus:181908:066, it slopes more sharply upwards to a level of 568.97 m. To the east of wall Locus:181908:066, a step in the virgin soil was observed, which was probably created for the erection of the wall (**Fig. C6: section C**). Past this step, the virgin soil slopes upwards to an elevation of about 569.42 m, thus reaching the same level as the highest preserved elevation of wall Locus:181908:066. More to the east, it moves upward to a level of approximately 569.70 m, as far as the eastern border of Square 181908. In the neighbouring Square, 182908,

52 Kreppner/Squitieri 2017a, 49 (“The Eastern Sector”); Herr 2019, 49–53.

53 In the northern portion of this trench, a 1×7 m strip had already been excavated in 2018, but it was uncovered again in 2019 by removing the old backfill in order to better understand the structure of wall LGR:0329.

54 Herr 2019, 49 and 53.



Fig. C7: Virgin soil close to the southeastern corner of Building P. Photo by Jens Rohde and Laura Tretow.

long, while the remaining part lies under the southern excavation limit. The northern end of the wall was disturbed by the construction of Grave 102 (§C3.5). Wall Locus:181908:066 consists of two rows of longish and roundish cobbles. In the northeast part of the wall three courses are preserved, corresponding to a height of about 40 cm, whereas in the remaining part only one course is preserved. On the western side of the wall, it is possible to see that roundish stones form the lowest course, while the second and third courses consist of longish cobbles set perpendicular to the wall's alignment. Smaller stones were placed to fill the gaps in between the cobbles. The longish cobbles vary in length between 30 cm and 45 cm and in width between 15-20 cm. The more round cobbles are between 20×30 cm and 30×40 cm in size. The width of the wall is slightly more than 60 cm and is very close to the width of wall Locus:181908:065, which is described below. No floor level belonging to wall Locus:181908:066 was intercepted; perhaps it was destroyed by the installation of another grave, called Grave 105 (§C3.5), and by the modern looting activities.

To the northwest of wall Locus:181908:066 lies wall Locus:181908:065. This wall is oriented SW-NE and it is preserved for a length of approximately 4.3 m (**Figs. C6: section D, C9, C10**). It continues towards the west, within the excavation limit. Wall Locus:181908:065 is about 65 cm wide and up to 40 cm high; it is made from a variety of cobbles with irregular shapes. These cobbles vary in size between 20-30 × 20-40 cm. Only a few are slightly larger. The cobbles are mostly perpendicular to the alignment of the wall, while only a few align with the wall. Smaller stones are visible in the gaps between the cobbles. The wall is formed by two rows of stones and is preserved to a height of four courses. A looting pit which damaged the



Fig. C8: Wall Locus:181908:066. Photo by Jens Rohde and Laura Tretow.

western part of the wall has revealed that its stone base extends even deeper here. The width and the orientation of walls Locus:181908:065 and Locus:181908:066, along with the similarities in their construction techniques, suggest that a corner existed to connect these two walls; it was likely destroyed by the installation of Grave 102.

Two pebble floors can be connected to wall Locus:181908:065. The pebble floor Locus:181908:071 abuts wall Locus:181908:065 from the south, and it is better preserved towards the west (**Figs. C6: section D, C10**). It is a pebble floor consisting of a dense and compact layer of small pebbles set in a clayey, greyish soil. To the south and west, the floor continues below the limits of our excavation. Originally, it may have extended further east, and it probably abuts wall Locus:181908:066. Only pottery sherds were found on this floor. Whether it belonged to an indoor or outdoor area is uncertain.

The second pebble floor, similar to the first, is Locus:181908:070, which extends north of wall Locus:181908:065 (**Figs. C6: section D, C10, C11**), and, very importantly, abutting it. More of this floor is preserved than of floor Locus:181908:071. However, in its eastern half the pebbles are not so visible, so that its original boundaries remain uncertain. Its relationship to the southern wall of Building P (LGR:0329) is clear: Locus:181908:070 continues below this wall, and therefore must represent an older building phase than the Main Occupation Period to which Building P belongs. Walls Locus:181908:065 and Locus:181908:066, and the pebble floor Locus:181908:071 must also belong to this same earlier phase as these features all predate the construction of Building P. Though this stratigraphic relationship is clear, it is not possible to say much more about the nature of the area enclosed by walls Locus:181908:065 and Locus:181908:066.

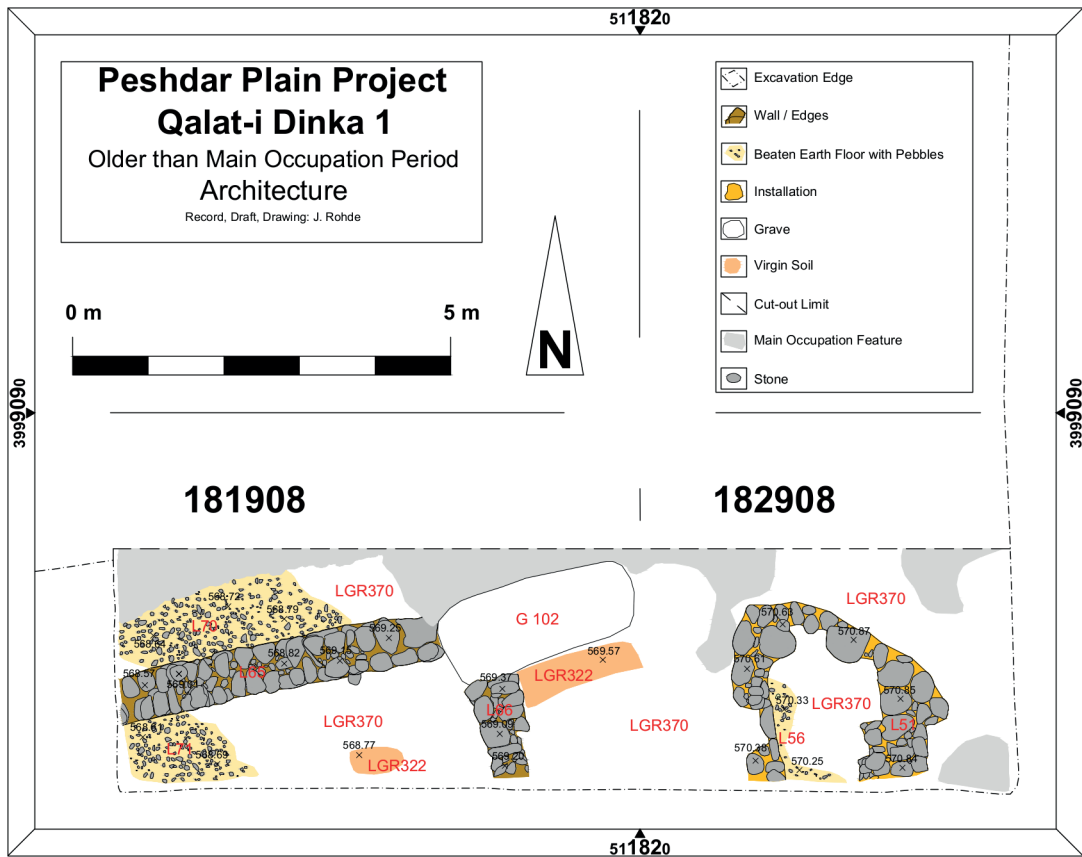


Fig. C9: Plan of the phase “Older than Main Occupation Period”. Prepared by Jens Rhode.

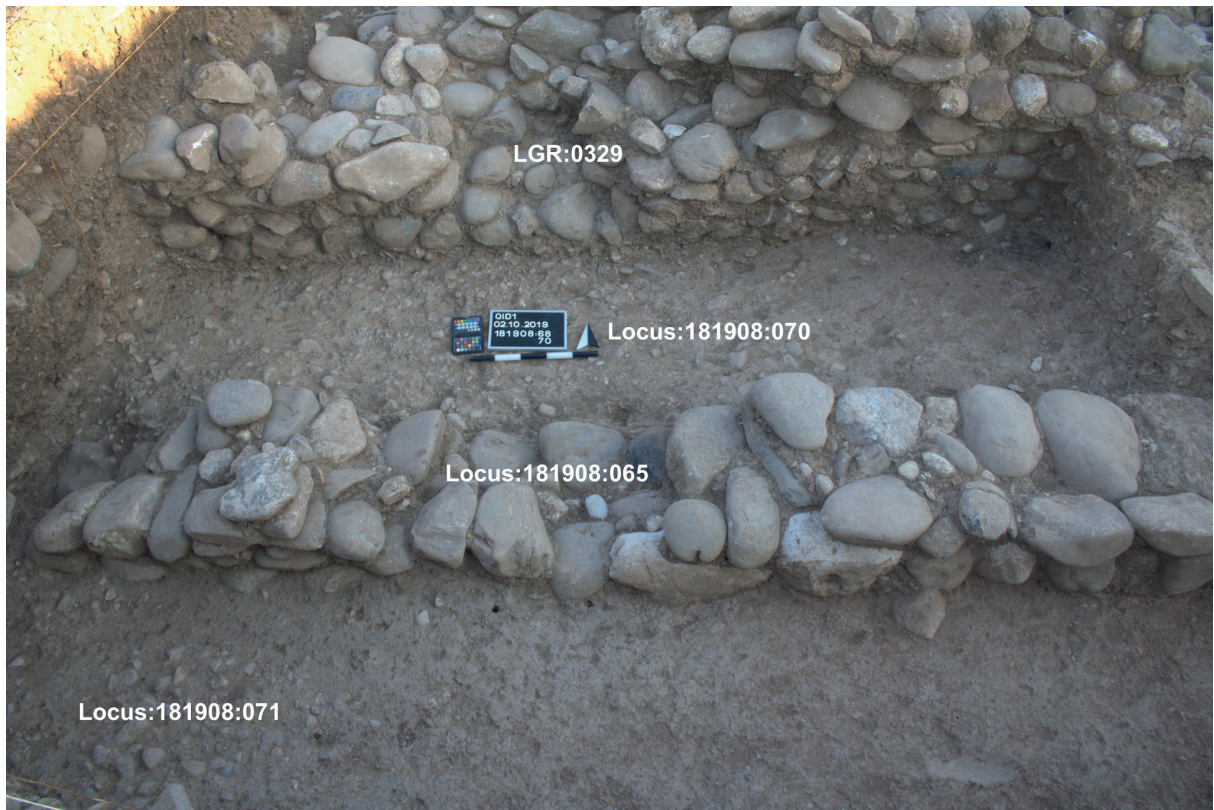


Fig. C10: Wall Locus:181908:065 and its surrounding. Photo by Jens Rohde and Laura Tretow.



Fig. C11: Floor Locus:181908:070. Photo by Jens Rohde and Laura Tretow.

C3.4 Wall LGR:0329 of Building P and the Outdoor Area 70 of the Main Occupation Period

The southern wall of Building P, that is LGR:0329, was partially exposed in 2016 in what, at that time, was called the “Eastern Sector”⁵⁵. By then, the top of the wall had been unearthed. In 2018, the northern face of this wall was uncovered down to the paved floor, named LGR:0324⁵⁶. At that time, the southern face of the wall was still covered. In 2019, we continued the excavation of the wall by exposing its southern face. While the northern face had been uncovered over a length of about 5.4 m, the southern face was exposed across a length of a little over 6 m (Figs. C5, C6: section D, C12). This face is preserved up to one meter high, and leans slightly towards the south. Due to its state of preservation, it shows from 3 to 9 courses of

stones of different sizes (Fig. C13). In the eastern part, the lower courses consist of small cobbles measuring 10-20 × 15-25 cm. In the western and upper parts, the cobbles are 20-30 × 20-40 cm in size. They are all set perpendicular to the alignment of the wall, with smaller stones filling the gaps between the cobbles. The wall’s width is not uniform. To the west, it is a little more than 1.2 m wide, while it measures about 1.45 m on the east (Fig. C12). Moreover, due to modern looting, the upper part of the wall is badly preserved, although the central and eastern sections are more visible. Overall, the layout and construction of wall LGR:0329 are comparable to those of wall LGR:0319, delimiting Building P to the north (§C6.1.1). Both walls run in a SW-NE direction and meet wall LGR:0321, located to the east, at right angles. Moreover, both walls display a step on their inner faces. In wall LGR:0329 this step is about 80 cm wide, extending about 2.5 m to the west from wall LGR:0321 (Fig. C14); behind this step the wall continues vertically with a width of about 70 cm. The step is only visible on the northern face of the wall, and is about 70-75 cm higher than the floor level of Room 58. As we will see below (§C6.1.1), a similar step is found on the inner face of the northern wall LGR:0319.

The southern face of wall LGR:0329 provides the boundary for Outdoor Area 70 (Figs. C5, C12), which refers to the space extending south of Building P, up to the southern limit of the excavation area. This space seems to be an open area because, within the trench, no evidence was found that it was enclosed by walls. To the east, Outdoor Area 70 merges with Outdoor Area 71 (§C4.3.2), with no clear demarcation between the two. The modern looting has irremediably damaged the original walking surface of Outdoor Area 70; however, a thick pebble package, called LGR:0382, was found abutting the southern face of wall LGR:0329 (Fig. C15). This is interpreted as the remains of a Main Occupation Period walking surface in Outdoor Area 70. The same pebble package was also preserved in various spots in the trenches to the southeast, east, and north of Building P (see below).

On top of LGR:0382 a two-row stone installation was found, called LGR:0384, about 60 cm wide (Fig. C16). The southern row of this installation forms a relatively straight face made of longish cobbles set perpendicular to the orientation of the installation. The northern row is made of irregularly set cobbles and it directly borders wall LGR:0329. These cobbles are between 10-25 × 15-35 cm in size. The installation is two to three courses high. To the west, its limit is not clearly visible, while to the east, it continues into the neighbouring Square 182908, reaching a total length of about 2 m. The function of this installation is not clear.

55 Kreppner/Squitieri 2017a, 44.

56 Herr 2019, 49-52.



Fig. C13: Southern face of wall LGR:0329.
Photo by Jens Rohde and Laura Tretow.



Fig. C14: Northern face of wall LGR:0329.
Photo by Jens Rohde and Laura Tretow.



Fig. C15: Pebble package LGR:0382, abutting wall LGR:0329 from the south. Photo by Jens Rohde and Laura Tretow.

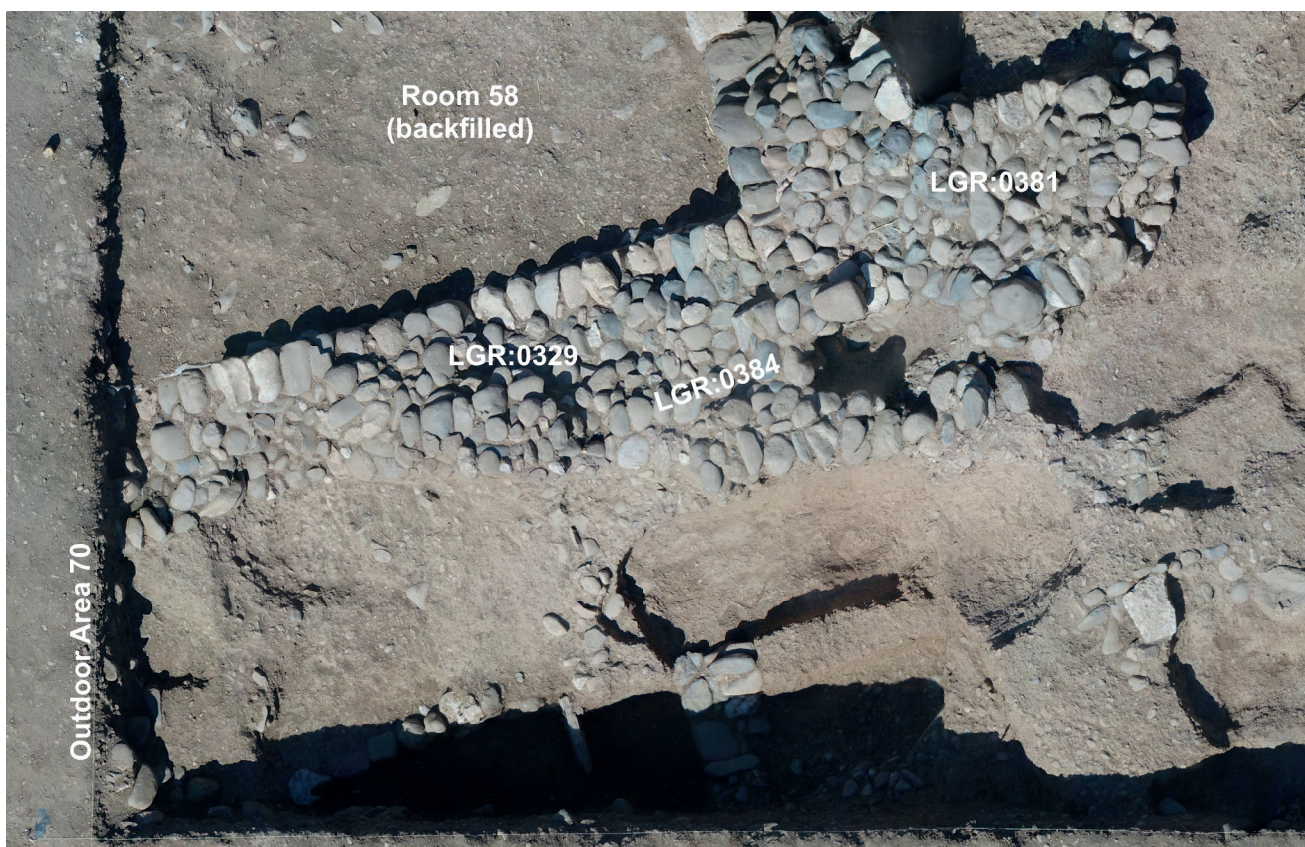


Fig. C16: Stone installation LGR:0384. Photo by Andrea Squitieri.



Fig. C17: Plan of the graves excavated in 2019 in QID1. Prepared by Jens Rohde.

C3.5 Graves 102 and 105

Two cist graves, Grave 102 and Grave 105, were identified south of wall LGR:0329 (Figs. C5, C17). Unfortunately, both had been heavily disturbed by looters, and consequently neither yielded any skeletal remains or *in situ* items. Only a few bits of their architecture were found *in situ*.

Grave 102 (Fig. C18) is a cist grave which seems to have been cut into the Main Occupation Period pebble package of LGR:0382; however, because of the modern disturbances, this stratigraphic relationship is difficult to ascertain. What is certain is that Grave 102 cuts the walls Locus:181908:065 and Locus:181908:066, both of which are older than the Main Occupation Period, and also cuts into the virgin soil LGR:0322. The cist is about 2 m long and 90 cm wide (measured from within), and is oriented from SW-NE. Its architecture, Locus:181908:038, consists of a stone lining made of roundish cobbles set in 4 to 5 courses on both the northern and southern sides, while flattish white boulders were placed upright to create the grave's western and eastern boundaries (Fig. C19). On the west



Fig. C18: Cist Grave 102 before the removal of the remains of the capping. Photo by Jens Rohde and Laura Tretow.



Fig. C19: Cist Grave 102 after removing the capping. Photo by Jens Rohde and Laura Tretow.

side, this boundary is created by one almost-rectangular boulder, while six boulders of different sizes form the eastern edge. Similar white, flattish boulders of different shapes were used to cap the grave. Three of them were still covering the tomb when it was excavated, while the others were found inside the tomb itself. The fills inside the grave architecture were excavated as Locus:181908:035, Locus:181908:036, Locus:181908:040 and Locus:181908:041. Because the grave had been robbed in modern times, these fills must be considered disturbed contexts. Along with many fragments of modern items left by the looters, ancient items were also found, particularly numerous bronze studs and several white appliques (see §E1, nos. 15 and 18). It is noteworthy that these ancient finds were concentrated in the area west of the grave, while none were found in Locus:181908:41 located to the east; likely this had to do with the method used by the looters to rob the grave. The upper grave fill and the fills right above the grave, labelled Locus:181908:033, Locus:181908:034 and Locus:181908:037, also contained finds that may be assigned to the original grave furniture (see §E1, nos. 14 and 63 and the arrowheads of Variant d discussed in §E4.1.4).

Southwest of Grave 102, close to the southern excavation limits, the remains of another cist grave were found: Grave 105 (Figs. C17, C20). Its architecture is labelled Locus:181908:055. Its northern boundary is about 2.8 m long and consists of a series of cobbles, about 15-30×15-20 cm in size, up to five courses. On the eastern side, only one flattish white stone block is preserved, about 80 cm wide, standing upright. This block closely resembles the ones used for the architecture of Grave 102. The southern and western boundaries of the grave seem to continue south beyond the excavation limit; however, part of the architecture is lost, and hence no remains of this grave are visible in the southern section. No skeletal remains were found inside, since the grave had been completely robbed. The looted fill inside the grave architecture (named Lo-



Fig. C20: Cist Grave 105. Photo by Jens Rohde and Laura Tretow.

cus:181908:051 and Locus:181908:055) yielded fragments of an Egyptian Blue bead (§E1, no. 27) along with some modern remains left behind by looters. Right above the grave architecture, the looted fills Locus:181908:044 and Locus:181908:048 also yielded numerous finds, some of which probably originated from Grave 105 (§E1, nos. 63, 69, 78, 80, 84, 85, 88 and 93). A large, whitish, flat stone block found in the fill above the grave was likely part of the original grave architecture. Because of the looting, the stratigraphic position of Grave 105 is difficult to ascertain; however, the similarities in architecture might suggest contemporaneity with Grave 102.

East of Grave 105 and south of Grave 102, a cut into the virgin soil LGR:0322 was observed; it is very similar to the cut opened in the virgin soil to accommodate Grave 102. Moreover, the fill excavated here, Locus:181908:050, yielded two fragments of bronze pins, remains of Egyptian Blue beads, and a bronze bead (§E1, nos. 79, 87 and 97), all of which would fit the item repertoire of a grave. Hence, it is possible that another grave was once present here.

C3.6 The modern looting pits and the topsoil

As mentioned above, evidence for recent looting activity was abundant across the entire trench (Fig. C21). Looting pits reached down to the virgin soil in several spots and irremediably confused the stratigraphy of the operation. The cuts and fills of these pits have been documented in separate loci, which are now collected into one locus group (LGR:0370). The fills of the looting pits were characterised by a loose dark-brown soil, including pebbles, ceramics, animal bones and, more rarely, charcoals. Several modern finds (e.g., plastic fragments, cigarette filters, aluminium pieces) were also found in these fills, along with ancient objects. Occasionally, accumulations of medium-sized stones were encountered that represented stones dislocated and accumulated by the looters; these accumulations had already been observed during the 2016 and 2018 campaigns⁵⁷. Both the soil characteristics and the presence of modern finds helped in the identification of the looting pits, though it has not always been easy to delineate their cuts because in most cases the pits superimposed and cut each other.

The looted fills connected to Graves 102 and 105 have been already discussed above, as they contained finds that possibly originated in these two graves. In addition, one more looted fill is worth mentioning: Locus:181908:029.

This fill extended across the length of the trench. Though it had no direct connection to any of the graves, it yielded several ancient finds, some of which may have belonged to a grave (§E1, nos. 62, 63, 66 and 82 and cf. the discussion of arrowhead “Variant c” in §E4). Among these objects is a complete bronze bowl (§E1, no. 61; Fig. E1.14), found upside down, about 2 m west of Grave 102. This bowl’s fill (Locus:181908:052) contained bones from a human hand. It is possible that this bowl originated in one of the graves. Due to a lack of collagen, the attempt to radiocarbon date one of the bones was unsuccessful.

The table below summarises the looted fills encountered in this trench, grouped into LGR:0370. Their locations are given in the plan shown in Fig. C21.

Looted fills in trench Square 181908 (part of LGR:0370)	
Locus numbers	Notes
Locus:181908:025, Locus:181908:028 Locus:181908:039, Locus:181908:045 Locus:181908:054, Locus:181908:057 Locus:181908:058, Locus:181908:059 Locus:181908:060, Locus:181908:061	Generic disturbed fills containing pottery sherds, animal bones, charcoals and modern items, all embedded in a dark-brown, loose soil matrix.
Locus:181908:027, Locus:181908:029 Locus:181908:043, Locus:181908:044 Locus:181908:046, Locus:181908:048 Locus:181908:050, Locus:181908:056 Locus:181908:062, Locus:181908:067 Locus:181908:068	Disturbed fills yielding several ancient finds, some of them possibly originating from a nearby grave.
Locus:181908:030, Locus:181908:031 Locus:181908:047, Locus:181908:049 Locus:181908:064	Stone accumulations gathered by looters.
Locus:181908:033, Locus:181908:034 Locus:181908:035, Locus:181908:036 Locus:181908:037, Locus:181908:040 Locus:181908:041, Locus:181908:051 Locus:181908:055	Disturbed fills inside or right above Graves 102 and 105, yielding finds which likely originated from these graves.
Locus:181908:052	Fill from inside the complete metal bowl (§E1, no. 61) containing the bones of a human hand.

Finally, all the deposits and features described above were covered by topsoil, which did not bear any trace of looting. It was excavated in three separate loci (Locus:181908:024; Locus:181908:026; Locus:181908:042), grouped into a single locus group LGR:0368. The 2018 backfill was partly re-excavated as Locus:181908:023, and along with the topsoil, it was covered by the site surface Locus:181908:022.

⁵⁷ Kreppner/Squitieri 2017a; Herr 2019, Fig. D20.

C3.7 Conclusions

Due to the heavy looting activity that occurred in modern times, the stratigraphy of the trench in Square 181908 cannot be reconstructed clearly. Nevertheless, some conclusions may be drawn. In particular, it seems that at least four phases were encountered:

- A phase stratigraphically older than the Main Occupation Period, represented by two walls and two pebble floors.
- The Main Occupation Period, to which the southern wall of Building P, the pebble package, and a stone installation belong. This phase was dated to the Iron Age (see **Tables C1-C2**).
- Cist Graves 102 and 105. The dating of the graves is uncertain, and their stratigraphic relationship to Building P is not very clear. Due to their architecture, it is possible that both graves are contemporary with each other, and because Grave 102 seems to cut into the Main Occupation Period pebble package, it is possible that it is later than the latter period. However, given how disturbed the stratigraphy of the trench is, we can not rule out the possibility that these graves were contemporary to Building P. The objects that have been linked to these graves and in particular the arrowheads (**Table E4.2**) would suggest a 9th-6th century BC date for them.
- The Modern Occupation Period, consisting of many looting pits reaching the virgin soil in several spots.

C4. The trench in Square 182908

Jana Richter & Hero Salih Ahmed

The trench in Square 182908 is located to the east of the previously discussed trench in Square 181908 (§C3), and covers 5×5 m in the southeastern corner of operation QID1 (**Figs. C3, C5**). It was opened with the primary goal of uncovering both the southeastern corner of Building P and the features located next to this building to the southeast. The sections below present the features and deposits excavated, in stratigraphic order from the oldest to the youngest.

C4.1 Virgin soil

The virgin soil was reached in several places across the trench. As throughout QID1, it is composed of a clayey, reddish soil, with some pebbles and white inclusions. It is called LGR:0322.

C4.2 A stone structure older than the Main Occupation Period

Locus:182908:051 is possibly the oldest feature uncovered in this trench, located in its southern part (**Figs. C5, C6: section C, C9**). It is an irregularly shaped, yet structured, stone installation, which was set on the virgin soil. It encloses an area of c. 1.4×1.7 m, with the southern limit of the space extending beyond the southern limit of our excavation area. In its western and eastern inner limits, this feature shows well-aligned stone faces (**Fig. C22**). The northern end is marked by larger stones up to 55 cm long, forming an approximate corner, while protruding into the enclosed space. One more regular course of stones exists in the northwestern part of the feature, where a clear outer corner is formed. The northeastern outer limit of this structure gives the impression of an almost circular or nearly diagonal shape. In most parts, only one course of stones is preserved. In the southwestern part, two elongated stones are set in a lower position than the others, possibly forming a threshold (**Fig. C22**). Some patches of loosely distributed small pebbles and pottery sherds were found abutting the inner faces of the installation inside the stone structure, close to its southern end, and were interpreted as faint traces of a floor (Locus:182908:056).

The stone structure Locus:182908:051 has no clear function. It is not clear if it was part of a building unit, although the possible presence of a threshold would suggest it might be part of a room. It is also possible to interpret this structure as a platform or a large basin. Admittedly, there is no strong evidence that this stone installation is older than the structures of Building P as no stratigraphic connection was identified; however, it seems that the thick Main Occupation Period pebble package that extends all



Fig. C22: Stone installation Locus:182908:051, with the remaining floor Locus:182908:056 towards the southeast. A patch of the pebble package Locus:182908:049 visible in the foreground. Photo by Jana Richter.

around Building P covered this installation, making it older than the Main Occupation Period. More data, however, are needed to ascertain this stratigraphic relationship.

C4.3 Structures and features of the Main Occupation Period

C4.3.1 The southeastern corner of Building P

A portion of the southeastern corner of Building P was uncovered within this trench. It was assigned Locus:182908:053, part of LGR:0381 (**Figs. C5, C12, C16**). The corner is built of roundish and longish cobbles of maximum lengths between 25 and 45 cm. The longish stones sit perpendicularly to the outer wall face. Up to three courses of stones are preserved above ground, but in most places fewer are visible. Following the technique used for the construction of the whole eastern part of Building P, which was built into the slope of the hill, the southeastern corner was also set against a cut opened into the virgin soil. This became visible when we made a small sounding near the looting pit (Locus:182908:023) which disturbed the area directly next to the corner. There, the removal of some virgin soil below the lowest visible stone course of the wall corner showed the presence of two to three additional courses of stones going deeper into the virgin soil. As they increase in depth, they recess towards the interior of the building, thus undercutting the outer wall edge. When seen from above (**Figs. C5, C12, C16**), the southeastern corner of Building P does not form a sharp angle, but follows a curved line that smoothly connects

the southern wall (LGR:0329) to the outer eastern wall of Room 59 (Locus:182909:035).

Two more features were found in connection to Building P. One is a patch of a pebble layer located south of the Building P's southeastern corner. It extends west into the neighbouring Square 181908, where it was described as LGR:0382. This layer, abutting the walls of Building P, may represent a remnant of the walking surface of Outdoor Areas 70 and 71 during the Main Occupation Period. LGR:0382 lies below a two-row stone installation, called LGR:0384, set against the southern face of Building P. This installation was also mentioned previously in our discussion of Square 181908.

C4.3.2 Outdoor Area 71

Outdoor Area 71 extends to the southeast and east of Building P, up to the excavation limits, merging to the west with Outdoor Area 70, which extends south of Building P (**Figs. C5, C12**). In Outdoor Area 71, we encountered several patches of a thick pebble layer, very similar to the aforementioned LGR:0382. It is made of pebbles mixed with several pottery sherds, going down to the virgin soil. This layer must have originally formed a large, thick pebble package that extended around Building P. It is better preserved on the east of this building in Square 182909 (§C5.2.4). Modern looting pits damaged this feature, leaving behind only a few distinct, discrete patches. The upper surfaces of these patches are interpreted as remains of the original walking surface of Outdoor Area 71, used at the time of the Main Occupation Period. Each patch

has been documented with two loci, one for the thick pebble layer and another for its upper surface. One is Locus:182908:047 (**Figs. C23, C24: section B**), located in the northeastern quarter of the trench. It continues to the north into Square 182909, where it corresponds to the pebble layer Locus:182909:063 (**Fig. C24: section A**). The latter abuts Building P from the east; hence, the pebble accumulation Locus:182908:047 is also deemed to belong to the construction of Outdoor Area 71 during the Main Occupation Period. Above this, Locus:182908:047 shows a flat horizontal surface, which was given the name Locus:182908:057 and likely represents the ancient walking surface. This surface also continues north into the neighbour-



Fig. C23: Pebble surface Locus:182908:047 in Outdoor Area 71, damaged by modern looting pits. Photo by Jana Richter.

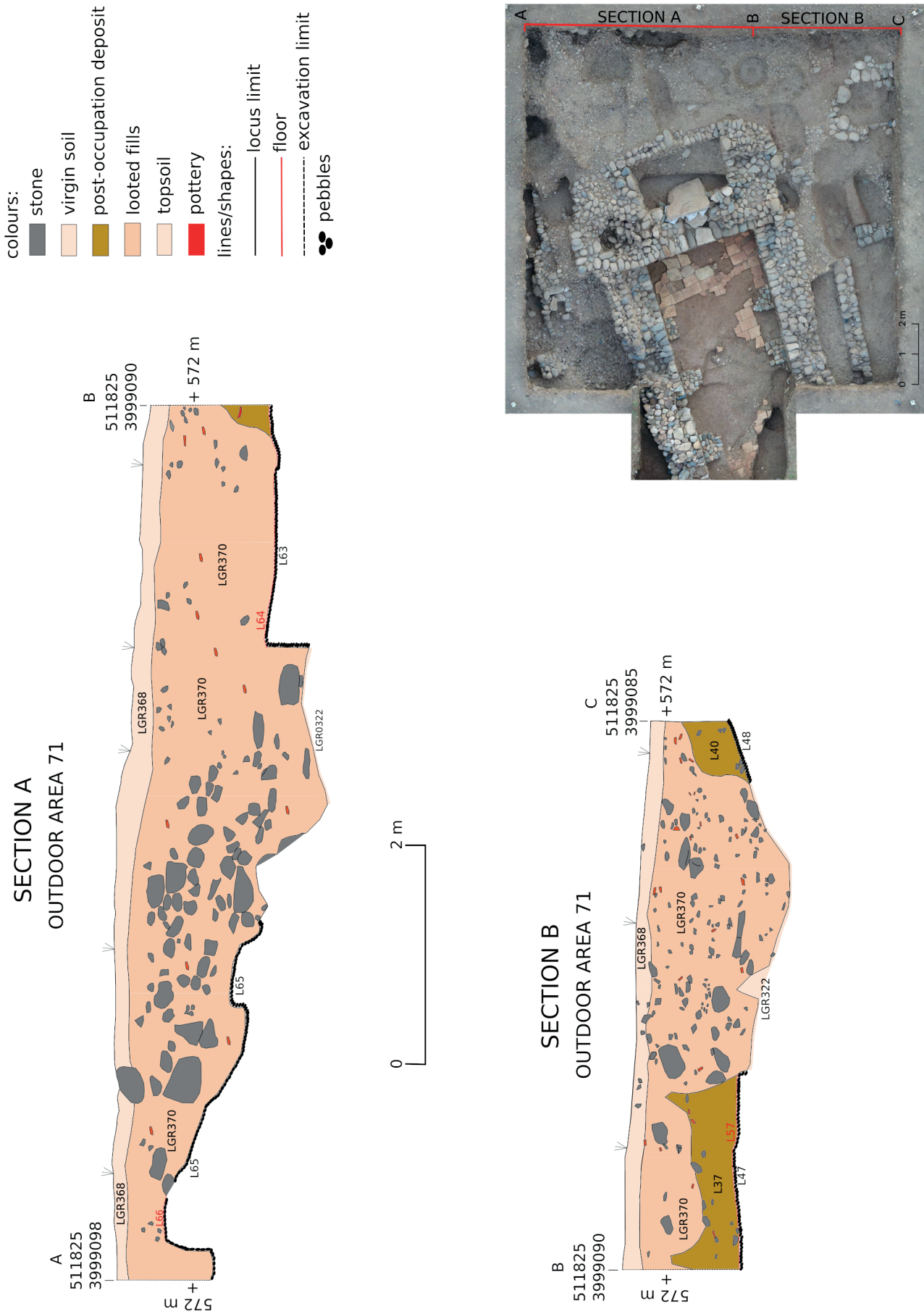


Fig. C24: Section A: eastern section drawing in Square 182909 (drawn by Jean-Jacques Herr and Abubakr Qasim). Section B: eastern section drawing in Square 182908 (drawn by Jana Richter). Digitisation by Alessio Palmisano. Prepared by Andrea Squitieri.

ing Trench 182909, where it is called Locus:182909:064 (**Fig. C24: section A**).

Right in the southeastern corner of the trench is another patch of pebbles, called Locus:182908:048. Though physically separated from Locus:182908:047, it may be equated with it (**Figs. C5, C24: section B**). To the northwest, near the feature LGR:0384, a pebble package (Locus:182908:049) was also found; it slopes upwards between two looting pit cuts (**Figs. C5, C22**). A portion of this pebble layer covers the western part of the stone feature Locus:182908:051, described above, thus suggesting that the latter is older than the Main Occupation Period. However, Locus:182908:049 is composed of stones which appear to be larger than those observed in the rest of the pebble package across Outdoor Area 71. For this reason, and also due to the lack of any physical connection, it is not clear that Locus:182908:049 belongs to the Main Occupation Period or constitutes a part of the pebble package extending across Outdoor Area 71.

C4.4 Deposits of the Post-Main Occupation Period

Some patches of the pebble package in Outdoor Area 71 were covered by deposits made of a hard and clayey soil with a yellowish colour. These deposits were clearly distinguishable, both in appearance and composition, from the darker, loose fills of the modern looting pits; they are interpreted to be the preserved remains of fills formed during the Post-Main Occupation Period, that is after the structures of the Main Occupation Period had been abandoned. One such deposit is Locus:182908:037 (**Fig. C24: section B**), located in the northeastern portion of the trench, where it covers the pebble package surface called Locus:182908:057. One additional post-occupation deposit is Locus:182908:040, covering a pebble layer (Locus:182908:048), located in the very southeastern corner of the trench (**Fig. C24: section B**). No diagnostic ancient find was retrieved from either deposit. Their affiliation to the Post-Main Occupation Period is only based on their colour and consistency, which, as mentioned, differ from the surrounding looting pits.

C4.5 Grave 103

In the southwestern portion of the trench, the burial Grave 103 was identified (**Figs. C5, C17**). This is a NE-SW-oriented cist burial measuring c. 1.6×0.6 m. Its lining is made of two courses of stones (Locus:182908:018) (**Fig. C25**). The cist was clearly set on top of installation Locus:182908:051

because the stones belonging to the latter were visible at the bottom of the grave pit. Most of the northern and eastern part of the cist were preserved, whereas the western and southern parts had been disturbed by modern looting activity. One trapezoidal, whitish stone slab, c. 50 cm wide, was found covering the central part of the cist. Most likely it was *in situ* or very close to it. Despite having been robbed, parts of the skeleton, (Locus:182908:041) were found. This skeleton (**Fig. C26**) was in an extended supine position. The pelvis and femur areas were better preserved as they were covered by the stone slab. The other bones were fragmented into many pieces held together by the surrounding soil. Remains of the elbow bones indicate that the left arm was originally in a flexed position; the right arm's bones were not preserved at all. Some teeth were found within the area of the crushed jaw and skull. They were sampled for dating purposes but proved to be unsuitable for radiocarbon analysis. A few items were found on the skeleton, most notably a well-preserved bronze ring, found inside the pelvic cavity (**§E1, no. 19**). The dark brown grave fill was excavated as Locus:182908:019. It contained some pottery sherds, as well as two iron pins (PPP 182908:019:003, PPP 182908:019:004, **§E1, no. 22**), one small iron bracelet (PPP 182908:019:002, **§E1, no. 21**), and fragments of at least two more iron rings (PPP 182908:019:005, PPP 182908:019:008, **§E1, no. 23**). Immediately above the grave, a looted fill was excavated as Locus:182908:042. In it, a bronze bead (**§E1, no. 99**) was found that may belong to the Grave 103 furniture; also the looted fill Locus:182908:011, which partially covered Grave 103, probably derived from the looting of that same grave; it contained an iron rod (PPP 182908:011:003: **§E1, no. 62**) that may have originated there.

Because Grave 103 is a cist grave, and includes the remains of a white stone slab used as a capping, it is possible that it is contemporary with Graves 102 and 105, described above (**§C3.5**). See also **§K**.

C4.6 The modern looting pits and the topsoil

The stratigraphy of this trench was irremediably damaged by the recent heavy looting activity (**Fig. C21**). As in the rest of QID1, the fills of the looting pits consisted of loose, dark brown soil, which assumed a more greyish colour in some cases. These fills contained pebbles, pottery sherds, animal bones, and several modern finds amongst the ancient ones. The cylinder seal PPP 182908:008:006 was found in fill Locus:182908:008 (**§E3.1**). The pit cuts were not always clear as they frequently superimposed on each other. Nevertheless, it seems that, on the eastern side of the trench, looters proceeded in a north-south direction, as some pits

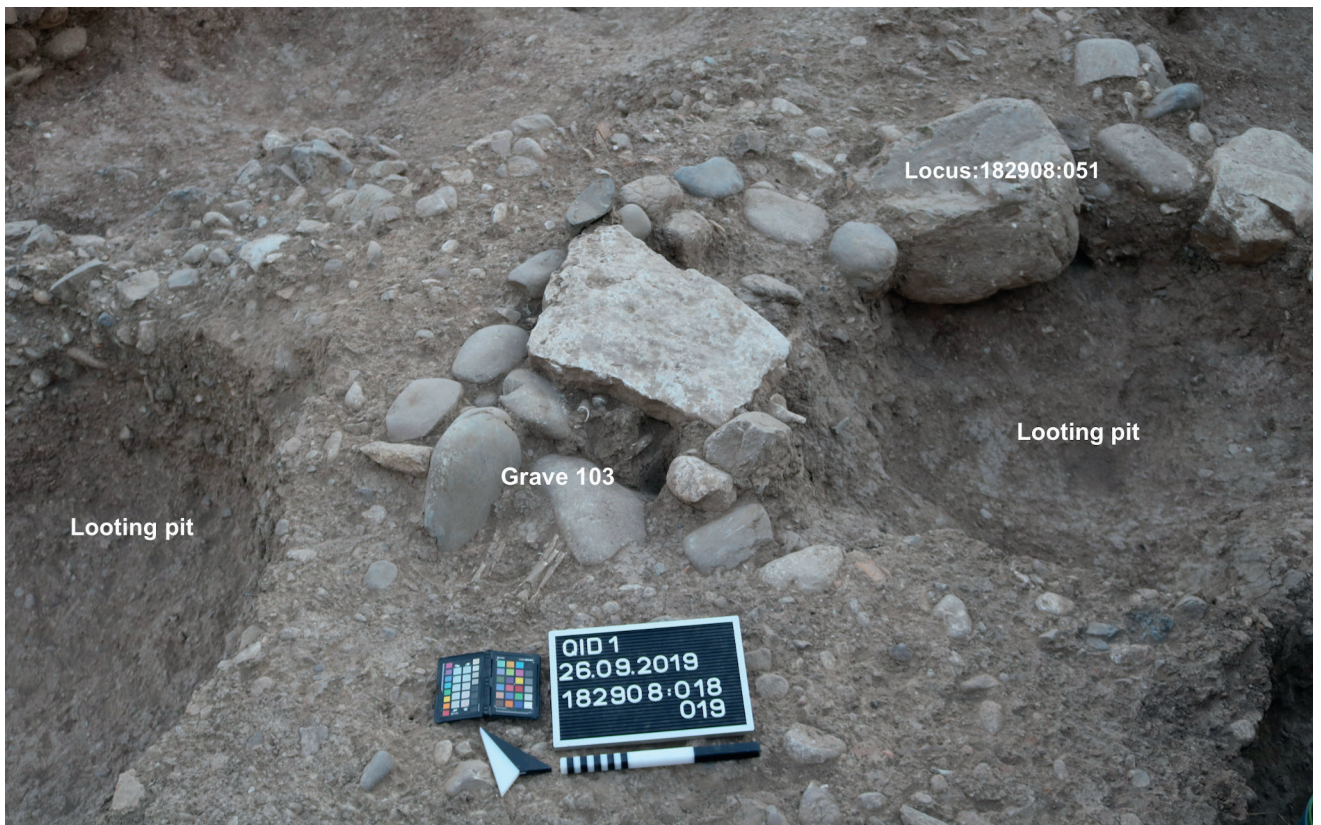


Fig. C25: Cist Grave 103 with the remains of its capping (white stone slab). Photo by Hero Salih Ahmed.

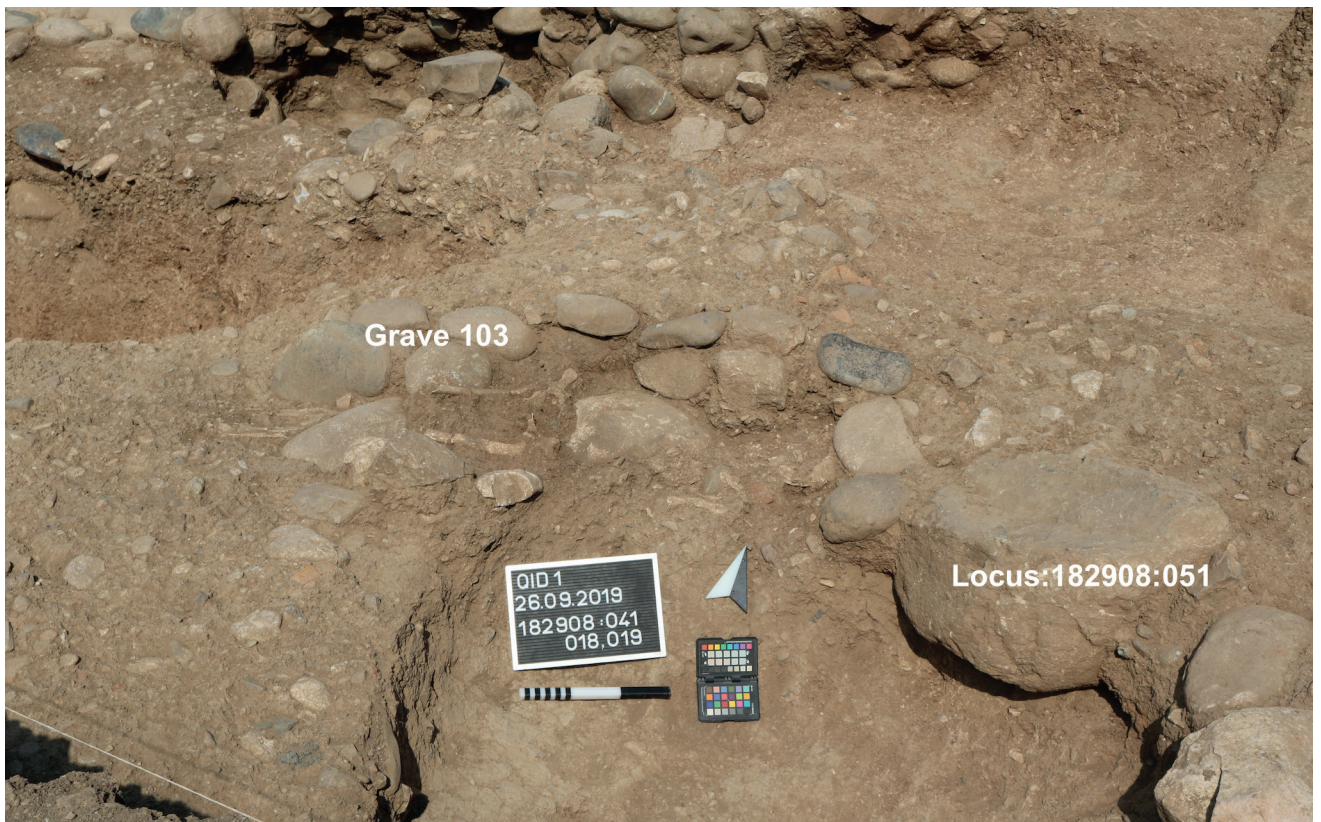


Fig. C26: Skeleton of Grave 103. Photo by Hero Salih Ahmed.

were aligned this way (for example, Trench 182909). As we have done before, all looting pits were grouped into the single locus group LGR:0370. The table below summarises the looted fills grouped within LGR:0370.

Looted fills in trench Square 182908 (part of LGR:0370)	
Locus numbers	Notes
Locus:182908:004, Locus:182908:020 Locus:182908:010, Locus:182908:028 Locus:182908:029, Locus:182908:012 Locus:182908:021, Locus:182908:039 Locus:182908:043, Locus:182908:045 Locus:182908:052, Locus:182908:055 Locus:182908:003, Locus:182908:027 Locus:181908:032, Locus:182908:015 Locus:182908:017, Locus:182908:024	Generic disturbed fills containing pottery sherds, animal bones, and modern items, all embedded in a dark-brown or greyish soil, alternating between a loose and a more compact consistency.
Locus:182908:005, Locus:182908:007 Locus:182908:026, Locus:182908:038 Locus:182908:046, Locus:182908:008 Locus:182908:033, Locus:182908:013 Locus:182908:034, Locus:182908:035	Disturbed fills yielding several ancient finds, some of them possibly originating from a nearby destroyed grave. A cylinder seal was found in fill Locus:182908:008 (§E3.1).
Locus:182908:042, Locus:182908:011	Disturbed fills connected to Grave 103, yielding finds which in part may have originated there (§E1, nos. 62 and 99).

All features excavated in this trench were covered by the topsoil. The latter was excavated in three loci, namely Locus:182908:002, Locus:182908:006, and Locus:182908:022, then grouped together into locus group LGR:0368. The topsoil did not show any trace of looting.

C4.7 Conclusions

Overall, more than 70% of the entire volume of excavated material from the trench in Square 182908 was composed of looting deposits. Despite this considerable level of disturbance, four pre-modern phases could be observed:

- A phase older than the Main Occupation Period, to which the stone structure Locus:182908:051 belongs.
- The Main Occupation Period, to which the southeastern corner of Building P and various patches of the pebble package of Outdoor Area 71 belong.
- A Post-Main Occupation Period, to which some deposits, missed by the looters, belong.
- The partially disturbed Grave 103, surely younger than the stone structure Locus:182908:051, but whose stratigraphic relation to Building P and the pebble package is not clear. Given its architecture, it is possible that it is contemporary with Graves 102 and 105.

C5. The trench in Square 182909

Jean-Jacques Herr & Louise König

The trench in Square 182909 extends by 8×5 m to the east of Building P, and to the north of the previously discussed trench in Square 182908 (Figs. C4, C5). It was opened with two principal goals. First, to complete the excavation of Building P Room 59, which had been partially uncovered in 2018⁵⁸; second, to investigate the features located east of Building P, in the area dubbed Outdoor Area 71. The sections below will present the excavated features in stratigraphic order, from the oldest to the youngest, although the heavy looting activities that occurred in the modern period have, in many cases, made it difficult to establish precise stratigraphic relationships.

C5.1 Virgin soil

The virgin soil was reached in several locations, designated with different loci numbers and grouped into the locus group LGR:0322 (composed of Locus:182909:069, Locus:182909:070, Locus:182909:071, Locus:182909:017). As throughout QID₁, the virgin soil is a reddish, clayey soil with white inclusions, devoid of any artifacts. It may represent the ancient slope of the hill against which, and partially cutting into, Building P and the features of Outdoor Area 71 were set.

C5.2 Features of the Main Occupation Period

C5.2.1 Room 59 of Building P

Room 59 (Figs. C5, C12) is a small room located east of the much larger Room 58, to which it is connected via a 1.2 m wide threshold (Locus:181909:022), uncovered in 2018. Room 59 has a slightly trapezoidal layout, measuring about 1.6 × 2.9–3.3 m. It is bordered on the north and the south by the northern and southern walls of Building P. To the west, the room is bordered by the wide wall LGR:0321 (equipped with a threshold, as mentioned above), while to the east, it is bordered by a thinner wall about 3.3 m long. Because the eastern side is longer by about 40 cm than the western side, Room 59 has a trapezoidal layout. During 2018, only the western part of the room was excavated. Its excavation was completed during the 2019 campaign.

⁵⁸ Herr 2019, 53–55.

C5.2.2 The walls of Room 59

The walls of Room 59 lie on virgin soil. The southern wall was only partially exposed in 2018, when it was named Locus:181909:032; by then it was already clear that this wall was set at a higher level than the wall of the adjacent Room 58 (LGR:0321), thus conferring a stepped profile to the entire structure of Building P. The threshold between Room 58 and Room 59 is 90 cm higher than the floor of Room 58, indicating that Room 59 was intended to be at a higher level. In 2019, wall Locus:181909:032 continued to be excavated to the east as LGR:0381 (Fig. C27). Although it was badly damaged by looting activity, on the eastern part it is possible to see that this wall is about 1 m high, and is composed of 6 courses of large cobblestones set perpendicular to the wall's alignment. The wall's core was filled with smaller stones. Its eastern face, which corresponds to Building P's southeastern corner, is set partly against the virgin soil, and, as already noticed in Square 182908, has a curved shape (Fig. C16).

The northern wall of Room 59 was uncovered in 2018 and documented as Locus:181909:030, now part of



Fig. C27: Room 59, the southern and eastern walls. Photo by Jean-Jacques Herr and Louise König.



Fig. C28: Room 59, the eastern and northern walls. Photo by Jean-Jacques Herr and Louise König.

LGR:0376. It is made of 4-5 courses of cobblestones (about 70 cm in total height), which, in contrast to the southern wall, are aligned with the direction of the wall (Fig. C28). In 2019, it was discovered that this wall is part of a larger structure constituting the northeastern corner of Building P, which, despite being heavily damaged by looters, clearly differs from the southeastern corner. This corner will be better described in the discussion of Square 181909.

The eastern wall of Room 59, called Locus:182909:035, contrasts strikingly with the other walls of Building P as, at 40-50 cm wide, it is considerably thinner (Fig. C29). Moreover, only its inner face is visible, while the opposite face is completely covered by the pebble package that forms the walking surface of Outdoor Area 71. The wall is made up of only one row of cobblestones, about 20-30 cm long, laid in 5-6 courses, and set perpendicularly to the wall's direction. Like the southern wall, it is preserved at an elevation of about 1 m. In the middle of the wall, one larger boulder, about 65 cm long, was set in the uppermost course of stones. It appears that in order to build this wall the virgin soil had been dug so that the wall could lean against it. On the inside, it can be seen that the wall is not straight but slightly slanted towards the west. On the top, the wall's cobblestones are doubled, with the addition of another row of stones. Here, the upper part of the wall meets the walking surface of the pebble package Locus:182909:065, which extends to the east of Building P (Fig. C30).

C5.2.3 The large stone slab and the floor of Room 59

In 2018, when the western portion of Room 59 was excavated, it was already clear that this room had been completely looted, down to the virgin soil. In that year, we found a massive stone slab in an upright position in



Fig. C29: Room 59, the eastern wall. Photo by Jean-Jacques Herr and Louise König.



Fig. C30: Outdoor Area 71 in the foreground, with the looting pits damaging its pebble floor abutting the eastern wall of Room 59. Photo by Jean-Jacques Herr and Louise König.

the middle of the room, called Locus:181909:026⁵⁹. In order to proceed with the excavation, it was necessary to lean it against the eastern limit of the excavation area (see Fig. C31, depicting the situation during the 2018 campaign). Because we continued excavation towards the east in 2019, we moved the massive stone to the western limit of Room 59 (supporting it with bags of soil). This stone slab was described in detail in the previous excavation report; the following comments are only a brief summary of that information. It is a squarish, 14 cm thick, quarried block of white limestone, measuring 1.55×1.27 m. It shows a carved circular depression on one corner, with a diameter of 19 cm. Despite the additional excavation of this room, its original use remains unclear. It is possible that it was lifted up by looters expecting to find a grave underneath, which would explain why we found it in an upright position in 2018. Whether it was originally part of the floor of the room, with the circular depression functioning as a door socket, or whether it was used in other ways (e.g., as a podium) is not certain. It is also possible

that it was misplaced by the looters and its original location must be sought elsewhere in the vicinity.

The 2019 excavations in this area revealed that the looters must have stopped at the room's floor level on the eastern side of the room. This appears as a concentration of pebbles and pottery sherds embedded in a greyish soil matrix, called Locus:182909:023 (Fig. C32), and extending along Room 59's entire length. Perhaps it was the original walking surface that had been destroyed by the looters in the western part of the room. Assuming that Locus:182909:023 was the original floor level of Room 59, then the difference in height between it and the threshold leading to Room 58 is about 30 cm.

C5.2.4 Outdoor Area 71

In the eastern side of Room 59, we encountered a thick and dense layer of pebbles mixed with pottery sherds embedded in a grey-brown soil, which was lying directly above the virgin soil (Figs. C5, C12, C33, C34). This pebble package covers the entire extension of the trench. It continues into the southern trench in Square 182908, as mentioned above (§C4.3.2), and parts of it were also un-

59 Herr 2019, 53-55.

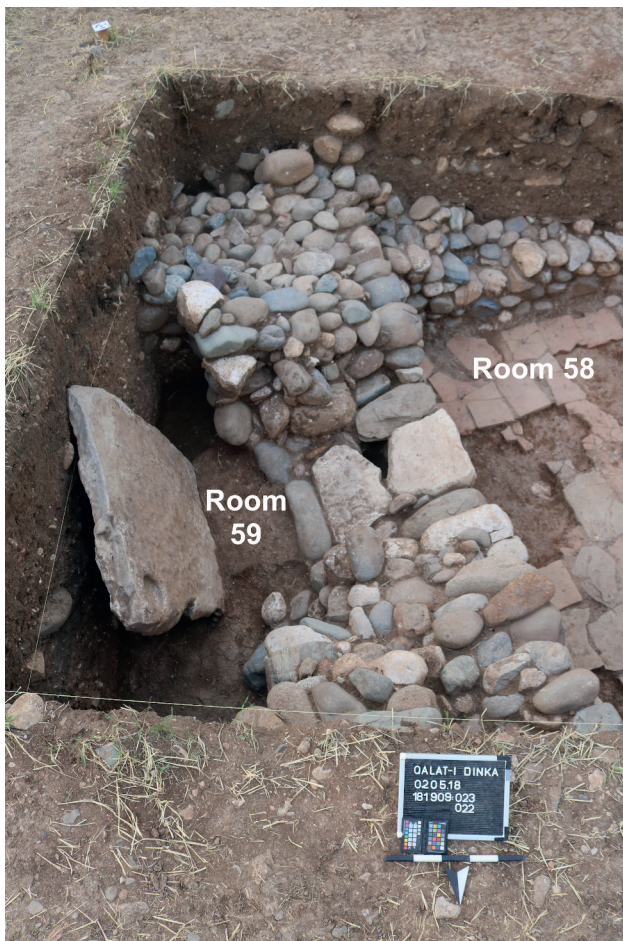


Fig. C31: Room 59 at the end of the 2018 excavation campaign with the large stone slab Locus:181909:026 found in the room in upright position. Photo by Jean-Jacques Herr.

covered in the trench 181908 (§C3.4). This pebble package was heavily damaged by looting pits, whose excavation showed that the package of pebbles and pottery sherds reach a depth of about 1.5 m (Figs. C21, C34, C35). The various spots where it had been left undamaged were assigned different loci. In particular, each spot was assigned a locus for the pebble package itself, and one for its upper surface. The pebble packages are Locus:182909:065, Locus:182909:063, Locus:182909:068 (Figs. C21, C24: section A), to which the following surfaces correspond: Locus:182909:066, Locus:182909:064 and Locus:182909:072, respectively (Figs. C21, C24: section A). These surfaces are thought to belong to the Main Occupation Period as they represent the walking surfaces used at that time. It is noteworthy that the pebble package abuts Building P from the east, and for this reason it is considered contemporaneous with the latter.



Fig. C32: The pebble floor of Room 59. Locus:182909:023. Photo by Jean-Jacques Herr and Louise König.

C5.3 Graves 101, 109 and 110

In the northern portion of the trench, three graves were found (Fig. C17). Graves 101 and 109 are cremation burials, while the Grave 110 is a simple pit grave. They had been all partially robbed, but some of their features can be reconstructed. Most notably, Grave 110 yielded a partially preserved skeleton, from which a tooth (Locus:182909:067:017) has yielded the radiocarbon dates of 767-488 calBC (see Table C1). The sections below describe the graves and discuss their stratigraphic position in relation to the Main Occupation Period features.

C5.3.1 Grave 101

Grave 101 (Figs. C5, C17) is a cremation burial whose urn was found intact: fortuitously, it was missed by the looters. However, the rest of the burial was affected by looting so it is not possible to clearly define its outer boundaries (Fig. C35). The edges of the grave seem to have been defined by a burnt clay lining that is orange in colour with darker spots (Locus:182909:044). This lining defines a rectangular pit, measuring about 2 m from east to west. In the southeastern portion, this lining was completely obliterated by looters. Inside the lining we found ashy layers (Locus:182909:008 and Locus:182909:048), along with a dark brown fill (Locus:182909:009, Locus:182909:033 and Locus:182909:045). The limits of the grave pit were identified thanks to the discovery, at the bottom of the pit, of a powdery, white-grey, ashy layer, which included many heavily fragmented bones (Locus:182909:008 and Locus:182909:048) (Fig. C36). The urn was located inside the pit. This carinated jar with a neck (PPP 182909:009:002) was found intact, standing on the bottom of the pit



Fig. C33: The pebble floor of Outdoor Area 71, damaged by the looting pits. Photo by Jean-Jacques Herr and Louise König.



Fig. C34: Northeastern corner of Outdoor Area 71. Photo by Jean-Jacques Herr and Louise König.



Fig. C35: The cremation burial Grave 101, with the cremation burial Grave 109 in the background. Photo by Jean-Jacques Herr and Louise König.

(§D1.2.2); its top became visible around 60 cm below the site surface. The urn's mouth was covered by a broken, but complete, carinated bowl (PPP 182909:009:003), set upside down (§D1.2.2 and Fig. C37). Around and underneath the urn (Fig. C38), several other grave goods were unearthed, most notably six decorated hollowed bone tubes (§E1, no. 7), fragments of metal items, and a golden earring (§E1, no. 9).

The urn contained a dark brown soil (Locus:182909:022) in which several fragments of human and animal bones were found. The bones were very fragile, and many of them looked as if they had been exposed to fire⁶⁰. A human long bone was sent to the laboratory for radiocarbon analysis; unfortunately, it did not contain enough collagen for dating. No artifacts were found inside the urn, with the exception of one shapeless metal fragment (§E1, no. 10). Four drop-shaped pebbles were found, which did not look worked. Three of them are dark red, while the fourth is translucent white (§E1, no. 11).

⁶⁰ According to the assessment of the archaeozoologist Anja Prust after her on-site autopsy of the bones in autumn 2019.

The characteristics of the grave lining (Locus:182909:044), which seems to have been exposed to fire, and the presence of ashy and powdery layers at bottom of the pit would point to a fire event. In our reconstruction, the pit was created to host the cremation ritual. After the incineration, the pit may have been partially cleaned, and the bones (or some of them) gathered into the urn. Finally, the urn, with its bowl lid, and most of the goods were placed into the pit. Most of the grave goods did not look burnt, as was the case of the fragmented decorated bone tubes; however, a bronze item was also found next to the urn which appeared to have been melted (Fig. C38, no. 6). Hence, it is possible that some grave goods had been deposited with the body before incineration, while others were placed there afterwards. Further analysis is required to better understand and reconstruct the process of this cremation. Due to the modern disturbances, the stratigraphic relationships of Grave 101 are not easily reconstructed; however, it seems that the grave cut the pebble package, Locus:182909:066. This would make Grave 101 younger than the construction of the Outdoor Area 71 floor.



Fig. C36: Cremation burial Grave 101, with its withish and ashy layer at the bottom of the grave pit. The red × shows the location of the urn. Photo by Jean-Jacques Herr and Louise König.

C5.3.2 Grave 109

About 2 m east of Grave 101, another cremation burial was found, named Grave 109 (Figs. C5, C17, C35 and C39). Unfortunately, it had been damaged by two looting pits on the southern and the eastern sides. As in the case of Grave 101, Grave 109 also seems to cut the pebble package of Outdoor Area 71. The edge of Grave 109's pit has been preserved on its western side; this edge consists of a line of burnt clay with an orange colour and some darker spots; it is similar to the lining of Grave 101. The upper fill of the pit was a light brown soil with pebbles (Locus:182909:050), which covered a carinated bowl set upside down (PPP 182909:051:001, see §D1.2.3). The bowl was embedded in a fill of brown and white ashy soil (Locus:182909:051). In the northeastern part of the pit, we found an accumulation of fragments of fragile human bones (PPP 182909:051:002) (Fig. C40). This ac-



Fig. C37: The urn of Grave 101 as it was found still *in situ*, with a broken but complete bowl on top of its mouth in an upside down position. Photo by Jean-Jacques Herr and Louise König.



Fig. C38: Positions of some of the items collected from around the urn (no. 8, after removal) of Grave 101. For the bone tube fragments nos. 1-5 see §E1, no. 7; and for the bronze fragments nos. 6-7 see §E1, nos. 1-2. Photo by Jean-Jacques Herr and Louise König.

cumulation included parts of a cranium, as well as some finger bones. North of the carinated bowls, a few ribs were also found. Underneath the bowl were the remains of an epiphysis of a femur along with a loose, powdery, white fill (Locus:182909:052) (Fig. C41). Some of the bones which were underneath the bowl had an intensely white or grey colour, possibly because they had been exposed to fire. Unfortunately, none of these bones were suitable for radiocarbon dating. The grave goods consisted of a single white stone bead (PPP 182909:052:005), found underneath the bowl (§E1, no. 12). Like Grave 101, Grave 109 showed traces of fire on the preserved walls of the grave pit. As we have seen, this was filled with ashy layers including several bone fragments, both around and underneath the bowl, which looked as if they had been exposed to fire. For these reasons, we interpret



Fig. C39: Cremation burial Grave 109. Photo by Jean-Jacques Herr and Louise König.



Fig. C40: Grave 109 with a bone concentration on the north-eastern side. Photo by Jean-Jacques Herr and Louise König.



Fig. C41: Bones found underneath the bowl in Grave 109. Photo by Jean-Jacques Herr and Louise König.

Grave 109 as a cremation burial. Unlike Grave 101, however, the bones of Grave 109 were not all gathered inside an urn, but were partly below and around it. Whether this was intentional or the product of later disturbances is not clear.

C5.3.3 Grave 110

Another grave was identified about 2 m south of Graves 101 and 109: Grave 110 (Figs. C5 and C17). Unlike the previous two, Grave 110 is an inhumation burial in a simple pit. Unfortunately, it was damaged by looters who dug two pits on either side of the grave (Locus:182909:013 and Locus:182909:025) (Fig. C42). It was possible to observe that the grave pit cut the pebble package of Outdoor Area 71, which in this spot is called Locus:182909:065. The southern part of the grave is missing where a looting pit was dug. However, the northern part still contained the grave's fill (Locus:182909:059) and the remains of the up-

per part of a skeleton (Locus:182909:067), which lay directly on top of the pebble package Locus:182909:065 (Fig. C43). The body was laid on its back, with its head facing east. The lower skeleton is missing, from the ilium to the phalanges of the feet. The left arm was bent so that the mouth was covered by the hand, and the left thumb was found next to the left clavicle. The lower ends of the humerus, radius, and ulna were not preserved as they were damaged by the looters. The thoracic vertebrae were in place, and there the ribs were in contact with each other. The scapulae were badly preserved, which prevented us from removing them in one piece. On the right side of the skeleton, the humerus was extended and the lower epiphysis is missing as well as the radius, ulna, and the hand. Although fractured, the cranium was well preserved with visible sutures. The mandible and the maxillary were well preserved, although not in contact with each other. The left and right maxillaries still joined. The mouth was found open, likely due to taphonomic processes. As mentioned previously in §C2.1, a tooth was radiocarbon dated to 767-488 calBC (Table C1).

During the excavation of Grave 110, it became clear that some of the bones had shifted position. The mandible had fallen down, leaving the mouth open. The ribs had all moved towards the lower part of the body, as had the clavicles. The joints between the metacarpal bones and the finger phalanges showed a depression, as if this part also had fallen down. Moreover, the sternum and rib cage were missing and the centre of the preserved thoracic vertebrae looks badly damaged. To explain these changes in position, we hypothesise that the body was not buried directly in the soil, but was originally covered by stone slab or a wooden lid. This capping must have prevented the body from being fully covered by soil before it completely decomposed, thus allowing some of the bones to shift position (namely the mandible, ribs, clavicles). If the body



Fig. C42: Inhumation Grave 110 with the remaining part of the skeleton. Photo by Jean-Jacques Herr and Louise König.



Fig. C43: The skeleton of Grave 110 with two of the objects still visible *in situ*: 1: Fibula PPP 182909:067:004 (discussed in §E2); 2: cylinder seal PPP 182909:067:007 (discussed in §E3). Photo by Jean-Jacques Herr and Louise König.

had been fully covered with soil when it was interred, these bone movements would not have occurred. Concerning the age, we could not find the third molars, and

the epiphyses had not finished joining with the diaphysis. Hence, the individual may have been young⁶¹.

Grave 110 yielded several grave goods, some visible in **Fig. C43**. Next to the lower part of the left humerus, we found a completely preserved cylinder seal, PPP 182909:067:007, with its glass cap PPP 182909:067:008 (§E3.2). From the area of the left pectoral and underneath the ulna, we found two bronze fibulae, named PPP 182909:067:010 and PPP 182909:067:011 (§E2.1). Next to the right shoulder, another bronze fibula was found (PPP 182909:067:004) (§E2.1). One carnelian bead (PPP 182909:067:001) and one white incised bead (PPP 182909:067:003) were found next to the right ear (§E1, nos. 48-49). A shapeless, rock crystal (quartz) fragment, PPP 182909:067:009, was found underneath on one of the left ribs (§E1, no. 46). A fragment from an Egyptian Blue bead PPP 182909:067:005 was found in the fill, along with tiny fragments of gold (§E1, nos. 46-47).

Given the available evidence that these graves cut the pebble package of Outdoor Area 71, it is possible to give the graves a *terminus post quem* following the construction of the Main Occupation Period floor.

C5.4 The modern looting pits and the topsoil

C5.4.1 The fill of Room 59

As mentioned above, the fill of Room 59 had been completely looted and contained no undisturbed remains. In 2019, this fill was excavated as Locus:182909:016. The fill is part of the locus group LGR:0305, which was created in 2018 to incorporate all of the looted fills in the area of Room 59⁶². This locus group is comparable to LGR:0370, which (as described above) combines all the remaining looted fills of QID1.

C5.4.2 Outdoor Area 71

As mentioned previously, Outdoor Area 71 had been extensively damaged by several looting pits (**Fig. C21**). These pits were filled with a dark brown soil mixed with variously-sized stones which must have originated from the ancient structures. We also found some irregular

⁶¹ The preliminary anthropological observations contained in this section were carried out by Jean-Jacques Herr and some of them may have to be revised once in-depth analyses can be carried out by a specialist in physical anthropology.

⁶² Herr 2019, 59, Fig. D21.

stone accumulations which must have been gathered by the looters. Some pits were circular, others were more ovoid, and they seemed to have been excavated in roughly regular rows in 50 cm to 1 m intervals. However, the pits frequently cut each other, which has made identifying the individual cuts very difficult. Apart from soil and stones, the looting pit fills yielded a combination of fragments of modern items, such as pieces of aluminium packages and cigarette filters, and ancient objects. The table below summarises the looting pit fills excavated in this trench, and grouped into LGR:0370.

Looted fills in trench Square 182909 (part of LGR:0370)	
Locus numbers	Notes
Locus:182909:018, Locus:182909:039	Generic disturbed fills containing pottery sherds, animal bones, and modern items, all embedded in a dark-brown, loose soil matrix.
Locus:182909:042, Locus:182909:053	
Locus:182909:054, Locus:182909:056	
Locus:182909:012, Locus:182909:032	
Locus:182909:041, Locus:182909:030	
Locus:182909:038, Locus:182908:032	
Locus:182909:006, Locus:182909:007	Disturbed fills yielding several ancient finds.
Locus:182909:010, Locus:182909:015	
Locus:182909:019, Locus 182909:024	
Locus:182909:027, Locus:182909:034	
Locus:182909:055, Locus:182909:014	
Locus:182909:026, Locus:182909:043	
Locus:182909:028, Locus:182909:047	Stone accumulations gathered by the looters.
Locus 182909:046	

All of the looting pits were covered with topsoil (LGR:0368) which did not bear any traces of looting activity, although it showed plough tracks left by the most recent agricultural activities (Fig. C44).



Fig. C44: The surface of the topsoil in Square 182909. Photo by Andrea Squitieri.

C5.5 Conclusions

As a result of the 2019 investigations in Square 182909, we have now completed the excavation of Room 59, having reached a pebble surface that very likely constitutes the room's floor. To the east of Room 59, Building P seems to have occupied an isolated position, as no other architectural structures have been identified there. Outdoor Area 71 extends to the east of Building P. Its walking surface is characterised by a pebble package mixed with pottery sherds. Because this pebble package abuts Building P, we consider both to belong to the Main Occupation Period.

We identified three graves which seem to have been cut into the pebble package. Two are primary cremation burials (Graves 101 and 109) while one is a simple inhumation pit (Grave 110). The latter yielded a radiocarbon date range of 767-488 calBC (Table C1). These graves seem to be stratigraphically younger than the Main Occupation Period. However, it is not possible to establish whether they were all contemporary with each other. Finally, several looting pits have been encountered that damaged the graves, the pebble package, and the fill of Room 59.

C6. The trench in Square 181909

Alessio Palmisano & Sophie Pietsch

The 2019 trench in Square 181909 extends the northern portion of the 2018 excavation area (Figs. C3, C5). In total, this trench measures 4 m towards the north and 7 m towards the east, where it connects with the trench in Square 182909. The goals for this trench were to complete the excavation of the northern wall (LGR:0319) and north-eastern corner (LGR:0376) of Building P, and continue the excavation of what, in the 2018 campaign, was labelled Room 60 but in the 2019 campaign was renamed Outdoor Area 60: a seemingly open space extending north of Building P. The following sections will describe the features excavated in this trench in stratigraphic order.

C6.1 The Main Occupation Period

C6.1.1 The northern portion of Building P

During the 2019 campaign, we exposed the northern face of wall LGR:0319, Building P's northern wall, which runs parallel to wall LGR:0329 on the south. A portion of it had

already been partially exposed in 2016 and 2018⁶³. Combining the results from the previous campaigns, LGR:0319 appears to be a large wall, exposed for a length of about 8 m (Figs. C5, C12). However, its original length may be longer, as its westernmost limit has yet to be reached. It is 1.4 m wide on the west, increasing to about 1.6 m in the east, and it runs parallel to the southern wall LGR:0329, whose width also increases as it moves east. In the portion of the wall exposed in 2019, we uncovered two looting pits: one about 80 cm west of wall LGR:0321; and another, larger, about 2.5 m to the west of the previous one. Several stones were removed by looters; however, the wall structure is still clear. The northern face of wall LGR:0319 is about 1.6 m high, and shows 7 to 9 courses of cobblestones (Fig. C45). The cobblestones are c. 30-45 cm long and are set perpendicularly to the wall's alignment; they encase a core of smaller stones with a diameter of about 10-25 cm. No mortar was observed between the stones. It shares a particular feature with southern wall LGR:0329. On its southern face, an approximately 2.5 m long step can be



Fig. C45: Northern face of wall LGR:0319, the northern wall of Building P. Photo by Alessio Palmisano.



Fig. C46: Southern face of wall LGR:0319. Photo by Alessio Palmisano.

seen. It is about 80 cm wide, and it begins at the eastern wall LGR:0321 (Fig. C46). Behind it, a narrower portion of the wall rises for another 50-55 cm. As with southern wall LGR:0329, this step is only found on the inner face, and it is about 70-75 cm higher than the floor level of Room 58. It is too regular to be the result of the modern looting, so we assume that it was part of the original wall structure. Beyond the step, towards the west, the wall is solid with no signs of any similar step. The function of these steps in both walls LGR:0319 and LGR:0329 is not clear.

As we observed in 2018, the eastern wall LGR:0321 is higher than both wall LGR:0319 and wall LGR:0329, thus forming a stepped structure. However, the northeastern corner of the building, which had been completely exposed in 2019, appears to differ from the southeastern corner, described above. The northeastern corner, called LGR:0376, is a squarish structure measuring 3.3 m in NE-SW direction and 2.1 m in NW-SE direction (Fig. C47). It is built with 35-45 cm long boulders, and flattish, 20-25 cm long cobblestones. This structure connects to wall LGR:0321 in the south, and with wall LGR:0319 to the west. The northern face was partially damaged by a looting pit. There had possibly been a revetment as some reddish remains of burned clay were found still adhering to it (Fig. C47). The top of LGR:0376 was unfortunately damaged by looters, who opened a round pit in the middle of it. Nevertheless, looking at the plan (Figs. C5, C12), LGR:0376 has a different appearance than the southeastern corner of Building P, giving the building an asymmetrical layout. It is possible that LGR:0376 had a different function from the southeastern corner, which is as yet unclear.



Fig. C47: Northeastern corner of Building P, LGR:0376. Photo by Alessio Palmisano.

63 Kreppner/Squitieri 2017a, 52 ("The Northern Sector"), Fig. C6 (labelled Locus:100000:006); Herr 2019, 49-52, Fig. D10.

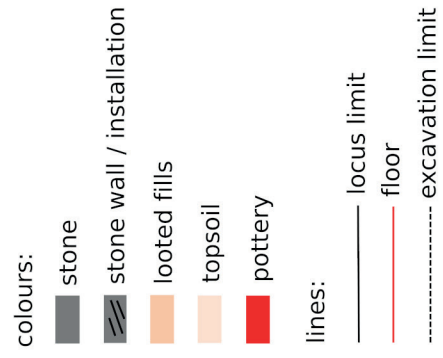
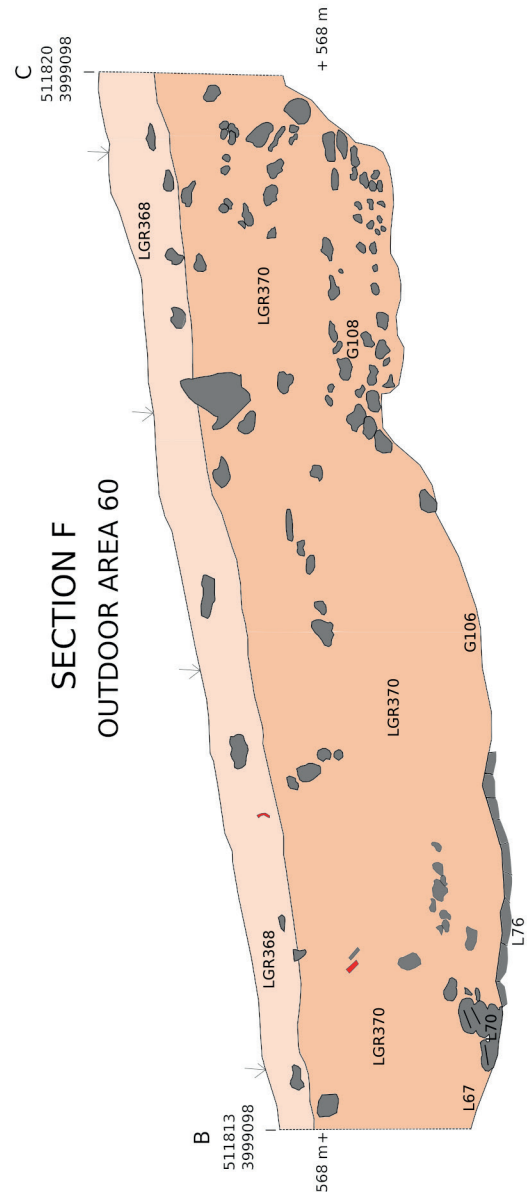
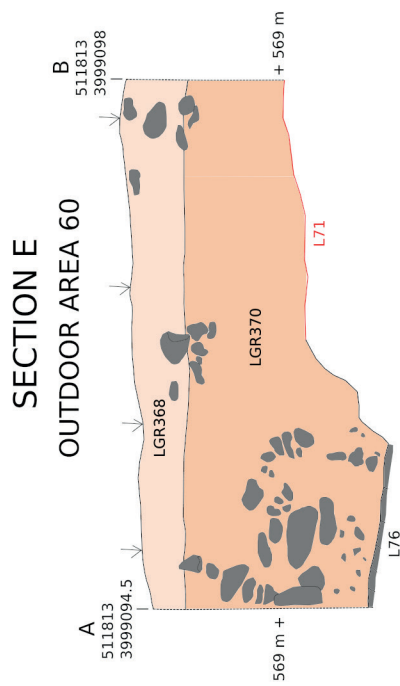
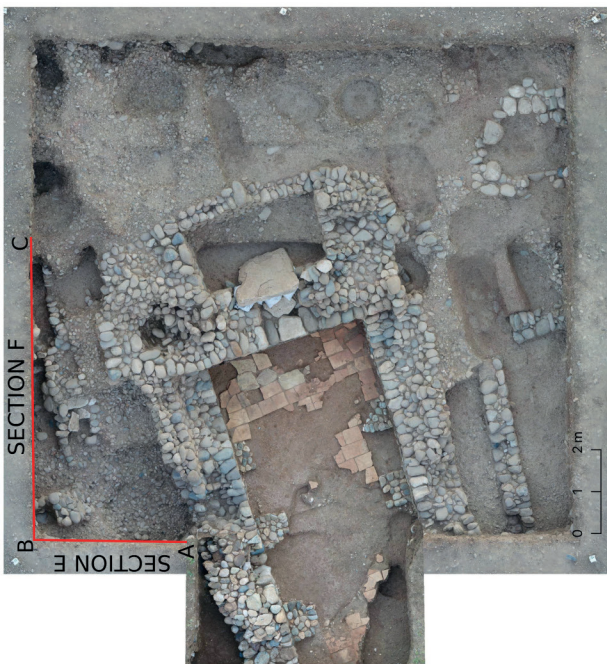


Fig. C48: Section E: northwestern section drawing. Section F: northern section drawing. Drawn by Sophie Pietsch, digitised by Alessio Palmisano. Prepared by Andrea Squitieri.

C6.1.2 Outdoor Area 60

Open Area 60 is a space measuring about 4×7 m located to the north of Building P (Figs. C5, C12). The western portion of this space was partially exposed in 2018, when it was named Room 60⁶⁴. In 2019, we expanded its excavation to the east and the north. As it appears to not be a walled space, we renamed it Outdoor Area 60. In the western part of the outdoor area, we reached a layer that was about 45-50 cm thick and made of a mixture of cobbles and pebbles, named Locus:181909:076 (Figs. C5, C12 and C48: sections E and F, C49). The cobbles are ovoid-shaped and measure approximately 15-20 x 10-15 cm. This layer abuts the lowest course of wall LGR:0319. We interpreted it to be a levelling layer laid beneath the outdoor area's floor. This floor was exposed in two spots: Locus:181909:061 and Locus:181909:071 (Figs. C49-C50). Before describing the floor, we need to mention a stone structure that was uncovered near the northwestern corner of the excavation area, labelled Locus:181909:070 (Figs. C5, C12 and C48: section F, C49, C50). This is a north-south-oriented structure that extends for about 1 m from the northern excavation limit (and continues beyond it). It is about 70 cm high and 80 cm wide and is made of four preserved courses of stones. Its northwestern section was partially damaged by a looting pit (pit cut: Locus:181909:066). Its size suggests that it is a preserved portion of a stone wall; however, the top view reveals none of the usual structural forms found in walls. To compare, the two walls in Square 181908, Locus:181908:065 and Locus:181908:066 (Figs C8 and C10), which are comparable to Locus:181909:070 in width, display two clear rows of stones with gaps filled with smaller stones in between when looked at from above; other similar walls exposed in 2016 also have the same structure⁶⁵. In contrast, Locus:181909:070 does not show clear rows of stones. It is possible that it represents another type of wall, built using different techniques, or that it is simply a badly preserved wall; however, it is also possible that Locus:181908:070 had a separate function which at the moment remains unclear.

The floors of Outdoor Area 60, Locus:181909:061, are formed by a mixture of cobbles, pebbles, and pottery sherds lying flat on the surface (Figs. C49-C50). Some of the cobbles are flattish and roundish, and measure 5-10 cm in diameter; others are ovoid and measure approximately 10-15 x 5-10 cm. This floor is only preserved to the north of Wall LGR:0319 and to the west of the northeast-

ern corner of Building P LGR:0376. The preserved portion is 1.65 m long and 1.25 m wide and it covers approximately a surface of 2 sqm. This surface abuts Wall LGR:0319 to the south and the northeastern corner of Building P (LGR:0376) to the east. The deposit found directly on the floor is called Locus:181909:055. It yielded several pottery sherds, bone fragments, and a complete ceramic bowl (PPP 181909:055:001, see §D1.1.1, Fig. D1.1.3).

Another small portion of the outdoor area's floor, called Locus:181909:071, is similar to Locus:181909:061, and was found in the north-western corner of the excavation trench, where it seems to abut the stone structure mentioned above (Locus:181909:070) (Figs. C5, C12 and C48: section E, C50). In the remaining areas, the floor of Outdoor Area 60 was heavily damaged by several looting pits. West of Locus:181909:061, and at a higher level, a pebble package called Locus:181909:077 was found (Figs. C5 and C47). This package seems to be the continuation of the thick pebble layer found in several spots in Outdoor Area 71 in Square 182909 (§C5.2.5). As with Outdoor Area 71, it is possible that the top surface of this pebble package was the Main Occupation Period walking surface. A step which was created by the looters during their illicit excavations is visible between Locus:181909:077 and floor Locus:181909:061. Originally, this spot must have been a sloping portion of the floor connecting Locus:181909:077 and Locus:181909:061.

As we saw also with Outdoor Areas 70 and 71, the distinction between Outdoor Area 60 and Outdoor Area 71 is not clear, as both areas seem to be part of the same open space around Building P, extending (at least within the limits of our excavation) to the north, east, and south of this building.

C6.2 The Graves 106, 107 and 108

Three burials were found within the trench: Graves 106, 107, and 108 (Figs. C5 and C17). In addition, a loose skull (Locus:181909:084) was found in a looting pit (fill: Locus:181909:067), located in the northwestern corner of the excavated area (Fig. C50). The burials had all been severely looted; however, Grave 106 yielded both human remains and artefacts. Stratigraphically, the graves seem to be later than the Main Occupation Period as they cut into features of Outdoor Area 60, namely (from east to west) Locus:181909:077, Locus:181909:061, and Locus:181909:076.

64 Herr 2019, 55.

65 Kreppner/Squitieri 2017a: Locus:100000:028 and Locus:100000:023, Figs. C12, C19.

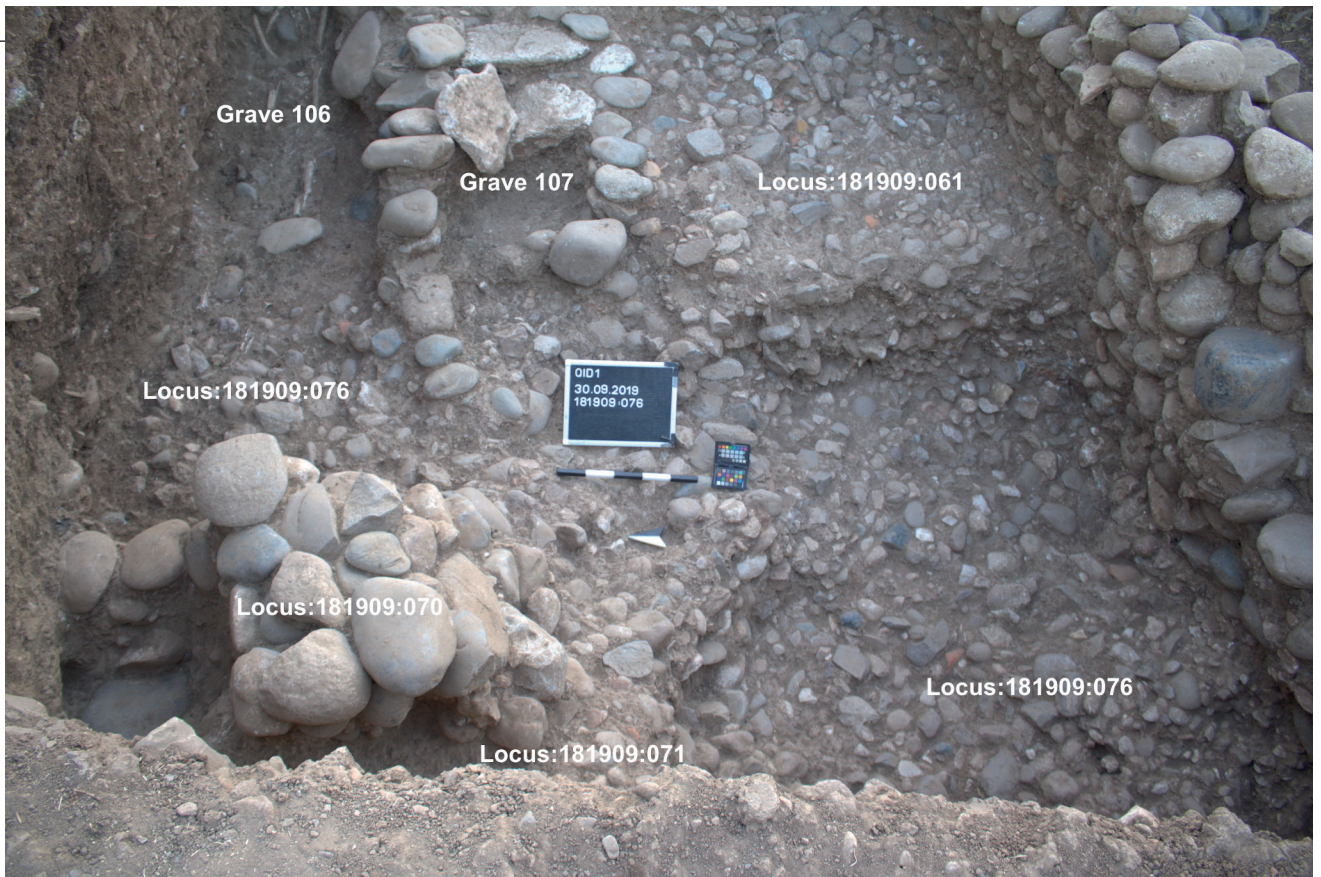


Fig. C49: The features in Outdoor Area 60, and the two later graves. Photo by Alessio Palmisano.

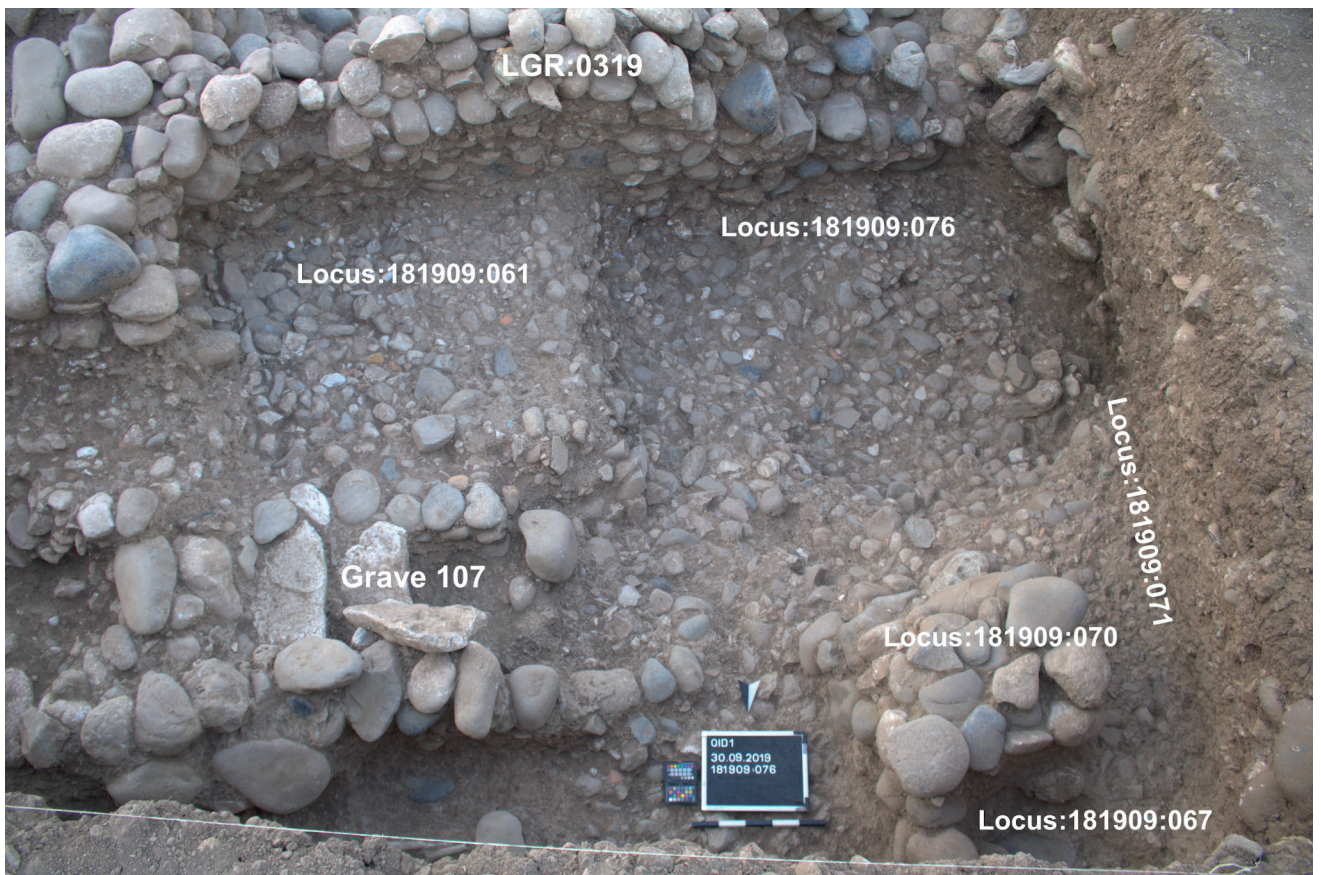


Fig. C50: The features in Outdoor Area 60, with the later Grave 107, and on the right the looted fill Locus:181909:067 from where the radiocarbon dated tooth was derived. Photo by Alessio Palmisano.

C6.2.1 Grave 107

Grave 107 is the only grave in this trench with preserved architecture (Figs. C17, C50-C51). It is a cist grave, about 1.75 m long and 1 m wide, lined with medium-sized, 20-25 cm diameter stones, set in three visible courses. It was originally capped with approximately 50 cm long white stone slabs, of which two are still visible *in situ* in approximately the middle of the grave. The grave was looted from the west, and therefore no finds remained. Structurally it closely resembles Graves 102, 103, and 105 (discussed above), which suggests that they were contemporaneous with each other.

C6.2.2 Grave 106

We found Grave 106 immediately north of Grave 107 (Figs. C5, C17 and C49). It yielded the remains of one or two individuals (Figs. C51-C52). No architecture was found in connection to this grave: whether the architectural details were completely destroyed by looters, or whether Grave 106 was a simple pit burial (like Grave 110) is not clear. The



Fig. C51: Graves 107 and 106. Photo by Alessio Palmisano.



Fig. C52: Human remains in Grave 106. Photo by Alessio Palmisano.

burial is 2 m long and 55 cm wide. The skeleton(s) lay on the back(s). The burial fill, Locus:181909:069, has yielded several pieces of jewellery, described in detail in §E1 (nos. 28-45). It also yielded a broken iron arrowhead (PPP 181909:069:019), described in §E4.1.6.

C6.2.3 Grave 108

Grave 108 is a cist grave located immediately east of Grave 106 (Figs. C5, C17 and C48: section F). Though not complete, the southern part of its stone lining is visible. This lining is formed from two courses of medium sized (ca. 20-25 cm diameter) stones (Fig. C53). The grave is approximately 2 m long and 85 cm wide. Unfortunately, the stone capping was removed by looters; however, a large white stone slab that may have been part of the missing grave capping was found in the fill above the grave (Locus:181909:063). No human or manufactured remains were found. It is possible that Grave 108 was contemporaneous with the other cist graves discussed above (Graves 102, 103, 105 and 107).

About 1 m south of Grave 108 (Fig. C5), there are some stones that are partially aligned in the form of an ovoid cist. It is possible that another cist grave was once here, now irrevocably destroyed by the looters.

C6.3 Skull Locus:181909:084 from a looting pit: evidence for Early Iron Age burials

In the northwestern corner of the trench, a looting pit was excavated, with a fill named Locus:181909:067 (Figs. C48: section F, C50) and cut Locus:181909:066. Its position at the edge of our excavation means that the complete extension of this pit is unknown; however, it is clear that it damaged the stone structure Locus:181909:070. The pit



Fig. C53: The remains of Grave 108. Photo by Alessio Palmisano.

fill contained a bronze fibula (Locus:181909:067:001, discussed in §E2.2) and a cylinder seal (Locus:181909:067:003, discussed in §E3.3). Whether these items originated from one of the nearby graves cannot be definitively established, but is very likely.

In this pit, also a skull was found (Locus:181909:084) as well as a tooth (Locus:181909:067:006), which was collected close to the skull and most likely came from it. The tooth was radiocarbon dated to 1210–1029 calBC (Table C1). The tooth's context does not allow us to connect these dates to any of the known graves. Nevertheless, it is noteworthy that this date range is very close to the dates obtained from a skeleton excavated in 2018 (Grave 99): 1259–1117 calBC (95.4 % probability)⁶⁶. These human remains demonstrate that graves from the late second millennium BC existed in the area; most likely, they preceded the excavated structures of Building P and the graves described above.

C6.4 The modern looting pits and the topsoil

As elsewhere in QID1, the trench in Square 181909 bears signs of the heavy looting that occurred recently (Fig. C21). The looted deposits, grouped in LGR:0370, yielded a mix of both modern and ancient materials. Some of the ancient finds may have originated from either the graves or the occupation period of Outdoor Area 60; however, this is difficult to establish. Fragmented human bones were frequently found in these deposits, as were medium-sized stones, which may have originally been part of the now-destroyed graves. None of the original stratigraphy of these deposits was intact, so it was not possible to identify any post-occupation deposits that may have formed following the abandonment of the Main Occupation Period structures. The table below summarises the looted fills found in this trench and grouped into LGR:0370.

Looted fills in trench Square 181909 (part of LGR:0370)	
Locus numbers	Notes
Locus:181909:053, Locus:181909:072 Locus:181909:060, Locus:181909:065 Locus:181909:073, Locus:181909:078	Generic disturbed fills containing pottery sherds, animal bones, and modern items, all embedded in a yellowish dark brown, loose soil matrix.
Locus:181909:051, Locus:181909:052 Locus:181909:058, Locus:181909:063 Locus:181909:050, Locus:181909:062	Disturbed fills yielding several ancient finds.

Looted fills in trench Square 181909 (part of LGR:0370)	
Locus numbers	Notes
Locus:181909:056	Stone accumulations gathered by the looters.
Locus:181909:067	Disturbed fill in which tooth PPP 181909:067:006 was found. Radiocarbon date from the tooth: 1210–1029 calBC.

Finally, the topsoil, excavated as Locus:181909:050, Locus:181909:051, and Locus:181909:062 (grouped in LGR:0368), did not show any signs of looting, but was characterised by recent ploughing marks.

C6.5 Conclusions

The excavations of the trench in Square 181909 yielded the following results:

- Building P, to the north, appears to be isolated. Outdoor Area 60 extends here, and seems to be the continuation of Outdoor Area 71, located to the east.
- Building P's northeastern corner seems to be a massive structure that is architecturally different from the southwestern corner. Therefore Building P has a slightly asymmetrical layout.
- Cist Graves 106, 107, and 108 postdate the features of the Main Occupation Period (Building P and Outdoor Area 60). One of them, Grave 107, closely resembles Grave 102 in Square 181908. Considering their architectural similarities, it is possible that all these graves were contemporaneous.

C7. Preliminary assessment of the 2019 excavations at QID1

F. Janoscha Kreppner & Andrea Squitieri

The 2019 excavation campaign on the western slope of Qalat-i Dinka continued investigations in operation QID1, prompted by the discovery, during the 2016 and 2018 campaigns, of portions of a monumental building, dubbed Building P. The 2019 excavations covered an area of about 150 m² and they focused on completing the investigation of Building P and its surrounding area. As was already recognised during the prior campaigns, the entire excavation area had been disturbed by several recent looting pits, which has made it very difficult to reconstruct the stratigraphy for the entire operation.

The 2019 campaign brought to light evidence (§C3.3) of an architectural phase older than Building P, consisting of two walls and a pebble floor. Unfortunately, it is not possible to assign these older features to a specific chronological period. It is worth mentioning that both the construction technique and the size of these older walls are consistent with some of the walls uncovered during the 2016 campaign in QID1 (Fig. C12: L24 in Outdoor Area 69 and L28 in Room 61), as well as in the operations of the Lower Town (namely Gird-i Bazar, DLT2 and DLT3). However, whether this resemblance indicates contemporaneity is difficult to ascertain.

During the 2019 campaign, our knowledge of Building P and its immediate surroundings was furthered. This building stands out from the other buildings of the Dinka Settlement Complex for its distinctive characteristics: it has wide walls, a brick paved floor, and a monumental threshold connecting Room 58 with Room 59. The eastern wall of Room 59 was uncovered in 2019. Its 40-50 cm width contrasts with the wider walls found in the rest of the building. Because Building P was built against a natural slope it has a stepped structure: the northern and southern walls of Room 58 meet the eastern wall of this room at a lower level, and there is an approximately 90 cm difference in height between the floors of Room 58 and Room 59. Moreover, Building P has two slightly asymmetric corners: the northeastern corner has a wide, squarish shape, while the southeastern corner has a rounded profile. When observed in detail, some of the architectural features of Building P are consistent with the other structures of the Dinka Settlement Complex. The use of unworked cobbles for walls and the use of baked bricks to pave the floor can be found elsewhere across the settlement; however the scale of Building P's architecture is greater than any other of the buildings there. Other architectural features, on the other hand, are only attested in Building P. The protruding stone bases in Room 58, the steps visible in this room's northern and southern walls, and the use of quarried blocks for the threshold and in Room 59 (although in Room 59 this block's purpose is not clear as it had been moved by the looters) are all features that contribute to differentiating Building P from the other structures so far unearthed at the Dinka Settlement Complex. Building P's affiliation to the Iron Age is confirmed by a charcoal sample collected in 2018 from directly above the floor of Room 58, which provided a radiocarbon dating of 1001-847 calBC, indicating that Building P was in use at the same time as at least some of the other buildings of the Lower Town (§A and Table C1). In relative stratigraphy, we refer to this period as the Main Occupation Period.

During the 2019 campaign, it became clear that Building P was situated in an open space that extended around it towards the north, east, and south (called Outdoor Areas 60, 70, and 71). The western portion of Building P is not completely uncovered so this part remains unclear. A thick package of pebbles and pottery sherds was deposited across these open areas abutting the outer walls of Building P. The top layer of this package served as a walking surface during the Main Occupation Period. However, due to the extensive modern looting activity, only a few patches of this surface layer have survived. Moreover, the looting activities blended the fills in the outdoor areas as well as in the rooms of Building P, irreparably damaging the original stratigraphy.

The features described above were cut by graves that have since been plundered, but must have originally been equipped with valuable finds. The remains of some cist graves are still preserved (Graves 102, 103, 105, 107). In a few cases, skeletal remains were found together with finds (Graves 106, 110). In addition to these inhumation burials, two cremation burials were also detected (Graves 101 and 109). Although it seems that some of them cut the Outdoor Area floors from a higher elevation, which would make them younger than Building P, it is not impossible that some of the graves were contemporary with, or even older than, Building P. In fact, the radiocarbon dates provided by the human remains unearthed in QID1 in both 2018 and 2019 reveal that the area was used as a cemetery across a long span of time. Two radiocarbon dates from human remains are available that pre-date the charcoal sample from Building P Room 58's floor (see Chapter A and Table C1). These results came from a tooth associated with Grave 99 dated to 1259-1117 calBC, and a tooth from a looting pit (not associated with any grave) dated to 1210-1029 calBC. They predate the charcoal from Room 58's floor, which was dated to 1001-847 calBC. These older human remains indicate that graves existed in this area before Building P was built.

The chronological sequence was advanced by a tooth from Grave 110, which yielded the radiocarbon date of 767-488 calBC (Table C1). Grave 110, therefore, seems to be later than Building P; however, whether the other graves excavated in 2019 also belong to the Grave 110's period is unclear. Finally, a human bone connected to Grave 98 (found in 2018 above the northern wall of Building P) was radiocarbon dated to 355-93 calBC, pointing to the existence of even later graves. How the undated graves relate to each other chronologically, and how they relate to Building P remains uncertain, and clarifying this should be the target of future investigations.

D. Pottery studies

D1. The 2019 pottery from Qalat-i Dinka (QID1)

Jean-Jacques Herr

The main challenge for the analysis of the pottery collected during the 2019 campaign⁶⁷ at QID1 has been the heavy looting that occurred relatively recently, which altered the entire stratigraphy of the operation and made it difficult to associate pottery sherds with specific deposits and structures.

Only two groups of sherds were found in contexts with comparatively good stratigraphic information. One group comprises sherds collected from the deposits above the floors of Outdoor Area 60 and Outdoor Area 71, which were found in a relatively good state of preservation, although looting damage was still present (§C). Based on both their stratigraphic context and their morpho-technological features, these sherds can be assigned to the Main Occupation Period of the Dinka Settlement Complex (DSC), roughly spanning the 12th-8th centuries BC (**Tables C1 and C2**). Another group of sherds comes from the inhumation Grave 106 and the cremation burials Graves 101 and 109. These burials had been left partially intact by the looters, hence some pottery sherds could be assigned to them with certainty. In this chapter, these two groups of sherds will be discussed in sections §D1.1 and §D1.2.

Finally, there is a third, large group of sherds that came from both the topsoil and the looting pits that were excavated across the entire operation. Within this group, some sherds could be related to specific chronological horizons based on parallels. Pottery sherds belonging to the 12th-8th centuries BC could be identified, thanks to the parallels coming from the well-preserved contexts of the DSC (particularly in the Lower Town). These sherds belong to the so-called Main Occupation Period in relative stratigraphy (§C, **Table C2**). Some potsherds could be dated to the Chalcolithic period based on parallels in the Chalcolithic kiln excavated in operation DLT3 (§I) and comparisons to other Chalcolithic sites of the area. Finally, some sherds

could be assigned to the third/second millennia BC and the Middle Islamic Period (MIP) on the basis of morphological and technological comparisons with other sites in the region⁶⁸. However, because no architectural evidence dating to the third/second millennia BC or the MIP has been found so far in the DSC, we do not have any reference material from stratigraphic contexts within the DSC itself to help us better identify sherds of these periods. Finally, there are sherds that could not be assigned to any chronological horizon with certainty, although their technological and morphological features clearly distinguish them from the Main Occupation Period pottery. §D1.3 and §D1.4 deal with a selection of sherds that came from the looted contexts of QID1.

The methodology applied to the study of the QID1 pottery follows the Peshdar Plain Project's systematic and standardised protocol established in 2015, which focuses on morpho-stylistic and technological features of the pottery to reconstruct the *chaînes opératoires*⁶⁹.

D1.1 Pottery from DSC's Main Occupation Period

D1.1.1 Outdoor Area 60

The deposit Locus:181909:055, found above the floor of Outdoor Area 60, has yielded five collections of potsherds and one complete and weathered carinated bowl (PPP 181909:055:001). The analysis of the sherds has assigned most of them to the techno-petrographic groups Tech-P6a and TechP6b, both very common in the DSC, while a

67 During the 2019 campaign, 40 collections were sorted in order to identify the Techno-Petrographic groups (TechPs) and morphological variants which could be dated to the first half of the first millennium BC. For the description of the TechP, see Herr 2017; Herr *et al.* 2018; 2019.

68 On the third/second millennium BC and Middle Islamic Period pottery from DSC, see Herr *et al.* 2019, 110-112. For the Chalcolithic period pottery from DSC, see §I and Herr *et al.* 2019.

69 During the 2019 autumn campaign at Qalat-i Dinka, the pottery was processed by Jean-Jacques Herr, Jamal Jameel Asaad, and Abubakr Qasim (General Directorate of Antiquities of Iraqi Kurdistan), assisted by Hamrin Mala Issa, Emo Muhamad Mala Issa, and Mahdi Qasim. I am indebted to Hero Ahmed Salih for making drawings of the potsherds and for providing me with important information regarding the technique of some of the collections stored in the Archaeological Museum of Sulaymaniyah that I could not physically check for myself, due to the coronavirus crisis of 2020.

few sherds from large jars were made with TechP9⁷⁰. Rim sherds of carinated bowls (Figs. D1.1.6; D1.2.2-5), hemispherical incurved rim bowls (Fig. D1.2.1) and flat (Fig. D1.2.6-7) and disc bases have been found. Two sherds from a closed vessel are made with Fabric B (calcite temper) and might be associated with cooking pots (Fig. D1.2.8-9). The complete carinated bowl PPP 181909:055:001 (Fig. D1.1.3) has a round, 9.5 cm diameter rim and a convex base. It belongs to a morphological type that has not been found in any of the other operations of the DSC. Two holes were drilled on the outer edges before firing. The diagnostic sherds from this bowl belong to TechP6a, made with the typical Fabric C1 (Figs. D1.1.6; 15), and to TechP6b, made with the typical Fabric D (Figs. D1.2.1-7). These diagnostic features allow us to assign the carinated bowl PPP 181909:055:001 to the Main Occupation Period of the DSC.

D1.1.2 Outdoor Area 71

In Outdoor Area 71, only a few sherds were collected from the surface of the pebble package (Locus:182909:066). They included burnished fragments of carinated bowls made with TechP6a (Figs. D1.1.8: 11), sherds of necked jars made with TechP9 (Figs. D1.1.12-13) and a flat base made with TechP6a (Fig. D1.1.16). One sherd from a cooking pot made with TechP4⁷¹ (Fig. D1.2.10) has also been recovered in this area. All these potsherds have good parallels with pottery recovered in the Main Occupation Period levels of the DSC.

D1.2 Graves

Graves 106, 101, and 109, despite having been partially robbed, yielded pottery sherds that can be assigned to the burials with certainty. Graves 101 and 109, two cremation burials, yielded three complete vessel profiles, while no complete vessels were found in Grave 106, an inhumation burial.

D1.2.1 Grave 106

The looted fill of Grave 106 (§C6.2.2) (Locus:181909:069) yielded 61 sherds, of which 13 are diagnostic. Fragments of hemispherical incurved rim bowls and carinated bowls made with TechP6a (Figs. D1.1.1-5) were found; they can be dated to the Main Occupation Period (c. 12th-8th centuries BC). One grooved rim sherd from a pot (Fig. D1.1.14) shows the base of a closed spout⁷². The base of another (possible) closed spout is detectable on a sherd with a narrow neck and a small vertical handle belonging to either a shouldered beaker or a small jar (Fig. D1.1.10)⁷³. Based on its level of preservation, we can conclude that this sherd is made with Fabric C1 and it is burnished on the outside with a vertical pattern, as used in TechP9. If this sherd was part of a beaker, we might assign it to the well-known “tankard”-type vessels, which spread across northwestern Iran from the mid-second to the early first millennium BC. “Tankard”-type vessels used for drinking and pouring liquid are a regular part of burial furniture in the Zagros area⁷⁴.

D1.2.2 Grave 101

Grave 101 (§C5.3.1) is a cremation burial that was partially looted. Fortuitously, the looters missed both the urn containing human bones and the bowl that covered its mouth, which were therefore both found in a good state of preservation.

The urn consists of a biconical jar with a cylindrical neck (PPP 182909:009:002) (Fig. D1.1.17). Its mouth was covered with a burnished, carinated bowl with a disc base (PPP 182909:009:003) (Fig. D1.1.15), set upside down. The bowl is made with Fabric C1 (§D2: sample PPP 116). The rim is everted and rounded in section – a type of rim that had already been encountered in other areas of the DSC⁷⁵. The biconical jar was made using the wheel coiling technique, but bears no traces of burnishing, in contrast to the traditional surface treatment observed on the small and medium jars of the Main Occupation Period at DSC (TechP9). The fabric is Fabric C1, as is the case for the majority of the Main Occupation Period pottery recovered at the DSC (§D2: sample PPP 115). Morphological parallels

70 TechP6a: Fabric C1 + Coiling + Slow wheel + Burnishing. TechP6b: Fabric D + Coiling + Slow wheel + Burnishing. TechP9: Fabric C1 + Coiling + Slow Wheel + Planing. For the descriptions of the technological and petrographic groups, see Herr 2017, Herr *et al.* 2018; 2019.

71 TechP4: Fabric B + Coiling + probably Slow wheel + Brushing on while clay was of leather hard consistency.

72 The spout might have been tubular, similar to those recovered in pit Locus 271927:030 at Gird-i Bazar. See Herr 2016, 91.

73 Less than 25% of the diameter is preserved. Therefore, it is not possible to know if the original shape had two handles or only one.

74 Danti/Cifarelli 2013, 199.

75 See for instance in DLT3: Herr *et al.* 2019, 104, Fig. G1.3.4 or in DLT2: Herr *et al.* 2018, 122, Fig. F1.1.5.

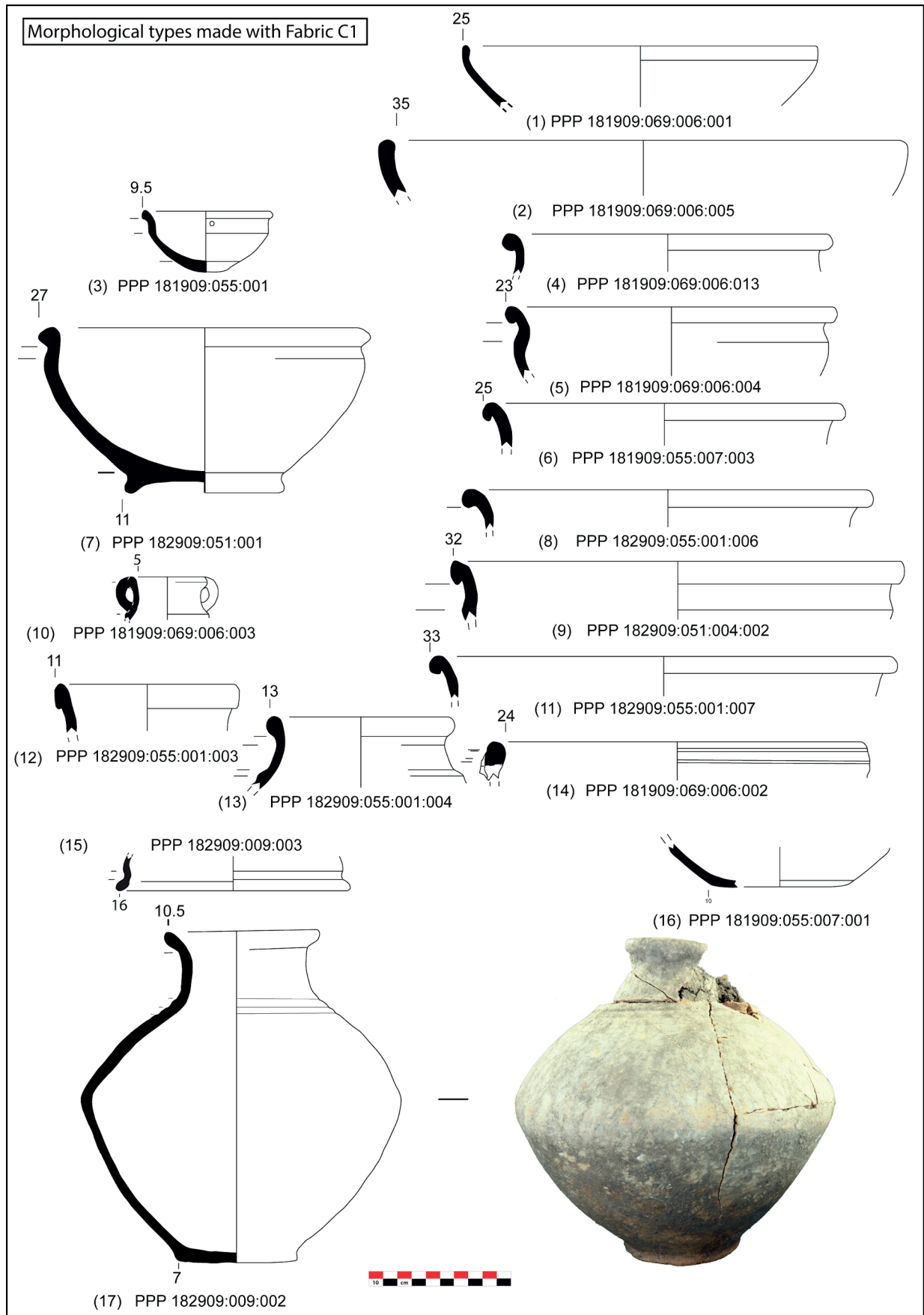


Fig. D1.1: QID1 pottery. Hemispherical incurved rim bowls (1-2), carinated bowls (3-6; 8-9; 11; 15), hemispherical bowl with a ring base (7), beaker (10), pot/jar with a spout (14), base (16) and necked jars (12-13; 17) made with Fabric C1. Drawings by Jamal Jameel Asaad; vectorised drawings by Hero Ahmed Salih. Prepared by Jean-Jacques Herr.

for this jar occur in the burials at Dinkha Tepe (north-western Iran), dating to the Iron Age II Levels II and III, as well as in the Iron Age inhumation burials recovered in Luristan⁷⁶.

D1.2.3 Grave 109

Grave 109 (§C5.3.2) is a cremation burial, encountered partially looted. Four diagnostic sherds and one complete vessel have been found in the grave fill (Locus:182909:051).

Among the diagnostic sherds, the best preserved one belongs to a carinated bowl made with TechP6a (Fig. D1.1.9). The complete vessel is a hemispherical carinated bowl (PPP 182909:051:001) (Fig. D1.1.7, and see Fig. C40); it was found upside down covering part of a burnt femur embedded in a layer of ashy material (Fig. C41). Its fabric is similar to Fabric C1 (§D2: sample PPP 117); its shape, however, is different from the usual carinated bowls found in Main Occupation Period levels, as it has a ring base. So far, only flat and disc bases have been found in the Main Occupation Period layers of the DSC. Carinated bowls with ring bases like PPP 182909:051:001 are rarely found in the second/mid-first millennium BC sites of the northern Zagros area. The rim consists of a coil set on the exterior of a straight wall with a pronounced triangular section. This rim type has parallels in Qal'eh Siah, about 100 km north of Lake Urmia⁷⁷ and in Hasanlu (Level IVC)⁷⁸, with a chronological range spanning from the mid-13th to the 8th century BC.

D1.3 Glazed pottery

As in 2018⁷⁹, a few sherds of glazed pottery were found during the 2019 campaign. These came from the looted deposits (Locus:181909:052:001) covering the northern part of the trench, above the looted Graves 106 and 107 (Fig. C17). One sherd (Fig. D1.3.1) was part of a jar with a cylindrical neck and a rim diameter of less than 10 cm. The walls are coated with a white glaze, and black splashes decorate the top of the rim. The fabric is porous and was probably tempered with organic material. It is similar

to the fragments recovered in 2018⁸⁰ and also most probably was part of a small jar or bottle. The second sherd decorated with a white glaze (Fig. D1.3.2) consists of a fragment of a ring base; it has an orange colour similar to the pottery recovered in the deposit above the floor of Room 58 and it is probably made with Fabric C1⁸¹.

The presence of glazed pottery in the topsoil and looted deposits might be related to the practice of depositing goods in graves. The funerary practice of depositing glazed vessels in burials is also attested by graves found in the Zagros that date to the first half of the first millennium BC⁸².

D1.4 Middle Islamic Period pottery

As also in 2018, the 2019 excavations in QID1 yielded some diagnostic Middle Islamic Period (MIP) potsherds, easily recognisable due to their white slip and green glazed surface treatment (also called “Gārrus ware”⁸³). We found these sherds on the site surface (Locus:182908:001), in the topsoil (Locus:181908:024, part of LGR:0368), and in the looted deposits (Locus:181909:052, part of LGR:0370) (Fig. D1.4).

The new specimens consist of fragments of open vessels coated with a white slip or “engobe,” which was then covered with a green glaze on the inner walls (Figs. D1.4:1 and D1.4:3) or on both walls (Fig. D1.4:2). We have also again noticed the same *sgraffiato*-type decoration that was seen on some of the sherds found in 2016 and 2018⁸⁴ (Fig. D1.4:1). This decoration consists of a curvilinear pattern incised into the white slip and then covered with a transparent glaze. The green glazed sherd from a small bowl with two grooves on the outside (diameter less than 10 cm) has an almost identical morphological parallel among the sherds recovered in the topsoil of QID3 (Locus:176904:002), excavated in 2018⁸⁵.

In the MIP pottery of the DSC, the fabric is highly levigated and few inclusions have been observed macroscopically⁸⁶. The colour of the fabric is pink-reddish.

76 For jars with biconic bodies: Muscarella 1974, Fig. 43 (B 10b, burial 8; Fig. 49; Fig. 52). See also morphological parallels decorated with incised triangles in Luristan in the War Kabud graves (Haerinck/Overlaet 2004a, 35, Fig. 11)

77 Kroll 1976, 38, Abb. 10.18.

78 Danti/Cifarelli 2013, 232, Fig. 4.41.T and 242, Fig. 4.46.R

79 Herr *et al.* 2019, 103-107.

80 Herr *et al.* 2019, 115, Fig. G1.8.1-4.

81 Herr *et al.* 2019, 115, Fig. G1.8.5.

82 Hassanzadeh 2016.

83 See Herr *et al.* 2019, 11, Fig. G1.7; we found other sherds similar to the pottery sherds (1) (= PPP176909:002:001:148), (2) (= PPP100000:007:001:021), and (3) (= PPP176904:002:001:063) depicted there.

84 Herr *et al.* 2019, 111, Fig. G1.7.1-2.

85 Herr *et al.* 2019, 111, Fig. G1.7.3.

86 Herr *et al.* 2019, 112; 2018, 125.

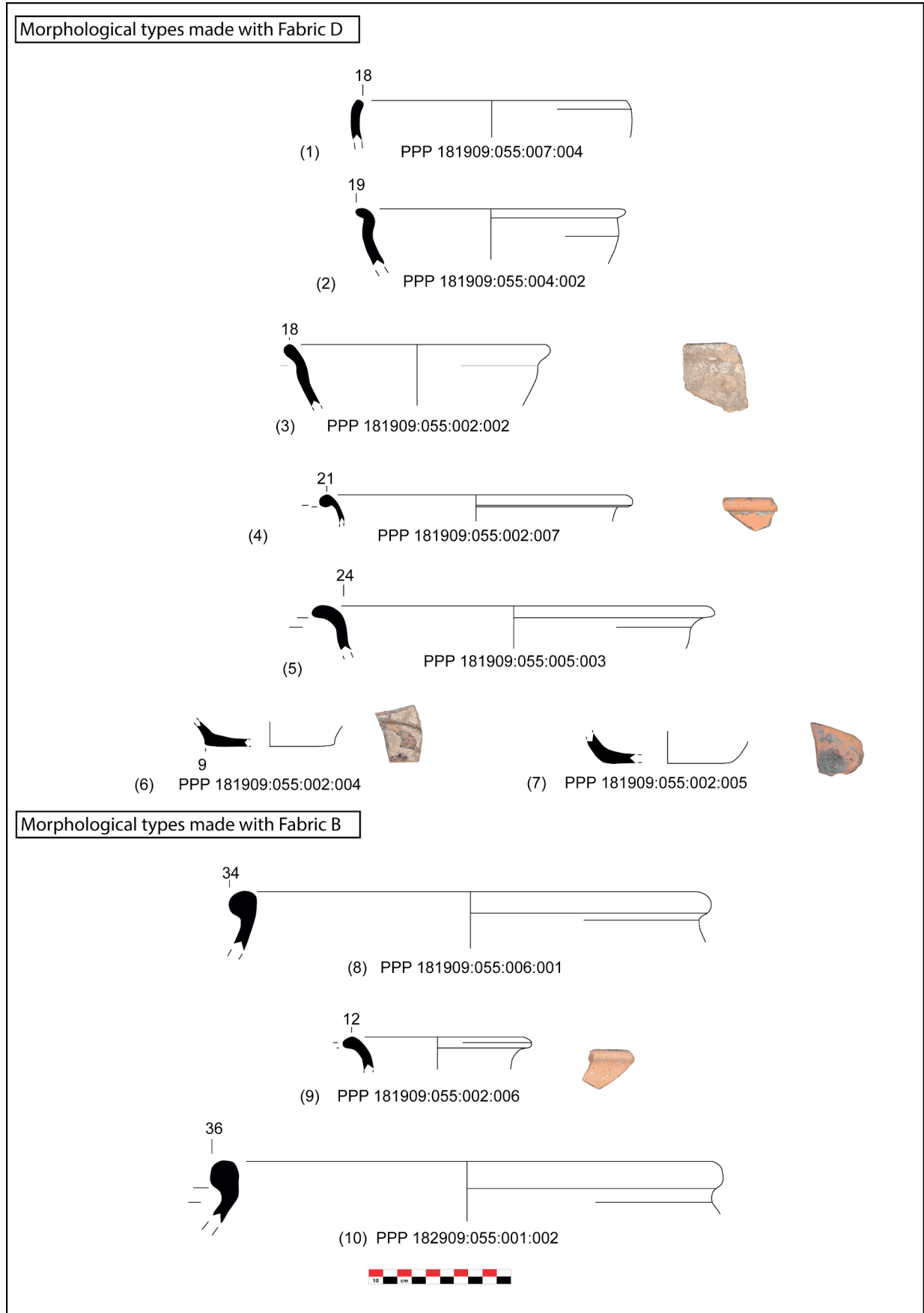


Fig. D1.2: QID1 pottery: Hemispherical incurved rim bowl (1), carinated bowls (2-5), disc base (6) and flat base (7) made with Fabric D. Cooking pots (8-10) made with Fabric B. Drawings by Jamal Jameel Asaad; photos by Abubakr Qasim; vectorised drawings by Hero Ahmed Salih. Prepared by Jean-Jacques Herr.

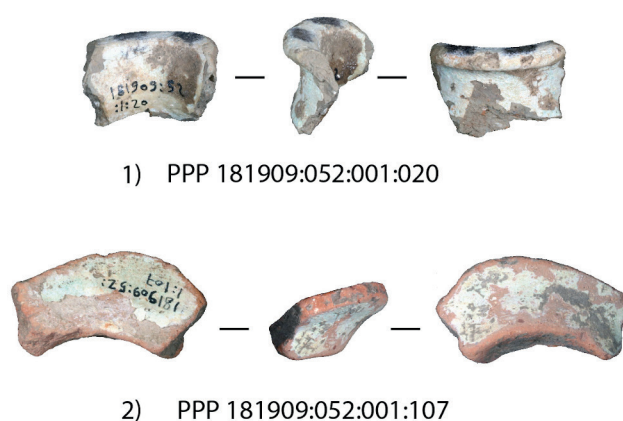


Fig. D1.3: Glazed pottery sherds from QID1: Necked jar made with an organically tempered fabric (1) and base of a vessel made with Fabric C1 (2). Photos by Jamal Jameel Asaad and Abubakr Qasim. Prepared by Jean-Jacques Herr.

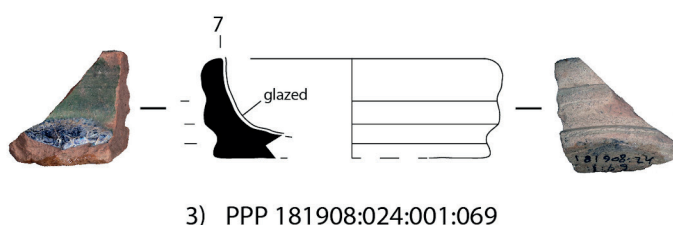
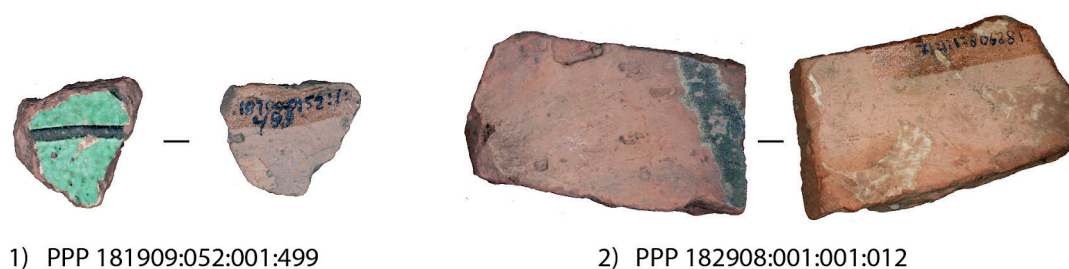


Fig. D1.4: Glazed pottery sherds from QID1: opened vessels made with levigated clay (1-3). Drawings by Jamal Jameel Asaad; photos by Jamal Jameel Asaad and Abubakr Qasim. Prepared by Jean-Jacques Herr.

D1.5 Conclusions: putting the QID1 pottery in its wider context

Despite the large amount of pottery that could not be assigned to a precise context due to modern looting activity, we have seen that some sherds can be connected to some of the graves excavated in QID1 during the 2019 campaign. In order to set these sherds into a wider context, in this section I will outline the archaeological information currently available about pottery deposited in first millennium BC burials in the northern and central Zagros regions.

Burnished, bridgeless-spouted and bridged spout jars, “tankards”, pedestal goblets, and “worm bowls” (characterised by double drilling)⁸⁷ have been regularly found among the assemblage of grave goods in the northeastern pediment of the Zagros, near the Urmia basin. Reference sites are Dinkha Tepe (old periodisation: II-III)⁸⁸,

⁸⁷ Danti/Cifarelli 2013, 207-209.

⁸⁸ Muscarella 1974.

the Lower Mound north of Hasanlu (Level IVB)⁸⁹, Geoy Tepe⁹⁰, and Haftavan Tepe⁹¹. Indeed, the deposition of pottery into a grave, alongside the body, is a ritual frequently observed in western Iran for that period. For instance, at Hasanlu, 90 % of the furnished graves have yielded complete vessels of the types mentioned before⁹². The second important collection of pottery deposited in graves of the first half of the first millennium BC comes from the region of Luristan⁹³. The excavations conducted by the Belgian Archaeological Mission in Iran (BAMI) in the Pusht-i Kuh cemetery have yielded a large collection of complete pottery vessels dated to the first half of the first millennium BC, subdivided into the “Iron Age I-III” phases (1300-c. 650 BC)⁹⁴. Many different shapes have been associated with specific phases of this periodisation. The BAMI archaeologists have consistently found vessels associated with the consumption of liquids, such as pitchers with pinched spouts, carinated beakers, small jars with biconic and globular shapes (occasionally decorated with an incised triangle on the shoulder), and “teapot” pottery fired in a reducing atmosphere (so-called “grey ware”) in these graves⁹⁵.

Compared to the northern Zagros area and Luristan, the central Zagros area is less well known due to the scarcity of archaeological investigations there. However, recent excavations have documented graves in Sanandaj⁹⁶, Kul Tarike⁹⁷, Mala Mcha⁹⁸, Kani Koter⁹⁹, and Sarrez¹⁰⁰. Pottery vessels are part of the grave goods deposited with the inhumations. Vessel types that vary from the ones found in the northern Zagros area and Luristan have been recovered, such as small globular bottles, “petal-form beakers,” glazed bottles, flared rim carinated bowls, and s-shaped profile beakers¹⁰¹. These vessels might be dated to c. 8th-6th century BC, a period referred to as “Iron Age III”.

Finally, in the western Piedmont of the Zagros, in Iraqi Kurdistan, only a few graves dating to the beginning of the first millennium BC have been excavated. Ghabrestan-i Topzawa¹⁰² yielded a large quantity of pottery

vessels that have parallels in the pottery from the Main Occupation Period of the Dinka Settlement Complex. Farther west, the excavations at Gir-Gomel¹⁰³ and in Erbil, in the modern urbanised area of Arab Kon¹⁰⁴, have provided, respectively, primary cremation pits and collective burials, with pottery similar to the northern Mesopotamian tradition dated to the Neo-Assyrian period (9th-7th century BC). The assemblages consist of small globular pots, small jars or bottles with cylindrical necks, glazed bottles, carinated bowls, lamps, and beakers.

In QID₁, the lack of complete ceramic vessels from inhumation graves is striking, and it might be related to the heavy level of looting activity. The collection of potsherds recovered in the disturbed Grave 106 documents the existence of hemispherical bowls, a (probably) bridgeless-spouted pot or jar (only one rim sherd was found), and a possible “tankard.” Such fragments offer some hints about the funerary rituals, which might have consisted of depositing drinking vessels or, more generally, pottery associated with commensality. This follows the wider trend of funerary rituals attested in both northern Mesopotamia and in the Zagros during the late second/early first millennium BC.

The primary cremation burial Grave 101 demonstrates the funerary practice of collecting the bones that remained following the cremation and depositing them into a small jar covered by another open-shaped vessel. This practice, common during the first half of the first millennium BC, has been observed across the broad area of the fertile crescent, and beyond¹⁰⁵. The deposition of the burned remains of cremated bodies into a vessel has not been documented in the southern part of the Zagros¹⁰⁶.

In conclusion, the graves discovered in QID₁ during the 2019 campaign contribute to our knowledge of funerary practices in both northern Mesopotamia and in the Zagros area. They further our knowledge of funerary practices in the central part of the Zagros near the Qandil

89 Danti/Cifarelli 2013; Cifarelli 2018.

90 Burton-Brown 1951; Danti/Cifarelli 2013, 192.

91 Burney 1970; 1972; 1973; 1975.

92 Cifarelli 2018, 86.

93 Cinquabre 1978, 339-342.

94 Overlaet 2005.

95 Haerinck/Overlaet 2004b, 128-134; Overlaet 2005.

96 Amelirad *et al.* 2012; Radner *et al.* 2020.

97 Rezvani/Roustaei 2007.

98 Amelirad *et al.* 2017.

99 Amelirad/Azizi 2019.

100 Amelirad/Razmpoush 2015.

101 Amelirad *et al.* 2017, Fig. 23.

102 Danti 2014.

103 Morandi Bonacossi *et al.* 2018, 82-86.

104 van Ess *et al.* 2012.

105 In the Upper and Middle Euphrate Valley, see for instance the burials in Yunus, near Karkemish (Woolley 1939) or the area H in Tell Shiukh Fawqani (Tenu 2005; al-Bahloul *et al.* 2005, 997-1048). In eastern Anatolia, in sites of the Urartu area, see Derin 1992, 49-62; Herles 2012, 60-90; and Kroll *et al.* 2012, 32-33. In Iran, see Dinkha Tepe (Muscarella 1974). For some examples of cremation in an urn in northern Mesopotamia, see Assur (Haller 1954, 12-13; Hauser 2012, 204-206) and Tell Sheikh Hamad (Kreppner 2014, 175).

106 In the Susiana, at the site of Chogha Zanbil, a few infant cremation burials dating to the Neo-Elamite period (1000-520 BC) follow this practice but this seems to have been exceptional in this area. See Wicks 2018, 209.

mountain range, and provide for the first time a funerary context associated with a settlement in this specific area.

The sorry state of the burials also shows how widespread and systematic modern looting activities have become across the Zagros mountain range, where graves have typically been the primary targets for looters, lured by the quantity of material deposited during ancient funerary rituals¹⁰⁷.

D2. Petrographic analysis on Iron Age pottery from Graves 101 and 109

Silvia Amicone

A petrographic study was carried out on three ceramic samples from Graves 101 and 109, which were given the laboratory numbers PPP 115, PPP 116, and PPP 117¹⁰⁸. Their respective registration numbers are:

- Laboratory no. PPP 115 = registration no. PPP 182909:009:021
- Laboratory no. PPP 116 = registration no. PPP 182909:009:020
- Laboratory no. PPP 117 = registration no. PPP 182909:051:012

Samples PPP 115 and PPP 116 come from the cremation burial Grave 101 (**§D1.2.2**). PPP 115 was taken from the biconic jar used as a urn (PPP 182909:009:002, **Fig. D1.1.17**), while PPP 116 is from the carinated bowl found upside down on the urn's mouth (PPP 182909:009:003, **Fig. D1.1.15**). The third sample PPP 117 comes from the bowl found in the cremation burial Grave 109 (PPP 182909:051:001, **Fig. D1.1.7**). Petrographic analysis revealed that all these samples have a paste similar to Fabric C1, which characterises most of the Main Occupation Period sherds of the Dinka Settlement Complex¹⁰⁹. The specimens are marked by rounded inclusions of micritic calcite and fragments of metamorphic rocks (**Fig. D2.1.a-d**). These results show that the clay sources used to make the pottery vessels in both Graves 101 and 109 were the same as those used for the rest of the pottery dating to the Main Occupation Period.

¹⁰⁷ As in the case of Hasanlu (Danti/Cifarelli 2015), Kul Tarike (Retzvani/Roustaei 2007), Ziwiye (Ghirshman 1979, 9-10) and Baba Jilan (Hasanpur *et al.* 2015).

¹⁰⁸ The petrographic analysis was carried out by Silvia Amicone at the Competence Center Archaeometry – Baden-Wuerttemberg (CCA-BW) of the University of Tübingen.

¹⁰⁹ Amicone 2017a; 2018; 2019.

However, Fabric C1 alone cannot be considered strongly diagnostic of a chronological phase. This paste is made from local clay sources, minimally processed, and it has been found associated also with Chalcolithic ceramics (**§I; Fig. I15**). Therefore, the use of this fabric across different periods reflects a choice dictated by the interaction between people and the landscape of the Bora Plain, rather than a choice that can be connected to a specific cultural milieu. In other words, the various communities inhabiting the Bora Plain across time found it beneficial to select this type of non-calcareous clay as it requires minimal manipulation (e.g. cleaning) to be plastic enough to produce the majority of vessels, such as tableware.

Detailed description of the fabric of the analysed samples¹¹⁰

Quartz (sa.-eq., max=0.30 mm, mode=0.10 mm) and fragments of foliated metamorphic rocks (sr.-el., max=2.8 mm, mode=0.80 mm) composed of quartz, muscovite and biotite are frequent. Micrite and sparry calcite (wr.-eq., max=2.5 mm, mode=0.85 mm) are common (especially in PPP 117). Few inclusions of plagioclase (sr.-eq., max=0.50 mm, mode=0.20 mm), biotite (sr.-el., max=0.35 mm, mode=0.20 mm), muscovite (sa.-el., max=0.30 mm, mode=0.20 mm) and clay pellets (wr.-eq., max=0.65 mm, mode=0.50 mm) were observed. Very rarely epidote (sa.-eq., max=0.35 mm, mode=0.30 mm). The grain size distribution is polymodal. Voids are vesicles and vughs, and they do not show any preferential orientation. The matrix is light brown in PPL and orange to brown in XP. The matrix is non-calcareous, and the samples exhibit high to low optical activity.

Frequency of inclusions	%
Predominant	> 70 %
Dominant	50-70 %
Frequent	30-50 %
Common	15-30 %
Few	5-15 %
Very few	2-5 %
Rare	0.5-2 %
Very rare	< 0.5 %

¹¹⁰ Abbreviations: el. = elongate; eq. = equant; a. = angular; sa. = sub-angular; vr. = very angular; r. = rounded; sr. = sub-rounded; wr. = well rounded.

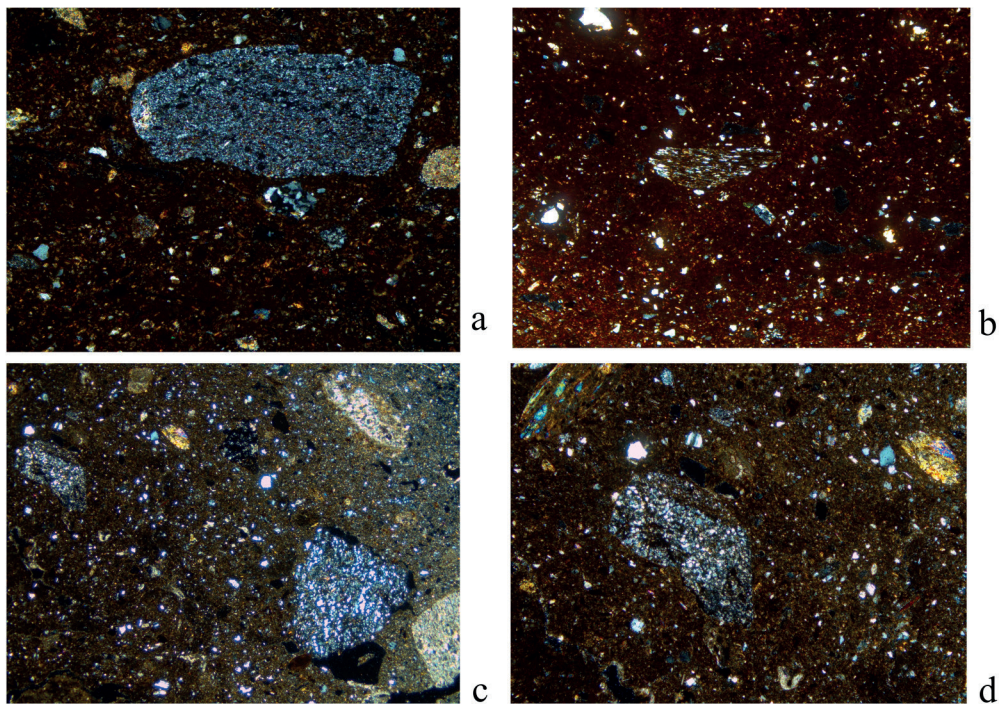


Fig. D2.1: Thin section photomicrographs of selected ceramics from Graves 101 and 109: (a) Fabric C1 (PPP 115), with a fragment of metamorphic rock composed of quartz and biotite XP; (b) Fabric C1 (PPP 116), with a fragment of foliated metamorphic rock XP; (c) Fabric C1 (PPP 117), with fragments of metamorphic rocks and calcite XP; (d) Fabric C1 (PPP 117), with a fragment of metamorphic rock and muscovite XP. Image width = 1.5 mm (a), 3 mm (b, d), 6 mm (c). Prepared by Silvia Amicone.

E. Small finds from the Dinka Settlement Complex, 2015-2019

This section includes six chapters dealing with various groups of small finds excavated at the Dinka Settlement Complex. §E1 presents the new small finds retrieved during the 2019 excavations on Qalat-i Dinka (QID1), supplemented by two detailed studies on the fibulae (§E2) and the cylinder seals (§E3) found there. All arrowheads found between 2015-2019 (originating in excavations at Gird-i Bazar and QID1) are analysed in §E4, followed by an archaeometric analysis of the “Bodkin type” arrowhead found in 2015 at Gird-i Bazar (§E5). Finally, all artefacts made of faunal remains that have been found at the Dinka Settlement Complex between 2015-2019 are collected and discussed in §E6.

E1. The 2019 small finds from Qalat-i Dinka (QID1)

Andrea Squitieri

E1.1 Introduction

This chapter deals with the small finds collected from operation QID1 during the 2019 campaign. Overall, the 2019 small finds from QID1 amount to about 500 items, which join the approximately 200 items collected during the 2016 and 2018 campaigns. As was the case in previous campaigns, modern looting affected the operation QID1 severely, altering the entire stratigraphy of the operation and making the association between finds and specific deposits or structures very problematic. As a consequence, not all the small finds from QID1 can be presented in a stratigraphic sequence.

For this reason, the small finds have been subdivided into three groups based on their origin:

Group 1: Finds associated with looted graves.

Small finds from this group have been assigned to specific graves on the basis of the following criteria:

- They were located inside the grave architecture (Graves 102 and 105);
- They were found in direct contact with the skeleton (Graves 103 and 110);

- They were found in the fill immediately above the skeleton (Grave 106).

The cremation burial Grave 101 represents a lucky case because several items were found in a section of the grave pit that had been left undisturbed by the looters. The finds from Group 1 are discussed in §E1.2 below.

Group 2: Ancient finds found in looting pits.

These finds constitute the largest group. They were collected from the fills of the looting pits excavated throughout the operation. These items are discussed in §E1.3, organised by category and material. It was not possible to establish a stratigraphic sequence for them. In some cases, finds found in those fills that were located very close to graves are singled out as they may have originated from the graves themselves. Items that were more likely to have originated in the structures of Building P, and not from graves, are discussed in the final section §E1.4.

Group 3: Modern finds found in the looting pits.

This constitutes quite a large group of items, comprising aluminium pieces, cigarette filters, fragments of modern metal tools, and plastic remains, which were left behind by recent looters. They have helped us identify and follow the looting pits during the excavation. None of the 2019 modern finds provided any information on the date of the looting event, in contrast to 2016, when a biscuit wrapper was found bearing a production date of 1999¹¹¹, thus providing a *terminus post quem* for the looting. Modern items will not be discussed in the present chapter.

Assigning chronological horizons to the items from Groups 1 and 2 can prove to be challenging. As shown in §A and §C (Table C1), radiocarbon dates available from the excavation area QID1 range from the beginning of the Iron Age to almost the end of the first millennium BC. Among the objects in both Groups 1 and 2, only those from Grave 110 can be connected to an absolute date (767-488 calBC). However, some items show stylistic connections that help narrow the wide chronological range provided by the radiocarbon dates. These connections and their chronology

¹¹¹ Kreppner/Squitieri 2017a, 56.

are discussed in the following sections, and especially in §E2, §E3 and §E4.

E1.2 The small finds from graves (Group 1)

In the following sections, the small finds from graves are discussed, starting with the cremation burials (Graves 101 and 109), continuing with the cist graves (Graves 102, 103 and 105) and concluding with the simple pit burials (Graves 106 and 110). Basic information about the objects from each grave is summarised in tables¹¹² that also contain their registration and catalogue numbers. Only particularly interesting objects are discussed in greater depth.

E1.2.1 Grave 101

Grave 101 is a cremation burial found in Square 182909 (§C5.3.1). It is formed by a grave pit whose lining shows burnt traces, and contains ashy layers on the bottom. An urn was found standing in the pit, along with some items around it. Although the grave had been looted, the urn was left intact. Some bronze fragments found around the urn were possibly modified by heat, while the other items did not show any trace of burning or heat modification, suggesting that they were placed in the grave pit after the combustion had taken place. Among these items were six decorated bone tubes, which are discussed in greater detail below. No absolute date for this grave is available as the attempt to radiocarbon date a human bone fragment from inside the urn was unsuccessful. Stylistic dating may be possible for at least some of the grave items.

Registration no.	no.	Description	Context
PPP 182909:008:001	1	6 shapeless bronze fragments, possibly modified by heat. L. < 5 cm.	Around the urn
PPP 182909:009:013-014,			
PPP 182909:009:004	2	Shapeless bronze fragment, L. 8 cm, possibly from a bowl modified by heat.	Around the urn
PPP 182909:009:007	3	3 iron fragments, L. 3 cm; W. 0.3 cm, possibly belonging to one or more pins.	Around the urn

¹¹² Abbreviations used in this section, including the object tables: L. = length; W. = width; H. = height, Th. = thickness; D. = diameter. The materials of the objects discussed in this chapter have been identified by eye, unless indicated otherwise. The term "bronze" as used in the present discussion designates any copper-alloy.

Registration no.	no.	Description	Context
PPP 182909:009:017	4	Iron stick, L. 18 cm, W. 1.5, hollowed, made of a rolled piece of iron, tapering to one end. It probably had a bone handle (no. 7) (Fig. E1.2).	Around the urn
PPP 182909:009:018	5	Iron pin, fragment. L. 6 cm, W. 0.3 cm.	Around the urn
PPP 182909:009:006	6	Ceramic object, cylindrical, L. 4 cm, with a wider base. Broken. Possibly the foot of a beaker.	Around the urn
PPP 182909:009:005	7	6 decorated bone tubes, partially preserved (see below).	Around the urn
PPP 182909:009:008-011			
PPP 182909:009:016			
PPP 182909:048:004	7	Decorated bone tube, in fragments (see below).	Near the urn
PPP 182909:048:005-006, PPP 182909:048:008	8	3 shapeless bronze fragments, L. < 5 cm.	Near the urn
PPP 182909:048:007	9	Golden crescent-shaped earring. L. 1 cm; Th. 0.2 cm decreasing to 0.1 cm at the extremities. Weight: 1 g (Fig. E1.3).	Near the urn
PPP 182909:022:001	10	Metal fragment, shapeless. L. 4 cm.	Fill inside the urn
PPP 182909:022:002	11	4 ovoid unworked stones, L. 2 cm. PPP 182909:022:002 is translucent white, possibly made of alabaster (translucent gypsum). The other stones are dark reddish and opaque.	Fill inside the urn
PPP 182909:022:003			
PPP 182909:022:004			
PPP 182909:022:005			

(7) Decorated bone tubes (registration numbers: PPP 182909:009:005, PPP 182909:009:008-011, PPP 182909:009:016 = Fig. E1.1, and PPP 182909:048:004)

Material: Bone.

Dimensions: PPP 182909:009:005: L. 7 cm, D. 2.5 cm, broken; PPP 182909:009:008: broken into four fragments, the largest with L. 8 cm, D. 2.5 cm; PPP 182909:009:009: L. 5 cm, D. 2.5 cm, broken; PPP 182909:009:010: broken into four fragments, the largest with L. 5 cm, D. 2.5, PPP 182909:009:011: broken into seven fragments, the largest with L. 4 cm; D. 2.5 cm. PPP 182909:009:016: best preserved: L. 11 cm; D. 2.5 cm, PPP 182909:048:004: broken into eight fragments, the largest with L. 2 cm.

Six decorated bone tubes, of which five were found surrounding the urn, while one was below it. They are all in fragments, except for PPP 182909:009:016, which is the best preserved and has been restored. PPP 182909:009:016 is a hollowed bone tube, showing a rounded perforation



Fig. E1.1: Decorated bone tube PPP 182909:009:016 (7) from Grave 101. Restored by Akam Omar Qaradaghi. Photo by Haymin Noori.



Fig. E1.2: Iron stick PPP 182909:009:017 (4) from Grave 101. Photo by Andrea Squitieri.



Fig. E1.3: Golden crescent-shaped earring PPP 182909:048:007 (9) from Grave 101. Photo by Louise König.

(D. 0.5 cm) near one edge. The surface is decorated with motifs distributed in three horizontal bands. The first shows a cross-hatched motif, the second a herringbone pattern, and the third repeats the first motif. They are separated by two plain camps. The other five bone tubes are not as complete as this one, however they show the same decorative patterns so it can be assumed that they resembled PPP 182909:009:016 originally. The fragmented tubes also preserve, in many cases, the 0.5 cm diameter circular perforation. The tubes are made from a long *mammalia* bone, but it is not possible to define the species. **Comparisons:** Decorated bone tubes similar to our examples date back to the Early Bronze Age, when they can be found across the Aegean and the Levant¹¹³. During the first millennium BC, they are found in several sites throughout the Levant and Mesopotamia, concentrating from the 9th century BC through the Achaemenid period. They were recovered from a variety of contexts (not just funerary)¹¹⁴.

¹¹³ Genz 2003; Rahmstorf 2010.

¹¹⁴ See e.g., **Iron Age:** Assur (Wicke 2011, Pl. 46: V31-V32; Miglus *et al.* 2016, Pl. 90c); Yunus cemetery (Woolley 1939, Pl. 21.22), Zincirli (Luschan 1943, Pl. 59: r, s), Deve Hüyük (Moorey 1980, Fig. 15), Tell Ali Al-Hajj (Ishida *et al.* 2014, Fig. 6.96.34), Megiddo (str. XIII and IV: Lamon/Shipton 1938, Pl. 99: 3; Loud 1948, pl. 196: 2-6); Nippur (McCown *et al.* 1978, Pl. 68: 4D, 337); **Achaemenid:** Til Barsip (Thureau-Dangin/Dunand 1936, Pl. 16: 8-9; Pl. 18: 7-8), Kamid el-Loz (Poppa 1978, Graves 2, 6, 8, 11, 12, 58, 71, 72, and 78); **Hellenistic-Parthian:** 'Atlit (Johns 1933, Fig. 7), Nippur (University of Pennsylvania Museum of Archaeology and Anthropology, object no. B14660). It should be noted that the bone tubes from QID1 and their comparisons here discussed are not to be confused with ivory pyxides. These are items which can show similar decorative patterns to bone tubes, but have a wider diameter and are frequently equipped with lids (see Wicke 2008).

Concerning their use, some have suggested that they were intended as kohl tubes, others as handles. The first interpretation is supported by evidence from some Levantine graves, where decorated bone tubes were found along with kohl sticks¹¹⁵; however, because the examples from Grave 101 show a perforation near the edge, which could have been used to fix the tube to another object, and they do not show any discoloration from the presence of kohl, they seem to have been used as handles. The iron stick, 18 cm long (**no. 4**, **Fig. E1.2**), which was found near the urn, was possibly equipped with one of the bone tubes as a handle. Similar iron sticks, although without handles, were found at the cemetery of Dinkha Tepe II-III (Iron Age II)¹¹⁶.

Finally, it is worth mentioning that only one decorated bone tube comparable to the QID1 examples has been reported from western Iran, from Surkh Dum in Luristan¹¹⁷. Other decorated bone tubes from western Iran differ from our examples with their square sections, thick walls, and

¹¹⁵ E.g., Kamid el-Loz, Grave 11; Til Barsip, Burial C.

¹¹⁶ Muscarella 1974, Figs. 7, 16.

¹¹⁷ Muscarella 1981, 348, no. 27.



Fig. E1.4: Bronze button PPP 181908:033:005 (14) from Grave 102. Photo by Andrea Squitieri.



Fig. E1.5: White applique PPP 181908:036:012 (18) from Grave 102. Photo by Andrea Squitieri.

E1.2.4 Grave 103

Grave 103 is a cist grave located in Square 182908 (§C4.5). It had been robbed, but the skeleton was partially preserved. A flat ring was found in the pelvis area, and two unworked pebbles were found near the elbow and the knee respectively. The other items come from the fill directly above the skeleton.

Registration no.	no.	Description	Context
PPP 182908:019:007	19	Bronze flat ring, with thicker edges. D. 2.3 cm, H. 1 cm. Decorated parallels come from Iron Age III graves at Mala Mcha and Ruwar (both in Iranian Kurdistan).	With the skeleton, in the pelvis.
PPP 182908:019:009 PPP 182908:019:010	20	2 unworked pebbles, D. 2 to 3 cm. PPP 182908:019:009 is roundish and pink in colour; PPP 182908:019:010 is white and oval in shape.	With the skeleton: the first near the knee, the second near the elbow.

Registration no.	no.	Description	Context
PPP 182908:019:002	21	Complete iron bracelet with overlapping extremities, D. 4.7 cm, Th. 1.2 cm. Due to corrosion, it is not clear if the terminals are decorated.	Looted grave fill
PPP 182908:019:003-004	22	2 iron pins, fragments. L. 4.6 cm and L. 8 cm.	Looted grave fill
PPP 182908:019:005 PPP 182908:019:008	23	2 iron rings in fragments. D. < 2 cm.	Looted grave fill
PPP 182908:019:006	24	Iron fragment, L. < 1 cm, original shape cannot be determined.	Looted grave fill

* Amelirad *et al.* 2017, Fig. 30; Ghasimi *et al.* 2019, Fig. 20.

E1.2.5 Grave 105

Grave 105 is a cist grave located in Square 181908 (§C3.5). Only part of the architecture was found, while the fills had been looted and the skeleton completely obliterated. The items listed below were found inside the grave architecture. The fill above the grave architecture, called Locus:181908:044, may also have contained some of the items coming from this grave (§E1.3).

Registration no.	no.	Description	Context
PPP 181908:051:002	25	Iron fragment, possibly from a ring, L. 4.5 cm.	Looted grave fill
PPP 181908:055:006	26	Iron fragment, L. 1.8 cm, original shape cannot be determined.	Looted grave fill
PPP 181908:055:002	27	Fragments of a blue material, possibly from an Egyptian Blue bead.	Looted grave fill

E1.2.6 Grave 106

Grave 106 (§C6.2.2) is an inhumation grave located in Square 181909. It lies between the northern border of the excavation area and Grave 107, of which only the architecture has been found but no objects (Figs. C5, C17). No architecture connected to Grave 106 has been found. Partially-articulated human remains were found, which perhaps belonged to two individuals. The items shown in the table below were found in the fill immediately above the skeleton(s), and some of them are discussed in more detail after the table. Several pieces of personal ornamentation were found, plus the arrowhead (PPP 181909:069:019) discussed in §E4.

Registration no.	no.	Description
PPP 181909:069:001	28	2 bronze pins with spiral decoration (see below).
PPP 181909:069:005		
PPP 181909:069:002	29	Bronze fragments, possibly of needles. L. 6.8 cm (max), Th. 0.1 cm.
PPP 181909:069:010	30	Bronze dome-shaped perforated disc (see below).
PPP 181909:069:011	31	Bronze open ring with flat surface, D. 2.7 cm, Th. 0.1 cm.
PPP 181909:069:022	32	Bronze tube formed from a rolled sheet, L. 5.5 cm, D. 0.4 cm. Parallels from Kalhu (Nimrud), Deve Hüyük and Hasanlu (Level IV)*.
PPP 181909:069:003	33	Bronze bead, oblate shape. D. 0.7 cm.
PPP 181909:069:023	34	3 bronze coils (see below).
PPP 181909:069:024		
PPP 181909:069:029		
PPP 181909:069:025	35	3 bronze crescent-shaped earrings (see below).
PPP 181909:069:027		
PPP 181909:069:031		
PPP 181909:069:032	36	Bronze-iron mirror, broken (see below).
PPP 181909:069:019	/	Iron arrowhead, broken (see §E4).
PPP 181909:069:007	37	3 iron bracelets, decorated (see below).
PPP 181909:069:008		
PPP 181909:069:009		
PPP 181909:069:012	38	3 iron rings: D. 2.6 cm / 2.7 cm / 1.5 cm, Th. 0.4 cm / 0.4 cm / 0.1 cm. The last has overlapping extremities.
PPP 181909:069:016		
PPP 181909:069:020		
PPP 181909:069:013	39	11 iron curved fragments, L. max 2 cm, original shape cannot be determined.
PPP 181909:069:015		
PPP 181909:069:021	40	Iron crescent-shaped earring. D. 2.6 cm, Th. 0.6 cm.
PPP 181909:069:017	41	Truncated bicone bead in Egyptian Blue decorated with vertical grooves. D. 0.25 cm.
PPP 181909:069:018	42	Fragments of a blue material, possibly from an Egyptian Blue bead.
PPP 181909:069:014	43	2 red carnelian beads, oblate shape. D. 1 cm; D. 0.4 cm.
PPP 181909:069:030		
PPP 181909:069:028	44	Cylindrical white bead, L. 1.4 cm; D. 0.7 cm, possibly in chalk.
PPP 181909:069:026	45	Black stone beads, PPP 181909:069:026 possibly has an etched decoration. L. 1.5 cm / 1.4 cm / 0.8 cm; D. 0.4 cm / 0.5 cm / 0.5 cm.
PPP 181909:069:033		
PPP 181909:069:034		

* Kalhu (Nimrud): Curtis 2013, Pl. 74; Deve Hüyük: Moorey 1980, Fig. 16: 423; Hasanlu IV: Muscarella 1988, cat. no. 129.

(28) Pins with spiral decoration (registration numbers PPP 181909:069:001 = Fig. E1.6, and PPP 181909:069:005).

Material: Bronze.

Dimensions: PPP 181909:069:001: L. 6.3 cm; Th. 0.1 cm; PPP 181909:069:005: L. 2.6 cm; Th. 0.2 cm, broken.

PPP 181909:069:001 is a roll-headed pin with spiral decoration. PPP 181909:069:005 is thicker than the first pin,



Fig. E1.6: Pin with spiral decoration PPP 181909:069:001 (28) from Grave 106. Photo by Andrea Squitieri.

and its extremities are not preserved. It shows the same spiral decoration as the first.

Comparisons: Roll-headed pins, although not decorated like the examples here, are attested in various sites, e.g., Kalhu (Nimrud), Dur-Šarrukin (Khorsabad), Deve Hüyük, and Megiddo, and in Iran at Dinkha Tepe and Talish (Gilan Province)¹¹⁹.

(30) Domed-shaped perforated disc (registration number PPP 181909:069:010; Fig. E1.7)

Material: Bronze.

Dimensions: D. 4.2 cm; H. 1.2 cm.

Dome-shaped disc with a perforation (D. 0.3 cm) in the middle. Partially covered with patina, and with a short crack visible on the side. It was perhaps used as a decorative element, for example as a metal boss to decorate a handle terminal.



Fig. E1.7: Domed-shaped perforated disc PPP 181909:069:010 (30) from Grave 106. Photo by Andrea Squitieri.

Comparisons: Similar examples have been found in the Iron Age graves of Dinkha Tepe (levels III-II) and of Sanandaj (8th-7th centuries BC)¹²⁰.

119 Kalhu and Dur-Šarrukin: Curtis 2013, Pl. 93: 1161; Deve Hüyük inhumation cemetery: Moorey 1980, Fig. 14: 357-358; Dinkha Tepe: Muscarella 1974, Fig. 36; Megiddo stratum V and I: Lamon and Shipton 1938, Pl. 84: 11-13; Talish: Bassampour 2014, Fig. 5

120 Dinkha Tepe: Muscarella 1974, Fig. 7: 622 and Fig. 48: 714-715; Sanandaj: Amelirad *et al.* 2012, Pl. 18.



Fig. E1.8: Bronze coils (left: PPP 181909:069:023, right: PPP 181909:069:024) (34) from Grave 106. Photo by Andrea Squitieri.

(34) Coils (registration numbers PPP 181909:069:023 = **Fig. E1.8 left**; PPP 181909:069:024 = **Fig. E1.8 right**; PPP 181909:069:029).

Material: Bronze.

Dimensions: PPP 181909:069:023: L. 2.1 cm, D. 1 cm; PPP 181909:069:024: L. 1 cm, D. 0.4 cm; PPP 181909:069:029: L. 0.6 cm, D. 0.4 cm (broken).

Three bronze coils made of a thin, looping bronze string. The first has an ovoid shape with the string forming a sort of hook on one extremity (broken); the other two have a cylindrical shape. They were possibly used as beads, or in the case of PPP 181909:069:023, as pendants.

Comparisons: Similar items are known from the inhumation graves at the cemetery of Sanandaj, dated to the 8th-7th centuries BC; from the Iron Age II graves (c. 1050-800 BC) of Hasanlu; from Dinkha Tepe, and from Iron Age III graves in Luristan at the cemeteries of War Kabud and Baba Jillan. Parallels in silver are known from Kul Tarike cemetery, dated to around the 7th century BC¹²¹.

(35) Crescent-shaped earrings (registration numbers PPP 181909:069:025 = **Fig. E1.9**, PPP 181909:069:027, and PPP 181909:069:031).

Material: Bronze.

Dimensions: PPP 181909:069:025: D. 1.1 cm; Th. (max): 0.4 cm; PPP 181909:069:027: D. 1 cm, Th. (max) 0.2 cm; PPP 181909:069:031: D. 0.9 cm; Th. (max): 0.3 cm.



Fig. E1.9: Crescent-shaped earring PPP 181909:069:025 (35) from Grave 106. Photo by Andrea Squitieri.

Three crescent-shaped earrings with touching extremities.

Comparisons: Several earrings of this shape have already been found on Qalat-i Dinka during the 2016 and 2018 campaigns¹²². Crescent-shaped earrings occur frequently across the Near East throughout both the Bronze and Iron Ages¹²³.

(36) Mirror (registration number PPP 181909:069:032; **Fig. E1.10**).

Material: Bronze and iron.

Dimensions: plaque: L. 11.4 cm, W. 4.4 cm, Th. 0.8 cm; stem: L. 2.1 cm, D. 1.3.

Four fragments, of which the largest has a bronze stem attached to a flat circular plaque in iron, broken in half. The other three fragments are smaller and are likely also parts of the plaque. The object is interpreted as a mirror, based on its shape.

121 Sanandaj: Amelirad *et al.* 2012, Pl. 19b-c, Pl. 21; Hasanlu: Danti/Ci-farelli 2015, Fig. 23h (Grave SK111); Dinkha Tepe: Muscarella 1988, cat. no. 31, Muscarella 1974, Fig. 45: 1002; War Kabud: Haerinck/Overlaet 2004a, Fig. 36: G3-G4; Baba Jillan: Hasanpur *et al.* 2015, pl. 11; Kul Tarike: Rezvani/Roustaei 2007.

122 Kreppner/Squitieri 2017a, Fig. C26; Squitieri 2019, Fig. H8.

123 E.g., Curtis 2013, Pl. 86; Ilan 2014.



Fig. E1.10: Fragments of a bronze-iron mirror PPP 181909:069:032 (36) from Grave 106. Photo by Andrea Squitieri.

(37) Bracelets, possibly decorated (registration numbers PPP 181909:069:007 = **Fig. E1.11:** left, PPP 181909:069:008, and PPP 181909:069:009 = **Fig. E1.11:** right).

Material: Iron.

Dimensions: PPP 181909:069:007: D. 9 cm, Th. 1 cm; PPP 181909:069:008: D. 9.1 cm; Th. 0.7 cm; PPP 181909:069:009: D. 6.1, Th. 0.7 cm.

PPP 181909:069:007 is an open iron bracelet, while PPP 181909:069:008 and PPP 181909:069:009 have overlapping terminals. All three have highly corroded surfaces, which obscure any decorative motifs that may exist on their terminals. Similar bracelets from other Iron Age sites often have terminals decorated with stylised animal heads of caprids or serpents.

Comparisons: Iron Age examples of similar bracelets are attested in many sites, for example Kalhu (Nimrud), Hasanlu, the cemetery of Sanandaj, as well as in Luristan and the Gilan Province of Iran¹²⁴.



Fig. E1.11: Iron bracelets (left: PPP 181909:069:007, right: PPP 181909:069:009) (37) from Grave 106. Photo by Andrea Squitieri.

¹²⁴ Kalhu (Nimrud): Curtis 2013, 107-110, Pl. 84-85; Hasanlu: Muscarella 1988, 36; Sanandaj: Amelirad et al. 2012, Pl. 36; Luristan: Baba Kilan, Hasanpur et al. 2015, Pl. 21; Gilan Province (Talish): Bassampour 2014, Fig. 10.

E1.2.7 Grave 110

Grave 110 (§C5.3.3) is an inhumation pit grave found in Square 182909 (**Figs. C5, C17**). It was partially looted, but the upper part of the skeleton was preserved. Three bronze fibulae and a cylinder seal with its glass cap were found in direct association with the skeleton, and are discussed in detail in §E2 and §E3. The other finds include beads found in the fill directly above the skeleton. This grave yielded a radiocarbon date of 767-488 calBC (see **Table C1**).

Registration no.	no.	Description	Context
PPP 182909:067:010	/	Bronze fibula (see §E2.1).	Near the left clavicle
PPP 182909:067:004	/	Bronze fibula (see §E2.1).	Near the right clavicle
PPP 182909:067:011	/	Bronze fibula (see §E2.1).	Near the left elbow
PPP 182909:067:007	/	Cylinder seal with hunting scene (see §E3.2).	Next to the left elbow
PPP 182909:067:008	/	Glass cap for cylinder seal found with seal PPP 182909:067:007 (see §E3.2).	Next to the left elbow
PPP 182909:067:009	46	Shapeless rock crystal (quartz) fragment, translucent, L. 2.3 cm; W. 1.7 cm; H. 1 cm.	On a left rib
PPP 182909:067:002	47	Tiny and shapeless fragments of gold	Grave fill
PPP 182909:067:001	48	Carnelian barrel bead, L. 1 cm; D. 0.6 cm (Fig. E1.12).	Grave fill
PPP 182909:067:003	49	White oblate bead decorated with vertical grooves, D. 0.4 cm.	Grave fill
PPP 182909:067:005	50	Fragments of a blue material, possibly from an Egyptian Blue bead.	Grave fill



Fig. E1.12: Carnelian bead PPP 182909:067:001 (48) from Grave 110. Photo by Andrea Squitieri.

E1.2.8 General considerations on the grave goods (Group 1)

Only the items from Grave 110 can be connected to an absolute date derived from radiocarbon analysis (767-488 calBC). Based on their style, the items from the other graves may also belong to a chronological horizon very close to that of Grave 110. Though many of the grave goods can occur across a very long span of time (e.g., the crescent-shaped earrings and the carnelian beads), others have parallels only among the Late Iron Age and Achaemenid-period sites of the Levant, northern Mesopotamia and western Iran. Overall, it seems that a date spanning from around the 9th century BC to the end of the Achaemenid period would be appropriate for the grave items analysed in this section (see also below §E1.4). Additional items from graves, some of which having a chronological significance are discussed in the following §E2, §E3 and §E4.

E1.3 Small finds from looted fills and the topsoil (Group 2)

The sections below will deal with the ancient items found in the fills of the looting pits (Group 2). Because they lack stratigraphic information, they have been organised by material and category. Ancient finds from the topsoil are discussed here also, as they too do not provide any stratigraphic information.

The finds discussed below are divided into the following categories:

- 1) Stone tools;
- 2) A complete metal bowl;
- 3) Metal rods and studs;
- 4) Pieces of personal ornaments formed from metal;
- 5) Beads in various materials;
- 6) Perforated ivory/bone items;
- 7) Perforated ceramic discs.

To this list, we should add the items from looted fills that are discussed in other sections:

Registration no.	Item	Chapter
PPP 181909:067:001	Fibulae	§E2
PPP 182909:020:007		
PPP 182908:008:006	Cylinder seals	§E3
PPP 181909:067:003		
PPP 181908:025:009	Arrowheads	§E4
PPP 181908:029:030		
PPP 181908:029:055		
PPP 181909:052:016		
PPP 181909:052:017		
PPP 181909:063:011		
PPP 181909:063:013		

E1.3.1 Stone tools

Stone tools are divided into morphological categories following the classification established in the previous publications of the stone tools from the Dinka Settlement Complex¹²⁵. Basic information is first provided in the table below, then each category is discussed in greater detail.

Registration no.	no.	Description
PPP 182909:006:005	51	2 half-broken querns. PPP 182909:006:005: L. 12 cm, W. 11.5 cm, H. 7.5 cm. It shows a flattish surface smoothed through use, and a curved dorse. It seems to be too wide to be a handstone. Stone may be granite. PPP 182909:020:011: L. 11 cm, W. 13.5 cm. Similar to PPP 182909:006:005.
PPP 181908:044:042	52	3 broken handstones. PPP 182909:019:003: L. 11.1 cm; W. 7.4 cm; H. 5.5 cm. Working surface flat polished through use, convex dorse easy to grip. Stone is basalt. PPP 182909:014:002: L. 8 cm, W. 6.5 cm, H. 4 cm. Working surface rough, convex dorse.
PPP 182908:007:013	53	4 pounders. PPP 182908:007:013: L. 8 cm, W. 6.5 cm. Ovoid pebble with pecking marks on the surface. Stone: basalt. PPP 182909:051:002: D. 6.5 cm. Ovoid pebble (broken) with pecking marks. Speckled stone, may be granite. PPP 181909:051:002: L. 8 cm, W. 7 cm. Spheroid pebble, with pecking marks. Stone is whitish, and could be limestone. PPP 182909:005:004: D. 7 cm. Spherical pebble made of basalt with pecking marks.
PPP 181908:029:011	54	9 perforated stones. D. between 10-15 cm. They are in white limestone, and show a biconic perforation of about 2-3 cm in the middle of a roughly-worked, disc-shaped cobble.
PPP 181908:029:033		
PPP 181908:044:019		
PPP 181909:062:005		
PPP 181909:062:006		
PPP 182908:006:005		
PPP 182908:022:005		
PPP 182908:046:004		
PPP 182909:021:004		
PPP 181908:029:006	55	4 pebble mortars. D. < 13 cm. They have two shallow depressions on opposite sides carved into slightly-worked pebbles. Stone is limestone except for PPP 182908:038:002 which is basalt
PPP 181908:044:044		
PPP 182908:038:002		
PPP 182908:006:007		
PPP 181908:029:038	56	4 spheroid pebbles (weights?). D. around 5 cm, polished surface.
PPP 181908:029:054		
PPP 181909:050:004		
PPP 181909:050:006		

¹²⁵ Squitieri 2017; 2018; 2019.

Registration no.	no.	Description
PPP 182909:006:006	57	4 broken whetstones, 1 entirely preserved.
PPP 182909:004:004		They have square sections, smooth
PPP 182909:020:002		sides showing tiny linear marks, and
PPP 182909:026:004		rounded extremities (when preserved).
PPP 182909:020:008		PPP 182909:006:006: L. 7.5 cm, W. 2.8;
		PPP 182909:004:004: L. 7.5 cm, W. 3.5 cm;
		PPP 182909:020:002: L. 5 cm, W. 2.5; PPP
		182909:026:004: L. 6 cm, W. 4 cm; PPP
		182909:020:008: L. 8 cm, W. 3 cm. This
		whetstone is completely preserved and
		contains a bi-conic perforation of D. 0.3
		cm used to hang the tool with a string.
PPP 181908:062:004	58	Spindle-whorl. Material: limestone. D. 2.7
		cm; H. 0.7 cm.
PPP 181908:048:009	59	Polished stone fragment, L. 6.5 cm, W.
		3.7 cm, with triangular section, slightly
		pointed. It may be the broken leg of a
		tripod bowl. Stone is basalt.
PPP 182909:006:004	60	Ring base and curved body fragment of a
		bowl. Made of basalt.

(51) Querns.

These are grinding tools with a triangular section and a flat working surface. Mainly used to grind grain. Two half-broken querns were found in QID₁, possibly made of granite.

(52) Handstones.

These are upper tools used for grinding in conjunction with querns. They have a flattish, smoothed working surface and a curved dorse. Usually they can be easily distinguished from querns by their size, which must be small enough to easily grip in the hand. While the examples from QID₁ are broken, they have been interpreted as handstones because they are narrower and easier to handle than the querns. Their stone is basalt.

(53) Pounders.

These are defined as spheroid or ovoid pebbles usually with one dimension larger than 5 cm which makes them easy to grip and use to pound without harming the fingers. They also show pecking marks on their surface due to use. Four examples made of basalt and limestone were found in QID₁. These tools have close parallels from the Lower Town¹²⁶.

(54) Perforated stones.

Disc-shaped stones, with diameters between 10 and 15 cm, usually roughly worked at the edges, and showing coarse-

ly made, bi-conic perforations in their centres. Their function is not clear, and it is possible they had multiple purposes. Among these, they may have been used as weights for digging sticks. It is unlikely that they were used as weights for weaving as they are too heavy (heavier than 500 g) and irregular. For a similar reason, they were probably not used to weight fishing-nets. We should also exclude their potential use as fly-wheels and door-sockets, firstly because they are not consistent enough to allow a smooth rotation, and secondly because door-sockets at the Dinka Settlement Complex look very different from these perforated stones. Several such perforated stones were also found in the Lower Town¹²⁷.

(55) Pebble mortars.

These are disc-shaped stones, never more than 13 cm in diameter, showing two shallow depressions on the opposite sides, carved into an unworked or slightly worked body. They are also called cupmarks. The depressions are irregular and do not show evident wear marks inside. These tools may have had many uses connected to grinding small substances. Similar pebble mortars were also found in the Lower Town¹²⁸.

(56) Spheroid pebbles, possibly weights.

These are spheroid or ovoid pebbles, showing a smooth surface, with dimensions not exceeding 5 cm. They are similar in shape to pounders, however they lack visible pecking marks and their size makes them uncomfortable for pounding. Hence, they are interpreted as weights for a variety of purposes. Similar tools have also been found in the Lower Town¹²⁹. We do not have a sufficient number to make a statistical analysis of their weight distribution patterns, which might confirm their identification as weights.

(57) Whetstones.

These tools can be easily recognised by their squarish sections, rounded edges, and tiny linear wear marks on their smooth sides. The only entirely-preserved example from QID₁, PPP 182909:020:008, is also perforated near one end, allowing the tool to be hung by a string. Similar whetstones were found in 2018 during the operation QID₂ at Qalat-i Dinka, and many more have been found in the Lower Town¹³⁰. They were used to sharpen other objects, including metal items such as arrowheads.

127 Wilkinson/Squitieri/Hashemi 2016; Squitieri 2017; 2018; 2019.

128 Wilkinson/Squitieri/Hashemi 2016; Squitieri 2017; 2018; 2019.

129 Squitieri 2017; 2018; 2019.

130 Squitieri 2017; 2018; 2019.

126 Squitieri 2017; 2018; 2019.

(58) Dome-shaped spindle-whorl (Fig. E1.13).

This example is the only spindle-whorl in this shape found in the Dinka Settlement Complex. Spindle-whorls known from both Qalat-i Dinka and the Lower Town are made of ceramic and are disc-shaped (§E1.3.11).



Fig. E1.13: Dome-shaped spindle whorl from looting fill. PPP 181908:062:004 (58). Photo by Andrea Squitieri.

(59-60) Stone vessel fragments.

One has a triangular section, a pointed extremity and a polished surface; it may have been the foot of a tripod bowl. The other is a fragment of a ring base attached to a curved body, which belonged to a ring base bowl. They have no parallels in the Lower Town.

Many of the stone tools listed above have parallels from the Main Occupation Period structures of the Lower Town, namely the pounders, perforated stones, pebble mortars, spheroid weights and whetstones, thus establishing a material connection between the Lower Town and Qalat-i Dinka. The tools identified as handstones and querns in QID1, on the other hand, are much rarer (if not absent entirely) in the Lower Town; only one broken quern has been found in DLT2¹³¹. The stone tools described above are difficult to relate to graves. Although it is not impossible to find stone tools in funer-

ary contexts, these objects are more frequently part of the urban setting. Hence, it is possible that these stone tools originated in Building P. The dome-shaped spindle whorl represents the first of its kind ever found in the Dinka Settlement Complex, as do the two fragments of stone vessels. They could be pieces of furniture from a destroyed grave, since it is not uncommon to find such items in graves. However, due to the context of these finds, this is difficult to establish.

E1.3.2 A complete bronze bowl

(61) Flat-based metal bowl (registration number: PPP 181908:029:034 = **Fig. E1.14**).

Material: bronze.

Dimensions: D. 19 cm; H. 6 cm.

Complete bronze bowl with a flat base bowl, curved body, and flared rim. It was found in a looting pit fill, about 2 m west of the looted Grave 102 (§C3.5). It was in an upside-down position, and contained the bones of an almost complete human hand mixed with soil. On the basis of these contents, it is plausible that it came from one of the graves found in Square 181908. Although radiocarbon analysis was carried out on one of the bones, it was not successful due to the lack of collagen.

Comparisons: Bowls similar to PPP 181908:029:034 are often referred to as *phiale*¹³². They can be found across a vast area of the Near East throughout the Iron Age and the Achaemenid period. Many of these bowls bear decorative motifs, unlike ours which is plain¹³³. Although



Fig. E1.14: Complete metal bowl PPP 181908:029:034 (61) found in a looting pit close to Grave 102. It was found upside down with bones of a human hand in it. Restored by Akam Omar Qaradaghi. Photo by Haymin Noori.

¹³¹ Squitieri 2018, Fig. G8.

¹³² Lushey 1939.

¹³³ Iron Age: Howes Smith 1986; Achaemenid period: Dusinberre 1999.

an Assyrian origin has been suggested for their design¹³⁴, their appearance in the Late Bronze Age and Iron Age I Hasanlu points rather to a tradition that may have been inspired by the second millennium BC flared-rim bowls from south-eastern Anatolia, Iran, and Mesopotamia¹³⁵. Bronze *phiale* became popular after the 9th century BC, with several examples found in Assur¹³⁶ and Kalhu (Nimrud)¹³⁷, as well as outside Assyria¹³⁸. Some plain examples similar to PPP 181908:029:034 are also known from the Iron Age III graves in Iranian Kurdistan and Luristan¹³⁹. During the Achaemenid period, bronze *phiale* were even more widespread, and have been found across the area stretching from Central Asia to Greece¹⁴⁰.

E1.3.3 Metal rods and studs

This category is comprised of metal rods and studs which, although found in looting pits, may have been elements of grave furniture as they were found in close proximity to Graves 102, 103, and 105. Possibly they were used to assemble pieces of wooden furniture that were included in the grave goods, of which nothing more has been preserved.

(62) Curved metal rods (registration numbers: (A) PPP 181908:029:008 = **Fig. E1.15**; (B) PPP 181908:029:009; (C) PPP 181908:029:010; (D) PPP 181908:029:046; (E) PPP 181908:046:003; and (F) PPP 182908:011:003).

Material: iron.

Dimensions: A: L. 13.2 cm, Th. 2.1 cm; B: L. 5.3 cm, Th. 0.7 cm; C: L. 7.6 cm; Th. 0.7 cm; D: L. 6.7 cm; Th. 0.8 cm; E: L. 6.5 cm, Th. 0.7 cm; F: D. 4.3; Th. 0.8 cm

Six curved iron rods with rather thick bodies. They are broken, except for PPP 181908:029:008, which is complete. The rods were found in looting pits so their context cannot help to establish their function. However, it is noteworthy that four of them (A, B, C and D) were found in close proximity to one another, in the fill covering the architecture of Grave 102. It is therefore possible that they came from this grave. In support of this, we should mention that the

fill Locus:181908:029, where the rods were found, also contained a number of bronze studs (**no. 63**) matching those found inside Grave 102, which suggests that this fill may have contained parts of the original grave furniture. Rod F was found above Grave 103, and possibly derived from it.

Comparisons: Their shape and bodies resemble the connecting rods used in furniture from Kalhu (Nimrud)¹⁴¹. Some of the Kalhu examples show grooves on their bodies, a feature which is seen on PPP 181908:029:046 and possibly also on PPP 181908:029:009, although here it is obscured by corrosion.



Fig. E1.15: Curved iron rod PPP 181908:029:008 (**62**) from a looting pit near Grave 102. Photo by Andrea Squitieri.

(63) Metal studs (registration numbers PPP 181908:029:043 = **Fig. E1.16**; PPP 181908:029:049; PPP 181908:029:051; PPP 181908:042:003; PPP 181908:044:004; PPP 181908:044:008; PPP 181908:044:014; PPP 181908:044:035; PPP 181908:044:040; PPP 181908:033:005; PPP 181908:044:015; PPP 181908:044:033; and PPP 182909:043:003).

Material: all in bronze; except for PPP182909:043:003, which is in iron.

Dimensions: L. < 1 cm; head D. < 1 cm.

13 small metal studs with a rounded head, a flat head or a button-like head. They have a single pin, which in PPP 181908:033:005; PPP 181908:044:015; and PPP 181908:044:033 is not preserved. These small studs were possibly used to assemble wooden furniture. The bronze examples came from looted fill excavated above the Grave 105, and hence it is possible that they belonged to this



Fig. E1.16: Bronze stud PPP 181908:029:043 (**63**) from a looting pit near Grave 102. Photo by Andrea Squitieri.

¹³⁴ Curtis 2013, 69.

¹³⁵ Dusinberre 1999, 76; Danti/Cifarelli 2016, 366; Howes Smith 1986.

¹³⁶ Haller 1954.

¹³⁷ Layard 1853.

¹³⁸ See Curtis 2013, 71-72 for a list of sites.

¹³⁹ Sanandaj: Amelirad *et al.* 2012, Pl. 34: A10; War Kabud: Haerincq/Overlaet 2004a, Pl. 138: A37-4; Djub-i Gauhar: Haerincq/Overlaet 1999, ill. 15 no. 7, Pl. 33: 77b; Chamahzi Mumah: Haerincq/Overlaet 1998, Fig. 11.17.

¹⁴⁰ Dusinberre 1999, Fig. 2.

¹⁴¹ Curtis 2013, Pl. 58.681.

grave. The iron stud, on the other hand, came from a looted pit located near the eastern section of the excavated area, and hence it is not clear if it originated from a grave or another context. For comparisons, see **no. 15**.

E1.3.4 Metal pieces of personal ornamentation

Several pieces of rings, bracelets, earrings and pins were found across the operation. Many of them match those collected in previous campaigns. It is likely that they came from the graves destroyed by the looters. They are summarised in the table below, and potential parallels are included in the description.

Iron:

Registration no.	no.	Description
PPP 181909:052:010 PPP 181908:043:004	64	8 iron rings, with D. between 1.8 cm and 2.8 cm.
PPP 181909:058:005 PPP 181909:063:004 PPP 182908:006:004 PPP 182908:007:007 PPP 181909:050:003 PPP 182908:006:008		Very corroded. PPP 181909:058:004 has also some bronze patina because it was found along with bronze ring PPP 181909:058:004. PPP 181909:063:004 is thicker than the others (Th. 1.2 cm) so it is not clear whether it was a finger-ring or a small chain ring.
PPP 182908:007:014	65	Crescent-shaped iron earring, D. 1.6 cm; Th. 0.6 cm., highly corroded. For similar earrings in bronze, see below.

Bronze:

Registration no.	no.	Description
PPP 181908:029:021	66	Bronze pendant, L. 2.8 cm; D. 0.2-0.7 cm. Elongated object, thicker and rounded at one end, possibly a pendant.
PPP 181909:052:022	67	Bronze pendant, L. 2.4, D. max 1.1 cm. Composed of a spherical body with a smaller spherical shape on one end and a circular "loop" to which a hook is attached on the opposite side.
PPP 181908:043:005	68	Bronze spring ring, D. 1.8, made of a string looping on itself three times (Fig. E1.17). Perhaps used as a hair-binder. Parallels are attested in Iron Age III graves in Iranian Kurdistan ⁱ . See also parallels from Late Bronze Age and Iron Age graves from Hasanlu ⁱⁱ , Dinkha II-III ⁱⁱⁱ , from Iron Age III graves in Luristan ^{iv} , and from the Iron Age grave at Ruwar in Iranian Kurdistan ^v . See also similar items from Nimrud ^{vi} .

Registration no.	no.	Description
PPP 181908:044:005	69	Decorated bronze ring, D. 1.7 cm., with touching extremities and a ridged surface (Fig. E1.18). A similar decoration can be found on bracelets from Hasanlu (Level IV) ^{vii} .
PPP 181908:056:003	70	Decorated bronze ring, D. 2.3 cm; Th. 0.3 cm, with touching extremities. From the terminals along the body, the decorative motif is composed of: three transversal grooves, a cross and two longitudinal grooves along the rest of body. Very similar in shape and decoration to PPP 181909:038:055 found in 2018 ^{viii} .
PPP 181908:046:010 PPP 181909:063:006 PPP 182909:027:005	71	Bronze ring, D. 1.9 cm, with overlapping terminals. Bronze hair ring, D. 0.3 cm, with overlapping extremities. Bronze ring with overlapping terminals. D. 1.7 cm; Th. 0.1 cm. Similar rings with overlapping extremities are attested throughout a wide area.
PPP 181909:052:008	72	Broken bronze ring, D. 2 cm, Th. 0.2 cm.
PPP 181909:058:004	73	Bronze ring covered with iron corrosion (found with iron ring PPP 181909:058:005). D. 2.3 cm, Th. 0.3 cm.
PPP 181909:062:004	74	Bronze ring with touching extremities found with PPP 181909:062:007.
PPP 181909:062:007	75	Bronze ring with touching extremities found together with PPP 181909:062:004. D. 2.4 cm; Th. 0.1 cm.
PPP 181909:063:015	76	Open bronze ring, with tapering terminals. D. 2.9 cm; Th. 0.2 cm.
PPP 182908:002:004	77	Open bronze ring, D. 1.7 cm, with one spherical terminal.
PPP 182908:002:006 PPP 181908:044:057 PPP 182908:007:008 PPP 182908:007:015 PPP 182908:026:013	78	Crescent-shaped bronze earrings, D. between 0.8 cm and 1.6 cm, Th. between 0.1 cm and 0.3 cm. PPP 182908:007:015 is the only complete one (Fig. E1.19). See above for similar examples from Grave 106.
PPP 181908:050:003 PPP 181908:050:008	79	Two fragments of bronze items, possibly parts of pins. L. c. 2.5 cm; D. 0.1 cm

- i Amelirad *et al.* 2012, Pl. 15 (although these are thicker than our examples); Amelirad *et al.* 2017, Figs. 21b, 23 and 25; Amelirad/Azizi 2019, Fig. 17.
- ii Danti/Cifarelli 2013.
- iii Muscarella 1974.
- iv Haerinck/Overlaet 1999, Fig. 20; Haerinck/Overlaet 2004a, Fig. 27.
- v Ghasimi 2019, Fig. 10.
- vi Curtis 2013, Pl. 86.949-950, the latter in silver.
- vii Muscarella 1988, cat. n. 18 (University of Pennsylvania Museum of Archaeology and Anthropology, object number 59-4-126).
- viii Squitieri 2019, no. 8.



Fig. E1.17: Bronze spring PPP 181908:043:005 (68) from a looting pit. Photo by Andrea Squitieri.



Fig. E1.18: Bronze ring PPP 181908:044:005 (69) decorated with a ridged surface. Photo by Andrea Squitieri.



Fig. E1.19: Bronze crescent-shaped earring PPP 182908:007:015 (78) from a looting pit. Photo by Andrea Squitieri.

E1.3.5 Carnelian beads

Carnelian beads are very common across the Near East and can be found in virtually every period. Several examples come from the Sasanian graves of Gird-i Bazar, whose material has been identified by means of archaeometric analysis¹⁴². Because of their similarity in colour and shape,

the red beads from QID₁ are also thought to be carnelian. Interestingly, aside from QID₁, such beads have only been found among the Sasanian graves of Gird-i Bazar, while no such bead was found in the Iron Age structures of the Dinka Settlement Complex. This leads us to assign the carnelian beads to the graves of QID₁ rather than to Building P.

Registration no.	no.	Description
PPP 181908:024:005	80	Oblate shape beads with straight perforation, D. between 0.4 cm and 1 cm. Fig. E1.20: PPP 182908:005:006.
PPP 181908:026:003		
PPP 181908:044:059		
PPP 181909:052:026		
PPP 182908:005:006		
PPP 182908:005:008		
PPP 182908:008:003	81	Spherical shape beads. Distribution and size: see oblate beads above.
PPP 182908:008:013		
PPP 182908:038:006		
PPP 182909:006:007		
PPP 182909:015:003		
PPP 182909:021:008		
PPP 182908:001:005		
PPP 181909:052:023		
PPP 182908:005:004	82	Barrel shape beads, D. between 0.5 cm and 1.6 cm.
PPP 182909:021:007		
PPP 182909:055:004		
PPP 181908:029:014	83	Short cylindrical beads, broken.
PPP 181908:029:045		
PPP 181909:052:024		
PPP 182908:002:005		
PPP 182909:034:009		



Fig. E1.20: Carnelian bead PPP 182908:005:006 (80) from looting pit. Photo by Andrea Squitieri.

E1.3.6 Blue/white-blue beads

In this category, I have included beads or fragments of beads in blue and white-blue colours. Given their colour and consistency, they may be made of Egyptian Blue, faience, or frit. However, some of the blue beads from the 2018 campaigns were proven to have been made of

¹⁴² Greenfield 2017, 174-175; Downey 2018.

Egyptian Blue by means of archaeometric analysis¹⁴³. Therefore, by comparison, it is possible that the beads discussed below are in Egyptian Blue. These items may well have originally been located in the graves. However, one fragmented bead in Egyptian Blue was also found in the Lower Town, in the operation DLT₂¹⁴⁴. This means that this material was also used in the Main Occupation Period structures in the Lower Town. Hence, it is possible that at least some of the Egyptian Blue beads from QID1 belonged to Building P rather than to the graves.

Registration no.	no.	Description
PPP 181908:044:024	84	Cylindrical blue beads, D. between 0.2 cm and 0.4 cm; L. between 0.3 cm and 0.6 cm. Broken and highly weathered. From the fill above Grave 105 so perhaps originated there.
PPP 181908:044:025		
PPP 181908:044:027		
PPP 181908:044:028		
PPP 181908:044:030		
PPP 181908:044:043		
PPP 181908:044:045		
PPP 181908:044:049	85	Grooved cylindrical beads, L. between 0.5 cm and 0.7, D. between 0.2 cm and 0.3 cm. PPP 181908:044:036 is likely a fragment of the same type as L. 0.2 cm and D. 0.2 cm. They are bluish-white in colour. They come from the fill above Grave 105. Similar beads are found across a vast area from the Levant to western Iran*. Fig. E1.21: PPP 181908:044:026.
PPP 181908:044:026		
PPP 181908:044:031		
PPP 181908:044:032		
PPP 181908:044:036		
PPP 181909:069:023	86	Short oblate bead decorated with grooves. This category of beads is also very frequently found across a vast area, see references above for the grooved cylindrical beads.
PPP 181908:050:005	87	Powdery and shapeless fragments of an intense blue colour. Based on the colour, they are probably Egyptian Blue. They were found mixed with soil, and may come from disintegrated beads or other small items.
PPP 181908:053:002		
PPP 181908:055:002		
PPP 182908:008:008		
PPP 182908:008:012		
PPP 182908:008:015		
PPP 182908:046:005		
PPP 182908:046:006		

* See e.g., Megiddo: Lamon/Shipton 1938, Pl. 91: 37; Hasanlu: University of Pennsylvania Museum of Archaeology and Anthropology, object no. 75-29-199, Sanandaj: Amelirad *et al.* 2012, Pl. 21; War Kabud in Luristan: Haerincq/Overlaet 2004a, Fig. 36.F1.



Fig. E1.21: Egyptian Blue grooved bead PPP181908:044:026 (85) from a looting pit. Photo by Andrea Squitieri.

E1.3.7 White beads

White beads, made of a soft, whitish material. Although no analysis has yet been carried out on them, they were probably made of ivory or bone. It is likely that they originated in the graves. Similar beads were found in the 2016 excavation campaign in QID1¹⁴⁵.

Registration no.	no.	Description
PPP 181908:044:039	88	Disc shaped white beads, D. 0.2 cm.
PPP 181908:053:003		
PPP 182908:026:006		
PPP 181909:052:013	89	Ring shaped bead broken in half, D. 0.6 cm.
PPP 182908:038:003	90	Oblate bead decorated with vertical grooves, D. 0.9 cm.
PPP 182909:027:008	91	Spherical bead, D. 1.8 cm.

E1.3.8 Shell beads and pendants

These are beads and one pendant made of shells¹⁴⁶. They also may have originated in the graves, although it is not clear. Though rare, cowrie shells have also been found in the Lower Town in the Main Occupation Period structures; hence it is possible that some of the shell beads below originated in Building P of QID1 rather than in the graves. These items are also discussed in §E6.2.

¹⁴⁵ Kreppner/Squitieri 2017a, Fig. C28.

¹⁴⁶ I would like to thank Anja Prust for the identification of the species of these shells.

¹⁴³ Squitieri 2019, 131.

¹⁴⁴ Squitieri 2018, no. 10.



Fig. E1.22: Fragments of beads from the tusk shell of *Dentalium* sp. PPP 181908:034:012 (92) from a looting pit. Photo by Andrea Squitieri.

Registration no.	no.	Description
PPP 181908:024:004	92	Fragments of beads from the tusk shell of <i>Dentalium</i> sp., L. 1.2, D. 0.7 cm; L. 1.2 cm, D. 0.2 cm (largest fragment); L. 1 cm, D. 0.4 cm.
PPP 182909:034:012		
PPP 181908:044:022		
		Fig. E1.22: PPP 181908:034:012. Similar shell beads are quite widespread across the Near East*.
PPP 181908:044:038	93	Cowrie shells, L. < 2 cm. Their backs are removed so they were intended to be used as beads**.
PPP 182908:013:004		
PPP 182908:035:003		
PPP 182909:024:006		
PPP 182909:034:010		
PPP 182909:034:011		
PPP 182909:055:003		
PPP 181909:063:005	94	Ring bead, broken (shell <i>Gastropoda</i>), L. 2.5 cm.
PPP 182909:007:001	95	Ring bead, broken (shell <i>Gastropoda</i>), D. 1.7 cm.
PPP 182909:034:005	96	Pendant (bivalve shell), L. 2.8 cm; W. 2.5 cm, with perforation.

* For recent finds, see the Iron Age graveyard of Qara-Tappeh in northwestern Iran: Dehpahlavan *et al.* 2019, Fig. 18 (top left).

** On cowrie shells used in Egypt and the Near East as ornaments, see Golani 2014.

E1.3.9 Bronze beads

Registration no.	no.	Description
PPP 181908:050:004	97	Short oblate bead decorated with grooves, D. 0.9 cm.
PPP 182908:007:009	98	Flat disc-shaped bead, D. 0.6 cm.
PPP 182908:042:003	99	Spherical bead formed from a flat sheet folded on itself, D. 1.2 cm.
PPP 182909:010:008	100	Coil bead with cylindrical shape, L. 0.7 cm, D. 0.5 cm. See similar examples from Grave 106, no. 34 .
PPP 181908:046:011	101	Bronze bead formed from a rolled band, D. 0.9 cm.

E1.3.10 Perforated ivory/bone items

These two are rectangular fragments of perforated items in ivory/bone. Similar items were also found during the 2016 campaign at QID1. They were possibly used to decorate pieces of furniture.

Registration no.	no.	Description
PPP 181909:052:006	102	Two pieces of what appears to be a rectangular ivory/bone small plaque with a perforation in the middle. A triangular shaped fragment is missing. L. 2.9 cm; W. 1.2 cm; Th. 0.3 cm. Similar items were found during the 2016 excavations, coming from right above the floor of Room 58*.
PPP 181909:063:014	103	Fragment of a rectangular-shaped ivory/bone item, with a circular perforation in the middle. L. 1.8 cm, W. 1.5 cm, Th. 0.4 cm. Similar to no. 102 .

* Kreppner/Squitieri 2017a, Fig. C25.



Fig. E1.23: Two pieces of a rectangular ivory/bone small plaque with a perforation in the middle: PPP 181909:052:006 (102). Photo by Andrea Squitieri.

E1.3.11 Ceramic discs

These are seven flat ceramic discs with a perforation in the centre. They are crudely made, and most likely are re-worked sherds of broken pottery vessels. They were possibly intended to be used as spindle-whorls. Similar items were found in the Lower Town in the Main Occupation

period structures; hence it is possible that the ceramic discs from QID1 belong to Building P.

Registration no.	no.	Description
PPP 181908:027:005	104	7 perforated ceramic discs. D. between
PPP 181908:044:013		2.8 and 6.9 cm; perforation D. c. 0.5 cm.
PPP 181908:044:016		Fig. E1.24: PPP 182909:034:007.
PPP 182908:033:002		
PPP 182908:034:003		
PPP 182909:010:006		
PPP 182909:034:007		



Fig. E1.24: Perforated ceramic disc PPP 182909:034:007 (104) from a looting pit. Photo by Andrea Squitieri.

E1.4 Preliminary assessment of the 2019 small finds from QID1

The study of the small finds from QID1 presents several challenges because heavy looting has inevitably altered both the horizontal and the vertical positions of virtually every item.

In §E1.2, we discussed those items that can be established with certainty as originating from graves (Group 1). These include pieces of personal ornamentation such as fibulae, earrings, bracelets, beads, appliques, a mirror, and other types of objects such as decorated bone handles and metal studs. Many of these items have close parallels (e.g., the decorated bone tubes, **no. 7**) in the area extending from the Levant to West Iran. In some cases, their chronology can only be based on stylistic analysis, which would make a date between the 9th century BC through the Achaemenid period very likely.

Only for Grave 110 is a radiocarbon date range of 767-488 calBC available, which fits the results of the stylistic analysis conducted on the three fibulae (PPP 182909:067:010, PPP 182909:067:004, PPP 182909:067:011) found near the

skeleton (discussed by Friedhelm Pedde in §E2.1), and the cylinder seal (PPP 182909:067:007) showing a hunting scene in “Provincial Assyrian Style” (discussed by Anja Fügert in §E3.2). It is possible that at least some of the other graves also belong to the chronological horizon of Grave 110. The study on the arrowheads offered by Anja Hellmuth Kramberger in §E4 singled out one arrowhead (PPP 181908:033:004) from Grave 102 that can be dated to the 9th-6th century BC (see **Table E4.2**), a date range which is not so far off the radiocarbon date yielded by Grave 110.

Grave 106, which had the highest number of grave goods preserved, did not yield any radiocarbon date. However, the items retrieved from it, although not very diagnostic in nature, can easily be included in the 9th-6th century BC time horizon due to stylistic parallels from other sites.

Finally, based on the parallels identified for the decorated bone tubes, the cremation burial Grave 101 can only be dated to the time from the 9th through the Achaemenid period. This leaves open the possibility that the cremation burials (Graves 101 and 109) are of a later date than the inhumation burials, although further data are needed to ascertain this.

As we have seen, many objects come from looted fills and the topsoil (§E1.3). In some cases, they belong to the same object-types as items also found in graves. These are Egyptian Blue and carnelian beads, bracelets and rings with overlapping terminals, crescent-shaped earrings, and metal studs. It is possible that these items, although found scattered throughout the fills of the looting pits, came from graves that had been robbed or even completely destroyed by looting. Establishing a chronology for these items is very problematic if one considers that, based on the radiocarbon dates available from human remains in QID1 (see **Table C1**), these items may come from graves of various periods dating from the beginning of the Iron Age until the very late first millennium BC. It is also worth mentioning that the looting pits have also yielded pottery sherds belonging to before and after the first millennium BC (see Jean-Jacques Herr’s assessment in §D1), which makes it even more complicated to assign the QID1 objects from looted contexts to a specific period. The exceptions are two fibulae (PPP 181909:067:001 and PPP 182909:020:007, see Friedhelm Pedde in §E2.2) and two cylinder seals (PPP 182908:008:006 and PPP 181909:067:003, see Anja Fügert in §E3.3) that were found in looting pits but whose stylistic attribution to the Iron Age is certain.

We may also ask whether it is possible to identify, among the objects from looted fills, those which possibly came from the structures of Building P rather than from

graves. If we use the comparison with the items from the Lower Town (from the structures of the Main Occupation Period) as our criterion, then we may conclude that the stone tools (with only few exceptions), the perforated ceramics discs, some of the shell beads, and perhaps some of the Egyptian Blue beads may have come originally from Building P, since these objects all have parallels in the Lower Town. This attribution sounds reasonable, although the presence of Egyptian Blue beads in both QID1 graves and the Lower Town may indicate that these items may have originated from both graves and Building P.

The lack of stratigraphic information makes every attribution of objects to specific deposits or structures very tentative. The object horizontal distribution cannot be trusted either, as there is no way to know to what extent looters scattered the items around. However, it is noteworthy that the decorated ivory fragments¹⁴⁷ retrieved in 2018¹⁴⁸ during the excavation of the looted fills of Building P Room 58 do not have any parallels in the 2019 excavations, which concentrated outside this room. Moreover, some of these decorated ivory fragments from the 2018 campaign were also collected from the floor of Room 58 (although, it should be noted that the looters had reached this level). Hence, it can be suggested, based on the findings of the 2019 campaign, that the decorated ivory fragments of the 2018 campaign did originally belong to the furniture of Building P rather than to the graves¹⁴⁹. Of course, this assessment must be considered provisional as further investigations on QID1 may produce new evidence to help interpret the rich repertoire of small finds coming from this excavation area.

E2. Five fibulae from Qalat-i Dinka (QID1), 2019

*Friedhelm Pedde*¹⁵⁰

This chapter discusses five bronze fibulae found during the 2019 excavations at Qalat-i Dinka (QID1), three of which came from Grave 110, while the other two were recovered from the fill of looting pits identified within the excavation area.

¹⁴⁷ The material of these items has been tentatively identified as ivory; however, an in-depth analysis is required to decide whether their raw material is ivory or bone. See also §E6, Table E6.1.

¹⁴⁸ Squitieri 2019, 126-128.

¹⁴⁹ In the light of the 2019 discoveries, I corrected the interpretation given in Squitieri 2019, 132, where I had assigned to Building P also some pieces of jewellery, which may in fact belong to graves.

¹⁵⁰ Assur Projekt, Berlin.

E2.1 Fibulae from Grave 110

Grave 110 (§C5.3.3) yielded one skeleton of an individual, whose upper part was preserved and untouched, whereas the lower part was looted. Among other grave goods (§E1.2.7), the deceased was provided with three bronze fibulae of different types. They are all complete, with separately made and inserted needles.

Fibula 1: PPP 182909:067:004

Length 3.4 cm, height 2.2 cm, weight 6.89 g. Angle of the arms ca. 80°. Diameter pearls 0.6-0.8 cm, diameter discs 0.5-0.6 cm, diameter insertion segment 0.8 cm, length of the pin 3.3 cm.

This fibula was found near the right clavicle of the buried individual (Fig. E2.1). It is a small triangular fibula. The bow of the fibula has a sharp bend. Each arm has two circular beads, which are both flanked by two circular discs. One arm ends in a circular bead: the socket, or insertion segment, for the pin, which is bent in a spiral and is fixed in this segment. The other arm ends in a catch for the point of the needle, which slightly protrudes out of the catch. It is quite corroded, so it remains to be seen whether the catch has the form of a human hand.

The fibula belongs to group D2.2¹⁵¹. This group is clustered in the Assyrian heartland (Assur, Kalhu) and spreads widely from the Levantine coast to Iran¹⁵², where the type is found in particularly large quantities in Sar Kabud¹⁵³. Because of the wealth of examples, this group can easily be dated to the 7th century BC.

Fibula 2: PPP 182909:067:010

Length 3.9 cm, height 2 cm, weight 7 g. Angle of the arms 90°, diameter 0.4-0.7 cm. Needle length 2.8 cm.

This fibula was found on the other side of the skeleton, near the left clavicle (Fig. E2.2). This small piece also has a triangular shape, and the arms are bent at a right angle. The bend in the middle of the body is undecorated. This section, like the arms, has a rectangular or square profile and the arms are provided with a block. Its highly-corroded state does not allow any further analysis, but we can assume that after restoration these blocks will show a cross-hatching on their surface. There is no special segment for the insertion of the needle, which is simply inserted into the block. The other arm ends in a flat catch without any decoration. The pin has a double spiral and an additional loop at its end. The point of the needle does

¹⁵¹ Pedde 2000, 284-293, Pl. 66-68.

¹⁵² Pedde 2000, 285 (map).

¹⁵³ Van den Berghe 1978.



Fig. E2.1-5: The fibulae from Qalat-i Dinka (QID1) found during the 2019 campaign. (1) PPP 182909:067:004; (2) PPP 182909:067:010; (3) PPP 182909:067:011; (4) PPP 182909:020:007; (5) PPP 181909:067:001, after restoration by Akram Omar Qaradaghi. Photos by Andrea Squitieri (1-4) and Haymin Noori (5)

not protrude from the catch. The fibula seems to be part of group C8¹⁵⁴, which is mostly found in the Assyrian heartland, but also along the Levantine coast¹⁵⁵. Most of the fibulae of this group can be dated to the 7th or the beginning of the 6th century BC.

Fibula 3: PPP 182909:067:011

Length 4.2 cm, height 2.5 cm, weight 8.5 g. Diameter of the bow 0.4-0.6 cm, diameter of insertion segment 1.2 cm. Needle complete length ca. 3.3 cm.

This fibula was found near the left elbow (**Fig. E2.3**). In contrast to the others, it is a bow fibula. Some of the details remain obscured by corrosion. The bow is empty, but a pearl, flanked by two discs, is positioned close to the catch. It is unclear whether another such pearl and disc combination is positioned on the other side of the bow, close to the insertion segment. The bow swells slightly in the middle and is not properly circular in shape. The insertion segment is wider and seems to have the shape of a disc. All parts of the fibula have a round profile. The flat catch is widened, but undecorated. The needle is broken, but complete. Its end spirals horizontally twice and is obviously inserted in a circular segment.

This bow fibula is related to group B4.2¹⁵⁶, but is not entirely similar. This group seems to have its origin in the region of the Levant, but some pieces have been found in Babylonia and a single example was discovered in Nimrud¹⁵⁷. Most of them seem to belong to the 6th century BC, but some may be from the 7th century BC and therefore a bit earlier, which fits well with the other two fibulae in this grave.

In summary, the three fibulae from Grave 110 suggest a dating to the 7th century BC, which fits with the radiocarbon date available from this grave: 767-488 calBC (see **Table C1**).

E2.2 Fibulae from looting pits

Two more bronze fibulae, which may or may not have been grave goods, were found during the excavation at QID1.

Fibula 4: PPP 182909:020:007

Length preserved 3 cm, width 0.8 cm, weight 4 g. Diameter of the bow 0.4-0.7 cm, diameter pearls 0.7-0.9 cm.

This item is the bow of a fibula (**Fig. E2.4**) and was found in the looting pit fill part of LGR:0305 (**SC5.4.1**). The central part of the bow with a pearl is preserved. It is circular in profile, and perhaps flanked by two discs. Close to the break is a second pearl. The bow seems to have an irregular shape: between the two pearls the bow is much thicker than on the opposite side of the central pearl. Because it is so poorly preserved, an assignment to a fibula group is difficult. The fibula seems to be related to group A2.3¹⁵⁸. In this group the diameter of the bow is also thin on one side and swells on the other. In this case our object would be a one-piece fibula, bow, and pin cast as a single piece. This group originated in Cyprus and is also attested on the mainland (close to Cyprus) as well as in central Anatolia¹⁵⁹. Interestingly, the fibula discussed here would be the first one of this group to be found so far east. Moreover, it is also the oldest example among the fibulae from QID1, because group A2.3 dates to the 9th and first half of the 8th century BC.

Fibula 5: PPP 181909:067:001

Length 5 cm, height 3.40 cm, weight 19.4 g. Diameter bow 0.5-0.8 cm, diameter pearls 0.75 cm, diameter discs 0.65 cm; insertion segment length 1 cm, diameter 0.6 cm; block length 0.8 × 0.65 cm, pin length 4.7 cm.

This is a complete bow fibula (**Fig. E2.5**). The bow is long and empty, with a regular shape that swells in the middle. At both ends of the bow is a pearl, flanked by two discs. Between the pearl and the catch is a flat, rectangular block. The long catch itself widens slightly, but is undecorated. The insertion segment has the shape of a cylinder, in which the needle is fixed by hammering. Traces of this hammering, two hollows, are still visible. Apart from the block, all the parts of this fibula have a circular profile. The pin has a threefold spiral, and the point of the pin is fixed in the catch.

This fibula belongs to group C1.3¹⁶⁰, which is spread throughout northern Syria, particularly in the region between the Euphrates and the Orontes, but was also found in western Syria (Ebla) and Israel¹⁶¹. Most of these fibulae can be dated to the 7th century BC (or slightly earlier to the end of the 8th century BC). This fibula is the most eastern piece from this group yet found and was clearly imported from the west. The same looting pit fill where this fibula was found also contained a loose skull, one of whose teeth was radiocarbon dated to 1210-1029 calBC

154 Pedde 2000, 245-250, Pl. 55-56.

155 Pedde 2000, 246 (map); also recently found in Tušhan (modern Ziyaret Tepe), see Matney *et al.* 2017, 286.

156 Pedde 2000, 151-154, Pl. 17-18.

157 Pedde 2000, 151 (map).

158 Pedde 2000, 109-112, Pl. 6; Pedde 2001, Fig. 1.6.

159 Pedde 2000, 110 map.

160 Pedde 2000, 181-186.

161 Pedde 2000, 182 map.

(§C6.3, see also Table C1), suggesting the presence of a looted grave dating to this period. However, because the fibula is stylistically much younger than this date, it is very likely that it originated in another grave that had also been damaged by the looting pit.

E2.3 Conclusions

Most of the fibulae discussed are imports from the west, in particular from the Levantine coast. Though small in number, these grave goods demonstrate that a network of trade and exchange existed between western Iran and the Mediterranean coast. The types of fibulae that were typical of central Assyria, and found in abundance there, were not discovered at Qalat-i Dinka. Since fibulae function not only as grave goods, but are also indicators of particular types of clothing and costume, the geographic origins of the population found buried, or, rather, the identities of their trading contacts should be the subject of future investigation.

Table E2.1 sums up the dates suggested for the fibulae discussed in this chapter.

Registration no.	no.	Context	Suggested date
PPP 182909:067:004	1	Grave 110	7th century BC
PPP 182909:067:010	2	Grave 110	7th – beginning 6th century BC
PPP 182909:067:011	3	Grave 110	7th – 6th century BC
PPP 182909:020:007	4	Pit fill	9th – first half of 8th century BC
PPP 181909:067:001	5	Pit fill	end-8th – 7th century BC

Table E2.1: Summary table of the fibulae found at Qalat-i Dinka, 2019.

E3. Three cylinder seals from Qalat-i Dinka (QID1), 2019

Anja Fügert¹⁶²

In 2019, three cylinder seals were found during the excavation of QID1, situated on the western slope of Qalat-i Dinka. The seal PPP 182908:008:006 originated from a context disturbed by modern looting (Locus:182908:008), the seal PPP 182909:067:007 was found in Grave 110, and the seal PPP 181909:067:003 originated in another looting pit (Locus: 181909:067).

E3.1 A seal depicting a row of animals

The seal PPP 182908:008:006 (Fig. E3.1) originates from a looting pit located in the southeastern part of QID1 (Locus:182908:008, see §C4.6).

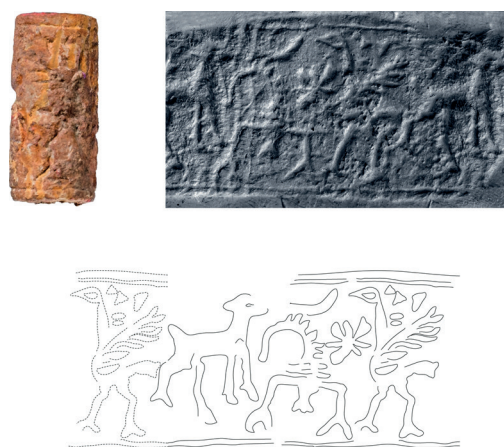


Fig. E3.1: Seal PPP 182908:008:006 and its impression. Seal and impression photos by Hayman Noori, drawing by Anja Fügert. Prepared by Anja Fügert.

Measurements: height: 2.4 cm, diameter: 1.1 cm, hole diameter: 0.4 cm.

Material and colour: limestone, beige-whitish.

Description of the impression: Animal row. The seal impression depicts three animals: a quadruped, a scorpion, and an ostrich. A quadruped facing right and an ostrich facing left flank the scorpion, which is depicted

¹⁶² German Archaeological Institute, Berlin. The author had no opportunity to examine the original objects; her comments are therefore based solely on the documentation available to her and must be considered preliminary. Special thanks go to Hero Salih Ahmed for taking measurements and additional photographs of the seals and their impressions in the Archaeological Museum in Sulaymaniyah.

upside down with its pincers above the bottom line and its tail curving left. Above the scorpion hover an eight-pointed star and a crescent. The quadruped resembles a calf, as it has no visible horns. There is a wedge-shaped element above the erect wing of the ostrich. A simple line border frames the image at top and bottom, although the quadruped is not positioned on the bottom line but hovers above it. The seal design is very crudely cut with hand-held tools.

Comparisons: Collon 2001, nos. 39, 86; Moortgat 1940, no. 722.

Discussion: Most probably the seal was produced locally. A date in the early centuries of the first millennium BC is feasible.

E3.2 A seal depicting a hunting scene

The seal PPP 182909:067:007 (**Fig. E3.2**) was found in an inhumation grave G110, which yielded a radiocarbon dating of 767-488 calBC (§C5.3.3, **Table C1**, and §E1.2.7). It was excavated together with a blue glass cap that allowed wearing the seal as a pendant (**Fig. E3.3**).

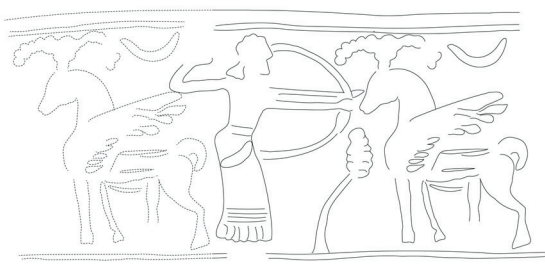


Fig. E3.2: Seal PPP 182909:067:007 and its impression. Seal and impression photos by Hayman Noori, drawing by Anja Fügert. Prepared by Anja Fügert.



Fig. E3.3: Glass cap PPP 182909:067:008 found with the cylinder seal PPP 182909:067:007. Photo by Andrea Squitieri.

Measurements: height: 3.6 cm, diameter: 1.2 cm, diameter hole: 0.3 cm.

Material and colour: faience or frit, whitish core, original surface most probably completely worn away.

Description: Hunting scene. A standing archer facing right aims an arrow at a standing quadruped (mouflon ram?) with ridged horns and wings. The archer wears an ankle-length fringed tunic under a thigh-length shawl, belted at the waist. The head of the archer is depicted with a beard; his hair is tied back at the neck. He wears either a headband or calotte-shaped headgear with a broad rim. There is a small tree consisting of only one branch and a curving stem that bends slightly to the right between the archer and the quadruped. A crescent hovers above the wings of the quadruped. A simple line border frames the image. The blurry appearance of the impression is characteristic of seals made of composite materials.

Comparisons: Collon 2001, nos. 27, 29, 31; Marcus 1996, nos. 64-65, 68 (“Provincial Assyrian Style”); Moortgat 1940, nos. 699-700, 706; von der Osten 1957, no. 318.

Discussion: Seals depicting the motif of the archer aiming at his prey were widely used, as many seals from the heartland of Assyria, Tell al-Rimah, the region around Carchemish, Babylon, Hasanlu, and even Karmir Blur attest¹⁶³. Most of them were executed as faience seals; stone seals bearing this motif are much rarer¹⁶⁴. Elements listed by Marcus as non-Assyrian, which can be confirmed for the present seal from Qalat-i Dinka, include the absence of feet on the depicted human figure, the high, ridged horns of the quadruped, and the curving of the stem of the tree¹⁶⁵.

E3.3 A seal depicting a contest scene

The seal PPP 181909:067:003 (**Fig. E3.4**) originates from a looting pit located in the north-western corner of QID1 (Locus:181909:067, §C6.4).

Measurements: height: 1.8 cm, diameter: 0.8 cm, diameter hole: 0.3 cm, slightly barrel-shaped due to use-wear?

Material and colour: faience or frit, light grey-beige core with traces of a light turquoise surface.

Description of the impression: Two-figure contest scene. A hero facing left holds a scimitar in his lowered left hand. With his right arm he grasps a rampant bull(?) by the foreleg. Parts of the bull’s body show a striation pattern. The standing hero wears a belted, long, fringed

¹⁶³ Collon 2001, 40.

¹⁶⁴ Collon 2001, 40.

¹⁶⁵ Marcus 1996, 45.



Fig. E3.4: Seal PPP 181909:067:003 and its impression. Seal and impression photos by Hayman Noori, drawing by Anja Fügert. Prepared by Anja Fügert.

garment. Between them are a small branch and two wedge-shaped elements; behind them, an eight-rayed star hangs in the sky with a highly stylized tree underneath. The design, which was originally quite detailed in execution, is worn, especially in its upper part. The hero was most probably shown bearded, with his long hair tied back at the neck. A simple line border frames the carved image.

Comparisons: Collon 2001, nos. 306, 307, 312; Fügert 2015, nos. 116, 122.

Discussion: The seal motif can be assigned to the Assyrian, or rather to the provincial Assyrian, group of two-figure contest scenes (often misleadingly referred to as “Babylonian contest scene”), since there are several examples of seals and seal impressions bearing this motif attested from Assyrian territory. This group of seals was possibly inspired by the incised decorations of Assyrian palace reliefs¹⁶⁶. The depiction of the hero wearing a long, closed (!) garment is only rarely attested. Characteristics that make this seal a provincial work are the striation pattern on the animal body and the hero’s missing feet¹⁶⁷. A date for this seal from the 9th to the 8th centuries BC is probable.

E3.4 Preliminary conclusions

The seals found on Qalat-i Dinka (QID₁) are most likely to have been local products and can be assigned to the group of “Provincial Assyrian Style” seals as defined by Marcus. In Hasanlu, this style of seal predominated, and it is most likely that the glyptic at Qalat-i Dinka followed the same pattern.

¹⁶⁶ See Fügert 2015, 166 and for examples of two-figure contest scenes on Assyrian wall reliefs, see Collon 2001, Pl. XLIV and Bartl 2014, 46, Fig. 32 and Pl. 39a.

¹⁶⁷ See Marcus 1996, 45.

E4. Iron arrowheads from the Dinka Settlement Complex, 2015-2019

Anja Hellmuth Kramberger¹⁶⁸

Between 2015 and 2019, 19 iron arrowheads emerged in various contexts of the Dinka Settlement Complex (DSC). Only a small selection of these has already been published (**Table E4.1**), namely an arrowhead with a square cross-section of the blade and tang (“Bodkin type”) from the topsoil of Gird-i Bazar (PPP 267931:011:004)¹⁶⁹, and a specimen representative for a group of nine similar arrowheads from Room 58 of Building P in Qalat-i Dinka (operation QID₁)¹⁷⁰. There, further arrowheads originated from the topsoil (PPP 181909:002:008-013) or a filling/layer below the topsoil that was disturbed by looting (PPP 181909:004:032, PPP 181909:004:049).

Apart from four arrowheads or arrowhead fragments that were recovered in the area of the disturbed Graves 102 (PPP 181908:033:004, PPP 181908:035:033) and 106 (PPP 181909:069:019), all other arrowheads from the 2019 campaign at QID₁ come from contexts disturbed by looting (PPP 181908:025:009, PPP 181908:029:055, PPP 181908:029:030, PPP 181909:052:016-017, PPP 181909:063:011, PPP 181909:063:013).

Table E4.1 summarises the find and publication information for the arrowheads from the Dinka Settlement Complex.

Arrowheads found in 2015 and 2018 and already published			
Registration no.	Operation	Context	Previous publication
PPP 267931:011:004	Gird-i Bazar	Topsoil	Wilkinson/Squitieri/Hashemi 2016, 102-104, Fig. D3.3
PPP 181909:002:008	QID ₁	Topsoil/	Squitieri 2019, 129
PPP 181909:002:009		dis-	
PPP 181909:002:010		turbed	
PPP 181909:002:011		layer	
PPP 181909:002:012			
PPP 181909:002:013			
PPP 181909:004:032			
PPP 181909:004:049			

¹⁶⁸ Institutum Studiorum Humanitatis, Alma Mater Europaea, Ljubljana (Slovenia).

¹⁶⁹ Found during the 2015 campaign at Gird-i Bazar, see Wilkinson/Squitieri/Hashemi 2016, 102-104, Fig. D3.3.

¹⁷⁰ Found during the 2018 campaign at QID₁, see Squitieri 2019, 129, Fig. H11.

Arrowheads from QID1 found during the 2019 campaign			
Registration no.	Operation	Context	Context information
PPP 181908:033:004 PPP 181908:035:033	QID1	Grave 102	§C3.5
PPP 181909:069:019	QID1	Grave 106	§C6.2.2
PPP 181908:025:009 PPP 181908:029:030 PPP 181908:029:055	QID1	Looting pit	§C3.6
PPP 181909:052:016 PPP 181909:052:017 PPP 181909:063:011 PPP 181909:063:013	QID1	Looting pit	§C6.4

Table E4.1: The arrowheads from the Dinka Settlement Complex, 2015-2019.

E4.1 Description of the attested arrowhead types

To date, a total of 19 arrowheads have been recovered and are preserved in whole or in fragmented form. All pieces fall into the group of bilobate arrowheads with a tang¹⁷¹. With this construction principle, the wooden arrow shaft encloses the tang below the arrow blade (the wing area), and there are examples from the Iron Age in Central Europe in which this part was glued with pitch/tar to create a stronger bond and additionally wrapped with cord or bast fibres¹⁷². In contrast to the arrowheads with tangs, the shafts of socketed arrowheads were sharpened at one end and fixed into a socket¹⁷³. So far, no arrowheads with sockets have been found in the Dinka Settlement Complex. The state of preservation or corrosion of iron arrow-

heads has a (more or less) significant effect on their type designation.

Four variants (called Variants a-d) of the bilobate or two-winged arrowheads with a tang (see **Fig. E4.1: a-d**) and the arrowhead with a square cross-section of the blade, already mentioned above, of the so-called “Bodkin type” (see **Fig. E4.2**) can be clearly distinguished. An additional five arrowheads are too fragmented and/or corroded, thus a type designation can only be made with reservations; they are listed here under the category “Others” (which includes Variant e).

E4.1.1 Variant a (Fig. E4.1: a)

The Variant a bilobate arrowheads represent by far the largest group (PPP 181909:002:008-013, PPP 181909:004:032 and PPP 181909:004:049). Six pieces were found relatively close together (PPP 181909:002:008-013) and it is more than likely that all of them originally came from one and the same quiver. The arrowheads have a length between 5.0-7.10 cm, and the maximum width of the leaf measures approximately 2 cm. This arrowhead variant is characterised by a proportionally relatively compact, arch-shaped blade, with the lower end of the blade being slightly concave at the transition to the tang. The tang has a stop at the top and a collar/stem¹⁷⁴, which means it is slightly thickened at the transition to the blade, with a round cross-section. The tang itself has a square cross-section.

E4.1.2 Variant b (Fig. E4.1: b)

A bilobate arrowhead with a triangular-shaped blade can be named under Variant b (PPP 181909:063:011), whose length is 5.10 cm. The strong corrosion makes the identification of any details difficult, so it cannot be clearly determined whether the lower end of the blade (wing section) is straight or possibly slightly convex, as it appears to be. In any case, the shape was not entirely symmetrical as is also the case in comparative finds (see below). A slight thickening and a stop on the tang below the blade can be recognised.

¹⁷¹ Also “Stielpfeilspitzen” in German, or rarely “arrowheads with thorn” in English. See e.g., Thornton/Pigott 2011, 139, Fig. 6.1; Szudy 2015, 122-124, Fig. 6.1 (left); Hellmuth Kramberger 2016, 9, Fig. 16 (left).

¹⁷² Examples include finds of double-winged iron arrowheads from the so-called princely burial mound of Eberdingen-Hochdorf, southwestern Germany, which dates to the second half of the 6th century BC (Biel 1998). The arrow shafts have been preserved and the wood could be identified. The arrow shafts were made from hazel, euonymus, snowball tree, cornelian cherry, and willow wood. E.g., Biel 1998, 65, Pl. 16 (middle row second from left).

¹⁷³ E.g., Hellmuth 2007, 469, Fig. 1.56.

¹⁷⁴ Compare terminology used by Thornton/Pigott 2011, 139, Fig. 6.1, or Szudy 2015, 122, Fig. 6.1 (left).

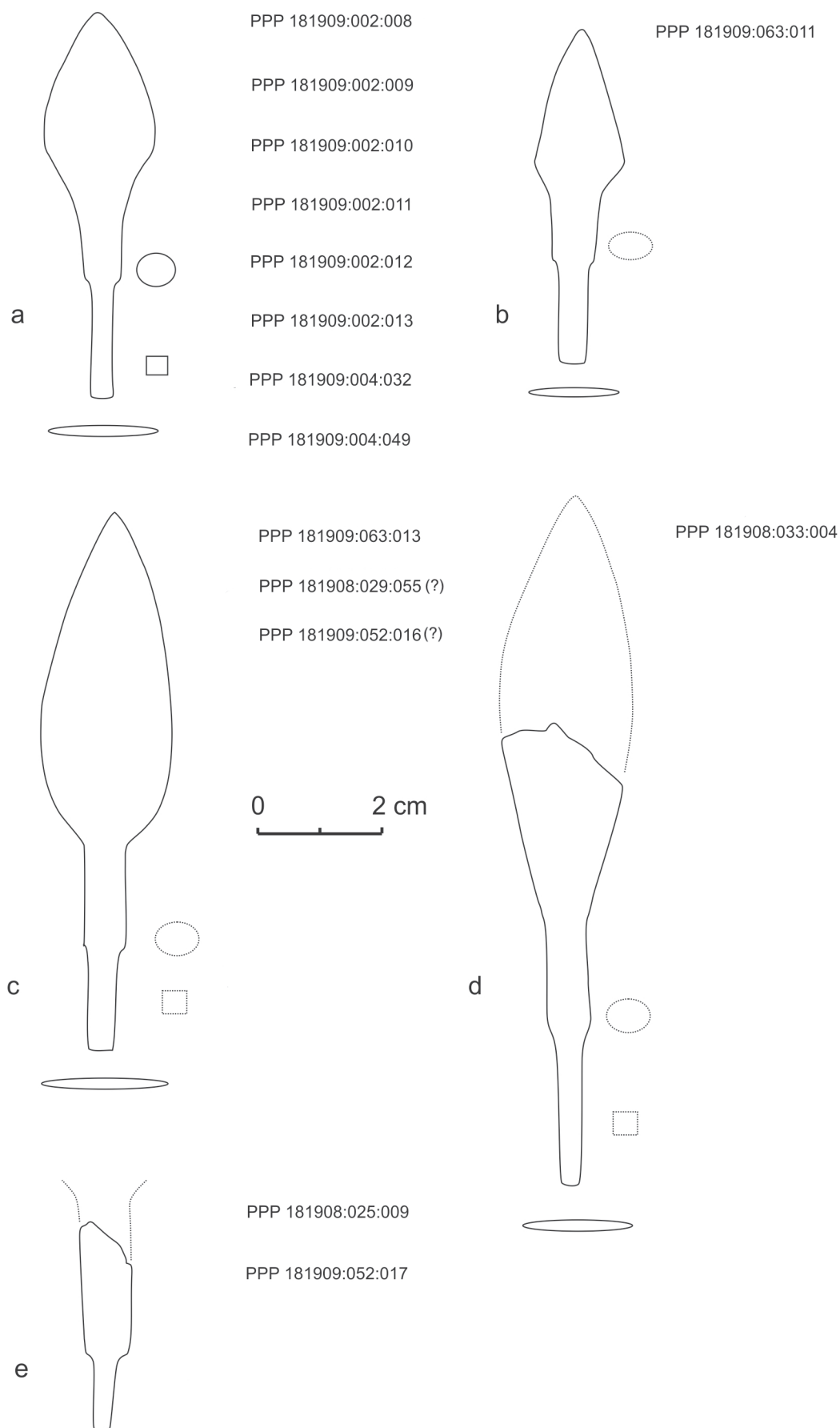


Fig. E4.1: Arrowhead variants from Qalat-i Dinka (QID1) in schematic representation. Drawings by Anja Hellmuth Kramberger.

E4.1.3 Variant c (Fig. E4.1: c)

Variant c is characterized by a bilobate almond-shaped blade (wing section). The widest part of the blade is in the rounded lower quarter, it narrows towards the tip. The tang has a more or less pronounced collar with a stop. In the case of the completely preserved arrowhead with the find number PPP 181909:063:013, we can only guess that the characteristic thickening is present due to its strong corrosion. The piece is preserved in a length of 7.7 cm, the 2 cm wide blade takes 4.0 cm. The weight is 11 g. Of the second arrowhead that can be assigned to Variant c (PPP 181909:052:016), only about two thirds, with a length of 5.70 cm, have survived. Although the upper half of the blade is missing and therefore the proportions of the arrowhead and the length ratio between blade and tang cannot be clearly determined, the rounded lower wing section and the tang with a square cross-section and a slight thickening (collar) with a weak stop are clearly recognizable. The weight of the fragmented arrowhead is 4 g. A third arrowhead, in which the upper tip of the blade is fragmented, most likely also belongs to this variant (PPP 181908:029:055). The piece was probably relatively large, since the preserved part alone measures 7.2 cm, with a blade width of 1.9 cm and a weight of 9 g. Overall, the dimensions are similar to the piece with the small find number PPP 181908:033:004 of Variant d, which is also preserved in fragmented form.

E4.1.4 Variant d (Fig. E4.1: d)

Variant d is very similar to Variant c; however, the widest point of the bilobate blade is not in the rounded lower quarter of the wing section, but in its middle part. In the case of the arrowhead PPP 181908:033:004 it should be noted that the upper half of the blade is missing, but the narrow lower half of the blade shows a gentle broadening towards the middle of the wing section. Thus, the transition from the shaft section with a tang with square cross-section and pronounced collar to the wing section appears smooth and the slender blade is reminiscent of a willow leaf. The arrowhead is overall significantly longer than all other pieces: the preserved part measures 7.1 cm with a maximum blade width of 1.5 cm. The weight is 8.5 g.

E4.1.5 "Bodkin type" (Fig. E4.2)

The characteristic of an arrowhead of the so-called "Bodkin type"¹⁷⁵ is the square cross-section of the blade. The total length of the arrowhead from Gird-i Bazar (PPP 267931:011:004) is 5.83 cm¹⁷⁶. The tang, which has a round cross-section, takes up a little less than a third of the total length. See Fig. E5.1–3.

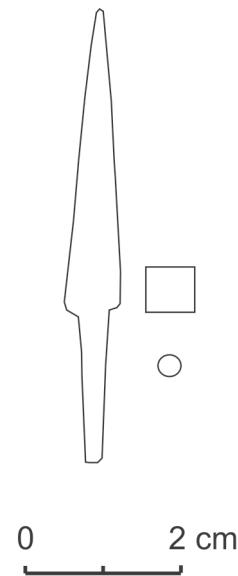


Fig. E4.2: Arrowhead PPP 267931:011:004 of the "Bodkin type", found in 2015 in the topsoil of Gird-i Bazar (see Wilkinson/Squitieri/Hashemi 2016). Drawing by Anja Hellmuth Kramberger.

E4.1.6 Variant e and "Others"

Two fragments measuring 3.3 cm and 2.5 cm long (PPP 181908:025:009 and PPP 181909:052:017) are very likely each a part of an arrowhead's tang with collar and stop; the transitions to the blades have not survived. They are both categorized as Variant "e" (Fig. E3.1: e).

As already noted above, there are also some pieces among the iron arrowheads that cannot be clearly assigned to a certain type due to their poor preservation; they are under the category "Others". A strongly corroded arrowhead with a length of 5.6 cm (PPP 181908:029:030) shows a tang with stop; the presumed wing section has a diameter of 1 cm. This could indicate that it was an arrowhead with a very pronounced mid-rib or even a four-winged respectively quadrilobate arrowhead¹⁷⁷. Several

¹⁷⁵ "Ahl-Spitze" in German.

¹⁷⁶ Wilkinson/Squitieri/Hashemi 2016, 102.

¹⁷⁷ See e.g., Hellmuth Kramberger 2016, 51.

iron fragments from the fill of Grave 106 are also very difficult to identify (PPP 181909:069:019). The largest, flat fragment with a length of 3.8 cm and a width of 1.3 cm could well represent the blade of a bilobate arrowhead, and the small, pin-shaped fragments could be fragments of the tang. Another fragment with a diameter of 0.8 cm and a length of 4.4 cm may also be a quadrilobate arrowhead. Finally, because of the lack of information about the fragment of an arrowhead PPP 181908:035:003 from Grave 102, it is not possible to assign this piece to a variant, and hence it has been assigned to the category “Others”.

E4.2 Comparisons and dating

In the following, comparisons and a possible dating of the arrowheads from the DSC are discussed based on morphological characteristics. In favour of greater clarity, the pieces are discussed in the same order of types and variants as described above.

E4.2.1 Variant a (Fig. E4.1: a)

The bilobate arrowheads of Variant a are relatively well preserved and their shape can be clearly determined and described. The rather compact, arch-shaped blade is slightly concave at the lower end at the transition to the shaft section, and a collar with a stop sits between the blade and the tang. The purpose of the stop on the top of the tang was to prevent the wooden arrow shaft from splintering on impact¹⁷⁸. While the collars of the arrowheads from the Dinka Settlement Complex have a round cross-section, the tangs show a square cross-section.

Bilobate iron arrowheads with a tang, collar/stem and a stop from Iron Age contexts have been described by several authors. J. Curtis, for example, refers to bilobate leaf-shaped iron arrowheads without mid-ribs and with a stop at the top of the tang as “Type 2”¹⁷⁹. Y. Gottlieb also names bilobate arrowheads of this form “Type II”, basing her typology on arrowhead finds from Lachish¹⁸⁰. C. P. Thornton and V.C. Pigott described the bilobate iron arrowheads with oval shaped blades and tang from Hasanlu (Period IVB) as “Type IB”¹⁸¹, M.J. Szudy calls this form “Type 5b-1”¹⁸². However, it must be pointed out that almost

every arrowhead recorded under the types mentioned, which appear by the thousands in Iron Age sites in north-western Iran, northern Iraq, northeastern Anatolia, north-western Syria and Israel, have a proportionally longer blade. Furthermore, the blades have either the shape of a willow leaf or they display an almond-shaped (oval) or a triangular-shaped blade.

Bilobate arrowheads with almond-shaped or willow leaf-shaped blades also occur at the Dinka Settlement Complex and are described here as Variants c and d (see below). In the following, it is therefore necessary to examine in more detail which archaeological sites and contexts contained bilobate iron arrowheads with a stopped tang and a compact, arch-shaped blade with slightly concave lower wing section. Good comparisons for the arched-shaped blade design with a slightly concave lower wing section can be found, for example, among the collection of arrowheads from the late 7th century BC from Kalhu (Nimrud)¹⁸³ (see here, e.g. Fig. E4.3: c). However, Szudy assigns these arrowheads to his “Type 5a-1”, which is characterised by a simple unstopped tang and which, with 434 specimens, is the most common type of Neo-Assyrian leaf-shaped iron arrowheads.¹⁸⁴ Undoubtedly, corrosion of the iron arrowheads complicates the detailed determination of the shape, but there are arrowheads from Kalhu listed as “Type 5a-1” that have an indicated collar/stem and stopped tang and should therefore, in my opinion, better be assigned to the “Type 5b-1” according to Szudy¹⁸⁵. Ultimately, however, even with our Variant a arrowheads, collars and stops at the top of the tangs are not equally pronounced on each piece and sometimes are hardly recognisable (e.g., PPP 181909:002:010). Furthermore, it should be noted that the arrowheads of “Type 5a-1” with a length of 3-3.5 cm recorded by Szudy are rather small on average, but this is related to the larger percentage of small sized arrowheads from Kalhu (Nimrud).¹⁸⁶ If the arrowheads from Kalhu are excluded from the statistics, the average length is between 4.5 and 5 cm, although there are also arrowheads with a length of up to 8.5 cm. In any case, the arrowheads of Variant a from the Dinka Settlement Complex with 5.0-7.1 cm tend to be in the upper size range of the “Type 5a-1” defined by Szudy. A similar blade

178 Szudy 2015, 292.

179 Curtis 2013, 40, pl. XII.

180 Gottlieb 2004, 1924-1928.

181 Thornton/Pigott 2011, 141, 142, Fig. 6.3.

182 Szudy 2015, 292ff.

183 Szudy 2015, Pl. 88, Nimrud 65 (Nimrud 65 5a-1 = ND 10944; British Museum) and 131 (Nimrud 131 5a-1 = ND 10944; British Museum).

184 Szudy 2015, 279ff.

185 See e.g., Szudy 2015, 292ff., Pl. 88, Nimrud 249 (Nimrud 249 5a-1 = ND 7534; British Museum), 131 (Nimrud 131 5a-1 ND 10944 British Museum), 79 (Nimrud 79 5a-1 = ND 10944; British Museum); Pl. 90, Nimrud 159 (Nimrud 159 5a-1 ND 10944 British Museum), 119 (Nimrud 119 5a-1 = ND 10944; British Museum).

186 Szudy 2015, 279-280, Fig. 9.37-38.

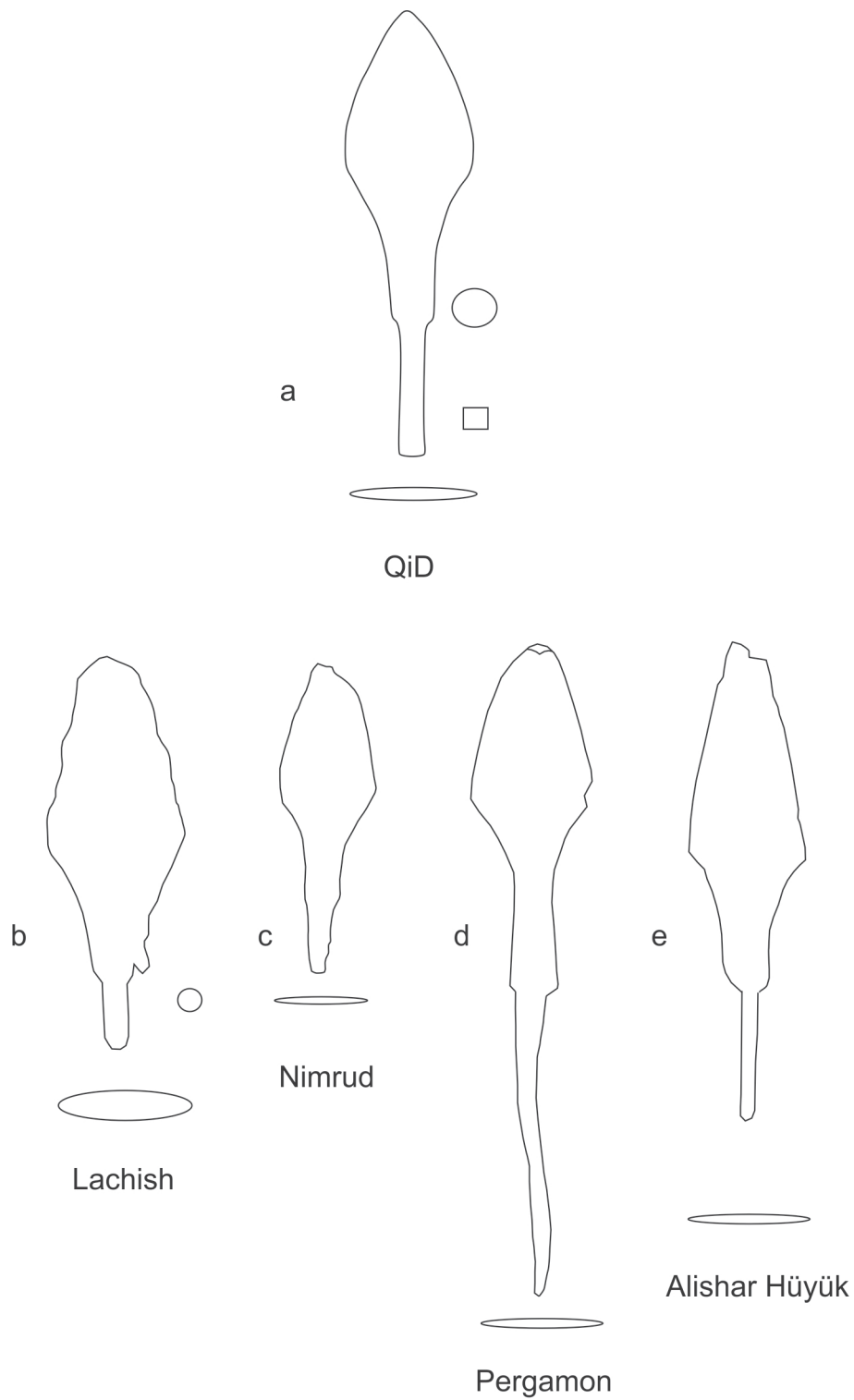


Fig. E4.3: Arrowhead of Variant a from Qalat-i Dinka (QID1), and comparisons. Drawings by Anja Hellmuth Kramberger.

shape, although perhaps a little more triangular, is shown on a bilobate iron arrowhead from Lachish¹⁸⁷ (Fig. E4.3: b). The arrowhead, of which the tang is probably not fully preserved, is 6.05 cm long and the weight is 11.7 g. The specimen was found in a fill below Level IV, but nevertheless an assignment to Level IV and thus a date in the 9th century BC is assumed¹⁸⁸.

Apart from the arrowheads from Kalhu and Lachish, for which an Iron Age dating between the 9th and 7th century BC holds, further comparisons can be pointed out; however, their chronological assignment is either unclear or certainly later, thus dating later than the Iron Age. A bilobate iron arrowhead with an elongated, arch-shaped blade and diagonally cut-off wings at the lower end of the blade (wing section), with a collar on the transition to the tang, comes from a grave in the necropolis Deve Hüyük II and probably dates to around the middle of the first millennium BC¹⁸⁹. Arrowheads from the Persepolis treasury also remind us of our Variant a of the bilobate arch-shaped arrowheads with stopped tang, but these have different mid-ribs¹⁹⁰. However, since the arrowheads of the Achaemenid period from Persepolis have been only selectively published, it cannot be ruled out that among the approx. 500 leaf- and lanceolate-shaped iron arrowhead specimens that correspond to our Variant a without a mid-rib may also exist. An arrowhead from the lower citadel (“Unterburg”) of Bastam, which was included in the finds from some mixed layers, shows a certain similarity, although this piece, as the drawing suggests, also had a central rib.¹⁹¹

The best comparisons for our Variant a arrowheads, judging according to formal criteria, come in the form of two arrowheads from Pergamon, even though the tang is slightly longer¹⁹² (Fig. E4.3: d). The two arrowheads belong to “Type A” defined by W. Gaitzsch for the arrowheads from Pergamon. With 35 pieces, this type represents by far the largest group. They are characterised by a triangular-rhombic outline of the blade, whereby the lower edges of the blade (wing section) can be diagonal and of different lengths and shapes, the stopped tang has a spherical to cylindrical collar/stem, and the lengths of the arrowheads vary between 3.5 and 7 cm¹⁹³. In the specimens mentioned, the arch-shaped blade is slightly con-

cave on the lower end towards the tang. “Type A” arrowheads, according to Gaitzsch, were found in Pergamon across the entire citadel mound and come mainly from late Byzantine contexts¹⁹⁴.

In Dur-Katlimmu (Tell Sheikh Hamad), an arrowhead, which corresponds to Gaitzsch’s “Type A” was found during excavations on the western slope of the settlement mound¹⁹⁵. The collar on the tang of this arrowhead, which was found in area 1927/IV in layer 1-2 (approx. 3rd century AD), is more spherical than cylindrical.

A bilobate iron arrowhead, with an elongated, triangular to arch-shaped blade with clearly concave lower end of the wing section and stopped tang, was found in the slope area in Alişar Hüyük¹⁹⁶ (Fig. E4.3: e). Regarding the find context, it was noted that the piece came from a layer that also contained fragments of *terra sigillata*. Another arrowhead, which corresponds to Gaitzsch’s “Type A”, was found in Alişar Hüyük in the waste from Mound A, which contained mixed material from Layers V-VI¹⁹⁷. However, this arrowhead is not very similar to our examples; it more closely resembles arrowheads of this type from Pergamon¹⁹⁸, since the leaf is strongly diamond-shaped and the collar/stem appears almost ring-shaped.

E4.2.2 Variant b (Fig. E4.1: b)

As noted above, the arrowhead with the find number PPP 181909:063:011 is relatively heavily corroded, which makes a detailed description of its original shape difficult. In general, it most resembles a bilobate arrowhead with a tang, whereby it seems that the tang has a stop and a slightly visible collar/stem, as is also the case with the bilobate arrowheads of our variants a, c and d. The blade is triangular in shape and appears slightly asymmetrical.

Despite the problems regarding a detailed description of the formal characteristics of the arrowhead, some parallels can be listed. J. Curtis has described bilobate leaf-shaped iron arrowheads with a thickening of the tang as “Type 1”¹⁹⁹. The outline of the blade can vary, from slender leaf-shaped to rhombus-shaped („diamond-shaped”), the

187 Gottlieb 2004, 1910-1911, Fig. 27.1, reg. no. 13. 31793/60, Area GW. fills of Level IV, Locus 4327.

188 Gottlieb 2004, 1913.

189 Moorey 1980, 62, Fig. 10, no. 188.

190 Schmidt 1957, 99, Pl. 76.4.

191 Kroll 1988, 159, Fig. 3.6, 160.

192 Gaitzsch 2005, Pl. 38: P5, Pl. 39: P17.

193 Gaitzsch 2005, 139-140.

194 A distinction between early and late Byzantine pieces is not possible, according to Gaitzsch 2005, 140.

195 Bernbeck 2005, 109, Fig. 116a-c; Hellmuth Kramberger 2016, 45, 86, no. 082.

196 Schmidt 1933, 71-72, no. 1147.

197 Schmidt 1933, 71-72, no. 375.

198 See e.g., Gaitzsch 2005, 140, Fig. 27A.

199 Curtis 2013, 39, Pl. XI; see also Szudy 2015, Pl. 51, Nimrud 66 (Nimrud 66 5a-1 = ND 10944; British Museum), Nimrud 125 (Nimrud 125 5a-1 = ND 10944; British Museum).

length of the arrowheads is between 3.5 and 8.21 cm, with an average length of 5 cm. 426 arrowheads of this type were discovered in Kalhu, especially in Fort Shalmaneser (see e.g., **Fig. E4.4: c**). Curtis assumes that arrows – arrow- and bow-equipment – were stored there at the time of the city's destruction in the late 7th century BC²⁰⁰.

In the arrowhead typology created by Thornton and Pigott for the material from Hasanlu Tepe, period IVB, bilobate arrowheads with a simple tang (thus, without a stop) appear under the designation “Type IA”; the majority were specimens with a proportionally longer triangular blade²⁰¹.

In his extensive study on bow armament in the Neo-Assyrian period, M.J. Szudy summarized bilobate, leaf-shaped iron arrowheads with unstopped tangs as “Type 5a-1”²⁰². Among the arrowheads he analyzed in his study, “Type 5a-1” with 434 specimens from different localities made up the largest share, and the majority of those pieces came from Kalhu (Nimrud).

Comparable arrowheads dating to the 9th-late 8th centuries BC originated in Lachish. Y. Gottlieb referred to the bilobate, leaf-shaped iron arrowheads with simple tang from Lachish as “Type I” with sub-types 1-3²⁰³, meaning that our piece would belong to sub-type 3 with a triangularly shaped blade²⁰⁴. For one arrowhead from Lachish²⁰⁵, found in a fill below Level IV and for which an assignment to Level IV is also assumed, a dating in the 9th century BC can be estimated²⁰⁶ (here **Fig. E4.4: d**). This arrowhead is 6.08 cm long, the weight is 5.8 g. Other arrowheads of the type described come from Level III in Area R,²⁰⁷ which is characterised by traces of a military attack and destruction that most likely occurred in the late 8th century BC (more precisely the year 701 BC²⁰⁸).

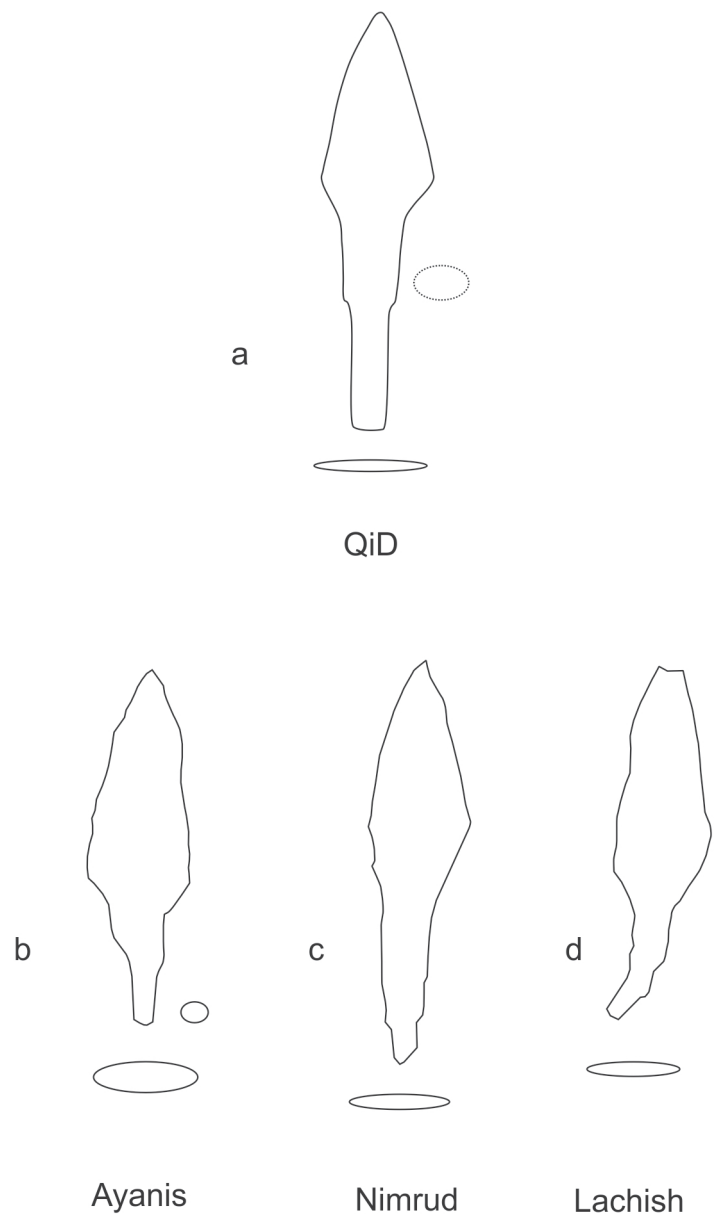


Fig. E4.4: Arrowhead of Variant b from Qalat-i Dinka (QID1), and comparisons. Drawings by Anja Hellmuth Kramberger.

Other arrowheads that clearly resemble our piece come from Agartı Kalesi-Ayanis²⁰⁹ (here **Fig. E4.4: b**). These also seem to show a thickening and a stop on the tang below the triangular-shaped blade, and here too the lower edges of the wing section appear slightly asymmetrical²¹⁰.

200 Curtis 2013, 39.

201 Thornton/Pigott 2011, 139-144, Fig. 6.2.

202 Szudy 2015, 279ff., Fig. 9.36 (left).

203 Gottlieb 2004, 1914-1922.

204 Gottlieb 2004, 1922.

205 Reg. no. 11018/60, Area GE, fills of Level IV, Locus 4093.

206 Gottlieb 2004, 1911-1913, Fig. 27.11.14.

207 E.g. Gottlieb 2004, 1937, Fig. 27.13, 17.

208 For more details, see below.

209 Derin/Muscarella 2001, 212, Fig. 2.8-9.

210 One wing side has a longer edge at the lower end. The same can also be seen in the case of some bilobate iron arrowheads with a triangular blade and marginally stopped tang with collar/stem from Lachish (Gottlieb 2004, 1937 Fig. 27.13.5), Bastam (Kroll 1979, 178, Fig. 16.4), Agrab Tepe (Muscarella 1973, 66, Fig. 27.5) or Carchemish (Woolley 1921, 125, Pl. 22b upper row second from left).

E4.2.3 Variant c (Fig. E4.1: c) and Variant d (Fig. E4.1: d)

As previously noted, Variants c and d show very similar formal characteristics – an almond- or willow leaf-shaped blade, a collar/stem and a stopped tang. Iron arrowheads of this shape are categorized by most authors as one type, within which there is usually no more detailed breakdown into variants, although variability within the group is emphasized. Under “Type 2” according to J. Curtis²¹¹, the bilobate leaf-shaped iron arrowheads without mid-rib with stopped tang, appear alongside arrowheads: with an almond-shaped blade²¹² (see here Fig. E4.5: c); with a slightly narrower willow leaf-shaped blade²¹³ (see here Fig. E4.6: c); with a triangular shaped blade²¹⁴; and specimens with a compact, arch-shaped blade²¹⁵. As Curtis emphasizes²¹⁶, apart from the different variations in the shape of the blades, there are also large deviations in the size and weight of the arrowheads of his Type 2. The size of the arrowheads varies between 4.1 cm and 10.8 cm, the weight between 4.9 g and 26.5 g, the average weight being 8.5 g.

Based on the arrowhead finds from Lachish, Y. Gottlieb also referred to bilobate arrowheads with collar/stem respectively with a thickening between the blade and the stopped tang as “Type II”²¹⁷, while plain leaf-shaped iron arrowheads with unstopped tangs represent “Type I” with three sub-types²¹⁸.

In D. Yalçıklı’s arrowhead typology for Anatolia²¹⁹, arrowheads with the characteristics mentioned above are referred to as “Type Ib1a2”; the majority of finds (92 %) are said to come from Toprakkale.

C.P. Thornton and V.C. Pigott label bilobate iron arrowheads with oval blade and tang from Hasanlu (Period IVB) as “Type IB”²²⁰ (see here Fig. E4.5: d and E4.6: b). Thornton and Pigott also refer to the different forms or variants in blade design, proportions, and size, and they rightly note that a more detailed breakdown into sub-types makes little sense since, on the one hand, arrowheads are forged (hammered) objects and therefore not

identical, and on the other hand, the strong corrosion of the iron arrowheads does not permit a detailed description of variants²²¹.

“Type 2” arrowheads according to Curtis and “Type IB” according to Thornton and Pigott were referred to as “Type IIa-neuassyrisch Variante d” for the iron arrowheads from the Neo-Assyrian period from Dur-Katlimmu (Tell Sheikh Hamad)²²².

Again, across the individual pieces that were assigned to this type, we find a relatively large variance in the size, details, and design of the blades. M.J. Szudy has categorised bilobate, leaf-shaped iron arrowheads with stopped tang as “Type 5b-1”²²³. Among the arrowheads he analysed in his study, “Type 5b-1” arrowheads which are represented by 340 pieces from different locations, make up the second largest share after the bilobate arrowheads with a simple, unstopped tang (“Type 5a-1”)²²⁴ with 434 examples²²⁵. The arrowheads examined by Szudy range in length between 2.2 and 9.0 cm (in the case of the fully preserved specimens), with average dimensions between 3.2 and 7.2 cm. This approximately corresponds to Curtis’ “Type 2” arrowheads, as well as to the almost completely preserved arrowhead with the find number PPP 181909:063:013 from Qalat-i Dinka.

Variant c and Variant d arrowheads were mainly distributed from northwest Iran, northern Iraq, northeastern Anatolia, and northwestern Syria to Israel. As Y. Gottlieb noted, they can be found in both Neo-Assyrian sites and those sites for which an encounter with the Assyrian army is documented²²⁶. They are found in large numbers, in particular from Kalhu (Nimrud), Lachish, and Tel Beer-Sheba. Large collections are documented in Hasanlu, Çavuştepe (Şardurihinili) and Agartı Kalesi-Ayanis.

106 “Type 2” (according to Curtis) or our Variant c iron arrowheads were found in Kalhu; 92 originated from Fort Shalmaneser, and others were found in the area of the city wall that bordered the east²²⁷ (see here Fig. E4.5: c). D. Stronach emphasised that numerous specimens were bent or had broken off tips, indicating their use in the final battle for the city in 612 BC, whereby the more “exotic”

211 Curtis 2013, 40, pl. XII.

212 E.g., Curtis 2013, Pl. XII, 181 (second row from the bottom, second from left).

213 E.g., Curtis 2013, Pl. XII, 181 (first row center).

214 E.g., Curtis 2011, Pl. XII, 181 (lower row on the left).

215 E.g., Curtis 2013, Pl. XII, 180 (second row from top, right).

216 Curtis 2013, 40.

217 Gottlieb 2004, 1924f.; see also Gottlieb 2016, 1195, 1197, Fig. 24.3 (middle).

218 Gottlieb 2004, 1914-1922.

219 Yalçıklı 2006, 215, 281, Table V, Map Ib.

220 Thornton/Pigott 2011, 141, 142, Fig.6.3.

221 Thornton/Pigott 2011, 142.

222 Hellmuth Kramerberger 2016, 38, Figs. 40, 41.

223 Szudy 2015, 292ff.

224 Which corresponds to “Type 1” according to Curtis (Curtis 2013, 39-40, Pl. XI), “Type I” with sub-types 1-3 according to Gottlieb (Gottlieb 2004, 1914-1922) or “Type IA” according to Thornton and Pigott (Thornton/Pigott 2011, 139-144, Fig. 6.2).

225 Szudy 2015, 279ff.

226 Gottlieb 2004, 1924.

227 Curtis 2013, 40; Stronach 1958, 170-171.

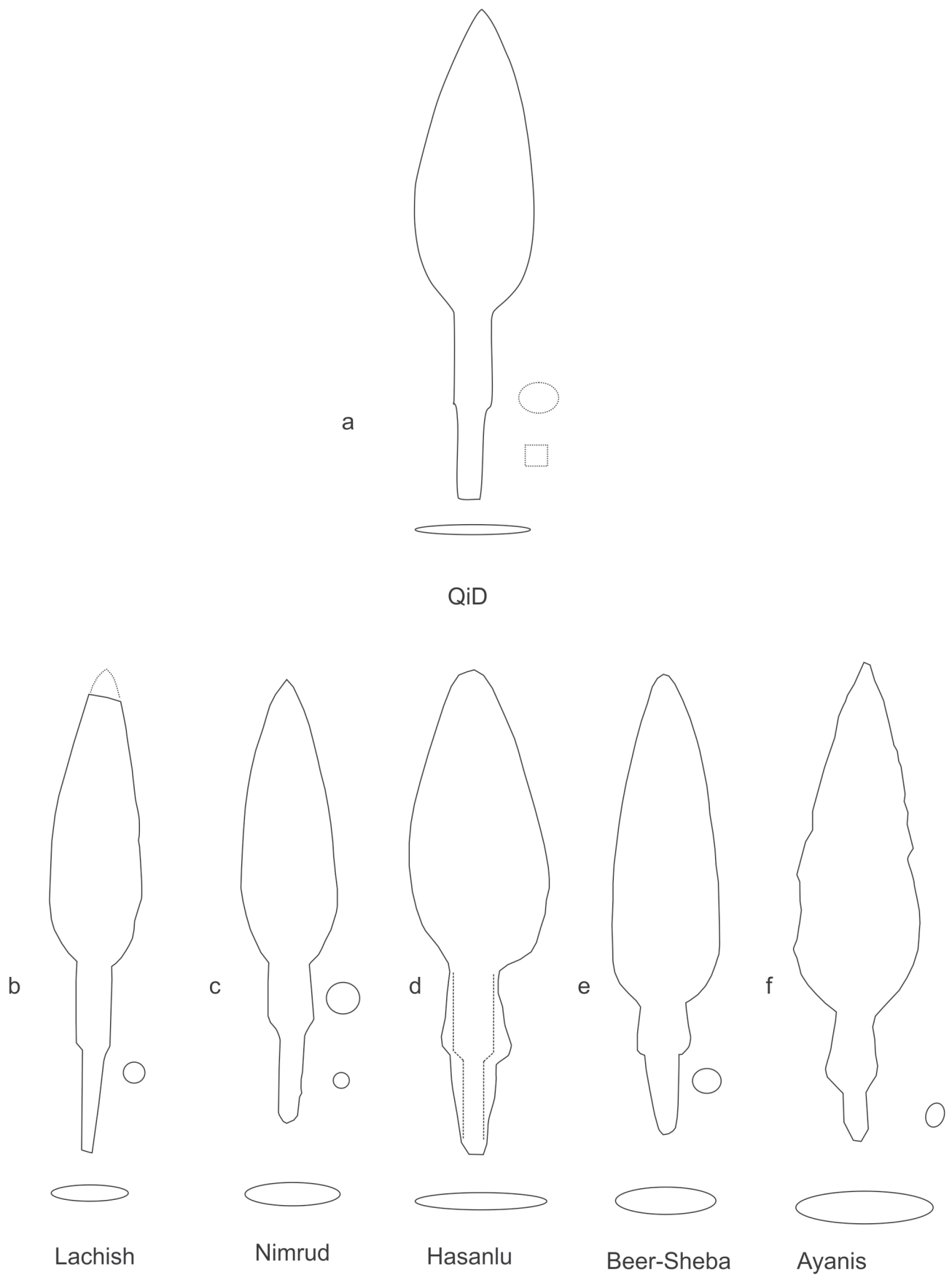


Fig. E4.5: Arrowhead of Variant c from Qalat-i Dinka (QID1), and comparisons. Drawings by Anja Hellmuth Kramberger.

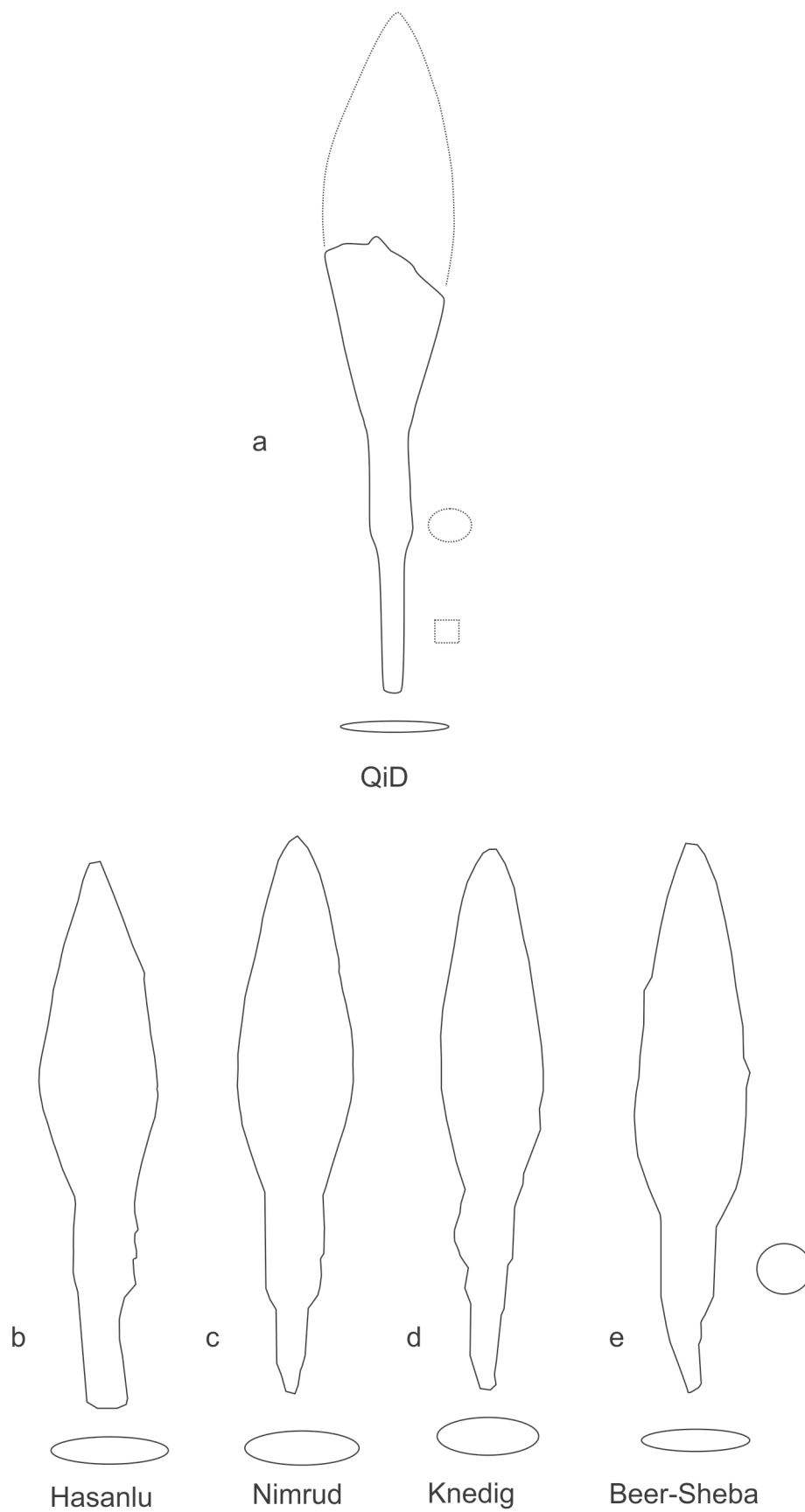


Fig. E4.6: Arrowhead of Variant d from Qalat-i Dinka (QID1), and comparisons. Drawings by Anja Hellmuth Kramberger.

arrowhead types²²⁸ may have been the weapons of the attackers²²⁹.

In Dur-Katlimmu (Tell Sheikh Hamad), an arrowhead of this type was found in the Middle Lower Town II in the “Neo-Assyrian Residences” (outside area FZ of House 1) in an earth unit that dates to the 7th century BC²³⁰. Two other specimens come from the “Red House” (also Middle Lower Town II) and are linked to the 6th century BC use phases²³¹.

136 leaf-shaped iron arrowheads with collar/stem and stopped tang were documented in Lachish²³² (see here **Fig. E4.5: b**). In contrast to the more than 900 examples of leaf-shaped arrowheads with a simple tapering tang that were discovered in Lachish²³³, they comprise a considerably lower percentage of the total finds and Gottlieb suspects that this is due to the more elaborate production required to make arrowheads with a stopped tang²³⁴. Arrowheads of this type were forged from an iron rod that had the width of the collar/stem²³⁵. The blade was hammered out of the upper part of this rod and the tang was dragged out of the lower part. The majority of the bilobate, leaf-shaped iron arrowheads with or without a stopped tang from Lachish originated in Level III, and their special significance lies in the fact that they provide evidence for a military attack. A map of the arrowheads in the excavated areas would clearly show that the number of arrowheads increases significantly from the outer section of the defenses to the main wall (Area R) – the course of the fighting can therefore be traced²³⁶. Gates generally represent a weak point in the defense of a city, and in Lachish the evidence of the attack was found in the area of the city gate (Areas GW and GE) as well as in the residential areas – testimony to the successful capture of the city²³⁷. This impressive evidence of a military attack in Lachish came with the Assyrian conquest in 701 BC under King Sennacherib²³⁸ and provides a *terminus ad quem* for dating of bilobate leaf-shaped iron arrowheads with tang.

Another archaeological site in modern Israel that brought to light a large number of arrowheads resembling

our Variant c and Variant d types is Tel Beer-Sheba²³⁹ (see here **Fig. E4.5: e** and **E4.6: e**). The arrowheads were mainly found in stratum II, where they make up 14% of the bilobate leaf-shaped iron arrowheads with tang; the majority of the 158 stratum II arrowheads from Tel Beer-Sheba have no collar/stem and stop at the tang²⁴⁰. Stratum II in Tel Beer-Sheba is sealed by a destruction horizon, and this, along with the large number of arrowheads, is associated with a military attack which (like Lachish, Level III) is linked to Sennacherib's 701 BC military campaign²⁴¹. In contrast to Lachish, however, where the distribution of the arrowheads in the area of the fortifications and the gate clearly make the course of the fighting traceable, the arrowheads in Stratum II in Beer-Sheba were more or less evenly distributed across the entire city area, thus it is more difficult to identify or assign weapons to either the attackers or the defenders²⁴².

Other sites where bilobate leaf-shaped iron arrowheads with tang were found in the contexts of the remains of military conflicts can be named. The oldest context is probably represented by the finds from Hasanlu (see here e.g., **Fig. E4.5: d** and **E4.6: b**). Thousands of artefacts, including 681 arrowheads, were recovered in the extensive destruction horizon that marked the end of the Hasanlu IVB period²⁴³. Leaf-shaped iron arrowheads with tang, Types IA and IB according to Thornton and Pigott, make up the largest percentage with 60%²⁴⁴. Remarkably, at least five bundles of arrowheads were found, undoubtedly representing the remains of quivers²⁴⁵, which may have fallen in place in the course of battle. The absolute dating of the destruction horizon of Hasanlu IVB is the subject of extensive discussion, and cannot be addressed at this point. A dating in the late 9th century BC is supported by radiocarbon testing²⁴⁶, while an alternative dating to the (late) 8th century BC is based on the stylistic characteristics of certain artefacts²⁴⁷.

Approximately 400 iron and bronze arrowheads provide evidence for the capture of the Urartian fortress Agartı Kalesi-Ayanis, shortly after the middle of the 7th century BC. Their locations were precisely documented

228 Very likely this means arrowheads of the Eurasian, Nomadic or so-called Scythian type, compare e.g., Stronach 1958, Pl. XXXIII, 7 or Curtis 2013, Pl. XIV, all under “Type 3”.

229 Stronach 1958, 171; see also Muscarella 1988, 321.

230 Hellmuth Kramberger 2016, 41, 69 No. 035.

231 Hellmuth Kramberger 2016, 41, 71, No. 039-040; see Kreppner/Schmid 2013, 360, Fig. 388, Supplement 1.

232 Gottlieb 2004, 1924.

233 Gottlieb 2004, 1916, 1920.

234 Gottlieb 2004, 1924.

235 Szudy 2015, 294.

236 Gottlieb 2004, 1951-1956.

237 Gottlieb 2004, 1957-1963.

238 Gottlieb 2004, 1907; Gottlieb 2016, 1192.

239 Gottlieb 2016.

240 Gottlieb 2016, 1202-1204, Figs. 24.7-24.13, 1221, Fig. 24.14.

241 Gottlieb 2016, 1212.

242 Gottlieb 2016, 1221-1222, Fig. 24.15.

243 Thornton/Pigott 2011, 137.

244 Thornton/Pigott 2011, 139.

245 Thornton/Pigott 2011, 140, Pl. 6.3, above, 141.

246 E.g., Muscarella 1966, 122; Dyson/Muscarella 1989; Thornton/Pigott 2011, 135; Danti 2013, 67-68.

247 E.g., Medvedskaya 1988; Magee 2008.

and mapped²⁴⁸. Of the 244 iron arrowheads recovered by 1998, 105 were completely deformed and broken by impact with the fortification walls. The majority of the iron arrowheads are bilobate leaf-shaped arrowheads with a tang, and the partial remains of their wooden shafts have been preserved²⁴⁹. A large number of the bilobate leaf-shaped arrowheads from Ayanis correspond to our Variant c and Variant d²⁵⁰ (see here **Fig. E4.5: f**). Iron arrowheads with a tang show a clear find concentration in Areas V and VI, thus in the area of the gate, on both sides of the west tower and along the southern wall (outer face) as well as the western buttresses, and especially in the interior of the fortress²⁵¹. Derin and Muscarella emphasise that the majority of the 146 bilobate bronze arrowheads with socket, which can be addressed as the nomadic, so-called Scythian type²⁵², were found in the outer area of the fortification wall²⁵³; they were probably fired in the direction of the wall. Since the latter arrowhead type should be considered foreign when it is found in the Urartian area, it may certainly indicate the origin of the attackers, or some of the attackers. A similar situation is also documented for numerous other Urartian fortresses²⁵⁴, such as Çavuştepe, where thousands of arrowheads of the so-called Scythian type were found, some of which are said to have still been embedded in the outer face of the walls²⁵⁵. A. Erzen dated the attack and its associated destruction to the final decade of the 7th century BC²⁵⁶. He considered the bilobate iron arrowheads with a tang to be the arrowheads used by the defending forces²⁵⁷. These correspond to the examples of bilobate arrowheads with an almond or willow leaf-shaped blade and stopped tang²⁵⁸ that we described previously from Kalhu, Lachish, Tel Beer-Sheba, Dur-Katlimmu, Hasanlu Tepe, and Agartı Kalesi-Ayanis, or to our bilobate Variants c and d arrowheads from the DSC.

Hundreds of arrowheads made of bronze and iron, including bronze arrowheads of the so-called Scythian type and bilobate iron arrowheads with a tang, were found in "House D" in the outskirts of Carchemish, and these have

been linked to the destruction that took place during the fall of the Neo-Assyrian Empire at the end of the 7th century BC²⁵⁹.

Other sites where bilobate, leaf-shaped iron arrowheads with stopped tangs have been found include: Hattusa (Boğazköy),²⁶⁰ Alişar Hüyük²⁶¹, Bastam²⁶², Toprakkale²⁶³, Agrab Tepe²⁶⁴, Tell Afis²⁶⁵, Naqsh-i Rostam²⁶⁶, Uruk²⁶⁷, and Tel 'Aroer²⁶⁸. Also interesting is a bone arrowhead from Toprakkale, which imitates the iron specimens²⁶⁹.

In connection with the appearance of destruction layers and the common occurrence of bronze arrowheads of the Scythian type and Assyrian iron arrowheads, the site of Grd-i Tle, located on the Raniyah plain northwest of the Peshdar Plain, is worth mentioning²⁷⁰. Among the arrowhead finds published so far, three-winged bronze arrowheads with an arched-shaped blade and a short to medium-long socket can be mentioned²⁷¹, which are a characteristic type of the late 8th and 7th centuries BC and which can be partly found also in contexts of the 6th century BC²⁷². Among the iron arrowheads from Grd-i Tle there can be named specimens from various periods. While one arrowhead with a triangular shaped blade and a tang with short stop/collar is probably Hellenistic²⁷³, the other one can be assigned to the Assyrian two-winged leaf-shaped iron arrowheads with a long tang²⁷⁴. In contrast to our two-winged, leaf-shaped iron arrowheads, however, it is a specimen with a midrib and a tang without stop/collar. According to its excavators, the arrowheads from Grd-i Tle seem to point to military conflicts in this region, probably in the 7th century BC²⁷⁵.

In addition to the numerous settlement finds, arrowheads of this type have also been found in graves, for example at Tall Knēdiğ and Deve Hüyük II. In Tall Knēdiğ, an arrowhead was found in Grave 59 (plateau of the south-

248 Derin/Muscarella 2001, 189, 211, Fig. 1.

249 Derin/Muscarella 2001, 189, 208-210, Fig. 2.5-23, Fig. 5.

250 Derin/Muscarella 2001, 213 Fig. 3.24-27, 29-34; 214, Fig. 4; 215, Fig. 5.57- 67;

251 Derin/Muscarella 2001, 191-192.

252 See also e.g., Hellmuth Kramberger 2016, 22-24, 23, Fig. 26; Hellmuth Kramberger 2017, 581.

253 Derin / Muscarella 2001, 190-192

254 Derin/Muscarella 2001, 192.

255 Erzen 1988, 49.

256 Erzen 1988, 50.

257 Erzen 1988, 46.

258 Erzen 1988, 47, Fig. 39 (middle row first and second from left, lower row first from left).

259 Woolley 1921, 125, Pl. 22b.

260 Boehmer 1972, Pl. 50, nos. 1585-1586.

261 von der Osten 1937, 115, 118, Fig. 113, d453, d733, and e611.

262 Kroll 1979, 172 Fig. 11.6; 160, 176.

263 Wartke 1990, 127, Fig. 32c; Wartke 1993, Fig. 90 (first and second from left).

264 Muscarella 1973, 66, Fig. 27.11.7, 67.

265 Matermawi 2005, 31, 166, Fig. 26.6.

266 Schmidt 1970, 74-75, Fig. 30.1.

267 van Ess/Pedde 1992, 68, no. 750.

268 Thareani 2011, 217, 381, Pl. 267.1.

269 Wartke 1993, Fig. 88 left.

270 Dezsó 2017; Kalla/Dezsó 2019.

271 Dezsó 2017, 98, Fig. 1.1-2.

272 Hellmuth 2010, 63-68, 271-281, 324-325.

273 Dezsó 2017, 98, Fig. 1.4, 108.

274 Dezsó 2017, 98, Fig. 1.3, 103- 107.

275 Kalla/Dezsó 2019, 10.

west mound, 93/8 NW) above the head of Skeleton I; others were found on the feet and right lower leg of Skeleton II. Some of these were highly fragmented²⁷⁶. Another leaf-shaped iron arrowhead with a stopped tang was discovered in the mudbrick debris on the plateau of the southwest mound, 94/1 NO²⁷⁷. The arrowheads from Tall Knēdiğ are thought to date to the Neo-Assyrian period²⁷⁸. One leaf-shaped iron arrowhead from a grave in Deve Hüyük II differs from the other arrowheads mentioned in that it probably features a mid-rib or a rhombus-shaped cross-section of the blade²⁷⁹. It weighs 15 g and was described by Moorey as a light spearhead; formally it corresponds to the arrowheads described here as Variants c and d.

Finally, based on the comparisons made, we can conclude that the bilobate, leaf-shaped iron arrowheads with a stopped tang – Variant c and Variant d – represent one of the most characteristic arrowhead types of the late 9th to 6th century BC, that is the Iron Age II-III period.

E4.2.4 “Bodkin type” (Fig. E4.2)

For the iron arrowhead of the “Bodkin type”, their parallels and possible dating have already been discussed in detail²⁸⁰; therefore a detailed treatise is not necessary at this point. Generally, “awl” or “bolt-shaped” arrowheads (called “bodkin”), with a round or square cross-section of the blade and a tang, represent a form that was produced in both the iron and bronze ages. The oldest arrowheads of this type feature a square cross-section, and they appeared in Anatolia by the third/second millennium BC²⁸¹.

Iron arrowheads of the “Bodkin type” with tang and square cross-section, “Type 1c-2” according to Szudy²⁸² or “Type IIIA” according to Thornton and Pigott²⁸³, have been found in various sites from the first half of the first millennium BC, however, they do not represent a large percentage of the total arrowheads in any location. They range from northwestern Iran, northern Iraq, northeastern and central

Anatolia, Syria to Israel,²⁸⁴ and they are found in Hasanlu Tepe²⁸⁵, Agartı Kalesi-Ayanis²⁸⁶, Dur-Katlimmu (Tell Sheikh Hamad)²⁸⁷, Hattusa (Boğazköy)²⁸⁸, and Toprakkale²⁸⁹.

It should be pointed out again²⁹⁰ that arrowheads of the “Bodkin type” continued to be used in much later periods²⁹¹, as discoveries from Pergamon or Bastam show. In Pergamon, arrowheads with a square cross-section form the second largest group, comprising 15% of the arrowheads with tang. Some of these pieces date from the late Hellenistic to the Middle Imperial period, while others came from a mixed antique-Byzantine context as well as from complexes of finds (FK 29 and FK 41) linked to late Byzantine buildings²⁹². The numerous “Bodkin type” arrowheads from the upper and middle citadel (“Oberburg” and “Mittelburg”) of Bastam were also found in the Medieval settlement debris²⁹³. They have partially deformed tips²⁹⁴, which clearly shows that they hit the walls during combat operations. The same observation can be made of some bronze arrowheads of the so-called Scythian type from Bastam²⁹⁵. Insofar as this can be assessed on the basis of drawings, the arrowheads from Pergamon and Bastam in particular are very similar to the piece from Gird-i Bazar, which could be an indication of a post-Iron Age dating (see also §E5 for even later examples).

E4.2.5 Variant e and “Others”

Among the highly fragmented arrowhead pieces from Qalat-i Dinka, it is only worth briefly mentioning PPP 181908:029:030, although its designation as an arrowhead has been made with reservations due to its poor state of preservation. As described above (§4.1.6), a stopped tang can be identified on the object, which merges into a suspected wing section with a diameter of 1 cm.

If, as assumed, this object represents an arrowhead with a very pronounced mid-rib or with a four-winged cross-section,

276 Klengel-Brandt *et al.* 2005, 305-306, Pl. 201, 1117-1118.

277 Klengel-Brandt *et al.* 2005, 306, Pl. 202.1124.

278 Klengel-Brandt *et al.* 2005, 305.

279 Moorey 1980, 61, Fig. 10, no. 183.

280 Wilkinson/Squitieri/Hashemi 2016, 102-104.

281 See Szudy 2015, 250. Szudy 2015, 243 rightly notes that especially “bodkin type” arrowheads (with a round cross-section of the blade) without a clearly visible stopped tang can hardly be distinguished from tools such as awls or punches. This could also be, in my opinion, the case with the suspected arrowhead of the “bodkin type” from Norşuntepe, which is an example of such an early arrowhead from the third/second millennium BC. See Szudy 2015, 205, Fig. 9.17.

282 Szudy 2015, Fig. 9.15, 251.

283 Thornton/Pigott 2011, 146, Fig. 6.6.

284 Wilkinson/Squitieri/Hashemi 2016, 103-104.

285 Thornton/Pigott 2011, 145, Fig. 6.6.

286 Derin/Muscarella 2001, 212, Fig. 2.1.

287 Hellmuth Kramberger 2016, 52, 95, no. 106.

288 Boehmer 1972, Pl. 51, 1554-1563A.

289 Wartke 1990, Pl. 39, b.8.

290 Compare Wilkinson/Squitieri/Hashemi 2016, 104.

291 Szudy 2015, 242 points out that arrows with “bodkin” tips were part of the standard equipment of archers in the European Middle Ages.

292 Gaitzsch 2005, 143, Fig. 27.G.

293 Kroll 1979, 151-152, 176, 161, Fig. 5.9-18.23-25; 163 Fig. 6.17-24; 165 Fig. 7.7-11; 167, Fig. 8.13; 169 Fig. 9.7-8; 177 Fig. 15.9-10; Kroll 1988, 155, 157, 160, 156 Fig. 1.5-10.14; 158 Fig. 2.21-23.26; 159, Fig. 3.17-23.

294 Kroll 1979, 165, Fig. 7.7-11; 167, Fig. 8.13; 177, Fig. 15.10.

295 E.g., Kroll 1979, 157, Fig. 3.2.

tion, a few parallels can be pointed out. For example, some arrowheads from Agartı Kalesi-Ayanis²⁹⁶ are worth mentioning; one specimen in particular is similar to our fragment²⁹⁷. Several specimens of Neo-Assyrian four-winged iron arrowheads have been found in Dur-Katlimmu and are described there for the first time as a separate type²⁹⁸. The arrowheads show a different state of preservation and come from the “Northeast Corner” of Lower Town II, locus (Grabungsstelle) “Citywall”²⁹⁹ and “Building F/W”³⁰⁰, from the “Neo-Assyrian Residences”³⁰¹, as well as from the “Red House”³⁰². All three of the fully preserved arrowheads found in Room YY of the “Red House” came from an earth unit that is linked to the construction of the second use phase of the building, meaning that they were used during the last third of the 7th and the first half of the 6th century BC³⁰³. The two completely preserved arrowheads from the “Neo-Assyrian Residences” were found in earth units of Phases 3b and 2b, which indicates a possible dating between the last quarter of the 8th and the last quarter of the 7th centuries BC, or a period between 612-593 BC³⁰⁴.

E4.3 Conclusions

In conclusion, it can be stated that the iron arrowheads from the Dinka Settlement Complex include, on the one hand, types or variants that represent characteristic arrowhead forms from the (late) 9th-6th century BC (our Variant b, Variant c and Variant d), and on the other hand arrowhead types whose dating cannot be clearly determined. The latter applies to our Variant a and the arrowhead of the “Bodkin type”. Although it is possible to categorise both forms, as we have discussed, there are parallels dating to the Iron Age II-III, and later comparable arrowheads from the Late Roman or even Medieval period also exist (see §E5).

Table E4.2 sums up the results of the typological analysis. Additionally, Variant e cannot be linked to a clear chronology. Finally, in the category “Others”, only the fragment PPP 181908:029:030 may be dated to the late 8th-6th century BC, although with some reservations.

Arrowheads found at the Dinka Settlement Complex in 2015 and 2018				
Registration no.	Operation	Context	Variant	Proposed Period
PPP 267931:011:004	Gird-i Bazar	topsoil	“Bodkin type”	Iron Age or later. Very possibly Medieval period (see §E5).
PPP 181909:002:008	QID1	topsoil/ disturbed layer	a	Iron Age or later
PPP 181909:002:009				
PPP 181909:002:010				
PPP 181909:002:011				
PPP 181909:002:012				
PPP 181909:002:013				
PPP 181909:004:032				
PPP 181909:004:049				
Arrowheads found at the Dinka Settlement Complex in 2019				
Registration no.	Operation	Context	Variant	Proposed Period
PPP 181908:033:004	QID1	Grave 102	d	9th - 6th century BC
PPP 181908:035:033	QID1	Grave 102	Others	/
PPP 181909:069:019	QID1	Grave 106	Others	/
PPP 181909:063:011	QID1	Looting pit	b	9th - 6th century BC
PPP 181908:029:055	QID1	Looting pit	c	9th - 6th century BC
PPP 181909:052:016	QID1	Looting pit	c	9th - 6th century BC
PPP 181909:063:013	QID1	Looting pit	c	9th - 6th century BC
PPP 181908:025:009	QID1	Looting pit	e	/
PPP 181909:052:017	QID1	Looting pit	e	/
PPP 181908:029:030	QID1	Looting pit	Others	late 8th - 6th BC ?

Table E4.2: Results of the typological analysis on the arrowheads from Gird-i Bazar and Qalat-i Dinka (QID1), 2015-2019.

296 Derin/Muscarella 2001, 212, Fig. 2.2-4.

297 Derin/Muscarella 2001, 212, Fig. 2.3.

298 Hellmuth Kramberger 2016, 51-52.

299 Hellmuth Kramberger 2016, 92, no. 99.

300 Hellmuth Kramberger 2016, 93, no. 100.

301 Hellmuth Kramberger 2016, 93, no. 101-102.

302 Hellmuth Kramberger 2016, no. 103-105.

303 See also Kreppner/Schmid 2013, 360, Fig. 388, Supplements 1 and 2.

304 Compare Kühne 2006-2008, Table on p. 550.

E5. Micro-CT study of the “Bodkin type” arrowhead from Gird-i Bazar

*Thilo Rehren*³⁰⁵, *Raouf Jemmali*³⁰⁶, *Silvia Amicone*³⁰⁷,
*Christoph Berthold*³⁰⁸

A well preserved iron arrowhead of the “Bodkin type” (length 58 mm, max. thickness of the square base of the pyramidal head 7.5 mm, weight 7 g) was found in the top-soil of Gird-i Bazar during the 2015 excavation season (**Fig. E5.1**)³⁰⁹. The artefact was very well preserved and only slightly corroded, therefore its shape was clearly identifiable. It was registered as PPP 267932:011:004. A discussion of its shape in comparison with other arrowhead types is offered in **§E4.1.5**. This chapter is dedicated to the results of the object’s micro-CT study.

For our comprehensive investigation, μ -X-ray computed tomography scans (μ CT) were performed to provide a more detailed characterisation of the outer shape of this object, and also to gain insights into its manufacturing process³¹⁰. The analysis was carried out at the Deutsches Zentrum für Luft- und Raumfahrt e.V. (DLR), German Aerospace Center, Institute of Structures and Design in Stuttgart using a high resolution μ CT-System (v|tome|x L 240/450, GE Sensing & Inspection Technologies GmbH, Wunstorf) consisting of a microfocus X-ray tube with a maximum accelerating voltage of 240 kV and a 16-bit flat panel detector (active area 2048 x 2048 pixels at 200 microns per pixel). The μ CT scan parameters are summarised in **Table E5.1**.

The resulting 2D X-ray images were reconstructed using a specific reconstruction algorithm known as Filtered Back Projection. The μ CT data were visualised and analysed with the VGStudioMax 3.2 commercial software package (developed by Volume Graphics, Heidelberg).

305 Science and Technology in Archaeology and Culture Research Center, The Cyprus Institute, Nicosia, Cyprus.

306 Deutsches Zentrum für Luft- und Raumfahrt e.V. (DLR), German Aerospace Center, Institute of Structures and Design, Stuttgart, Germany.

307 Competence Center Archaeometry – Baden-Wuerttemberg, Universität Tübingen, Germany

308 Competence Center Archaeometry – Baden-Wuerttemberg, Universität Tübingen, Germany.

309 Wilkinson/Squitieri/Hashemi 2016, 102.

310 The authors would like to thank the Excellence Initiative of the Eberhard Karls Universität Tübingen, the Ministry for Science, Research and Art of Baden-Württemberg and the Helmut Fischer GmbH, Institut für Elektronik und Messtechnik for the support provided to this research, and the Directorate of Antiquities of Sulaymaniyah for the export permit to study this artefact in our laboratory.

Parameters	Scan 1 (Overview)	Scan 2 (Detailed view)
Voxel size (mm)	0.035	0.010
Voltage (kV)	220	180
Current (μ A)	400	130
Timing (ms)	333	1000
Number of X-ray projections	1800	1800

Table E5.1: CT scan parameters

Micro-X-ray computed tomography (μ CT imaging) is a non-destructive imaging technique that uses X-rays to create high-resolution 3D reconstructions, and insight into the inner structures of objects via multiple projectional radiographs. Therefore, this technique is a perfect tool to study the internal microstructure of ancient finds which for curatorial, or other reasons, cannot be analysed through invasive analyses.

Similar studies on Roman arrowheads using neutron radiography³¹¹ have been able to reveal their original outline and corrosion condition, as well as offering guidance for any conservation treatment, all based on the high hydrogen content of the organic materials (fillers, adhesives) used. However, neutron radiography does not reveal much about an object’s internal metallurgical texture (e.g., about slag inclusions or voids). In contrast, the metallographic investigation of heavily corroded Crusader Period arrowheads from Tel Arsuf (Israel)³¹² revealed even minute remnants of solid metal, as well as slag inclusions, preserved within the corroded products, but was based on complete cross sections, which was not desirable for our purposes.

A μ CT image of the exterior appearance is shown in **Fig. E5.2** and typical images of the inner microstructure are displayed in **Fig. E5.3**. These sample images clearly show both the corrosion (medium grey material) pitting and penetrating the surface of the metal (bright), and also the defined, elongated and curved lines of dark material in the interior of the tip and the shaft. These are weld lines and strings of slag inclusions where the original iron bloom was consolidated by hammering to remove residual slag, charcoal, and other material leftover from the smelting stage, and then drawn out into the elongated shape desired for the arrowhead (then possibly folded back onto itself). In contrast to the more-or-less-rounded porosity typically left by a casting process, these extremely drawn-out/elongated and curvy lines of black porosity and greyish inclusions (i.e., the former slag particles con-

311 Salvemini *et al.* 2014.

312 Ashkenazi *et al.* 2013.



Fig. E5.1: Iron arrowhead of the “Bodkin type” from Gird-i Bazar: PPP 267931:011:004.
Photo by Peter Bartl.



Fig. E5.2: μ CT image of the outer shape of the arrowhead.
Prepared by Raouf Jemmali.



Fig. E5.3: μ CT image of the interior of the whole arrowhead (left) and shaft in detail (right).
Prepared by Raouf Jemmali.

centrated on the lines visible in the μ CT images) point to the production of the arrowhead by a smithing process, as would be expected for a pre-modern iron object.

This arrowhead's remarkably good state of preservation, evident from its outer shape, was corroborated by the limited level of corrosion seen in the CT cross sections, raising the question about the age of this find. Unfortunately, the find context in the topsoil does not contribute any stratigraphic information, and the shape of these arrowheads, or bolts, remained unchanged throughout their long period of use from the Iron Age to the end of the medieval period³¹³. Two larger, but morphologically very similar, and also barely corroded, iron bolts were reported by James and Taylor from Qasr Ibrim, a Late Antique site in Egypt³¹⁴, raising the possibility that the bolt from Gird-i Bazar may be dated to as late as the first or even the early second millennium AD (for additional morphological comparisons, see §E4.2.4).

E6. Artefacts made of faunal remains from the Dinka Settlement Complex, 2015-2019

*Anja Prust*³¹⁵

This section offers an overall view of the artefacts made of faunal remains that were found during the 2015-2019 campaigns at the Dinka Settlement Complex in the excavations in the Lower Town, that is Gird-i Bazar, DLT2 and DLT3, and on Qalat-i Dinka (QID1). These items are usually documented as individual finds during the excavation and therefore not included in the zooarchaeological statistics, which are provided in §F.

This section particularly deals with the artefacts found during the 2015-2018 campaigns that were not previously published. They are summed up in **Table E6.1**, where they are also given a catalogue number. This section also discusses some of the items found during the 2015-2018 campaigns and already published in previous volumes: they are summarised in **Table E6.2**, with the respective references. For completeness, **Table E6.3** shows the artefacts found during the 2019 campaign at QID1, which are discussed in detail in §E1.

Based on the information from the previous report by Tina Greenfield and the project database, 87 artefacts and one semi-finished object were documented during the 2015-2019 campaigns at the Dinka Settlement Complex.

Questions regarding the material still exist for some of the objects; consequently, the list given here is not necessarily complete. The artificially modified faunal remains from the DSC were mainly collected from secondary and tertiary fills (grave fills, pit fills); only a few objects were found in primary contexts such as floor deposits.

E6.1 Items made of mammal bones

Artefacts made of mammal bones are the most common; in addition to these, a few gastropods, bivalves, and scaphopods were modified. The bone artefacts from the Dinka Settlement Complex (n=61) include fragments of appliques, pendants, and ornaments or inlays, as well as beads, discs, decorated items – including seven decorated bone tubes (discussed in §E1, no. 7) – and pierced objects. One polished fragment of a proximal femur of a sheep/goat from DLT2 probably represents a partially-finished piece (**Table E6.1, no. 6, Fig. E6.1**).

Additionally, six specimens were worked into tools. Two are possible fragmented spatulae. One of these, already published, came from the excavation area DLT3, from the fill of Building Q Room 62; it shows tiny indentations on the preserved end (PPP 226922:044:002, see **Table E6.2**). The other, showing a flat, rounded end, is from QID1 (**Table E6.1, no. 10, Fig. E6.4**). A hook was found on Qalat-i Dinka on the floor of Building P, Room 58 (**Table E6.1, no. 8, Fig. E6.2**). It represents the only item of this category from the Dinka Settlement Complex.

A pointed tool made from a cattle ulna is from Gird-i Bazar (**Table E6.1, no. 7, Fig. E6.3**). It was found on the floor of Courtyard 18 of Building I. This area was devoted to pottery production³¹⁶; however, it is not clear whether the tool was involved in any of the steps of the pottery *chaîne opératoire*. Among the items published previously, it is worth mentioning a cattle horn core from Gird-i Bazar with “both ends chopped and smoothed down”³¹⁷, which was found in the bone collection PPP 269929:020:007 (**Table E6.2**). It came from the pottery kiln located in Outdoor Area 8³¹⁸. This kiln was partially reused as a rubbish pit after it had gone out of use.

Finally, two rectangular decorated fragments (**Table E6.1, nos. 12-13**) from QID1 are additions to the group of rectangular bars, discs, and other decorated fragments from this excavation area that were published previously and shown here in **Table E6.2**. The item **no. 12**, a rectan-

313 E.g., Potts 1998.

314 James/Taylor 1994, 94-95, Fig. 1 and 2.

315 LMU Munich.

316 Bartl 2018.

317 Greenfield 2019, 141.

318 Stone 2016, 66; Amicone 2017b.

gular fragment showing tiny parallel grooves, was part of a larger item that cannot be identified. The item **no. 13** is a fragment of a decorated bar showing a guilloche motif, and is very close in shape and decoration to other examples found in QID₁ during the 2018 campaign³¹⁹ (see also **Table E6.2**).

E6.2 Items made of marine species

During the course of the 2015-2019 campaigns, 22 artefacts formed from marine species were found. A total of 13 cowrie beads were collected from Gird-i Bazar and Qalat-i Dinka (QID₁). Five examples comprising two beads from the floors of Building I in Gird-i Bazar and three beads from QID₁, of which one was found on the floor of Building P Room 58 (**Table E6.1, nos. 1-5, Fig. E6.5**), had not yet been published. Seven beads were found during the 2019 campaign at Qalat-i Dinka (**§E1, no. 93**, see also **Table E6.2**), while one, already published (PPP 271929:045:006), was found in the Sasanian-period Grave 72 at Gird-i Bazar (**Table E6.2**). They all show abraded dorsa as they were used as adornments.

Furthermore, two rings made of gastropods (probably *Conus* shells), five beads made of scaphopods (*Dentalium* sp.), and one bivalve with a perforated umbo that may have been used as pendant were part of the faunal assemblage retrieved from QID₁ during the 2019 campaign (discussed in **§E1, nos. 92, 94, 95, 96**, see also **Table E6.3**). They all come from disturbed layers, and it is possible that they originated from the now-looted graves.

Finally, one half of a probably-unworked bivalve (PPP 271928:166:007, **Table E6.2**), is also interpreted as an artefact because its origin in the fill of the Sasanian-period Grave 72 at Gird-i Bazar points to its former use as a grave good or ornament.

Objects made from marine gastropods and shells were widely distributed since the Palaeolithic and have been reported for numerous sites and periods in the Near East³²⁰. It is certain that they reached our site via exchange or trade, most likely in the form of finished goods such as clothing and jewellery. Their distribution in the Dinka Settlement Complex does not reveal any particular pattern, as they can be found in both the Lower and the Upper Towns, among the Iron Age structures, and the Sasanian graves. This indicates that this type of item enjoyed a wide pattern of use.

E6.3 Conclusions

Altogether, there are only a few artefacts made from faunal remains attested at the Dinka Settlement Complex. While most of the decorated objects were found in grave contexts, tools were mainly excavated from fills and floor deposits in buildings and courtyards. The few objects made of bone and the two modified fragments of antler (**§F4.2**) point to the local production of tools and decorative objects – even though partially-finished products are scarcely attested. Elaborately decorated objects, such as the bone tubes and plaques, were probably acquired through exchange and trade, as was the case for the ornaments made of marine gastropods, bivalves, and scaphopods. Except for the decorated bone tubes that were found in Grave 101 (**§E1, no. 7**), there is no proof of the exploitation of animals in ritual practice, e.g. as funerary objects, offerings, or for ritual meals.



Fig. E6.1: Polished fragment of a proximal femur of sheep/goat, perhaps a semi-finished object? (DLT2, from collection PPP 236934:027:022). Photo by A. Prust.

319 Squitieri 2019, no. 2.

320 Bar-Yosef Mayer 2005.



Fig. E6.2: Hook, made of a mammal bone (Qalat-i Dinka, primary context, collection PPP 181909:038:057). Photo by Anja Prust.



Fig. E6.3: Pointed tool, made of a cattle ulna (Gird-i Bazar, primary context, collection PPP 266930:009:005). Photo by Anja Prust.



Fig. E6.4: Fragment of the spatula PPP 181909:004:036 from Qalat-i Dinka (QID1). Photo by Andrea Squitieri.

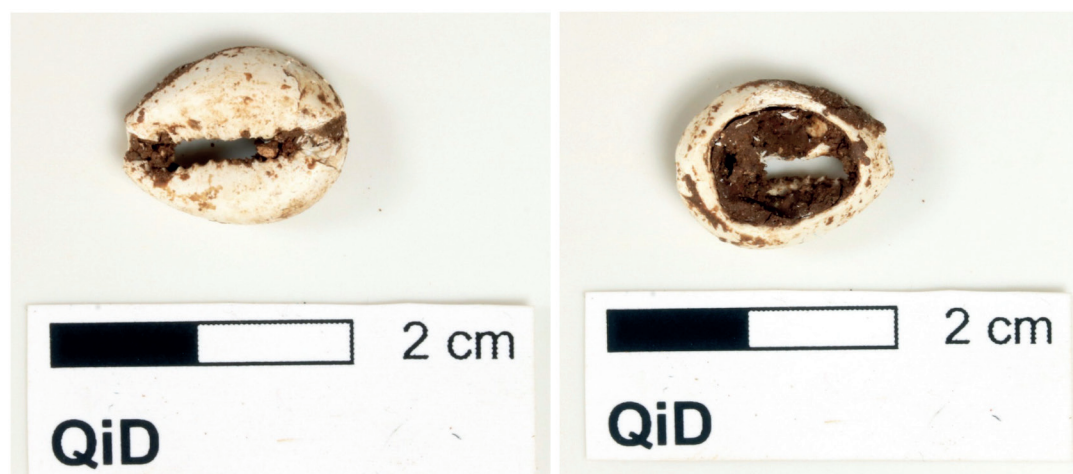


Fig. E6.5: Ventral and dorsal view of the cowrie bead PPP 181909:016:003 from Qalat-i Dinka (QID1).
Photo by Andrea Squitieri.

Artefacts from the Dinka Settlement Complex, 2015-2018, previously unpublished					
Registration no.	no.	Operation	Description	Context	Figure
Beads					
PPP 267930:036:030	1	GIB	1 cowrie bead	Floor of Building I Room 48	
PPP 267931:064:037	2	GIB	1 cowrie bead	Floor of Building I Room 46	
PPP 181909:016:003	3	QID1	1 cowrie bead	Disturbed fill	Fig. E6.5
PPP 181909:024:003	4	QID1	1 cowrie bead	Disturbed fill	
PPP 181909:038:058	5	QID1	1 cowrie bead	Floor of Building P Room 58	
Tools					
PPP 236934:027:022	6	DLT2	1 semi-finished polished item made from the femur of sheep/goat	Floor of Building K Room 40	Fig. E6.1
PPP 266930:009:005	7	GIB	1 pointed tool made from an ulna of cattle	Floor of Building I Courtyard 18	Fig. E6.3
PPP 181909:038:057	8	QID1	1 hook	Floor of Building P Room 58	Fig. E6.2
PPP 181909:006:007	9	QID1	1 worked bone fragment	Disturbed fill	
PPP 181909:004:036	10	QID1	1 spatula (fragment)	Disturbed fill	Fig. E6.4
PPP 181909:004:064	11	QID1	1 cylindrical fragment	Disturbed fill	
Decorated fragments					
PPP 100000:013:004	12	QID1	1 decorated fragment	Disturbed fill	
PPP 181909:038:025	13	QID1	1 decorated fragment	Floor of Building P Room 58	

Table E6.1: Worked animal bones and molluscs from the Dinka Settlement Complex, 2015-2018 (all previously unpublished).

Artefacts from Dinka Settlement Complex, 2015-2018, previously published			
Registration no.	Operation	Description	Reference
PPP 100000:021:013	QID1	9 circular beads	Kreppner/Squitieri 2017a, Fig. C28; Squitieri 2019, no. 4
PPP 100000:021:017			
PPP 181909:004:005			
PPP 181909:004:033			
PPP 181909:004:041			
PPP 181909:004:045			
PPP 181909:004:046			
PPP 181909:004:047			
PPP 181909:038:048			
PPP 181909:024:007			
PPP 181908:004:007			
PPP 181909:004:059			
PPP 181909:004:038			
PPP 100000:007:006			
PPP 181909:004:058			
PPP 181909:004:025			
PPP 181909:004:031			
PPP 181909:006:022			
PPP 100000:021:001	QID1	2 rectangular items with perforations	Kreppner/Squitieri 2017a, Fig. C25
PPP 100000:021:015			
PPP 271929:045:006	GIB	1 cowrie bead from the Sasanian Grave 93	Downey 2018, 182
PPP 269929:022:006	GIB	2 circular beads from the Sasanian Grave 32	Squitieri 2020, Table 1
PPP 269929:022:010			
PPP 271928:166:007	GIB	1 shell (unworked?) from the Sasanian Grave 72	Downey 2018, 180
PPP 269929:020:007	GIB	1 tool made from a horn core of cattle	Greenfield 2019, 141
PPP 226922:044:002	DLT3	1 fragment of spatula	Squitieri 2019, no. 32

Table E6.2: Previously published worked animal bones and molluscs found during the 2015-2018 campaigns at the Dinka Settlement Complex. Note that some of these items were previously described as being made of ivory.

Artefacts found during the 2019 campaign at QID1 and discussed in §E1	
Description	Reference in this book
7 fragments of decorated bone tubes	§E1, no. 7
20 appliques with pyramidal or hemispherical shapes	§E1, no. 18
3 disc-shaped beads	§E1, no. 88
3 beads made of <i>Dentalium</i> sp.	§E1, no. 92
7 cowrie beads	§E1, no. 93
2 rings made of gastropod shells	§E1, nos. 94-95
1 shell pendant, marine bivalve shell with pierced umbo	§E1, no. 96
2 rectangular items with perforation	§E1, nos. 102-103

Table E6.3: Worked animal bones and molluscs found during the 2019 campaign at QID1, as discussed in §E1.

F. Faunal remains from the Dinka Settlement Complex, 2015-2019

Anja Prust

The first analyses of faunal remains from the Dinka Settlement Complex, carried out by Tina Greenfield³²¹, aimed to reconstruct the local exploitation of animals, including species preferences, exploitation strategies, consumption, distribution and disposal practices. Her work was based on the analytical results from the Gird-i Bazar assemblages of the 2015 and 2016 campaigns, which indicated specific “patterns of behaviour in relation to food distribution, consumption and disposal” and “clear differences across the site, within and between spaces, buildings and rooms”³²².

The continuation of zooarchaeological research provides further data from various contexts and enables an intra-site comparison that largely confirms the previously observed strategies in local animal exploitation.

F1. Material

The analyses in 2019/2020 included faunal material from Gird-i Bazar (GIB)³²³, from Qalat-i Dinka (QID), and the two excavation areas in the Lower Town (DLT2 and DLT3), which were collected during the respective field campaigns from 2015–2019 (**Table F1**). According to the research design and sampling strategy for bioarchaeological

material³²⁴, the faunal remains were mainly collected by “*in situ* recovery” – meaning all specimens are collected by hand. Moreover, materials retrieved through flotation were studied as well.

The total faunal assemblage comprises 10,562 specimens (corresponding to 9.7 kg), including the bones and teeth of mammals, several fragments of molluscs, a few bird bones and a few remains of amphibians, fish and crustaceans. Of these, only 30.9 % (3,265 specimens) could be identified to the species or family level. As some contexts – especially graves – were disturbed, collections with mixed human and animal remains can be found occasionally. Respective finds were separated for anthropological research. The stratigraphic and chronological order is based on the entries in the Peshdar Plain Project database and personal communication³²⁵.

F2. Methods

The majority of the finds were analysed at the Institute for Palaeoanatomy and History of Veterinary Medicine (Ludwig-Maximilians-Universität, München)³²⁶. During the 2019 autumn campaign, collections retrieved by flotation (heavy

Operation	Analysed collections
GIB 2015, 2016	collections from <i>in situ</i> recovery & collections (heavy fraction & light fraction) retrieved from flotation
GIB 2017	collections from <i>in situ</i> recovery & collections (heavy fraction) retrieved from flotation
GIB 2019	collections (heavy fraction) retrieved from flotation
QID 2018, 2019	collections from <i>in situ</i> recovery & collections (heavy fraction) retrieved from flotation
DLT2 2017	collections from <i>in situ</i> recovery & collections (heavy fraction) retrieved from flotation
DLT2 2019	collections (heavy fraction) retrieved from flotation
DLT3 2018	collections from <i>in situ</i> recovery & collections (heavy fraction) retrieved from flotation
DLT3 2019	collections (heavy fraction) retrieved from flotation

Table F1: Analysed collections by operation and excavation campaign.

321 Greenfield 2016; 2019.

322 Greenfield 2019, 149.

323 The faunal material from Gird-i Bazar analysed here comprises both the material from the Iron Age levels and the material from the Sasanian period graves.

324 Greenfield 2016; 2017.

325 Thanks to Andrea Squitieri and Jean-Jacques Herr for their fruitful discussions. As a stratigraphic reference, see the stratigraphic tables published in the Peshdar Plain Project Publication volumes.

326 Many thanks to Joris Peters and Nadja Pöllath for helpful support during the analyses.

fraction) were analysed on site. Some were exported in order to be identified with the aid of the reference collection of the Bavarian National History Collections (section Palaeoanatomy).

The primary data were recorded in the database OsoBook,³²⁷ including basic archaeological information, taxon³²⁸, skeletal element and portion, side, number of specimens, epiphyseal fusion, tooth eruption and tooth wear, sex, specimen weight, pathologies, modifications, and biometrical data. If an identification to the species level was not possible, the higher taxonomic rank is given. Due to the poor state of preservation, some specimens could only be assigned to size categories, i.e. “large mammal” (e.g. horse, cattle, red deer), “medium-sized mammal” (e.g. sheep, goat, pig), “small mammal” (including dog, cat, fox, hare) and “micromammal” (e.g. murids). Unidentified specimens were listed as “indet.” or, when possible, according to taxonomic classes, e.g. “Mammalia indet.” or “Aves indet.”

For quantification, the standard units NSP (number of specimens), NISP (number of identified specimens) and MNI (minimum number of individuals) are applied. The quantification of antlers is problematic since only fragments are available; these were probably brought to the site as raw material. Furthermore, antlers may have been collected as isolated finds and do not necessarily represent hunting activities. Consequently, fragments of antlers were listed as single specimens, but were not included in statistics; their number is given in brackets.

The numerous and heavily fragmented specimens of land snails (*Helicidae*) cause problems as well. Since their relationship to individuals is unclear, every single speci-

men was counted; the minimum number of individuals is given in square brackets.

The situation is similar with the quantification of bivalves. Faunal assemblages seldom include both valves of an individual. Moreover, specimens and single valves could have been collected or traded as ornaments and are therefore not necessarily part of the consumption refuse. Consequently, each complete valve has been listed as a single specimen.

In order to obtain the most precise weight information possible for the material retrieved by flotation (heavy fraction and light fraction), the specimen weight was recorded to two decimal places. The weight of the material collected by “*in situ* recovery” was documented to only one decimal place. Age determination is based on the stage of epiphyseal fusion, tooth eruption, and tooth wear³²⁹.

The sample size does not offer representative data, especially if evaluated per operation and context (**Table F2**). Continuing Tina Greenfield’s analysis, data from both of the primary and secondary contexts – all representing Iron Age deposits – were combined “in order to observe some statistically significant patterns, which are indicative of the economic behaviour of the inhabitants of the site on the whole³³⁰”. The context categories given in this chapter are as follows: “primary contexts” are floor deposits and well-preserved grave fills; “secondary contexts” are undisturbed fills (e.g., fills of rooms or installations such as kilns); “tertiary contexts” are the topsoil, disturbed fills bearing signs of looting, and fills of modern pits.

Operation	Primary context	Secondary context	Tertiary context	Total
GIB	2,793 (2,282.75g)	1,106 (1,420.96g)	1,097 (1,381.81g)	4,996 (5,085.52g)
QID	175 (66.03g)	628 (216.23g)	2 (25.5g)	805 (307.76g)
DLT2	2,209 (1,165.54g)	428 (302.76g)	–	2,637 (1,468.3g)
DLT3	648 (457.52g)	669 (1,109.17g)	807 (1,266.93g)	2,124 (2,833.62g)
Total				10,562 (9,695.2g)

Table F2: Number of specimens (NSP) and specimen weight of the analysed material by operation and contexts.

327 Kaltenthaler, D., Lohrer, J., Kröger, P., van der Meijden, C., Granado, E., Lamprecht, J., Nücke, F., Obermaier, H., Stopp, B., Baly, I., Callou, C., Gourichon, L., Pöllath, N., Peters, J., Schibler, J.: OsoBook v19.5, Munich, Basel, 2020. (<http://xbook.vetmed.uni-muenchen.de/>).

328 The differentiation between sheep and goats is based on Boessneck *et al.* 1964, Zeder/Lapham 2010, and Zeder/Pilaar 2010. For the identification of molluscs, I relied on Fechter/Falkner 1989 and Schütt 2010.

329 The latter follows the criteria of Payne 1973 for sheep/goats and of Grant 1982 for cattle and pigs. All bone measurements follow the standards by von den Driesch 1976.

330 Greenfield 2019, 142.

	GIB		QID		DLT ₂		DLT ₃	
	NSP [MNI]	weight (g)	NSP [MNI]	weight (g)	NSP [MNI]	weight (g)	NSP [MNI]	weight (g)
<i>Homo sapiens</i>	8	0.58	2	6.12				
I. Domestic mammals								
<i>Equus caballus</i>			1	23.8			2	58.1
<i>Bos taurus</i>	149	2,015.57	6	20.29	24	166.86	107	1,042.85
<i>Ovis aries/Capra hircus</i>	171	454.63	10	33.39	121	129.9	145	406.03
<i>Capra hircus</i>	10	40.41			4	13.1	4	18.4
<i>Ovis aries</i>	3	28.4			3	14.41	21	126.4
<i>Sus domesticus</i>	234	1,122.61	6	7.04	126	504.04	72	335.34
<i>Canis familiaris</i>	1	1.7						
II. Wild mammals								
<i>Cervus elaphus</i>							1(+7)	2.5(+69.3)
<i>Gazella subgutturosa</i>	3	5.2			1	1.06	1	0.53
<i>Vulpes vulpes</i>							1	0.82
<i>Vormela peregusna</i>					4*1	0.62		
<i>Lepus sp.</i>					1	0.4		
<i>Meriones tristrami</i>	23*1	0.61						
<i>Mus musculus</i>	30*1	0.18			3*1	0.16	1	0.02
<i>Rattus rattus</i>	2*1	0.15						
Mustelide					2	0.4		
III. Birds								
<i>Gallus gallus dom.</i>	46*3	18.89						
<i>Alectoris chucar</i>					3*2	0.45		
<i>Anser anser</i>	2	5.82						
<i>Columba livia</i>					1	0.14		
IV. Amphibians								
<i>Rana sp.</i>							2	0.14
V. Fish								
Cyprinidae	1	0.12			1	0.03		

Table F3: List of faunal remains by operation; [xx]=MNI; *x partial skeletons with corresponding MNI; (+x)= antler fragments excluded from statistics.

	GIB		QID		DLT ₂		DLT ₃	
	NSP [MNI]	weight (g)	NSP [MNI]	weight (g)	NSP [MNI]	weight (g)	NSP [MNI]	weight (g)
VI. Molluscs								
Helicidae	659 [166]	21.57	47 [25]	2.44	12 [8]	0.24	23 [12]	3.15
<i>Helix cf. salomonica</i>	515 [125]	72.99	13 [4]	1.34	2 [1]	0.04	352 [30]	21.48
Hygromiidae	10 [7]	0.32						
<i>Monacha</i> sp.	8 [8]	1.35	11 [1]	0.1				
Cochlicopidae	21 [21]	1.14						
Chondrinidae	2 [2]	0.03						
Zonitidae	52 [19]	0.38						
Cecilioididae	166 [166]	0.28						
Cypraeidae	1	0.27	1	0.73				
VII. Crustaceans								
<i>Potamon</i> sp.	1	0.73						
NISP total	2118		97		308		732	
VIII. Indet.								
Large mammal	116	290.72	6	10.77	86	169.97	71	215.68
Medium-sized mammal	602	368.39	83	49.17	636	185.21	376	265.1
Small mammal	4	0.1	2	0.63	21	0.88	4	0.57
Micromammal	26*3	0.28			8	0.23	1	0.02
Mammalia indet.	2042	626.07	614	150.92	1,568	279.52	933	335.8
Aves indet.	7	3.16			7	0.59	5	0.51
Amphibia indet.	13	0.11						
Gastropoda indet.	68 [23]	2.76	3	1.02	3	0.05	2	0.18
Total	4,996	5,085.52g	805	307.76g	2,637	1,468.3g	2,124	2,833.62g

Table F3 (continued): List of faunal remains by operation; [xx]=MNI; *x partial skeletons with corresponding MNI; (+x)= antler fragments excluded from statistics.

	GIB primary & secondary context		GIB tertiary context	
	NSP [MNI]	weight (g)	NSP [MNI]	weight (g)
<i>Homo sapiens</i>	8	0.58		
I. Domestic mammals				
<i>Bos taurus</i>	120	1,677.36	29	338.21
<i>Ovis aries/Capra hircus</i>	108	266.03	63	188.6
<i>Capra hircus</i>	4	14.01	6	26.4
<i>Ovis aries</i>	2	26.9	1	1.5
<i>Sus domesticus</i>	150	818.11	84	304.5
<i>Canis familiaris</i>			1	1.7
II. Wild mammals				
<i>Gazella subgutturosa</i>	3	5.2		
<i>Merriones tristrami</i>			23*1	0.61
<i>Mus musculus</i>	30*1	0.18		
<i>Rattus rattus</i>			2*1	0.15
III. Birds				
<i>Gallus gallus dom.</i>			46*3	18.89
<i>Anser anser</i>	1	1.12	1	4.7
IV. Amphibians				
V. Fish				
Cyprinidae	1	0.12		
VI. Molluscs				
Helicidae	651 [165]	21.47	8 [1]	0.1
<i>Helix cf. salomonica</i>	458 [93]	29.39	57 [27]	43.6
Hygromiidae	7 [4]	0.12	3 [3]	0.2
<i>Monacha</i> sp.	1	0.2	7 [7]	1.15
Cochlicopidae	20 [20]	1.12	1	0.02
Chondrinidae	2 [2]	0.03		
Zonitidae	52 [19]	0.38		
Cecilioiidae	166 [166]	0.28		
Cypraeidae	1	0.27		
VII. Crustaceans				
<i>Potamon</i> sp.	1	0.73		
NISP total	1,786		332	
VIII. Indet.				
Large mammal	82	219.12	34	71.6
Medium-sized mammal	484	269.63	118	98.76
Small mammal			4	0.1
Micromammal	2	0.07	24 [1*]	0.21
Mammalia indet.	1,469	348.46	573	277.61
Aves indet.	1	0.01	6	3.15
Amphibia indet.	7	0.06	6*	0.05
Gastropoda indet.	68	2.76		
Total	3,899	3,703.71g	1,097	1,381.81g

Table F4: Gird-I Bazar. List of faunal remains by context; [xx]=MNI; *x partial skeletons with corresponding MNI.

	QID primary & secondary context		QID tertiary context	
	NSP [MNI]	weight (g)	NSP [MNI]	weight (g)
<i>Homo sapiens</i>	2	6.12		
I. Domestic mammals				
<i>Equus caballus</i>			1	23.8
<i>Bos taurus</i>	5	18.59	1	1.7
<i>Ovis aries/Capra hircus</i>	10	33.39		
<i>Sus domesticus</i>	6	7.04		
II. Wild mammals				
III. Birds				
IV. Amphibians				
V. Fish				
VI. Molluscs				
Helicidae	47 [25]	2.44		
<i>Helix cf. salomonica</i>	13 [4]	1.34		
<i>Monacha sp.</i>	11 [1]	0.1		
Cypraeidae	1	0.73		
VII. Crustaceans				
NISP total	95		2	
VIII. Indet.				
Large mammal	6	10.77		
Medium-sized mammal	83	49.17		
Small mammal	2	0.63		
Mammalia indet.	614	150.92		
Gastropoda indet.	3	1.02		
Total	803	282.26g	2	25.5g

Table F5: Qalat-i Dinka. List of faunal remains by context; [xx]=MNI.

	DLT ₂ primary & secondary context	
	NSP [MNI]	weight (g)
I. Domestic mammals		
<i>Bos taurus</i>	24	166.86
<i>Ovis aries/Capra hircus</i>	121	129.9
<i>Capra hircus</i>	4	13.1
<i>Ovis aries</i>	3	14.41
<i>Sus domesticus</i>	126	504.04
II. Wild mammals		
<i>Gazella subgutturosa</i>	1	1.06
<i>Vormela peregusna</i>	4*1	0.62
<i>Lepus sp.</i>	1	0.4
<i>Mus musculus</i>	3*1	0.16
Mustelide	2	0.4
III. Birds		
<i>Alectoris chucar</i>	3*2	0.45
<i>Columba livia</i>	1	0.14
IV. Amphibians		
V. Fish		
Cyprinidae	1	0.03
VI. Molluscs		
Helicidae	12 [8]	0.24
<i>Helix cf. salomonica</i>	2	0.04
VII. Crustaceans		
NISP total	308	
VIII. Indet.		
Large mammal	86	169.97
Medium-sized mammal	636	185.21
Small mammal	21	0.88
Micromammal	8*2	0.23
Mammalia indet.	1,568	279.52
Aves indet.	7	0.59
Gastropoda indet.	3	0.05
Total	2,637	1,468.3g

Table F6: Dinka Lower Town (DLT) 2. List of faunal remains by context; [xx]=MNI; *x partial skeletons with corresponding MNI.

	DLT ₃ primary & secondary context		DLT ₃ tertiary context	
	NSP [MNI]	weight (g)	NSP [MNI]	weight (g)
I. Domestic mammals				
<i>Equus caballus</i>			2	58.1
<i>Bos taurus</i>	45	549.55	62	493.3
<i>Ovis aries/Capra hircus</i>	88	237.99	57	168.04
<i>Capra hircus</i>	3	16.8	1	1.6
<i>Ovis aries</i>	9	89.3	12	37.1
<i>Sus domesticus</i>	45	152.57	27	182.77
<i>Canis familiaris</i>				
II. Wild mammals				
<i>Cervus elaphus</i>	1+(7)	2.5+(69.3)		
<i>Gazella subgutturosa</i>	1	0.53		
<i>Vulpes vulpes</i>	1	0.82		
<i>Mus musculus</i>	1	0.02		
III. Birds				
IV. Amphibians				
<i>Rana sp.</i>			2	0.14
V. Fish				
VI. Molluscs				
Helicidae	22 [11]	3.14	1	0.01
<i>Helix cf. salomonica</i>	117 [11]	7.28	235 [19]	14.2
VII. Crustaceans				
NISP total	333		399	
VIII. Indet.				
Large mammal	41	106.48	30	109.2
Medium-sized mammal	270	186.26	106	78.84
Small mammal	4	0.57		
Micromammal	1	0.02		
Mammalia indet.	661	212.17	272	123.63
Aves indet.	5	0.51		
Gastropoda indet.	2	0.18		
Total	1,317	1,566.69g	807	1,266.93g

Table F7: Dinka Lower Town (DLT) 3. List of faunal remains by context; [xx]=MNI; (+x)= antler fragments excluded from statistics.

F3. Taphonomic patterns

Altogether, the material is in a poor state of preservation, meaning that it is highly fragmented, surface weathered, and damaged by chemical and mechanical processes. While numerous finds show old damage, recent breakages – caused during excavation and transport – are fre-

quent as well. Completely preserved specimens are rare, and even small, more robust bones exhibit surface damage and breakage.

The difference in the state of bone and teeth preservation between the particular operations is striking. Reasons for this may be differing soil chemistry and sediment composition³³¹, as well as the type of deposit (disposed of



Fig. F1: State of bone preservation. A: Bone fragment, agglutinated with clayey soil (QID, collection PPP 176909:034:004); B: Bone fragment with calc-sinter encrustation (DLT3, collection PPP 225922:048:003); C: Calcaneus of domestic pig with weathered surface (GIB, collection PPP 267931:064:042); D: Bone fragment with highly-weathered surface and root etching (GIB, collection PPP 268930:063:002). Photos by A. Prust.

³³¹ Eckmeier/Tolbas/Weidenhiller 2018.

in open area or deposited in pits etc.). Most of the finds from Gird-i Bazar and DLT2 had an extremely heavy coat of clayey soil (**Fig. F1A**); cleaning was often not possible due to the fragile condition of the bones and teeth. Additionally, many specimens of the assemblages from Gird-i Bazar exhibit heavily-to-extremely weathered surfaces. Small channels pervade the bone surface that seems to be etched away (**Figs. F1C–D**). The material from the fill of the large well excavated in Gird-i Bazar (Locus:271929:039 and Locus:271929:042) is an exception. Although likewise fragmented and agglutinated with soil, most of the specimens are in excellent condition, without significant signs of surface weathering. In contrast, thick layers of calcium carbonate adhered to some bones and teeth from the DLT3 assemblage (**Fig. F1B**). Calcareous-sinter encrustations have only been observed on specimens from this operation.

Traces of fire, root damage, and gnaw marks are visible on various specimens from all operations, while cultural modifications (traces of butchery, dissection, and food

processing) are generally rare (see below, §F5). The faunal collections retrieved by flotation and sorted from the heavy fraction vary in their composition, but they almost always contain shell fragments of land snails and tiny, indeterminable bone fragments (**Figs. F2A, F2C**). Some samples also contain complete teeth and fragmented skeletal elements of large mammals (**Fig. F2B**). The collections retrieved from the light fraction of soil samples from Gird-i Bazar (2015/2016 seasons), comprise tiny fragments of bones and numerous completely preserved land snails (**Fig. F2D**).

The state of preservation has a strong influence on the data. The number of completely preserved specimens is extremely small. An evaluation of, for instance, age and size is therefore problematic and consequently, the interpretation of the finds must be taken with a certain level of reservation. The following statements are based on the current data only and should be understood as trends rather than hard evidence.



Fig. F2: Composition and state of preservation of faunal material retrieved from flotation. A: Heavy fraction (DLT2, collection PPP 235934:019:009:001); B: Heavy fraction (DLT3, collection PPP 225922:012:003:001); C: Heavy fraction (DLT3, collection PPP 226922:040:022:001); D: Light fraction (GIB, collection PPP 268932:066:003:003). Photos by Anja Prust.

F4. Taxonomic diversity

In all assemblages, the remains of domestic mammals dominate while wild mammals and birds were found only occasionally. There are only very few remains of amphibians, fish, and crustaceans in the material. The numerous molluscs are most likely intrusive.

F4.1 Domestic mammals

The most frequent species are sheep, goats, domestic pigs, and cattle. According to the current data, sheep and goat herding, as well as pig husbandry, were the dominant livestock management strategies. The percentage distribution seems to vary somewhat between the particular operations (**Table F8**). Considering the very small sample sizes, it is impossible to say if the differences between the particular contexts (primary/secondary contexts and tertiary contexts) and operations are the result of chance or due to different activities or treatments or origins.

Still today, small ruminants like sheep and goats form the basis of the livestock economy in the rural areas of Iraqi Kurdistan³³². Meat and dairy products are the primary interest in recent small-scale and subsistence farming. A similar husbandry strategy can be assumed for the ancient periods as well. Herds were kept outside the settlement in sedentary or transhumant pastoralism.

Because of the poor state of preservation, the morphological distinction between sheep and goat was possible only for a few specimens. The small sample size does not allow comments on the ratio of sheep to goats between the separate operations and also precludes meaningful statements on skeletal element distribution, since fewer than 60 elements are available from Gird-i Bazar and DLT2. At both operations, based on the pure data, mandibles, mandible teeth, and tibiae are distinctively overrepresented while bones with high-value meat portions (e.g. scapula, pelvis, humerus, femur) and elements typical of butchery waste (phalanges, horn cores) are underrepresented. Much more material is needed to judge whether this represents a specific pattern or a random

phenomenon. Age-at-death data for Iron Age assemblages is based on 35 specimens that permit comments on epiphyseal fusion; age determination by dental data is based on 15 mandibular teeth. While the fusion data shows the presence of mainly adult individuals, who died between 12 and 48 months, the tooth wear analyses revealed seven individuals aged 24–48 months and eight individuals older than 48 months (**Tables F9** and **F10**). None of the sheep and goat remains could be sexed. The small number of measurable elements restricts an evaluation and comparison of size and stature, but the few biometric data point to rather small animals (see **Table F16**).

Judging by the breakage patterns, the sheep and goat remains most likely represent the refuse of consumption and food processing. Skeletal elements typically disposed of during butchering (skulls and horncores, metapodials, phalanges) are missing or underrepresented. The slaughter and first dismembering of the carcasses obviously took place elsewhere. High-value meat body parts are underrepresented as well and may have been distributed to inhabitants who discarded their consumption refuse elsewhere. Thus, specific meat cuts of lower-value were processed and consumed in the areas of the settlement investigated here. The respective leftovers were disposed of on site. Moreover, the fact that mainly adult animals beyond the optimal slaughter age are present indicates (1) that sheep/goats were reared for secondary products or/and for reproduction and (2) that the consumers, whose refuse we deal with here, primarily ate the less valued meat of older animals.

Pig husbandry contributed to the animal protein supply of the community to almost the same extent as caprines (**Tables F3–F7**). As for the caprines, the skeletal element distribution for domestic pig is not representative, but the present data points to a remarkable overrepresentation of mandibles and mandibular teeth, a slight overrepresentation of pelvic bones and upper forelimbs, and a clear underrepresentation of vertebrae and hindlimbs. Elements characteristic of butchery waste are almost non-existent. The average age of slaughter was between 12 and 24 months. Neither epiphyseal fusion data nor dental data

	GIB prim.+sec. context	GIB tertiary context	DLT2 prim.+sec. context	DLT3 prim.+sec. context	DLT3 tertiary context
Cattle	120 (30.7%)	29 (12.6%)	24 (8.3%)	45 (23.3%)	62 (38.0%)
Sheep/Goat	114 (29.1%)	70 (30.3%)	128 (44.1%)	100 (51.8%)	70 (43.0%)
Pig	150 (38.4%)	84 (36.4%)	126 (43.4%)	45 (23.3%)	27 (16.6%)
NISP total	391	231	290	193	163

Table F8: Distribution (NISP per taxon and % of total NISP) of the most frequent domestic mammals per operation. NISP total without fragments of antlers and intrusives (rodents and molluscs).

332 Bendrey *et al.* 2016, 52.

fusion group (age in months)	element	GIB			DLT2			DLT3		
		unfused	in fusion	fused	unfused	in fusion	fused	unfused	in fusion	fused
A (0-6)	Radius prox.									2
B (6-12)	Scapula						1			1
	Humerus dist.							1		2
	Pelvis (Acetabulum)									
C (12-18)	Ph1	2		1						4
	Ph2			1			2			1
D (18-30)	Tibia dist.	1					1	1		
	Metacarpal dist.									
	Metatarsal dist.									
	Metapodial dist.				2		1			
E (30-48)	Radius dist.				1					
	Ulna prox.	1	1							
	Ulna dist.				1					
	Femur prox.	1			1		1	2		
	Femur dist.			1						
	Tibia prox.									
	Calcaneus						1			1
F (> 48)	Humerus prox.									
	Vertebrae				6	1	1	2	1	

Table F9: Epiphyseal fusion data for sheep/goat (n=47) from Iron Age layers by operation. Fusion ages based on Habermehl 1975 and Zeder 2006.

Phase	Taxon	0-2 m	2-6 m	6-12 m	12-24 m	24-48 m	> 48 m
GIB 1+2	Ovis/Capra						2
GIB 3	Ovis/Capra					2	2
QiD 1+2	Ovis/Capra					1	
DLT3 1+2	Capra hircus					1	
DLT3 1+2	Ovis aries						1
DLT3 1+2	Ovis/Capra					1	
DLT3 3	Ovis aries					2	2
DLT3 3	Capra hircus						1
		4-6 m	12-24 m	25-34 m	3-6.5 y	6.5-9 y	9-11.5 y
GIB 1+2	Bos		1				1
QiD 1+2	Bos						1
DLT3 1+2	Bos		1	2			
		0-2 m	2-6 m	6-12 m	12-24 m	24-36 m	> 36 m
GIB 1+2	Sus dom.				1		
GIB 3	Sus dom.		1	1	2		
DLT2 1+2	Sus dom.				1		

Table F10: Age estimates of caprine (n=15), cattle (n=6) and domestic pig (n=6) from tooth wear data. Age given in months (m) and years (y) based on Grant 1982. 1+2: primary/secondary contexts; 3: tertiary context.

indicate individuals older than 24 months (**Tables F10** and **F11**). Only one individual died aged between 2 and 6 months; another individual was 6 to 12 months of age. Consequently, a preference for the consumption of piglets is not attested.

The pig remains represent remains of food processing or/and consumption. As with the caprines, meat cuts with lower-value portions dominate. Modifications that point to the curing and storage of meat were not observed, but ultimately, such processing cannot be excluded.

Even today, cattle herding remains part of the local subsistence economy. Some households keep a few animals mainly for dairy production. During the day, local cowherds lead the animals to pasture outside the settlements³³³. According to the faunal assemblages, the percentage distribution of cattle remains varies depending on the particular operation. Here, too, functional differences and disposal strategies may be the reason.

The skeletal element distribution resembles the observations made for caprines and pigs. Mandibles and mandibular teeth are overrepresented, while scapulae and metatarsal bones are slightly overrepresented. Skeletal elements rich in meat, such as upper forelimbs and hindlimbs, are clearly less well represented. Elements characteristic of butchery refuse (in particular phalanges, skulls, and horn cores) are also underrepresented. The age determination based on epiphyseal fusion (n=15) resulted in one individual younger than 12–24 months (Gird-i Bazar) one individual aged between 12–24 months (DLT3) and two individuals older than 48 months (**Table F12**). The average age of slaughter was between 24 and 30 months. Tooth abrasion (n=6) indicates an average age of slaughter between 12 and 34 months; two individuals were older than 9–11.5 years (**Table F10**).

The very few bone measurements indicate rather small cattle for the Iron Age (**Table F16**). The remains of cat-

fusion group (age in months)	element	GIB			QID			DLT2			DLT3		
		unfused	in fusion	fused									
A (0–12)	Scapula	1											
	Humerus dist.		1										1
	Radius prox.	1	1										1
	Pelvis (Acetabulum)			1									
B (12–24)	Tibia dist.				1								
	Metacarpal dist.	1											
	Metatarsal dist.												
	Metapodial dist.	2								1			
	Ph1						1		1	3	2	1	
	Ph2			1				1		4			
C (24–30)	Fibula dist.												
	Calcaneus	2						1					
D (30–48)	Humerus prox.												
	Radius dist.	2									1		
	Ulna prox.							2			1		
	Ulna dist.												
	Femur prox.												
	Femur dist.	1											
E (>48)	Tibia prox.	2											
	Vertebrae	3						3			1		

Table F11: Epiphyseal fusion data for domestic pig (n=45) from Iron Age layers by operation. Fusion ages based on Habermehl 1975 and König/Liebich 2001.

333 Bendrey *et al.* 2016, 52. Also observed by the author in Qaladze and environs in autumn 2019.

fusion group (age in months)	element	GIB			QJD			DLT2			DLT3		
		unfused	in fusion	fused									
A (0–12)	Scapula			1									
	Pelvis (Acetabulum)												
B (12–24)	Radius prox.												
	Humerus dist.												
	Ph1						2				1	1	
	Ph2	1		1									
C (24–30)	Tibia dist.										1		
	Metacarpal dist.												1
	Metatarsal dist.			1									
	Metapodial dist.												
D (30–48)	Humerus prox.												
	Radius dist.												
	Ulna prox.												
	Ulna dist.												
	Femur prox.							1					1
	Femur dist.												
	Tibia prox.	1											
Calcaneus													
E (>48)	Vertebrae										2		

Table F12: Epiphyseal fusion data for cattle (n=15) from Iron Age layers by excavation area. Fusion ages based on Habermehl 1975 and König/Liebich 2001.

tle also most likely represent the remains of consumption and food processing. The few older individuals point to the exploitation of these animals for work and secondary products; worn-out individuals were certainly consumed as well.

The majority of working animals were probably herded and maintained outside the settlement core. Most likely, only animals intended for consumption – for the production of cuts of meat or cured meat – circulated within the settlement.

Equid remains are only present in assemblages from undated tertiary contexts (**Tables F5** and **F7**) and include one lower molar from a topsoil layer in Qalat-i Dinka, one fragment of a skull and one first phalanx from a refill. The latter two were collected in DLT3. All the remains were identified as deriving from horses (*Equus caballus*). The absence of equids from Iron Age strata seems quite remarkable at a first glance when one considers that the transport of goods was commonly done with donkeys. But if the meat of equids was not commonly consumed, their carcasses were usually disposed of far outside the settlements.

The fragment of a dog skull was uncovered in a topsoil layer in Gird-i Bazar. There is no evidence for the exploitation of dogs during the Iron Age so far, but the use of herding dogs must be assumed if we suppose that sheep, goats, and cattle were herded in the surrounding countryside. The context of this find, however, cannot be surely connected to the Iron Age period.

F4.2 Wild mammals

Based on the present data, there is no evidence for noteworthy hunting activity (**Table F3**); venison was less important as an additional source of meat. The “intriguing” small number of remains of wild species, especially cervids, was already mentioned by Tina Greenfield³³⁴. Although certainly present in the regional landscape, the remains of red deer (*Cervus elaphus*) are only occasionally found

334 Greenfield 2019, 143.

within the assemblages. This includes one lower molar (DLT₃, Outdoor Area 65) and seven fragments of antlers, which were all found in one fill (DLT₃, Locus:226922:012). All finds originate from Iron Age layers. Four out of these seven antler fragments – mainly fragments of the base and one from the crown or a tine – show dissection marks and most likely represent a raw material for craft production (Fig. F3). The scarce remains do not point to intensive hunting activities, especially since antlers may have been locally collected or may have reached the site as a commodity.



Fig. F3: Fragment of antler with chop marks (DLT₃, collection PPP 226922:012:002). Photo by Anja Prust.

Interpreting the gazelle remains is just as difficult. In total, five specimens of the goitered gazelle (*Gazella subgutturosa*) were identified (Table F3): two metacarpal bones and one talus from layers inside buildings in Gird-i Bazar; one pelvic bone of a juvenile individual from Building L in DLT₂; and one complete rib from Outdoor Area 69 in DLT₃. All the particular layers could have dated back to the Iron Age. Similar to the red deer, there are no elements of high-quality meat portions that point to the consumption of venison.

Further remains of wild mammals represent random finds and allow no conclusions about their exploitation. Besides the remains of red fox (*Vulpes vulpes*), marbled polecat (*Vormela peregusna*), and hare (*Lepus* sp.), a few specimens of mustelids, one partial skeleton of a Tristram's jird (*Meriones tristami*), two specimens of the black rat (*Rattus rattus*), and two partial skeletons of a house mouse (*Mus musculus*) were attested among the osseous remains. A few more specimens of small rodents were not identified to the species level. Fur-bearing animals were probably also hunted. Of note is the partial skeleton of the marbled polecat from a deposit right above the floor in Building L, Room 36 in DLT₂. The scapula of a hare was

found in the same context. The red fox is attested by only one pelvic bone found in a deposit right above the floor of Building S, Room 66 in DLT₃.

F4.3 Birds

Among the few bird remains, domestic chickens clearly dominate (Table F3). In total, 46 specimens – representing three individuals – were identified, including two partial skeletons of very young individuals. All specimens were found in tertiary contexts (topsoil, modern pits) in Gird-i Bazar. They most likely represent modern admixtures in the disturbed contexts, which is corroborated by the remarkable size of these animals.

Three bones of chukar partridge (*Alectoris chukar*) were collected from Iron Age layers in Building K, Rooms 39 and 40 in DLT₂ and represent one individual. It is notable that only the wing fragments are present (one left humerus and one left and right radius). This species is still widely distributed in the area.

Additional wild birds are attested by remains of the greylag goose (*Anser anser*) and the rock dove (*Columba livia*). The former is represented solely by one bone from a secondary context (in Building I, Courtyard 18) and one from the undated topsoil in Gird-i Bazar. The rock dove is attested by one sternum, found in Iron Age layers from Building L, Room 36 in DLT₂. Still today, the keeping and breeding of pigeons is very popular in this region and expresses a centuries-old tradition of dovecote culture. Furthermore, as synanthropic species, pigeons can be easily enticed and kept. Assyrian textual sources regularly mention the consumption of geese, pigeons, and doves in the course of secular and cultic feasts³³⁵. Moreover, they were kept for breeding and for sacrifices³³⁶. Considering the absence of ritual contexts and the presence of mainly lower-value meat cuts in the contexts presented here, the scarcity of these species is not surprising.

F4.4 Amphibians

Two fragments of a frog (family Ranidae) were found in a pit fill in DLT₃ (tertiary context). As these finds most likely end up in archaeological assemblages by chance, they represent intrusions without any relevance to ancient exploitation strategies.

³³⁵ Jancović 2004, 3-11; Gaspa 2012, 99-100.

³³⁶ Jancović 2004, 23.

F4.5 Fish

Despite the immediate proximity to the Lower Zab river, the number of fish remains is extremely low. Only two vertebrae from an unidentified member of the cyprinid family (Cyprinidae) were found. Both specimens were collected from the heavy fraction assemblages and originated in the Iron Age layers (secondary contexts) in Building A, Room 1 in Gird-i Bazar and Building L, Room 36 in DLT2. Unfortunately, a more precise identification to the species level was not possible.

Although the dearth of fish bones may have been partly caused by poor preservation at the site overall, the primary responsibility for this probably lay in local food preferences. For instance, fish bones are also surprisingly scarce in the Neo-Assyrian site of Tušhan (Ziyaret Tepe), located on the Tigris³³⁷. Seemingly, communities existed in the region who did not use this food source due either to their dislike of fish or perhaps to cultural or religious taboos. However, the possibility that fish was processed and consumed elsewhere cannot be ruled out.

F4.6 Molluscs

Referring to the number of identified specimens (NISP) and minimum number of individuals (MNI), molluscs represent the most frequent taxon on site (Table F3). Terrestrial snails clearly dominate while marine species occur only exceptionally. The higher species diversity in Gird-i Bazar is based on assemblages collected from the light fraction which are only available for this operation.

The most frequent species is *Helix salomonica*³³⁸, the easternmost species of the genus *Helix*³³⁹. The shells were found in almost every operation and context (buildings, rooms, courtyards, pits, graves) (Figs. F4 and F5). In total, at least 160 individuals were documented, excluding some recent shells that have been collected for comparative studies during the excavation campaign in 2015. *Helix salomonica* is reported from several archaeological sites in the Zagros region³⁴⁰, and frequently these shells are linked with human activity. The circumstances of their discovery and the specimens themselves yield evidence for whether a shell concentration was formed naturally or by anthropogenic impact. As Taylor and Bell state, while a wide “range of growth stages and species” and the “ab-



Fig. F4: *Helix cf. salomonica* (Naegele 1899), state of preservation (DLT3, collection PPP 226922:016:006). Photo by Anja Prust.

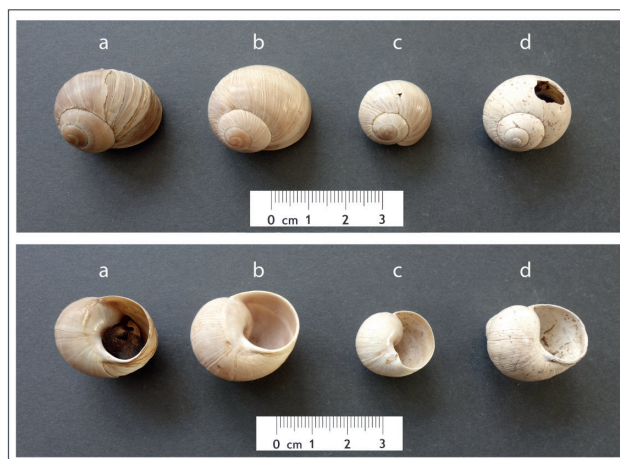


Fig. F5: *Helix cf. salomonica* (Naegele 1899); a: GIB, modern individual with epiphragm, collected during 2015 field campaign for comparison; b: GIB, secondary context (collection PPP 271929:009:003); c: GIB, tertiary context (collection PPP 271929:046:002); d: DLT3, primary context (collection PPP 226922:047:021). Photos by Anja Prust.

sence of associated anthropogenic artefacts” point to naturally-occurring deposits, the presence of “generally fully grown” specimens and of one or only a few particular species, occasionally modified or “heat-affected” and associated with cultural material in “specific contexts” suggest anthropogenic impact and consumption refuse³⁴¹.

With regard to the excavation areas in the Dinka Settlement Complex, there is no conspicuous quantity or concentration that points to shell middens. Nevertheless, the majority of *Helix salomonica* remains come from adult

337 Greenfield *et al.* 2013.

338 Naegele 1899.

339 Neubert 2014, 172.

340 Braidwood *et al.* 1983; Shillito 2013; Iversen 2015; Frahm/Tryon 2018.

341 Taylor/Bell 2017, 197.

individuals. Four individuals are affected by fire³⁴², but this may have been the result of taphonomic processes. Finally, while we cannot rule out that *Helix salomonica* could have been part of the local diet, they may also have got into the assemblages randomly since “large species often hibernate in colonies, often adhering to each other to create a seal to prevent drying-out and freezing”³⁴³.

Several specimens of small terrestrial land snails – species of the family Hygromiidae, Cochlicopidae, Chondrinidae, Zonitidae and Cecilioididae – were collected from the light fraction at Gird-i Bazar. The large family of Hygromiidae (leaf snails) is sometimes treated as a subfamily of Helicidae. A few specimens could be identified, such as *Monacha* sp., snails inhabiting humid, but also xerothermic habitats. The small shells of members of the Cochlicopidae (pillar snails) family are also widely distributed and often found in humid habitats. Furthermore, small shells of the Chondrinidae (snaggletooth snails), Zonitidae (trueglass snails) and Cecilioididae (blind snail/blind awl snail) families were collected only from the light fraction. The latter family is represented in particular by very small, burrowing, subterranean species that can be frequently found in the soil. All of the small terrestrial land snails are to be interpreted as intrusive.

The situation is different with two cowrie shells (Cypraeidae) found in the Iron Age layers of Gird-i Bazar (see §E6, Table E6.1, nos. 1-2), one in the Sasanian-period Grave 72 at Gird-i Bazar³⁴⁴, and ten from Qalat-i Dinka (QID) (§E6, Table E6.1, nos. 3-5 and §E1.3.8, no. 93) since they represent marine species. An identification to the species level was not possible, but the shell's size and shape is similar to *Monetaria annulus* (ring cowrie). The dorsum of both shells is missing, and the edges are regular. Most likely, the specimens were artificially modified. Worked cowrie shells are documented from numerous archaeological sites and various periods as they represent the most popular shell beads³⁴⁵. They were used as adornment, in ritual and cultic practices, and in gaming.

Unfortunately, the circumstances of the discovery of the Dinka Settlement Complex finds do not allow us any conclusions about their use. Further modified specimens, that have been already separately documented as artefacts (see §E6) were collected from fills in Qalat-i Dinka.

342 These include two partially carbonised shells from floor deposits in Gird-i Bazar (Building G, Room 16 and Building F, Room 22), one completely carbonised shell from a filling in Gird-i Bazar (Building F, Room 28) and one completely calcinated shell from Qalat-i Dinka (Grave 109).

343 Allen 2017, 21.

344 Downey 2018, 180.

345 Reese 1991; Golani 2014.

Quantities that indicate an economic importance and a local bead production are absent so far. These shells most likely reached the site in the form of finished goods, e.g. as elements of clothing or decorated objects.

F4.7 Crustaceans

One fragment of a pleopod from a freshwater crab (*Potamon* sp.) was collected during the flotation of soil samples from a floor deposit in Gird-i Bazar (Alley 4). It can possibly be identified as either *Potamon magnum* or *Potamon persicum*, both native species. Whether freshwater crabs were consumed or exploited for other purposes is unclear. A similar find has been reported from the Neolithic hunter-gatherer site M'lefaat near Mosul³⁴⁶ and was interpreted as “evidence that the river was exploited by the people of M'lefaat”³⁴⁷.

Considering the scarcity of remains of fish and wild mammals in the Dinka Settlement Complex assemblages, the exploitation of wildlife was rather negligible in general. Therefore, the fragment of a freshwater crab most likely also ended up in the assemblage accidentally.

F5. Modifications

8.8% (NSP 929) of the total material shows modifications, including 5.9% (NSP 621) with traces of fire, 2.2% (NSP 232) with root etching, 0.4% (NSP 45) with marks of butchery, dissection and/or food processing, 0.2% (NSP 22) with discolourations caused by chemical processes, and 0.09% (NSP 9) with gnaw marks from carnivores or rodents.

Remains that were exposed to fire are documented by the completely burnt (NSP 196) and calcined (NSP 384) specimens; a few specimens (NSP 41) are completely burnt and additionally partially calcined. There is no accumulation or context with higher frequencies of burnt remains. Even from the fill of the Chalcolithic kiln in DLT3 the proportion of specimens exposed to fire is less than 5%. The higher percentages of burnt remains from Building I, Room 46 in Gird-i Bazar (16.5%) and Building L, Rooms 35 and 36 in DLT3 (12.5%) may be the result of a specific function for those rooms (e.g., the presumed pottery workshop in Gird-i Bazar) or specific events and taphonomic processes (burnt horizon). However, it is most likely based on the different sample size and state of preservation.

346 Turnbull 1983, 693–695.

347 Turnbull 1983, 695.

Marks of dissection, butchery and food processing are documented on 45 specimens (**Table F13**): 11 specimens show chop marks, 32 have cut marks, and two specimens show a combination of both. Chop marks are predominantly found on vertebrae and ribs of cattle and long bones of pigs, indicating the dissection of the animal's body and preparation of cuts of meat. Cut marks were mainly documented on the long bones of pigs and large and small ruminants – including one pelvic bone of a goitered gazelle. The generally fine incision marks probably result from defleshing and consumption.

The discolouration of some bones from the Dinka Settlement Complex assemblages is undoubtedly the result of non-anthropogenic processes. Differences in the state of preservation between particular operations have already been mentioned. The discolouration of finds from DLT₃ is also part of this phenomenon. 19 specimens, from primary and tertiary contexts, show a selective black discolouration, most probably as a result of Manganese precipitation. Moreover, two specimens from Gird-i Bazar are discoloured dark brown and one long bone of a large mammal from DLT₃ is discoloured grey-brown. This may also be the result of its deposition in ash-layers or of post-depositional chemical processes in the soil.

Gnaw marks by animals may provide information on disposal strategies, e.g. the dumping of waste in open areas where it is easily accessible to carnivores or scavenging animals. Six specimens from Gird-i Bazar with gnaw marks from carnivores were collected from the topsoil and from a later fill; one specimen was found in a refill in DLT₃. These finds are not linked with the initial Iron Age occupation, but with later, undated events at the site. Gnaw marks from rodents were observed on one specimen each from an Iron Age fill in DLT₂, an Iron Age floor deposit in DLT₃ and a later pit fill in DLT₃.

F6. Pathologies

Pathologies were found only on three specimens. So, the three right molars from a cattle's upper jaw (Gird-i Bazar, fill of the well, tertiary context) and the lower, right third molar of a sheep/goat (Gird-i Bazar, floor deposits) show irregular dental attrition. The first phalanx of a goat (DLT₂, pit fills, secondary context) has a slight superficial exostosis at the base of the deep flexor tendon, probably the result of an irritation, inflammation, or trauma. None of these pathologies is related to an intensive exploitation of animals as work animals.

F7. Architectural contexts

In her zooarchaeological analysis of the faunal remains from Gird-i Bazar, Tina Greenfield provided preliminary statistics on the spatial distribution of faunal data according to architectural features “in order to establish patterns of domestic, utilitarian, industrial or ritual behaviour³⁴⁸.” These statistics are influenced by various parameters, such as the size of the excavated area, the volumes of fills and layers, the degree of fragmentation of the faunal material, the sampling strategy (flotation samples available or not) and the sample size in general. Due to these influences, an intra-site comparison is not carried out here. Instead, peculiarities of some archaeological features will be briefly discussed.

F7.1 Fill of large well in Gird-i Bazar

The assemblage originates from the fills of the deep well excavated in Outdoor Area 7 at Gird-i Bazar, Locus:271929:039 and Locus:271929:042³⁴⁹. In total, 352 specimens were collected, of which 101 specimens were identified to a species level (**Table F14**). Of note is the presence of only domestic mammals. For all taxa (cattle, sheep, goat, pig), mainly fragments of mandibles, single teeth, and vertebrae were found, while long bones are clearly underrepresented. For all bovids, horn cores were documented as well. Traces of dissection were observed on three specimens only (one vertebra of a cow and a humerus and a metacarpal bone of pig). This assemblage is dominated by refuse typical of butchery and meat processing (skull, vertebrae and lower fore- and hindlimbs). The small number of remains, the lack of partial and complete skeletons (disposal of deceased animals) as well as the lack of raw material and refuse from bone craft production also indicate that the well was not deliberately used as a waste pit. Further evaluation integrating all archaeological finds from the fill may support this hypothesis.

F7.2 Kiln fills in Gird-i Bazar and DLT₃

The fills of an Iron Age kiln in Gird-i Bazar (Locus:269929:020, Locus:269929:026 and Locus:269929:027) and a Chalcolithic kiln in DLT₃ (Locus:225922:049) were both categorised as secondary contexts³⁵⁰. Thus, primary deposited

³⁴⁸ Greenfield 2019, 144.

³⁴⁹ Rohde 2018.

³⁵⁰ Iron Age kiln: Stone 2016, Amicone 2017b; Chalcolithic kiln: Palmisano 2019 and **Chapter I**.

Taxon	Element (NSP)	Modification	Operation	Context
Cattle	Mandibula (1)	cut mark	DLT ₃	Secondary Context
Cattle	Humerus (1)	cut mark	DLT ₃	Tertiary Context
Cattle	Ulna (1)	chop mark	GIB	Secondary Context
Cattle	Costa (2)	cut mark	DLT ₃	Tertiary Context
Cattle	Costa (1)	chop mark	DLT ₃	Tertiary Context
Cattle	Costa (1)	chop & cut mark	DLT ₃	Tertiary Context
Cattle	Vertebra (1)	chop mark	GIB	Primary Context
Cattle	Vertebra (1)	chop mark	GIB	Tertiary Context
Cattle	Femur (1)	cut mark	DLT ₃	Secondary Context
Cattle	Tibia (1)	chop mark	GiB	Tertiary Context
Cattle	Patella (1)	chop mark	DLT ₂	Secondary Context
Cattle	Talus (1)	cut mark	DLT ₃	Tertiary Context
Cattle	Metatarsus (1)	cut mark	GIB	Primary Context
Goat	Talus (1)	cut mark	DLT ₂	Primary Context
Sheep/Goat	Radius (1)	cut mark	GIB	Secondary Context
Sheep/Goat	Costa (1)	cut mark	GIB	Tertiary Context
Sheep/Goat	Femur (2)	cut mark	GIB	Secondary Context
Sheep/Goat	Tibia (1)	cut mark	DLT ₃	Secondary Context
Sheep/Goat	Metapodium (1)	cut mark	DLT ₂	Primary Context
Domestic pig	Mandibula (1)	chop mark	GIB	Tertiary Context
Domestic pig	Humerus (1)	cut mark	GIB	Primary Context
Domestic pig	Humerus (1)	cut mark	GIB	Tertiary Context
Domestic pig	Metacarpus (1)	chop & cut mark	GIB	Primary Context
Domestic pig	Metacarpus (1)	cut mark	GIB	Tertiary Context
Domestic pig	Metacarpus (1)	cut mark	DLT ₃	Secondary Context
Domestic pig	Vertebra (1)	cut mark	DLT ₃	Tertiary Context
Domestic pig	Femur (1)	cut mark	QiD	Secondary Context
Domestic pig	Femur (1)	cut mark	DLT ₂	Primary Context
Domestic pig	Femur (1)	cut mark	DLT ₂	Secondary Context
Domestic pig	Femur (2)	chop mark	DLT ₃	Tertiary Context
Domestic pig	Calcaneus (1)	cut mark	DLT ₃	Tertiary Context
Domestic pig	Metatarsus (1)	cut mark	DLT ₂	Secondary Context
Medium-sized mammal	long bone (1)	chop mark	GIB	Secondary Context
Medium-sized mammal	long bone (2)	cut mark	GIB	Secondary Context
Medium-sized mammal	long bone (1)	cut mark	DLT ₂	Primary Context
Medium-sized mammal	long bone (1)	cut mark	DLT ₃	Tertiary Context
Large mammal	indet. (1)	cut mark	DLT ₃	Tertiary Context
Large mammal	long bone (1)	cut mark	DLT ₂	Primary Context
Large mammal	long bone (1)	chop mark	DLT ₃	Primary Context
Large mammal	long bone (2)	cut mark	DLT ₃	Tertiary Context

Table F13: Marks of dismembering/butchery/food processing (n=45).

	GIB large well	
	NSP [MNI]	weight (g)
I. Domestic mammals		
<i>Bos taurus</i>	56	916.6
<i>Ovis aries/Capra hircus</i>	17	73.5
<i>Capra hircus</i>	2	11.9
<i>Ovis aries</i>	2	26.9
<i>Sus domesticus</i>	24	173.2
NISP total	101	
VIII. Indet.		
Large mammal	2	11.2
Medium-sized mammal	9	22.8
Mammalia indet.	240	66.4
Aves indet.		
Total	352	1,302.5g

Table F14: Gird-i Bazar, fill of the well. List of faunal remains.

burnt material was not expected. In both assemblages, only domestic mammals are present (**Table F15**). There are no distinctive features in the skeletal element distribution such as complete or partial skeletons and no elements particularly dominate. In the DLT₃ assemblage, nine specimens were affected by fire (charred bones and completely carbonised bones), while from the DLT₃ assemblage only one fragmented humerus of a pig was completely calcined.

Based on this data, there seems to be no link between the functional aspect of the kilns and any specific exploitation of animal remains, e.g. as fuel, or in the form of remains of roasted meat portions. Rather, the finds of these features are the result of refuse deposits within the natural site formation processes.

F7.3 Buildings and rooms of the Iron Age period

Despite variations in the sample size across the Dinka Settlement Complex, the assemblages from buildings and related rooms show strong similarities in species distribution and skeletal element representation. Patterns indicating particular functions and behaviors are not identifiable. The largest collection of faunal remains from buildings was collected in DLT₂, Building L. Based on the size of the trench and the amount of soil that has been moved, the

	GIB Iron Age kiln in Outdoor Area 8		DLT ₃ Chalcolithic kiln	
	NSP [MNI]	weight (g)	NSP [MNI]	weight (g)
I. Domestic mammals				
<i>Bos taurus</i>	16	306.6	2	13.1
<i>Ovis aries/Capra hircus</i>	2	21.2	2	9.9
<i>Capra hircus</i>			1	2.7
<i>Ovis aries</i>			1	7.2
<i>Sus domesticus</i>	5	65.0	3	11.9
NISP total	23		9	
VIII. Indet.				
Large mammal	4	12.9	5	21.5
Medium-sized mammal	1	2.3	12	21.0
Mammalia indet.	64	28.6	73	19.3
Total	92	436.6g	99	106.6g

Table F15: Gird-i Bazar and Dinka Lower Town 3, kiln fills. List of faunal remains.

diversity of animal species is also quite large. Here too, no specific function and use patterns are detectable so far. Further spatial and functional analyses are in progress³⁵¹ and may provide more detailed information.

F7.4 Fills of the Sasanian period graves at Gird-i Bazar

Assemblages from grave contexts were either collected by “*in situ* recovery” (Graves 4, 8, 20, 21, 30, 72 and 85) or from the heavy fraction during flotation (Graves 3, 9, 88, 92 and 109). Heavily fragmented specimens of mammals dominate, followed by fragmented finds of terrestrial gastropods. Partial skeletons (one black rat and one Tristram’s jird) were found in fills from the Sasanian Grave 4 at Gird-i Bazar and should be interpreted as later intrusions. Consequently, the intentional deposit and use of animals in the course of funeral rites is not attested so far at Gird-i Bazar.

³⁵¹ Undertaken by Jana Richter, Westfälische Wilhelms-Universität Münster, as part of her PhD thesis.

F8. Animal exploitation in the Dinka Settlement Complex

Considering the size of the various excavation areas, the total number of faunal remains is conspicuously small. The excavators have repeatedly reported their impression of a “tidy settlement”³⁵². This phenomenon can also be seen from the zooarchaeological data since the majority of finds only represent refuse of consumption and probable meat processing.

Domestic mammals dominate, while wild species – mammals, birds, and fish – were of little importance as a source of food. Sheep, goat, cattle, and pig are the most frequent taxa. All of these species were exploited for food. The scarcity of typical butchery waste is noteworthy. Obviously, the slaughter and processing of meat mainly took place elsewhere, and cuts of meat were brought into the respective spaces³⁵³.

Because elements of lower-value meat portions were most frequently found within the assemblages, an intentional distribution of meat cuts must be presumed. Furthermore, specific functions of the buildings and outdoor areas may be a reason for this unusual selection. So, for example, the consumption of high-value meat cuts was more likely to have taken place in residential quarters than in workshops or public, administrative buildings. Because Gird-i Bazar and DLT2 might have been, respectively, a pottery workshop and a public/administrative structure, the function of these two areas may explain the overall high frequency of lower-value meat portions within the Dinka Settlement Complex. Social differences also come into question. To test these hypotheses, decidedly more material and detailed spatial and functional analyses of the architectural features are necessary.

The exploitation of secondary products (milk, wool, hair etc.) is very likely, but cannot be proven with certainty because the sample size for culling profiles is too low. The exploitation of cattle as work animals in agriculture and for transport is likely, based on the presence of older individuals. Sheep, goats, and cattle were herded outside the settlement as can still be seen today. It is conceivable that pigs were kept within the settlement, but the surrounding landscape offered pasture feeding and wood pasture as well.

Finally, some summary comments on activity zones and patterns of behaviour are necessary. As mentioned in the introduction, the first zooarchaeological investigation by Tina Greenfield focused on “patterns of behaviour in relation to food distribution, consumption and disposal” and “clear differences across the site, within and between spaces, buildings and rooms”³⁵⁴. She provided a detailed analysis of species distribution and consumption patterns within the architectural features in Gird-i Bazar and recognised discard areas and variations in body portion preferences between the buildings. By integrating this new data, some of the patterns observed can be confirmed: the exploitation of domestic animals as a major source of food, the presence of prepared cuts of meat while butchering took place elsewhere, and the presence of mainly lower-value portions of meat.

Statements referring to differences between spaces, buildings and rooms are problematic due to the small sample sizes. The trends regarding frequencies of faunal remains, taxonomic diversity and body part frequencies within buildings and in outside areas in Gird-i Bazar, that were noted in the first report³⁵⁵, could not be confirmed with the new material and will continue to vary with future finds. The zooarchaeological data from Qalat-i Dinka and DLT2 and DLT3 also show no marked differences in species frequency, skeletal element distribution, and consequently, animal exploitation strategies compared to Gird-i Bazar. Even the comparison between Iron Age assemblages and finds from later periods show few differences.

These apparently uniform patterns across the various excavation areas raise further questions: Where are the production sites and places for butchery? Which livestock species were also kept as working animals (e.g. draught animals, pack animals, animals for transport, herding dogs)? To what extent have secondary products been used? What happened to the higher-value meat portions? Were livestock production and the distribution of meat and animal products centralised? Were the locally available resources, such as game and fish, really so little exploited, or should we assume that their respective remains are simply located elsewhere? The current data allows at least one reliable statement about the local animal economy: it was a sedentary community that practiced livestock farming in a tradition that persisted for centuries.

The continuation of archaeological and zooarchaeological research will provide further data from a variety of contexts and features. Investigations of spatial distribu-

352 Thus Karen Radner, F. Janoscha Kreppner, and Andrea Squitieri, personal communication.

353 As also reported by Tina Greenfield in her preliminary conclusions (Greenfield 2019, 149). This observation also fits with the scarcity of grinding tools and other tools for food-processing (Squitieri 2018, 169).

354 Greenfield 2019, 149.

355 Greenfield 2019, 145; Table J8.

tions and activity zones are already in progress and may provide basic information necessary for a more detailed intra-site comparison and for testing hypotheses on strategies in animal exploitation in the Dinka Settlement Complex.

Bone measurements of caprines (sheep, goat) found in Iron Age layers				
Scapula	DLT_{3o}			
GLP	27.1			
LG	22.0			
BG	18.0			
SLC	17.6			
Radius	GIB_o			
Bp	28.5			
BFp	27.5			
SD	15.9			
Femur	DLT₂			
DC	19.4			
Tibia	DLT₂			
Bd	25.0			
Calcaneus	DLT_{2o}	DLT_{3o}		
GL		59.0		
GB	20.7	24.5		
Talus	DLT_{2c}	DLT_{3o}	DLT_{3c}	DLT₃
GLI	27.9	28.9	27.7	29.9
GLm	26.4			
DI	14.6	16.2	14.6	16.3
Bd	18.2	20.1		
Ph₁	DLT_{3c}	DLT₃	DLT₃	DLT₃
GL			29.9	
Bp	12.9	12.8	8.8	
SD		10.0	7.2	
Bd			8.6	11.6
Ph₃	GIB	DLT_{2o}		
DLS		26.6		
Ld		19.2		
MBS	5.2	5.0		

Bone measurements of cattle found in Iron Age layers.			
Scapula	GIB		
LG	50.4		
BG	41.5		
Os carpale II+III	DLT₂		
GB	29.2		
GD	24.4		
MT III+IV	GIB		
SD	c. 24.4		
Bd	48.0		
Ph₂	GIB	DLT₂	
GL	37.2	33.8	
Bp	26.8	23.0	
SD	22.6	18.8	
Bd	21.8	17.7	
Ph₃	GIB		
BF	19.7		

Table F16: Bone measurements of caprines (sheep, goat) found in Iron Age layers (o = *Ovis aries*; c = *Capra hircus*; no abbr. = *Ovis/ Capra*) and of cattle found in Iron Age layers.

G. Phytoliths from the Dinka Settlement Complex, 2015-2019: first results

Fatemeh Ghaheri

Phytoliths form in living plant tissues as silica, and are deposited in the soil after the death of the plant where they remain well-preserved in harsh conditions. Water carries silica from the soil into the plant through the roots, and it is then deposited within the epidermal tissue to form these microscopic structures³⁵⁶. Phytolith data help us answer paleoenvironmental and economic questions about agricultural expansion and strategies, environmental and micro-environmental settings, economy and the growth of complex societies, spatial distribution of various activities, irrigation farming, and types of agriculture. These are the types of issues that the phytolith analysis in the Peshdar Plain Project aims to investigate and elucidate. Especially considering the perfect environmental conditions of the Near East for forming and preserving this type of data, implementing it in our studies paints a picture of past agricultural and non-agricultural activities that took place, and provides information about activity areas and the general environment, complementing the information found through other archaeobotanical methods. This method is not widely used in ancient Near Eastern historical-period archaeology, unlike in many other parts of the world where it is employed for a variety of different time periods.

Through the study of phytoliths we can investigate the social development of the Dinka Settlement Complex (hereafter: DSC) and the impact that the Neo-Assyrian Empire had on landscape and agricultural strategies when the DSC was incorporated into the Empire in the late 9th century BC³⁵⁷. To achieve these aims, plant types are evaluated and reconstructed through systematic sediment sample collection and phytolith analyses, in order to understand and answer the following issues: plant exploitation, agricultural strategies, the use of micro-environments for agriculture, pastoral strategies, the scale of crop use, social classes, accessibility and distribution of crop resources, crop and food processing and the use of

building space, environments in which these plants were exploited, and what types of activities and activity areas can be drawn from them.

G1. On-site sampling strategy

The sampling strategy for this study was chosen in order to extract phytoliths that are suitable for investigating and answering the issues discussed above. In general, in phytolith analysis, the sampling strategies employed depend strongly on the research questions and problems under investigation. Based on the type of questions and problems to be evaluated in this research, the samples were collected from a variety of informative areas and layers within the site contexts and occupation units. These contexts included pits, houses, storage areas, alleys, outdoor areas, yards, and interior and exterior surfaces. These all represent different activities, environments of plant exploitation and cultivation, distribution, and level of access to resources and landscape.

Overall, 500 samples were collected from the Dinka Settlement Complex (campaigns 2015 to 2019), of which 150-200 have been selected for complete analysis. This chapter will discuss the 11 samples from Gird-i Bazar (=GIB) and DLT2 whose analysis has been completed (**Table G1**). The phytolith samples were taken using clean tools to avoid contamination; they were placed in plastic bags and, if moist, they were dried out in a clean, dust-free room with no air currents. Samples were taken from contexts with the potential for yielding a high number of phytoliths (e.g., fills of ovens, rubbish pits, burnt layers). In addition, samples were also taken from floors of rooms, alleys, and courtyards. Following the Peshdar Plain Project sampling protocol, floors were gridded with a 1 × 1 m square grid; from each grid square an average sample was taken by scraping the surface of each grid square. This system guarantees better spatial control over samples from floors. The location of every sample was measured with a dGPS, while for average samples the dGPS point was taken in the centre of each grid square.

³⁵⁶ Rosen 1999.

³⁵⁷ Radner 2016.

ID	Sample registration no.	Operation	Provenance	Context	Most occurring phytoliths
1	PPP 268931:022:002	GIB	Building D Courtyard 11	Floor deposit	Cyperaceae
2	PPP 268931:022:004	GIB	Building D Courtyard 11	Floor deposit	Rondel short cell; Cyperaceae
3	PPP 235934:012:007	DLT2	Alley 38	Floor deposit	Rondel short cell; Cyperaceae
4	PPP 235934:003:009	DLT2	Building L Room 35	Fill of storage vessel Locus:235934:037	Rondel short cell; Cyperaceae
5	PPP 235934:014:007	DLT2	Building L Room 35	Fill of storage vessel Locus:235934:038	Bulliforms
6	PPP 235934:018:006	DLT2	Building L Room 35	Floor deposit	Rondel short cell; Cyperaceae; Bulliforms
7	PPP 235934:019:011	DLT2	Building L Room 36	Floor deposit	Rondel short cell
8	PPP 236934:019:032	DLT2	Building K Room 39	Floor deposit	Rondel short cell; Cyperaceae; Bulliforms
9	PPP 236934:019:004	DLT2	Building K Room 39	Floor deposit	Rondel short cell; Cyperaceae; Bulliforms
10	PPP 236934:019:019	DLT2	Building K Room 39	Floor deposit	Rondel short cell; Cyperaceae
11	PPP 236934:027:014	DLT2	Building K Room 40	Floor deposit	Bulliforms

Table G1: List of phytolith samples discussed in this chapter. Prepared by Fatemeh Ghaheiri.

G2. Methodology for extracting phytoliths

The laboratory method for extracting phytoliths from the samples follows a protocol established by Prof. Arlene Rosen (University of Texas at Austin). The steps are: the sample is sieved in a 0.25 mm mesh to remove the coarse fractions, and 800 mg of the sieved sample is weighed for processing. It is then treated with 30 ml of 10% HCL, which removes the carbonate from the samples. In the next step, a deflocculant, such as Sodium pyrophosphate or Sodium hexametaphosphate (lab Calgon and distilled water), is added to allow the clay to start detaching from the sample, making its removal easier. The sample sits for one hour in an 8 cm column of water until the clay starts to suspend and any particles larger than 5 micrometers settle. After one hour, the clay is poured out, and this step will be repeated until the water becomes clear and the clay is completely removed. After this, the organic matter is removed by dry ashing at 500°C for two hours in a muffle furnace. A heavy density solution of SPT (Sodium

polytungstate and distilled water) calibrated to 2.3 specific gravity is then used to separate the phytolith and remove the remaining quarts and heavy minerals. The suspended phytolith is then transferred to a centrifuge tube, washed, centrifuged, dried, and mounted on a microscope slide using Entellan. The recovered phytoliths are then observed under the microscope at a 400× magnification and classified in comparison to the ICPN (International Code for Phytolith Nomenclature) and modern examples in the final step, which consists of counting. 200 to 300 single cells and 50 multi-cells (or as many as possible if there are fewer multi-cells) are counted on each slide³⁵⁸.

³⁵⁸ Rosen 1999.

G3. Preliminary results

G3.1 Environments of plants

The potential of phytoliths for reconstructing past environments lies in their morphologies, which vary according to types of environments and climate conditions. The rondel phytolith morphotype (indicative of pooid grass subfamilies) forms in C₃ grasses found in temperate and cooler climatic conditions, where they require more moisture. Cyperaceae (sedges) and fan-shaped bulliform (reed) phytolith morphotypes represent marshy environments where watery conditions are preferred³⁵⁹. In the phytolith assemblages from Gird-i Bazar (=GIB) and DLT₂ (**Table G1**), high ratios of rondel short cells (SC for short) can be observed in samples 2, 3, 4, 6, 7, 8, 9, 10. Cyperaceae are found in samples 1, 2, 3, 4, 6, 8, 9, 10 and Bulliforms in samples 5, 6, 8, 9, 11. This suggests that the environments where plant exploitation took place may have been marshy and wet, with a cool, temperate climate. The other type of phytoliths that dominate all of our samples are psilate long cells. Psilate long cells indicate stems, and they can be found where sedges and grasses grow. However, they are only of limited help to us for identifying plants and they do not reveal much about the environment. Based on this pattern, it is possible to suggest that the inhabitants of the site cultivated marshy plants in the margins of the fields and/or collected them from the surrounding areas. The likelihood that plants were imported to the site will be considered by further research.

G3.2 Pastoral activities

Phytoliths such as sedge cones, Cyperaceae, and dicots can be found in animal dung, especially depending on the specific locations and contexts where the samples are collected. An abundance of dicots and sedges (Cyperaceae) in the phytolith assemblages in the non-elite areas, particularly when found in outdoor areas and alleys, can indicate their use for livestock fodder. Cyperaceae, which could have been gathered and cultivated in the marginal lands and the woodlands of the hills and mountains, may also have been used for human consumption. Samples 1 and 2 from Courtyard 11 at Gird-i Bazar show a high concentration of grasses with a peak in sedges. Abundant sedges in these samples suggest the possible use of this marginal plant for livestock and non-elite consumption. Additionally, the abundant dicots in these samples sup-

port the presence of livestock on the site. Sample 3 from Alley 38 at DLT₂ has a high percentage of sedge cones and Cyperaceae, supporting the presence of pastoral activities among the occupants of the site. These findings can also indicate where animals were kept and fed, which in turn helps to interpret how indoor and outdoor spaces were used. In order to support these suggestions more strongly, more samples are currently under study.

G3.3 Wheat cultivation

Wheats that are cultivated in irrigated fields produce more multicell phytolith aggregates in comparison to rainfed wheat cultivation³⁶⁰. Preliminary results from the botanical remains of the DSC indicate the presence of wheat³⁶¹. The samples discussed in this chapter were characterised by the absence of wheat phytoliths; one possibility is that the wheat was cultivated with rainwater only, which is now, and has been, one of the common agricultural practices in the region. However, this conclusion is based on the restricted number of samples analysed in this chapter; future analysis conducted on a larger number of samples may change this scenario.

G3.4 Crop processing

The lack or presence of inflorescence phytoliths (shown by dendritic LC) inside, around, and in between buildings can indicate where crop processing activities took place. Due to the small sample size discussed in this chapter, it is not currently possible to determine the location and stages of crop processing; this will be better understood after future analysis.

G3.5 Activity areas, architectural evaluation and plant consumption

The interpretation and evaluation of phytolith distribution patterns across the DSC can provide information about the use of different spaces and the locations of activity areas. Since phytoliths indicate plant parts, they can be used to analyse building function and types of activities that took place in specific parts and locations of the site, including differentiating between areas where grain-processing was located, or where basketry or matting were

359 Ramsey/Rosen 2016.

360 Rosen/Weiner 1994.

361 Rosenzweig apud Greenfield 2017, 173.

present. For instance, remnants of plants which represent basketry can lead us to the conclusion that the space was used for some type of storage. Matted floors may indicate sleeping areas and residential space³⁶². Moreover, we can also analyse possible construction materials used in the buildings for roofing, flooring, and walls.

According to the current phytolith data, samples 5, 6, 9, and 10 show a high presence of sedges. Because these samples come from DLT2 which has been interpreted as a complex of buildings where storage facilities were also present, these results suggest the use of baskets, possibly for storage, and floor matting. A concentration of fan-shaped bulliforms, another indication of reeds, in samples 6, 8, 9, and 11 from DLT2 suggests that reeds were used as a construction material. To better interpret these preliminary data more samples are being studied.

G4. Preliminary conclusion and future research

So far, the samples studied have provided the general idea that the environments where plants were being cultivated and collected were wet and marshy. The data provides some patterns indicating that pastoral activities took place on the site. In addition, we have yielded some information about the architectural materials, and the presence of basketry and floor matting. However, to provide more complete answers to the problems proposed at the beginning of this section, more samples from among the informative rich contexts have been selected and are currently being studied in the laboratory. The results will be available in the near future.

³⁶² Rosen 1999.

H. Archaeobotanical remains from the Dinka Settlement Complex, 2015-2018: preliminary results

Melissa S. Rosenzweig & Anne Grasse

This report discusses the results of analysis conducted on 32 archaeobotanical samples collected from four different areas of the Lower Town of the Dinka Settlement Complex (hereafter: Dinka Lower Town): Gird-i Bazar eastern area, Gird-i Bazar western area, DLT₂, and DLT₃ (Fig. H1). Altogether, the data from this assemblage begin to provide insight into the plant and land use practices of the residents of the Dinka Lower Town, and offer additional information on the intra- and extra-mural activities within each of these areas. Preliminarily, the data demonstrate that the residents of the Lower Town grew and relied on a typical Near Eastern crop package of cereals and pulses supplemented by grapes, figs, and millet. Based on the ecologies of the domesticated and non-domesticated species recovered, the inhabitants of the Dinka Lower Town brought the Bora Plain under cultivation and utilised the steppe foothills and forested slopes of the Zagros Mountains, which would have been ideal landscapes for activities like livestock grazing, wild plant gathering, and wood collection. The spatial analysis suggests that occupants of the Dinka Lower Town stored, prepared, and ate crops in indoor rooms and reserved open, outdoor areas for crop processing, while sample-specific information opens up the possibility of mixed-cropping and wine-pressing practices at the settlement.

H1. Methods

In the field, excavators took a minimum 20-litre, bulk soil sample from secondary contexts, and collected 100% of the soil from primary contexts and features. Floor deposits were gridded into 1 × 1 m squares and samples were taken from each. Samples were then floated on-site in a high-capacity (300 litre), electric-powered flotation machine with settling tank designed for the Peshdar Plain Project.³⁶³ Light fraction remains were captured in a fine-weave (<1 mm²) mesh bag designed by Dr. Tina Greenfield

and dried on a clothesline set up in the shade of the Gird-i Bazar chicken farm. The authors would like to thank all the archaeologists and local workers who steadfastly collected and processed these samples over five years of excavation, and Karen Radner for investing, from the beginning, in large-scale archaeobotanical sampling at the site.

In the lab, samples were separated by 2 mm, 1 mm, and 500 µm sieves, and the size-graded plant remains were sorted and identified using a Leica stereoscopic microscope with 35x magnification. Taxa were identified to species when possible; otherwise, to genus or family. Taxa identified to possible genus or species were designated by “*cf.*” before the taxon name. The 32 samples selected for this analysis were targeted because of their secure primary context designations and promise of archaeobotanical preservation. Importantly, in this analysis, only the 2 mm and 1 mm size grades were analysed. Without data from the <1 mm fraction, this analysis skews toward an emphasis on larger, domesticated seeds (i.e. crops) and most likely underrepresents smaller, non-domesticated seeds (i.e. wild plants). Therefore, the discussions of plant diversity and ecology to follow should be considered preliminary and subject to change once the <1 mm remains have been sorted and integrated into the analysis.

Upon identification, botanical remains were recorded and tabulated using absolute counts. Any caryopsis (i.e. seed) or plant part received a value of 1. Halves of pulses (i.e. one cotyledon) were scored as 0.50. Fragments of grape (*Vitis vinifera*) were given a value of 0.25 each. Fragments of bedstraw (*Galium* sp.) were counted as 0.50 each. Wood charcoal fragments greater than 1 mm were weighed to 1/1000th of a gram.

H2. Assemblage composition

Table H1 provides details on the 32 samples selected for analysis. Fourteen samples come from Gird-i Bazar West, all derived from floor contexts with the exception of Sample 3, which was collected from a *tannur*, or clay bread oven, in Courtyard 21. Thirteen samples come from Gird-i

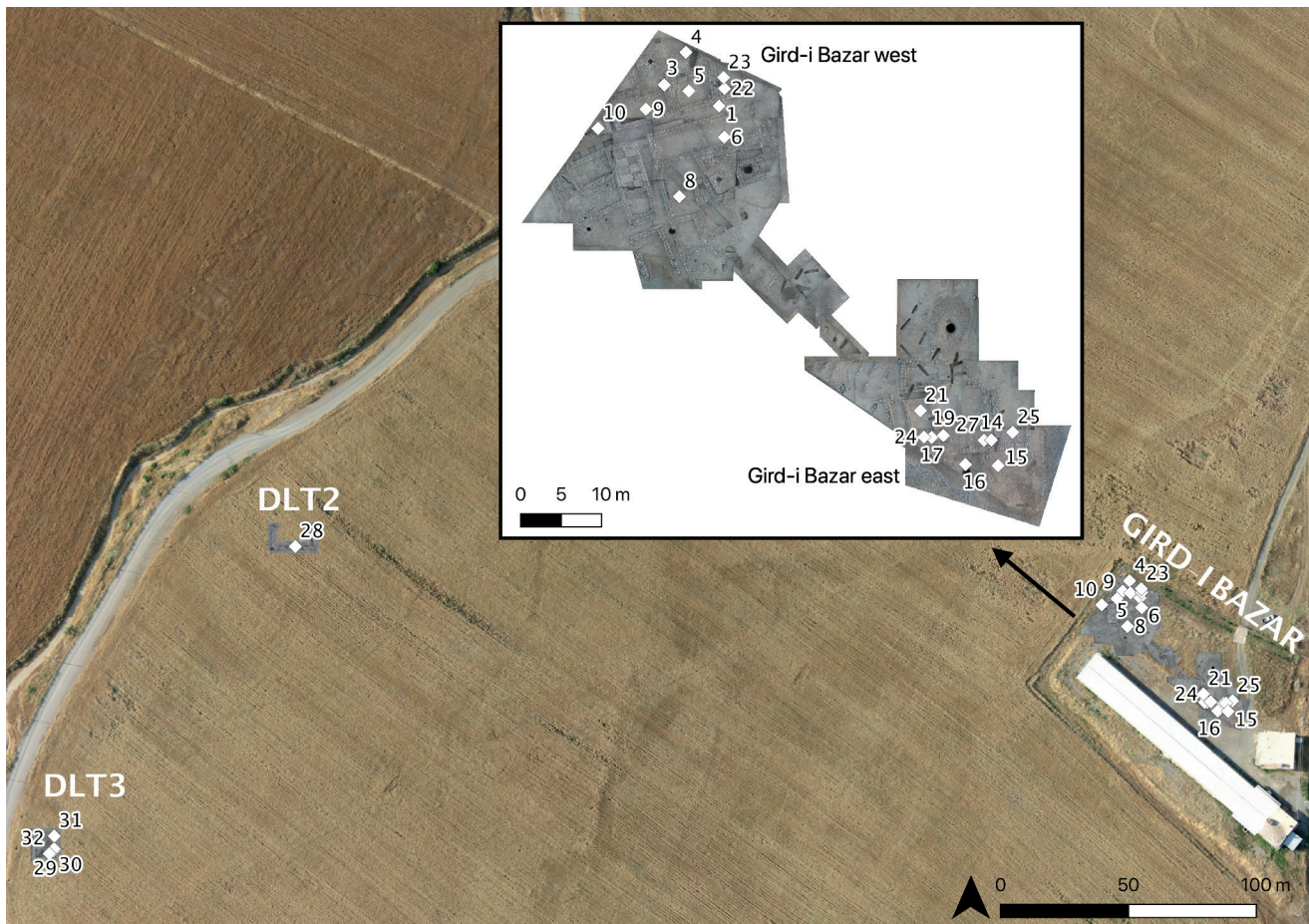


Fig. H1: Map of the excavation areas of Gird-i Bazar (=GIB), DLT2 and DLT3 from which the soil samples were derived. White dots indicate locations of the samples. Prepared by Andrea Squitieri.

Bazar East, and they were all taken from floor deposits. The assemblage contains one sample from DLT2, Sample 28, and it constitutes the contents of a storage vessel found *in situ* in Room 35. The remaining four samples in the collection come from floor deposit contexts in DLT3.

Altogether, a total of 1040 botanical remains were recovered from over 1404 litres of soil. Less than one plant item per litre of soil (<0.741) is a very low recovery ratio. A number of factors may be at play in explaining the poor preservation rate. The low rates of recovery may be a result of charred seed degradation in overly acidic soils (Mark Altaweel, personal communication) or other taphonomic conditions on the site, including bioturbation and anthropogenic disturbance, clearance, and destruction, both past and present. The dearth of archaeobotanical remains may also accurately reflect an extremely low level of plant use by the residents of the Dinka Lower Town. The latter proposition seems highly unlikely, however, given the importance of plant foods and plant materials in Iron Age communities in northern Iraq. The absence of evidence is not evidence of absence, so the archaeological

adage goes. We proceed, then, under the presumption that the diversity and abundance of plant remains presented here give us only a glimpse into what was most probably a much richer economy of human-plant interactions.

The scarcity of wood charcoal in this assemblage also deserves mention. Overall, there is less than 0.01 g of wood charcoal per liter of soil in this dataset. Only Sample 31 contained a significant amount of charred wood larger than 1 mm, 13.0 g. All the other samples produced less than half a gram of anthracological material. Typically, when wood charcoal is scant in a Near Eastern archaeobotanical assemblage, the presumption is that timber resources were unavailable or depleted, and dung fuel was the predominant fuel source for the community³⁶⁴. However, a reliance on dung fuel should also produce a significant wild plant to cultigen signature, if grazing was the primary means of feeding livestock. That, however, does not seem to be the case with the assemblage at

³⁶⁴ Miller 1984.

Sample ID	Operation	Registration no.	Unit	Context	Soil Volume (l)	Number of Plant Items	>1mm Wood Charcoal Weight (g)	Notes
1	GIB West	PPP 268932:042:001	Alley 13	floor deposit	46	15	0.013	
2	GIB West	PPP 268932:042:022	Alley 13	floor deposit	18	1	0.020	
3	GIB West	PPP 268932:052:002	Courtyard 21	tannur	48	50.5	0.036	
4	GIB West	PPP 268932:021:005	Courtyard 21	floor deposit	24	17.5	0.095	
5	GIB West	PPP 268932:051:007	Room 22	floor deposit	60	32.5	0.139	
6	GIB West	PPP 268931:032:017	Room 19	floor deposit	34	59	0.027	
7	GIB West	PPP 268931:026:005	Room 19	floor deposit	50	2	0.001	Indet. seeds found: not shown on distribution map
8	GIB West	PPP 268931:041:012	Courtyard 11	floor deposit	44	17.25	0.004	
9	GIB West	PPP 267932:017:013	Room 15	floor deposit	60	171	0.104	
10	GIB West	PPP 267931:014:009	Room 16	floor deposit	n/a	7	0.001	
11	GIB West	PPP 267931:014:004	Room 16	floor deposit	n/a	0	0.005	no seeds: not shown on distribution map
12	GIB West	PPP 267931:014:008	Room 16	floor deposit	n/a	0	0	no seeds: not shown on distribution map
13	GIB East	PPP 271927:021:020	Room 1	floor deposit	n/a	0	0.202	no seeds: not shown on distribution map
14	GIB East	PPP 272928:010:003	Room 29	floor deposit	40	4	0.074	
15	GIB East	PPP 272927:020:017	Room 23	floor deposit	30	119.5	0.227	
16	GIB East	PPP 271927:021:019	Room 1	floor deposit	n/a	74	0.058	
17	GIB East	PPP 271928:096:009	Room 3	floor deposit	26	9	0.039	
18	GIB East	PPP 271928:037:005	Room 3	floor deposit	n/a	0	0.366	no seeds: not shown on distribution map
19	GIB East	PPP 271928:110:003	Courtyard 2	floor deposit	30	14	0.231	
20	GIB East	PPP 271928:110:004	Courtyard 2	floor deposit	14	1	0.065	no seeds: not shown on distribution map
21	GIB East	PPP 271928:052:007	Room 3	floor deposit	n/a	14	0.003	
22	GIB West	PPP 268932:066:001	Room 28	floor deposit	114	3.5	0.119	
23	GIB West	PPP 268932:066:003	Room 28	floor deposit	60	27	0.045	
24	GIB East	PPP 271928:052:007	Room 3	floor deposit	78	10	0.011	
25	GIB East	PPP 272928:017:002	Outdoor Area 24	floor deposit	54	21	0.002	
26	GIB East	PPP 272928:010:006	Room 29	floor deposit	110	3	0.024	indet. seeds found: not shown on distribution map
27	GIB East	PPP 272928:010:001	Room 29	floor deposit	20	2	<0.001	
28	DLT2	PPP 235934:037:002	Room 35	vessel contents	36	170	0.134	
29	DLT3	PPP 226922:040:002	Room 64	floor deposit	50	27	0.050	
30	DLT3	PPP 226922:040:019	Room 64	floor deposit	100	57.5	0.040	
31	DLT3	PPP 226922:047:009	Room 63	floor deposit	128	92.25	13.000	
32	DLT3	PPP 226922:040:024	Room 64	floor deposit	130	18.5	0.060	
				TOTALS	>1404	1040	15.195	

Table H1: Catalogue of the soil samples analysed from Dinka Lower Town. GIB West = Gird-i Bazar western area; GIB East = Gird-i Bazar eastern area.

hand (**Table H2**). There are nearly three cultivated seeds to every wild plant seed. Because this analysis lacks data from the <1 mm size-grades, perhaps the wild plant signature of dung fuel has yet to be detected. It is also possible that the residents of the Dinka Lower Town chose to fodder their animals with cultivated grains and pulses, and this would explain the predominance of cultivars in this collection. But a heavy reliance on silage would mean that the agriculturalists of Dinka decided to ignore the endemic pastureland available to them in the steppic foothills of the Zagros. Another hypothesis is that wood was indeed the primary fuel source for Dinka's occupants, but poor archaeological preservation masks this practice. Clearly, further research is needed, and intended, to clarify the role that wood played at Gird-i Bazar. In addition to integrating data from the less than 1 mm fractions into future analyses, an expansion of the overall sample size and identification of the tree species present will help address these issues. In the meantime, we proceed under the assumption that wood was available and utilised by the residents of Gird-i Bazar, but underrepresented in this dataset.

Total cultigen count	251
Total wild plant count	88
Total cereal, chaff and pulse count	231
Cultigens : wild plants	2.852

Table H2: Ratio of cultigens to wild plants in the Dinka Lower Town assemblage.

Table H3 provides a complete accounting of the plant species recovered from the Dinka Lower Town assemblage, and their absolute counts. Altogether, 34 unique botanical taxa were identified in the collection, constituting significant richness in the plants associated with the occupation at Gird-i Bazar. With another 64 seeds to be identified, the richness of the assemblage stands to be even greater. Richness, or the number of unique taxa, is not the only measure of species diversity, however. Evenness, or the relative abundance of each taxon represented in the collection, also serves as a marker of diversity, with greater evenness associated with greater diversity. Simpson's Index of Diversity considers both richness and evenness by measuring the probability that two plant items randomly selected from the assemblage will represent two different taxa. Values range from 0 to 1, with higher numbers indexing greater diversity. The Simpson's Index of Diversity measure for this assemblage is 0.9304, indicating a highly diverse set of plant remains. Minimally, this score

suggests that the residents of the Dinka Lower Town took advantage of their area's natural resources and utilised a wide range of plants with consistency. Indeed, the mountain region in which Gird-i Bazar is located (**Fig. H2**) contains the greatest diversity of endemic plant species in Iraq (**Fig. H3**), and the MSU (Sulaymaniyah) district that contains the site of Gird-i Bazar is one of the most botanically diverse of all the physiogeographic zones of the country³⁶⁵ (**Fig. H4**). When one considers the low rates of preservation associated with this assemblage (less than one plant item per litre of soil), the high level of plant diversity is all the more remarkable, and suggestive of a very expansive human-plant economy.

When looking at the overall composition of the Dinka Lower Town assemblage (**Fig. H5**), 110 cereal grains and 16 chaff items constitute 35% of the identified plant remains recovered from the 32 samples, suggesting significant commitment to cereal crop agriculture at Gird-i Bazar. Winter cereals dominate the assemblage, and they include barley (*Hordeum vulgare*), emmer (*Triticum dicocum*), einkorn (*Triticum monococcum*), and free-threshed wheat (*Triticum aestivum/durum*). These grains would have been planted before the winter rains and harvested in the spring. Barley, a more drought-tolerant grain, would have been grown for both human and livestock consumption, while the wheat varieties, with higher water requirements, would have been reserved for humans alone. Contemporary records document an average annual rainfall of 700 mm to 900 mm in and around Gird-i Bazar³⁶⁶, plenty of precipitation to engage in dry farming. But as the discovery of *qanats* in the region attest³⁶⁷, risk buffering water systems were still built and utilised by agriculturalists in the Bora Plain, and the occupants of the Dinka Lower Town probably did not take water security for granted when making cropping decisions.

There is also one species of summer millet present in the cereal remains, broomcorn millet (*Panicum miliaceum*), represented by just one seed. Broomcorn millet is not unheard of in Iron Age Mesopotamian agriculture, but it is not considered a staple crop. Helbaek³⁶⁸ recovered caches of broomcorn millet from Kalhu/Nimrud (including at Fort Shalmaneser) in the Assyrian heartland, Rosenzweig³⁶⁹ detected it at Tušhan (Ziyaret Tepe) on the Upper Tigris, and Kubiak-Martens³⁷⁰ identified the summer cereal at

365 Ghazanfar/McDaniel 2016.

366 Guest/Al-Rawi 1966, 12, Fig. 5.

367 Altaweel/Marsh 2016 and §B1.

368 Helbaek 1966, 615.

369 Rosenzweig 2018.

370 Kubiak-Martens 2015.

Sample ID	1	2	3	4	5	6	7	8	9	10	11	12	13	14	15
Area	GIB West	GIB West	GIB West	GIB West	GIB West	GIB West	GIB West	GIB West	GIB West	GIB West	GIB West	GIB West	GIB East	GIB East	GIB East
Square	268932	268932	268932	268932	268932	268931	268931	268931	267932	267931	267931	267931	271927	272928	272927
Unit	Alley 13	Alley 13	Court-yard 21	Court-yard 21	Room 22	Room 19	Room 19	Court-yard 11	Room 15	Room 16	Room 16	Room 16	Room 1	Room 29	Room 23
Soil Vol. (!)	46	18	48	24	60	34	50	44	60	n/a	n/a	n/a	n/a	40	30
Wood Charcoal Weight (g)	0.013	0.02	0.036	0.095	0.139	0.027	0.001	0.004	0.104	0.001	0.005	0	0.202	0.074	0.227
CEREALS															
Triticum dicoccum (emmer wheat)									2						
T. durum/aestivum (free-threshed wheat)									3						
Triticum sp. indeterminate (wheat)				2					1						
Hordeum vulgare (barley)					1				5						1
Panicum miliaceum (broomcorn millet)									1						
Cereal grain indeterminate	2			2				4	36						1
CHAFF															
T. monococcum, spikelet fork (einkorn chaff)					1										
Triticum sp. spikelet fork (wheat chaff)															
Triticum sp. glume/base (wheat chaff)									1						
Cereal spikelet fork indeterminate (cereal chaff)								1							
Cereal culm (cereal chaff)									1						
Straw (cereal chaff)															

Table H3: Catalogue of the plant species recovered from each sample in the Dinka Lower Town assemblage.

Sample ID	1	2	3	4	5	6	7	8	9	10	11	12	13	14	15
Area	GIB West	GIB West	GIB West	GIB West	GIB West	GIB West	GIB West	GIB West	GIB West	GIB West	GIB West	GIB West	GIB West	GIB East	GIB East
Square	268932	268932	268932	268932	268932	268931	268931	268931	267932	267931	267931	267931	271927	272928	272927
Unit	Alley 13	Alley 13	Court-yard 21	Court-yard 21	Room 22	Room 19	Room 19	Court-yard 11	Room 15	Room 16	Room 16	Room 16	Room 1	Room 29	Room 23
Soil Vol. (l)	46	18	48	24	60	34	50	44	60	n/a	n/a	n/a	n/a	40	30
Wood Charcoal Weight (g)	0.013	0.02	0.036	0.095	0.139	0.027	0.001	0.004	0.104	0.001	0.005	0	0.202	0.074	0.227
PULSES															
<i>Lathyrus</i> sp. (lathyrus)															
<i>Lens culinaris</i> (lentil)		2.5			2										
<i>Pisum sativum</i> (common pea)															
<i>Vicia ervilia</i> (bitter vetch)															4.5
<i>Vicia sativa</i> (common vetch)															
cf. <i>Vicia faba</i> (faba bean)					1										
Large legume, indeterminate		10			2	8			7						31
OTHER CROPS															
<i>Ficus carica</i> (fig)															
<i>Vitis vinifera</i> (grape)					1										
<i>Vitis vinifera</i> (grape) pedicle															
<i>Vitis vinifera</i> (grape) fragment				0.5	3.5			0.25							
Nut shell indeterminate															
WILD PLANTS															
<i>Adonis</i> sp. (pheasant's eye)															
cf. <i>Alhagi</i> (camel thorn)										2					

Table H3 (continued): Catalogue of the plant species recovered from each sample in the Dinka Lower Town assemblage.

Sample ID	1	2	3	4	5	6	7	8	9	10	11	12	13	14	15
Area	GIB West	GIB West	GIB West	GIB West	GIB West	GIB West	GIB West	GIB West	GIB West	GIB West	GIB West	GIB West	GIB East	GIB East	GIB East
Square	268932	268932	268932	268932	268932	268931	268931	268931	267932	267931	267931	267931	271927	272928	272927
Unit	Alley 13	Alley 13	Court-yard 21	Court-yard 21	Room 22	Room 19	Room 19	Court-yard 11	Room 15	Room 16	Room 16	Room 16	Room 1	Room 29	Room 23
Soil Vol. (l)	46	18	48	24	60	34	50	44	60	n/a	n/a	n/a	n/a	40	30
Wood Charcoal Weight (g)	0.013	0.02	0.036	0.095	0.139	0.027	0.001	0.004	0.104	0.001	0.005	0	0.202	0.074	0.227
Anthemis sp. (may-weed)				2											
APIACEAE (CARROT family)															
ASTERACEAE (DAISY family)				2											
Astragalus sp. (milkvetch)															
Brassica sp. (wild mustard)															
Bromus sp. (brome grass)						1									
Buglossoides sp. (bugloss)									3						
Bupleurum sp. (hare's ear)															
Chenopodium sp. (goosefoot)															
cf. Eremopoa sp. (eremopoa)									1						
Galium (bedstraw) fragments															
Galium sp. (bedstraw)			1												
Grass -- to be identified															
Heliotropium sp. (heliotrope)															
Lolium sp. (rye grass)															
Medicago sp. (bur-clover)														1	

Table H3 (continued): Catalogue of the plant species recovered from each sample in the Dinka Lower Town assemblage.

Sample ID	1	2	3	4	5	6	7	8	9	10	11	12	13	14	15
Area	GIB West	GIB West	GIB West	GIB West	GIB West	GIB West	GIB West	GIB West	GIB West	GIB West	GIB West	GIB West	GIB West	GIB East	GIB East
Square	268932	268932	268932	268932	268932	268931	268931	268931	267932	267931	267931	267931	271927	272928	272927
Unit	Alley 13	Alley 13	Court-yard 21	Court-yard 21	Room 22	Room 19	Room 19	Court-yard 11	Room 15	Room 16	Room 16	Room 16	Room 1	Room 29	Room 23
Soil Vol. (l)	46	18	48	24	60	34	50	44	60	n/a	n/a	n/a	n/a	40	30
Wood Charcoal Weight (g)	0.013	0.02	0.036	0.095	0.139	0.027	0.001	0.004	0.104	0.001	0.005	0	0.202	0.074	0.227
POACEAE (GRASS family)			1	2		2									1
Portulaca sp. (purslane)															
Ranunculus sp. (buttercup)					1					1					
cf. Scorpiurus sp. (catpillar plant)															
Sinapis sp. (charlock)															
Thymelaea sp. (thymelaea)															
Trigonella sp. (fennugreek)															
MISCELLANEOUS															
Indeterminate seed	12	1	36	4	20	27	2	6	109	2			3	80	
To be identified	1			3		19		6	1	2				1	
Stem						2									
Seed coat															
	15	1	50.5	17.5	32.5	59	2	17.25	171	7	0	0	0	4	119.5

Table H3 (continued): Catalogue of the plant species recovered from each sample in the Dinka Lower Town assemblage.

Sample ID	16	17	18	19	20	21	22	23	24	25	26	27	28	29	30	31	32	TOTALS	
Area	GIB East	GIB East	GIB East	GIB East	GIB East	GIB East	GIB West	GIB West	GIB West	GIB East	GIB East	GIB East	GIB East	DLT3	DLT3	DLT3	DLT3		
Square	271927	271928	271928	271928	271928	271928	268932	268932	271928	272928	272928	272928	272928	235934	226922	226922	226922	226922	
Unit	Room 1	Room 3	Room 3	Court-yard 2	Court-yard 2	Room 3	Room 28	Room 28	Room 3	Outdoor Area 24	Room 29	Room 29	Room 29	Room 35	Room 64	Room 64	Room 63	Room 64	
Soil Vol. (l)	n/a	26	n/a	30	14	n/a	60	114	78	54	110	20	36	50	100	128	130	1494	
Wood Charcoal Weight (g)	0.058	0.039	0.366	0.231	0.065	0.003	0.045	0.119	0.011	0.002	0.024	<0.001	0.134	0.05	0.04	0.13	0.06	15.195	
CEREALS																			
Triticum dicoccum (emmer wheat)													3						5
T. durum/aestivum (free-threshed wheat)																			3
Triticum sp. indeterminate (wheat)												1	1			3			8
Hordeum vulgare (barley)	5															1			13
Panicum miliaceum (broomcorn millet)																			1
Cereal grain indeterminate	10			1			2		2				7	1		11	1		80
CHAFF																			
T. monococcum, spikelet fork (einkorn chaff)																			1
Triticum sp. spikelet fork (wheat chaff)										1							1		2
Triticum sp. glume/base (wheat chaff)																	1		2
Cereal spikelet fork indeterminate (cereal chaff)																			1
Cereal culm (cereal chaff)	1									3							1		6
Straw (cereal chaff)										4									4

Table H3 (continued): Catalogue of the plant species recovered from each sample in the Dinka Lower Town assemblage.

Sample ID	16	17	18	19	20	21	22	23	24	25	26	27	28	29	30	31	32	TOTALS
Area	GIB East	GIB East	GIB East	GIB East	GIB East	GIB East	GIB West	GIB West	GIB West	GIB East	GIB East	GIB East	GIB East	DLT2	DLT3	DLT3	DLT3	
Square	271927	271928	271928	271928	271928	271928	268932	268932	271928	272928	272928	272928	235934	226922	226922	226922	226922	
Unit	Room 1	Room 3	Room 3	Court-yard 2	Court-yard 2	Room 3	Room 28	Room 28	Room 3	Outdoor Area 24	Room 29	Room 29	Room 29	Room 35	Room 64	Room 63	Room 64	
Soil Vol. (l)	n/a	26	n/a	30	14	n/a	60	114	78	54	110	20	36	50	100	128	130	1404
Wood Charcoal Weight (g)	0.058	0.039	0.366	0.231	0.065	0.003	0.045	0.119	0.011	0.002	0.024	<0.001	0.134	0.05	0.04	13	0.06	15:195
PULSES																		
Lathyrus sp. (lathyrus)																2		2
Lens culinaris (lentil)													3			6		13.5
Pisum sativum (common pea)							1						2					3
Vicia ervilia (bitter vetch)																		4-5
Vicia sativa (common vetch)																1		1
cf. Vicia faba (faba bean)																		1
Large legume, indeterminate	1			1			2						11			7		80
OTHER CROPS																		
Ficus carica (fig)																		1
Vitis vinifera (grape)																		1
Vitis vinifera (grape) pedicel														2				2
Vitis vinifera (grape) fragment															1.5	1.25	0.5	7.5
Nut shell indeterminate																		1
WILD PLANTS																		
Adonis sp. (pheasant's eye)										1								1

Table H3 (continued): Catalogue of the plant species recovered from each sample in the Dinka Lower Town assemblage.

Sample ID	16	17	18	19	20	21	22	23	24	25	26	27	28	29	30	31	32	TOTALS
Area	GIB East	GIB East	GIB East	GIB East	GIB East	GIB East	GIB West	GIB West	GIB West	GIB East	GIB East	GIB East	GIB East	DLT3	DLT3	DLT3	DLT3	
Square	271927	271928	271928	271928	271928	271928	268932	268932	271928	272928	272928	272928	235934	226922	226922	226922	226922	
Unit	Room 1	Room 3	Room 3	Court-yard 2	Court-yard 2	Court-yard 2	Room 28	Room 28	Room 3	Outdoor Area 24	Room 29	Room 29	Room 29	Room 64	Room 64	Room 63	Room 64	
Soil Vol. (l)	n/a	26	n/a	30	14	n/a	60	114	78	54	110	20	36	50	100	128	130	1494
Wood Charcoal Weight (g)	0.058	0.039	0.366	0.231	0.065	0.003	0.045	0.119	0.011	0.002	0.024	<0.001	0.134	0.05	0.04	13	0.06	15.195
cf. Alhagi (camel thorn)																		2
Anthemis sp. (may-weed)									1									3
APIACEAE (CAR-ROT family)																	2	2
ASTERACEAE (DAISY family)																		2
Astragalus sp. (milkvetch)						1												1
Brassica sp. (wild mustard)															1			1
Bromus sp. (brome grass)																		1
Buglossoides sp. (bugloss)	1						9							1		5	1	20
Bupleurum sp. (hare's ear)													1		1			2
Chenopodium sp. (goosefoot)															2	5		7
cf. Eremopoa sp. (eremopoa)																		1
Galium (bedstraw) fragments								0.5					1					1.5
Galium sp. (bed-straw)													10					11
Grass -- to be identified						1												1
Heliotropium sp. (heliotrope)															1	2		3

Table H3 (continued): Catalogue of the plant species recovered from each sample in the Dinka Lower Town assemblage.

Sample ID	16	17	18	19	20	21	22	23	24	25	26	27	28	29	30	31	32	TOTALS
Area	GIB East	GIB East	GIB East	GIB East	GIB East	GIB East	GIB West	GIB West	GIB West	GIB East	GIB East	GIB East	DLT2	DLT3	DLT3	DLT3	DLT3	
Square	271927	271928	271928	271928	271928	271928	268932	268932	271928	272928	272928	272928	235934	226922	226922	226922	226922	
Unit	Room 1	Room 3	Room 3	Court-yard 2	Court-yard 2	Court-yard 2	Room 28	Room 28	Room 3	Outdoor Area 24	Room 29	Room 29	Room 35	Room 64	Room 64	Room 63	Room 64	
Soil Vol. (l)	n/a	26	n/a	30	14	n/a	114	60	78	54	110	20	36	50	100	128	130	1404
Wood Charcoal	0.058	0.039	0.366	0.231	0.065	0.003	0.119	0.045	0.011	0.002	0.024	<0.001	0.134	0.05	0.04	13	0.06	15:195
Weight (g)																		
Lolium sp. (rye grass)														1				1
Medicago sp. (bur-clover)	1						3											5
POACEAE (GRASS family)								1								7		14
Portulaca sp. (purs-lane)															1			1
Ranunculus sp. (buttercup)																		2
cf. Scorprius sp. (catepillar plant)						1												1
Sinapis sp. (charlock)																1		1
Thymelaea sp. (thymelaea)	1																	1
Trigonella sp. (fenu-greek)																1		1
MISCELLANEOUS																		
Indeterminate seed	48	7		8	1	11		10	7	6	2	1	130	22	50	27	6	638
To be identified	5	1		3			3	2		3	1		1			11	1	64
Stem	1																	3
Seed coat																		5
	74	9	0	14	1	14	3-5	27	10	21	3	2	170	27	57.5	92.25	18.5	1040

Table H3 (continued): Catalogue of the plant species recovered from each sample in the Dinka Lower Town assemblage.

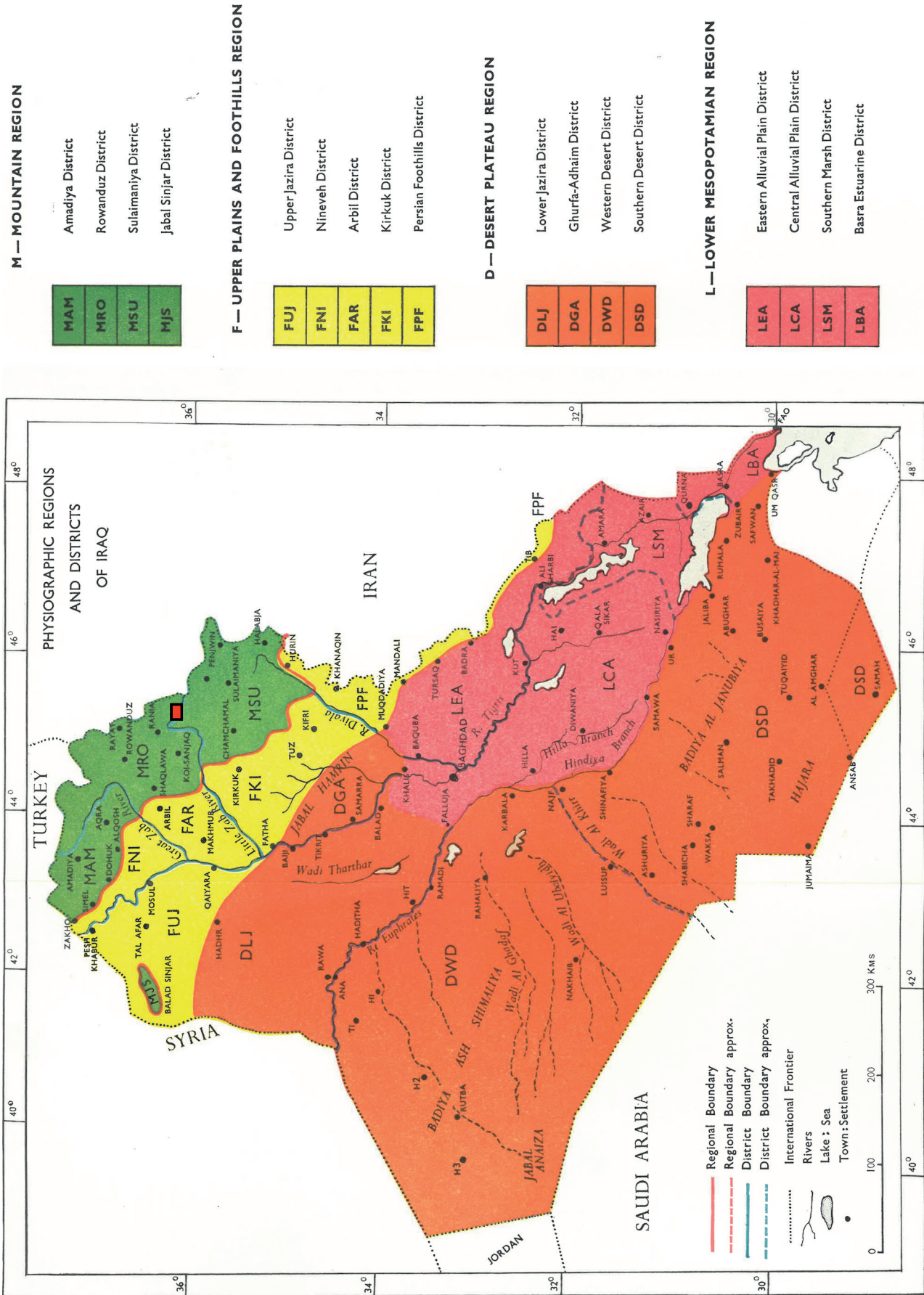


Fig. H2: Map of the physiographic districts of Iraq. From Guest/Al-Rawi 1966, frontispiece, Fig. 1. The red box shows the location of the Dinka Settlement Complex.

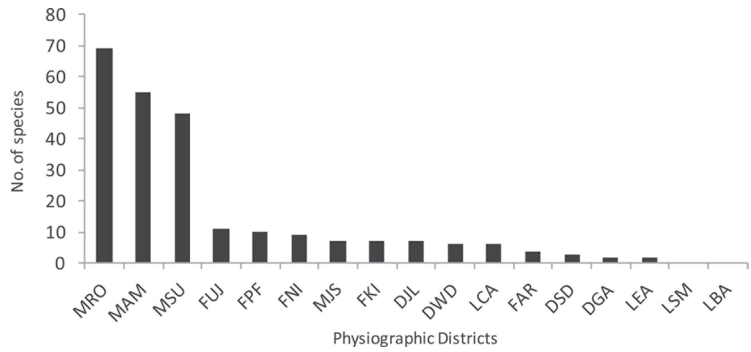
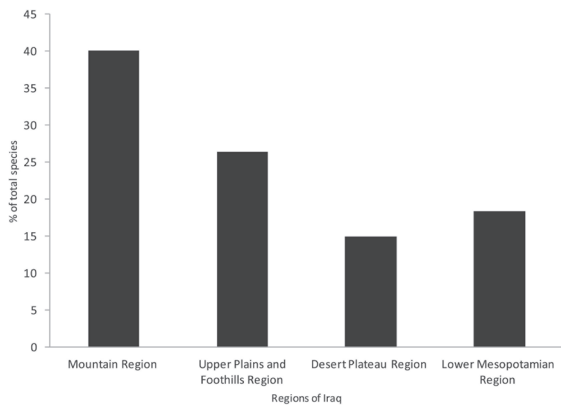


Fig. H3: Percent of total plant species in different physiographic regions of Iraq. From Ghazanfar/McDaniel 2016, 12, Fig. 7.

Fig. H4: Plant endemism in the physiogeographic districts of Iraq. From Ghazanfar/McDaniel 2016: 11, Fig. 6. The “MSU” district (= Sulaymaniyah district) is where the Dinka Settlement Complex lies.

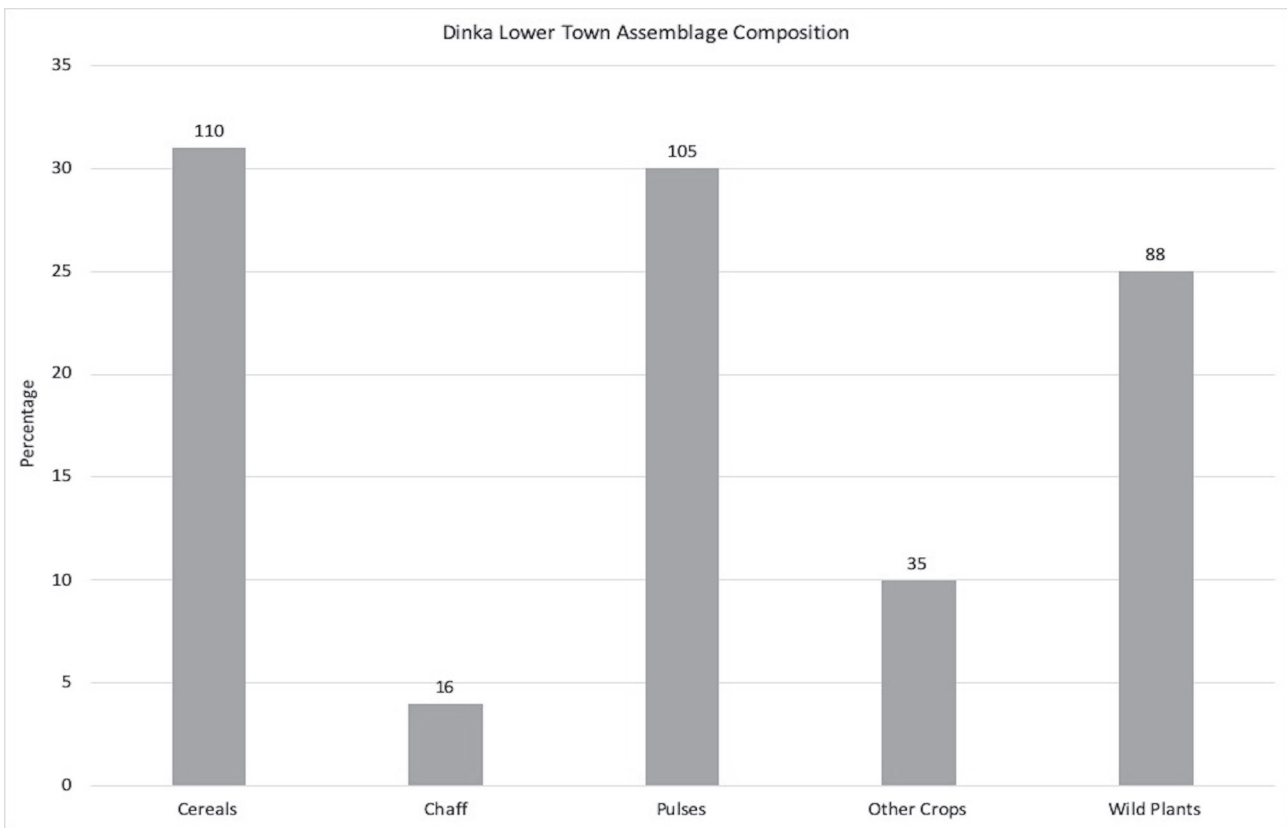


Fig. H5: Chart illustrating the proportional representation of the Dinka Lower Town plant remains by agricultural category. Absolute counts are provided above each bar chart. Prepared by Andrea Squitieri based on data provided by the authors.

Terqa (Tell Ashara) along the Middle Euphrates. Middle Assyrian written sources also reference millet as a secondary crop flanking larger fields of barley and wheat³⁷¹. Broomcorn millet at Gird-i Bazar would have mitigated the fallout of a poor winter harvest. Planted in the late spring or early summer, the fast-growing broomcorn millet would have been reaped by summer's end. Until or unless greater counts of millet are identified in the samples to be analysed, however, we cannot consider a summer grain harvest of importance to the agricultural calendar at the Dinka Settlement Complex.

Surprisingly, 105 pulse seeds were recovered, representing 30% of the overall assemblage. It is rare to encounter such an abundance of domesticated legumes in a Near Eastern archaeobotanical assemblage because these soft-bodied seeds tend to combust rather than char when exposed to fire, and thus elude discovery. Combined with the low levels of overall preservation for the Dinka Lower Town collection, the nearly 1 to 1 ratio of cereals to pulses preliminarily suggests that domesticated legumes were significant elements of Gird-i Bazar's agricultural economy. Six different pulses were distinguished: lathyrus (*Lathyrus* sp.), lentil (*Lens culinaris*), common pea (*Pisum sativum*), bitter vetch (*Vicia ervilia*), common vetch (*Vicia sativa*), and faba bean (*Vicia faba*). All of these species could have been grown as part of the winter harvest for both human and livestock consumption, but lathyrus can be poisonous to both humans and animals if eaten excessively, and bitter vetch has to be boiled before it is safe for human consumption. In addition to contributing to food supplies, pulses operate as nitrogen-fixing green manures that help retain nutrients in the soil of agricultural fields. The farmers of Gird-i Bazar could have interspersed these pulses with the barley and wheat and grown mixed crops, or seeded the fields with legumes after the grain had been harvested.

Additional edible plants found in the Dinka Lower Town assemblage include fig (*Ficus carica*), grape (*Vitis vinifera*), and unidentifiable nut. None of these supplemental fruits and nuts were found in great quantity, however, and they comprise only 10% of the overall collection. It is possible that the analysis of more samples from the Gird-i Bazar collection will reveal greater investment in viticulture and fig cultivation by the residents of the Dinka Lower Town, but the preliminary results do not find these fruits to be critical components of the Dinka economy or culinary culture.

The remaining 25% of identified botanical remains come from various species of wild plants. These 88 seeds

constitute plants that grow in a range of environmental habitats, and thus signal the extent of land use engaged by the humans and animals of Dinka Lower Town. The next section discusses these ecological signatures in greater detail.

H3. Plant ecologies and land use

The Dinka Settlement Complex is situated in the physiographically defined "mountain region" of Iraq (see **Fig. H2**). This region is further subdivided by vegetation into a forest zone 500–1800 meters above sea level, and a scrubby thorn-cushion zone at the higher altitudes of 1700–3000 meters above sea level (**Fig. H6**)³⁷². Oak (*Quercus* spp.) dominates the slopes of the forest zone, while milkvetch (*Astragalus* spp.) typifies the thorn-cushion, or sub-alpine, zone³⁷³. Nested within this broad overlay of forest and thorn-cushion scrub (some 30,000 km²), there lie areas of steppic and riverine vegetation. In some locations, degraded forest has transitioned to steppeland, and there are numerous lowland valleys that support riparian flora along riverbanks and out onto alluvial floodplains. The Bora Plain is one such location.

Information about land use by the residents of the Dinka Lower Town can be reconstructed from the plant ecologies of the wild plants identified through archaeobotanical analysis. In order to create this land use profile, we coded the wild plant taxa into categories of "alluvial plain", "steppe", "forest", and "non-diagnostic" based on their ecological signatures as provided in *Flora of Iraq*, focusing on species from the physiographic districts of Rowanduz (MRO), Sulaimaniya (MSU), and Amadiya (MAM) (see **Fig. H2**). For the taxa not covered by *Flora of Iraq* (the atlas is not yet complete), *Buglossoides* sp. and *Heliotropium* sp., we relied on ecological information provided in *Flora of Turkey* in the physiographic regions of southeastern Turkey. Next, we included the Dinka Lower Town's domesticated crops, and coded them for "fields", "orchards", or "vineyards". Wild plants common as weeds among agricultural crops were also coded as "fields". Finally, we added information about each taxon's altitudinal zonation and flowering period. These supplementary categories allow us to further infer the vertical extent of the residents' land use practices and construct a preliminary agricultural calendar, respectively. The resulting dataset is provided in **Table H4**.

371 Fales 2010, 78 n. 72.

372 Guest/Al-Rawi 1966, 67.

373 Guest/Al-Rawi 1966, 73.

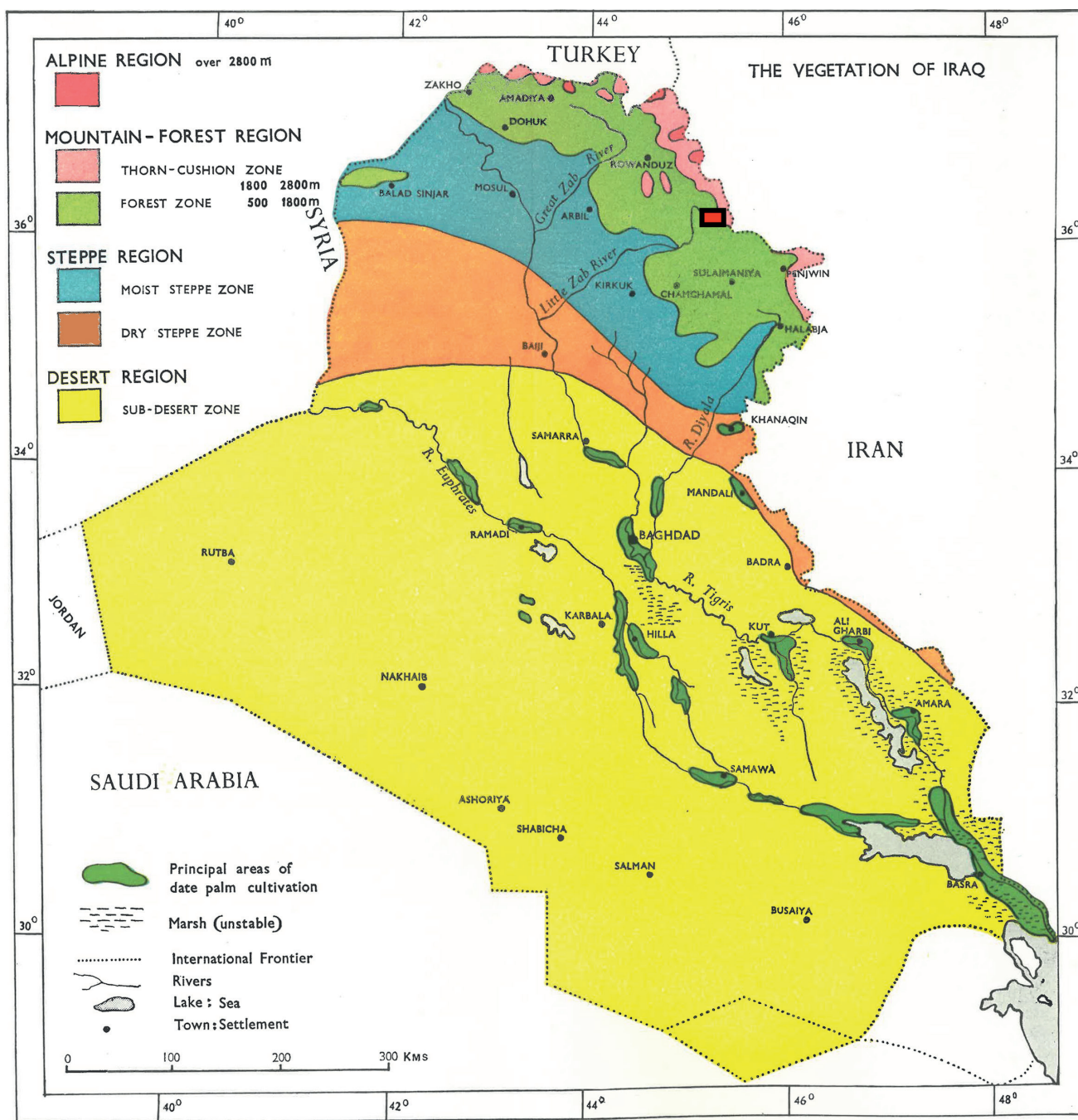


Fig. H6: Map of Iraq's zones of vegetation. From Guest/Al-Rawi 1966, 64, Fig. 15. The red box shows the location of the Dinka Settlement Complex.

In **Fig. H7**, two different expressions of the land use profile are presented. In **Fig. H7A**, the ecological signature of each taxon was given a value of 1, so that each species was equally weighed in the proportional representation of land use. The resulting chart illustrates that 35% (= 18) of the species recovered from the Dinka Lower Town are crops and weeds associated with settled agriculture (= bar label "Fields"). Another 27% (= 14) of the plants would have been found in the steppeland of the foothills and degraded forest slopes (= bar: Steppe), where Dinka's pastoralists would have taken their livestock to graze. Nearly one quarter (= 12) of the assemblage contains wild plants of the forest, suggesting that during the period of the Lower Town's occupation, the forests of the Zagros Mountains were still intact and well-utilised by the Dinka Lower Town community. The alluvial plain is represented by only two species: buttercup (*Ranunculus* sp.) and purslane (*Portulaca* sp.). These are both water-loving plants found along riverbeds and mountain streams. Buttercup is particularly fond of moist mountain meadows, and purslane enjoys growing alongside irrigation ditches. Neither plant is exclusive to the alluvial plain and could have just as likely derived from the forest zone. The lack of wild plants exclusive to the alluvial plain, combined with the prevalence of field crops and weeds, infers that the agriculturalists of the Dinka Lower Town had largely brought the Bora Plain under cultivation. Vineyards and orchards, however, are negligibly represented by grape and fig, respectively.

The bar chart in **Fig. H7B** relies on the absolute count of each taxon, and thus does a better job of conveying the impact of agriculture on the land use profile. Field use jumps to 46% (= 86.5) and vineyards to 5% (= 10.5). Meanwhile, use of the steppe declines, representationally, to 18% (= 33.5), and the forest falls to 16% (= 30.5). However, both charts make it clear that the steppe and forest remained critical landscapes for human and animal activity and the Dinka Lower Town's overall plant economy, despite the inhabitants' investment in crop agriculture.

The Dinka Lower Town sits at approximately 540 meters above sea level within the Bora Plain, itself a component of the larger Peshdar Plain created by the valley of the Lower Zab River. The alluvial plain is surrounded by the Qandil foothills, part of the Zagros mountain chain, beginning at around 700 m a.s.l., followed by mountains ascending to 2200 m a.s.l. The highest peak of the Qandil mountain range is 3,587 m a.s.l. We can begin to approximate the vertical extent of land use undertaken by the residents of the Dinka Lower Town by charting the altitudinal zonation of each plant species identified in the assemblage (**Fig. H8**). Elevation adds a dimension of movement to the land use profile, including the possibility of vertical transhumance.

Tracking altitude by both taxon (**Fig. H8A**) and absolute count (**Fig. H8B**), it is apparent that the occupants of the Dinka Lower Town obtained most of their plant resources from landscapes between 100 and 1500 m a.s.l., secondarily utilised the vegetation in the thorn-cushion zone, and rarely ventured into the alpine zone above 2800 meters for plant use. The sub-desert zone encompasses Lower Iraq (see **Fig. H6**), and it is characterised by 75-150 mm of annual rainfall and scattered small shrubs of the *Artemisia hera-alba* variety³⁷⁴. In the dry-steppe zone, precipitation increases to 200-350 mm per annum, the bare minimum for dry-farming cereals³⁷⁵. This region is characterised by sparse grassland and scattered shrubs. The so-called moist-steppe zone is a region of grasslands and semi-woody and herbaceous shrubs supported by 350-500 mm of rainfall per year. While relatively wetter than the dry-steppe zone, it is still a semi-arid environment where agriculture is best supported by irrigation. In the case of the Dinka Lower Town, the representation of plant species at 0 - 500 m a.s.l. should not necessarily be read as proof that the settlement's residents traveled far south for plant resources. All of the identified wild plant taxa capable of growing <500 m a.s.l. have great vertical range, and could have been found in the foothills, or higher, depending on the species; e.g. *Bromus* sp. and *Ranunculus* sp. Likewise, several of the taxa falling into the sub-desert and dry-steppe zones are domesticated crops and their attendant field weeds, like *Galium* sp. These plants, while capable of growing at lower altitudes in more arid environments, were much more likely to have been grown on the Bora Plain itself, or on the surrounding foothill terraces, where water was much more secure.

More assuredly, measures of altitudinal zonation in the forest zone extending from 500 - 1800 m a.s.l. capture the importance of this region for land use by the residents of the Dinka Lower Town. Annual rainfall in the lower zone of the mountain region ranges from 700 - 1400 mm per annum³⁷⁶, and it provides ideal habitats for many plants. In fact, every single plant taxon in the dataset is capable of living within this zone, and 1800 m a.s.l. marks the most common limit of the tree-line in the mountains, delineating the importance of this zone for timber resources³⁷⁷. At 700 m a.s.l., when the altitudinal zonation begins to peak by taxon and absolute count, the plain turns into foothills upon which Dinka's residents could have not only grown cereals and pulses, but also attended to vineyards, culti-

374 Guest/Al-Rawi 1966, 71.

375 Guest/Al-Rawi 1966, 71.

376 Guest/Al-Rawi 1966, 72.

377 Guest/Al-Rawi 1966, 85.

Taxon	Common Name	Land Use Designation	Altitudinal Zonation (masl)	Flowering/Fruiting Period	Absolute Count
<i>Adonis</i> sp.	pheasant's eye	steppe, forest	250 - 1500	April - June	1
cf. <i>Alhagi</i> sp.	camelthorn	steppe, forest	650 - 1500	June - August	2
<i>Anthemis</i> sp.	mayweed	non-diagnostic	50 - 2500	March - October	3
<i>Astragalus</i> sp.	milkvetch	steppe, forest	250 - 3500	March - September	1
<i>Brassica</i> sp.	wild mustard	steppe, forest	50 - 1700	February - June	1
<i>Bromus</i> sp.	brome grass	non-diagnostic	50 - 1700	February - August	1
<i>Buglossoides</i> sp.	bugloss	non-diagnostic	0 - 2500	February - June	20
<i>Bupleurum</i> sp.	hare's ear	steppe, forest	50 - 2800	April - August	2
<i>Chenopodium</i> sp.	goosefoot	fields	0 - 1500	May - September	7
cf. <i>Eremopoa</i> sp.	eremopoa	steppe, forest	100 - 1600	March - July	1
<i>Galium</i> sp.	bedstraw	fields, steppe, forest	0 - 2650	March - September	12.5
<i>Heliotropium</i> sp.	heliotrope	fields, steppe	0 - 1400	June - September	3
<i>Lolium</i> sp.	rye grass	fields, steppe, forest	250 - 1900	March - June	1
<i>Medicago</i> sp.	burclover	fields, steppe, forest	100 - 2200	March - September	5
<i>Portulaca</i> sp.	purslane	forest, alluvial plain	0 - 1500	April - August	1
<i>Ranunculus</i> sp.	buttercup	forest, alluvial plain	50 - 3100	March - September	2
cf. <i>Scorpiurus</i> sp.	caterpillar plant	fields, steppe	0 - 850	March - June	1
<i>Sinapsis</i> sp.	charlock	fields, steppe	100 - 1100	March - June	1
<i>Thymelaea</i> sp.	thymelaea	steppe, forest	300 - 1300	April - August	1
<i>Trigonella</i> sp.	fenugreek	steppe	50 - 1500	March - June	1
<i>Ficus carica</i>	fig	orchards	500 - 1300	April - July	1
<i>Vitis vinifera</i>	grape	vineyards	700 - 1600	May - June	10.5
<i>Lathyrus</i> sp.	lathyrus	fields	50 - 2000	March - August	2
<i>Lens culinaris</i>	lentil	fields	500 - 1450	March - June	13.5
<i>Pisum sativum</i>	common pea	fields	700 - 1600	April - May	3
<i>Vicia ervilia</i>	bitter vetch	fields	800 - 1100	April - June	4.5
<i>Vicia sativa</i>	common vetch	fields	0 - 1300	March - May	1
cf. <i>Vicia faba</i>	faba bean	fields	250 - 1000	March - May	1
<i>Hordeum vulgare</i>	barley	fields	0 - 800	March - May	13
<i>Triticum monococcum</i>	einkorn	fields	100 - 1000	June - July	1
<i>Triticum dicoccum</i>	emmer	fields	700 - 1300	May	5
<i>Triticum aestivum/durum</i>	free-threshed wheat	fields	0 - 1000	April - June	3
<i>Panicum miliaceum</i>	broomcorn millet	fields	0 - 1000	June - August	1

Table H4: Catalogue of the plant ecology information on each identified species in the Dinka Lower Town assemblage.

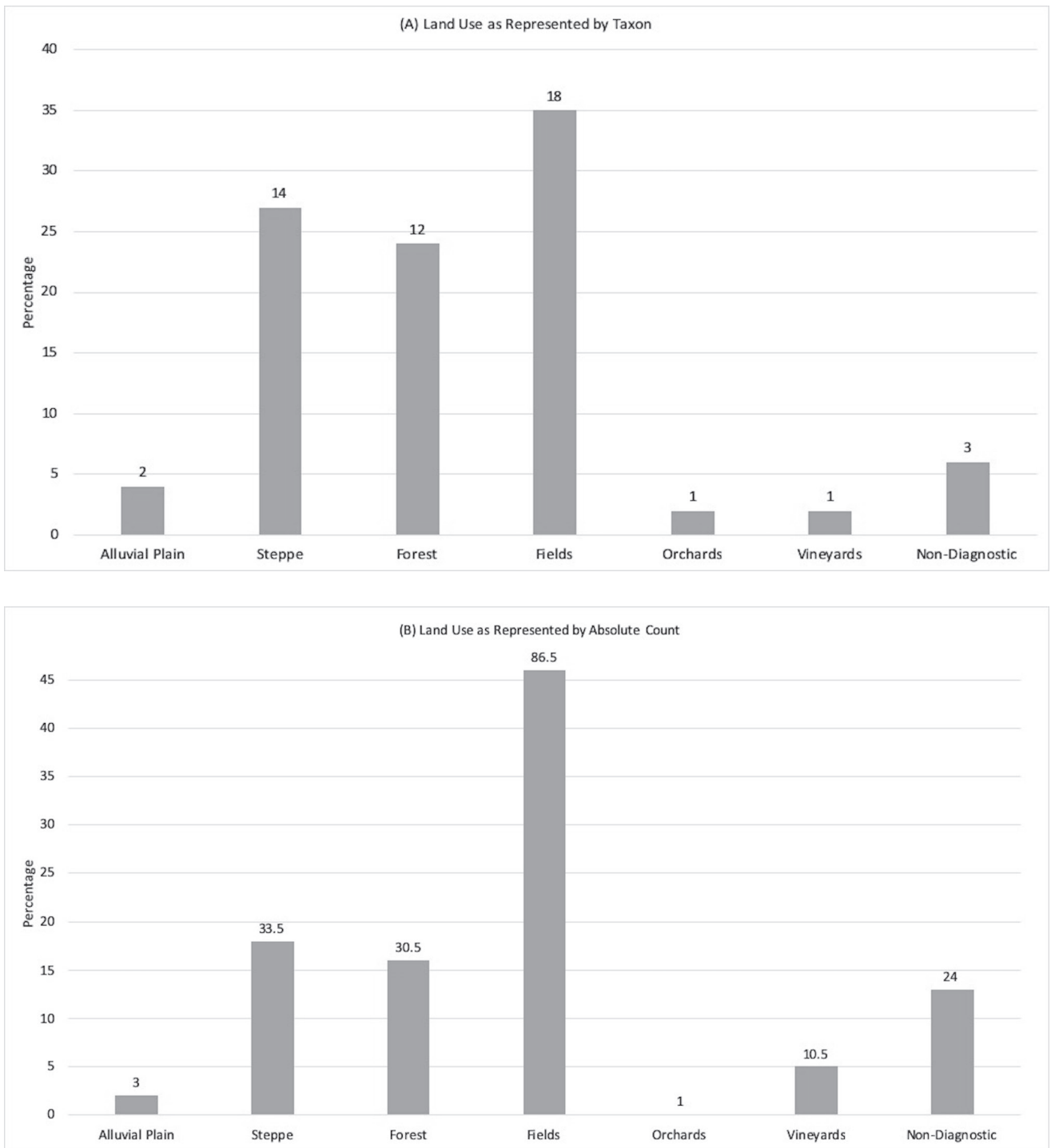


Fig. H7: (A) Land use as represented by the ecological signature of each taxon in the Dinka Lower Town assemblage. (B) Land use as represented by the weighted ecological signature of each taxon's absolute count in the Dinka Lower Town assemblage. Absolute counts are provided above each bar chart. Prepared by Andrea Squitieri based on data provided by the authors.



Fig. H8: (A) Altitudinal zonation by taxon. (B) Altitudinal zonation by absolute count. Prepared by Andrea Squitieri based on data provided by the authors.

vated groves of fig, and managed stands of oak and wild pistachio (*Pistacia atlantica*). Indeed, based on the plant remains, the inhabitants of Dinka Lower Town obtained at least 60% of their plant resources from the forest zone (Figs. H9A-B), and possibly upwards of 80% if the taxa capable of living below 500 m a.s.l. were actually growing at higher altitudes, as explained above.

At 1800 m a.s.l., the timber-line is reached and the landscape transitions to thorn-cushion, an open shrubland formation³⁷⁸ exposed to over 1000 mm of precipitation from rain and snow. Fewer and fewer of the plants from the Dinka Lower Town assemblage are capable of growing in this zone, and when elevations reach the alpine zone at 2750 m a.s.l., botanical representation becomes negligible. While there is no reason to preclude the possibility that the residents of the Dinka Lower Town traveled to heights greater than 1800 m a.s.l. to procure plant resources, all of the taxa represented in the thorn-cushion and alpine

zones could have been found at lower elevations, among the valleys and lower slopes of the forest zone, for example.

Fig. H10 depicts an agricultural calendar for the Dinka Settlement Complex, based on the flowering and fruiting periods for each of the plant species identified in the collection. April, May and June would have been a busy period of the spring harvest, when the bulk of the community's agrarian resources would have been reaped: wheat, barley, pulses, grapes and figs. A secondary summer harvest of broomcorn millet would have been planted as early as May and collected as late as September. Meanwhile, during these same spring and summer months, (agro-)pastoralists would have been taking their flocks and herds into the foothills and higher to graze on the many wild plants in season. Sometime around October, the agrarian economy would shift to the sowing of the fields, ahead of the winter rains, and shepherds would transition their livestock to grazing the crop stubble in the fields. Once the stubble had been consumed, the primary source of food for the settlement's animals would have

³⁷⁸ Guest/Al-Rawi 1966, 73.

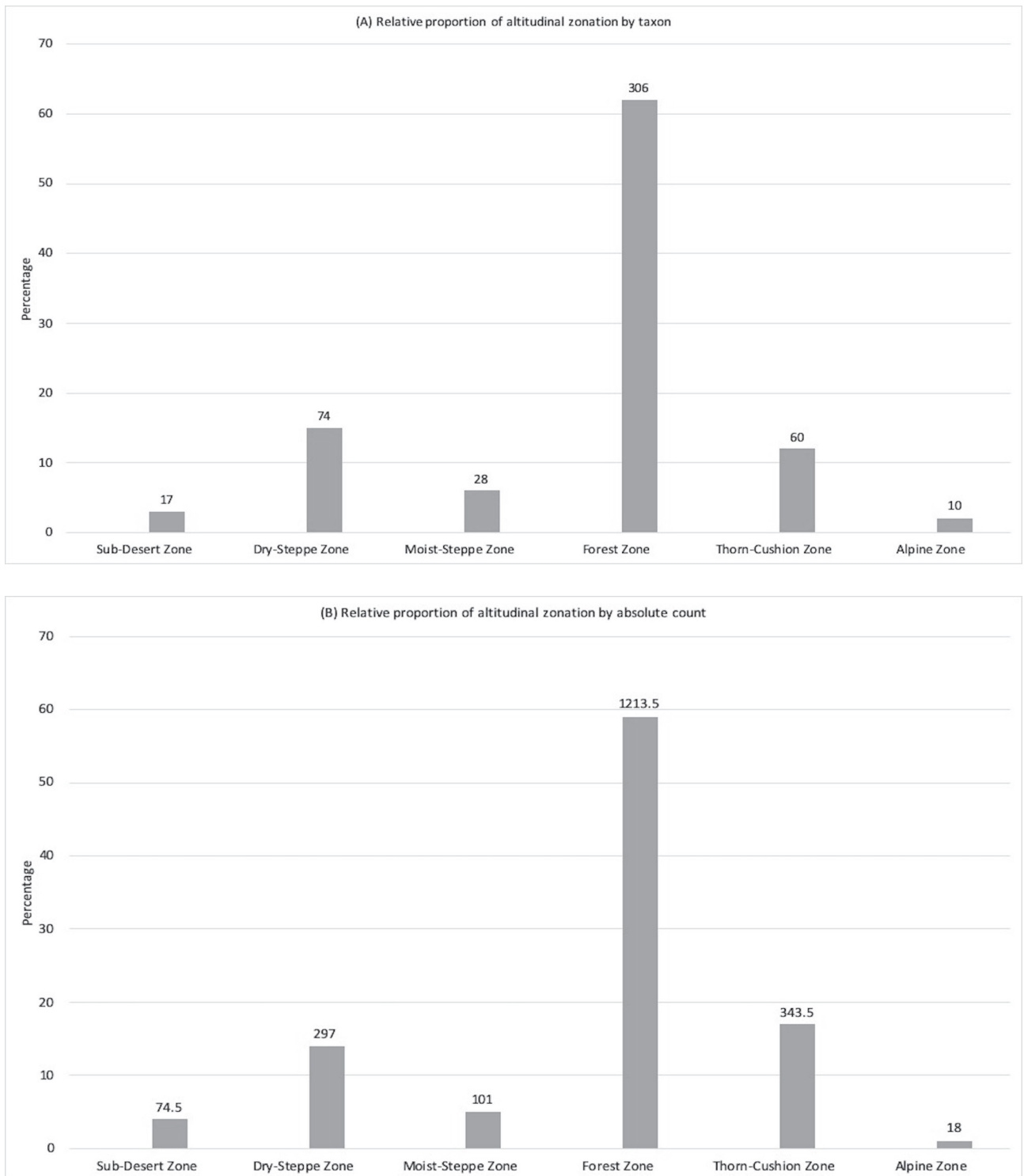


Fig. H9: (A) Relative proportion of altitudinal zonation by taxon. (B) Relative proportion of altitudinal zonation by absolute count. Absolute counts are provided above each bar chart. Prepared by Andrea Squitieri based on data provided by the authors.

Taxon	JAN	FEB	MAR	APR	MAY	JUN	JUL	AUG	SEP	OCT	NOV	DEC	Common Name
Cereals													
<i>Triticum monococcum</i>													Einkorn
<i>Triticum dicoccum</i>													Emmer
<i>Triticum durum/aestivum</i>													Free-threshed wheat
<i>Hordeum vulgare</i>													Barley
<i>Panicum miliaceum</i>													Broomcorn millet
Pulses													
<i>Lathyrus</i> sp.													Lathyrus
<i>Lens culinaris</i>													Lentil
<i>Pisum sativum</i>													Field pea
<i>Vicia ervilia</i>													Bitter vetch
<i>Vicia sativa</i>													Common vetch
cf. <i>Vicia faba</i>													Fava bean
Fruits, Nuts & Oils													
<i>Ficus carica</i>													Fig
<i>Vitis vinifera</i>													Grape
Weeds													
<i>Adonis</i> sp.													Pheasant's eye
cf. <i>Alhagi</i> sp.													Camel Thorn
<i>Anthemis</i> sp.													Chamomile, Mayweed
<i>Astragalus</i> sp.													Milkvetch
<i>Brassica</i> sp.													Wild mustard
<i>Bromus</i> sp.													Brome grass
<i>Buglossoides</i> sp.													Corn Gromwell
<i>Bupleurum</i> sp.													Hare's Ear
<i>Chenopodium</i> sp.													Goosefoot, Lamb's quarters
<i>Eremopoa</i> cf.													Eremopoa
<i>Gallium</i> sp.													Bedstraw
<i>Heliotropium</i> sp.													Heliotrope
<i>Lolium</i> sp.													Rye Grass
<i>Medicago</i> sp.													Burclover
<i>Portulaca</i> sp.													Purslane
<i>Ranunculus</i> sp.													Buttercup
<i>Scorpiurus</i> cf.													Caterpillar Plant
<i>Sinapsis</i> sp.													Charlock
<i>Thymelaea</i> sp.													Thymelaea
<i>Trigonella</i> sp.													Fenugreek
		Winter Rains Livestock Foddering			Spring Harvest			Summer Harvest		Sowing		Winter Rains Livestock Foddering	
						Livestock Pasturing							

Fig. H10: Agricultural calendar for the Dinka Settlement Complex, based on the flowering and fruiting periods for each identified plant species.

been stored fodder from the winter and summer harvests. The agriculturalists of the Dinka Lower Town would have needed to maintain a careful balance, however, because these same plant food stores had to last until spring for the human residents of the settlement as well.

H4. On-site plant use

We now turn to intra-site plant use at the Dinka Lower Town, based on the spatial distribution of the plant remains. Moving east to west (Fig. H1), we begin with Gird-i Bazar East (Fig. H11). The Iron Age strata in this area have been heavily disturbed by later Sasanian graves and modern activities. In addition, the excavators were unable to discover any diagnostic finds or identifiable installations that might clarify the function of this space. The plant remains are equally enigmatic, to an extent. The near lack of chaff remains, except in Outdoor Area 24 (Sample 25), implies that the residents of Gird-i Bazar East did not conduct crop processing indoors, preferring to reserve these activities, like threshing, winnowing and sieving, for outdoor spaces. However, it should be noted, that the unit labeled "Outdoor Area 24" had been severely damaged by later interventions (both Sasanian and modern), hence the possibility cannot be ruled out that it was originally a room rather than an open space³⁷⁹. Only Samples 15 (Room 23) and 16 (Room 1) produced enough botanical remains to establish a viable plant composition profile, and the results are contrasting uses of space for plant activities. The floor of Room 23 mostly contained a spread of pulses, bitter vetch and indeterminate large legumes, while the floor of Room 1 primarily contained a scatter of barley and indeterminate cereal grains. Preliminarily, then, there appears to be a division of space for plant activities, based on the hypothesis that if homogenous plant activities were taking place across Gird-i Bazar East, then the plant profiles across the area would be more similar. The distinctions could be a result of distinct storage, cooking, and consumption practices, and/or a reflection of social differentiation in plant use, like class, age, and/or gender. Lacking supporting lines of evidence, like a distinctive, *in situ* artefact assemblage, however, even additional sample analysis from rooms in this area may not clarify the human-plant relationships in Gird-i Bazar East.

Gird-i Bazar West is an area dedicated to pottery production where the excavators have identified a pottery workshop. Some food was also stored and/or consumed

in this industrial area. *Tannurs* were found in Room 48, Room 28, and Courtyard 21, and food processing may have taken place in Room 16, where the excavators found traces of ashes on a floor in association with stone tools. Like Gird-i Bazar East, there are notably very little to no chaff remains in these intramural contexts, suggesting that the interior rooms of Gird-i Bazar West were not locations of crop processing (Fig. H12). Instead, these potters' rooms appear to have been reserved for plant storage and consumption. In addition, each room generates a unique plant composition profile (with the exception of those rooms only containing 1-3 plant items), not unlike Gird-i Bazar East. This room-by-room diversity suggests context-specific plant activities. For example, the floor of Room 15 (Sample 9) contains an abundance of cereal remains relative to the other samples analysed in this area, and may have been a space dedicated to grain-based plant activities. Sample 9 also contains at least one representative of all the cereals present at Gird-i Bazar, with the exception of einkorn, and it is the origin of the only item of broomcorn millet. Just on the other side of a passageway to the north of Room 15, in Sample 3 from a bread oven (*tannur*), however, there are no cereal remains at all. Instead, the sample is dominated by lentils and unidentified pulses. Sample 6 in Room 19 displays the most similar pulse-heavy profile. Room 22, on the other hand, just east of Room 15, had a variety of plant remains on its floor (Sample 5). Here, we find evidence of Room 22's occupants utilising einkorn (chaff), barley, lentil, faba bean, and grape. It is difficult to further interpret and explain these room-by-room differences. Suffice to say, however, that the spatial organisation of pottery production also appears to extend to plant activities in Gird-i Bazar West. Disparate plant activities appear to be taking place in each room, not unlike the spatial division of labour in Gird-i Bazar West's *chaîne opératoire* of pottery production.

Plant use in Dinka Lower Town 2 (DLT2) is represented in this dataset by one sample, Sample 28, in Room 35 (Fig. H13). These plant remains come from the fill of a large storage vessel found *in situ* in Room 35. Notably, this cache could be representative of a mixed, or maslin cropping system. The vessel contained seeds of equal parts cereals, pulses, and field weeds, similar to the profile of a maslin crop. The cereals represented include emmer, unspecified wheat, and indeterminate cereals (i.e. wheat or barley). The pulses present are lentil, common pea, and indeterminate large legumes. The wild plants are dominated by bedstraw (*Galium* sp.), a very common field weed in winter crops. Tantalisingly, Sample 28 thus hints at the strategy of planting cereals and pulses in tandem to reduce the risk of total crop failure. Separation of wheat,

³⁷⁹ A. Squitieri, personal communication.

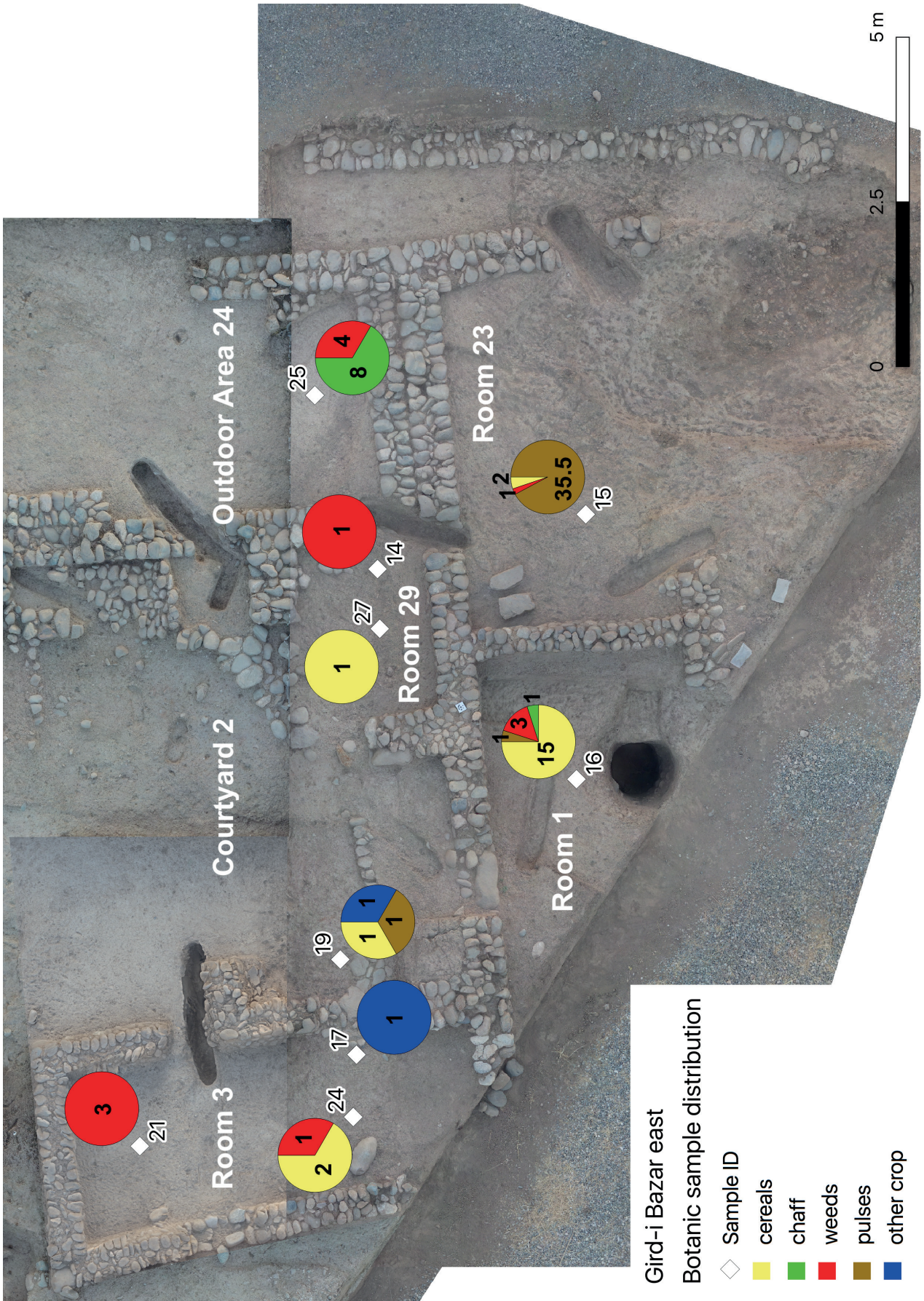


Fig. H11: Map of the plant composition of the samples from Gird-i Bazar East. Map created by Andrea Squitieri.

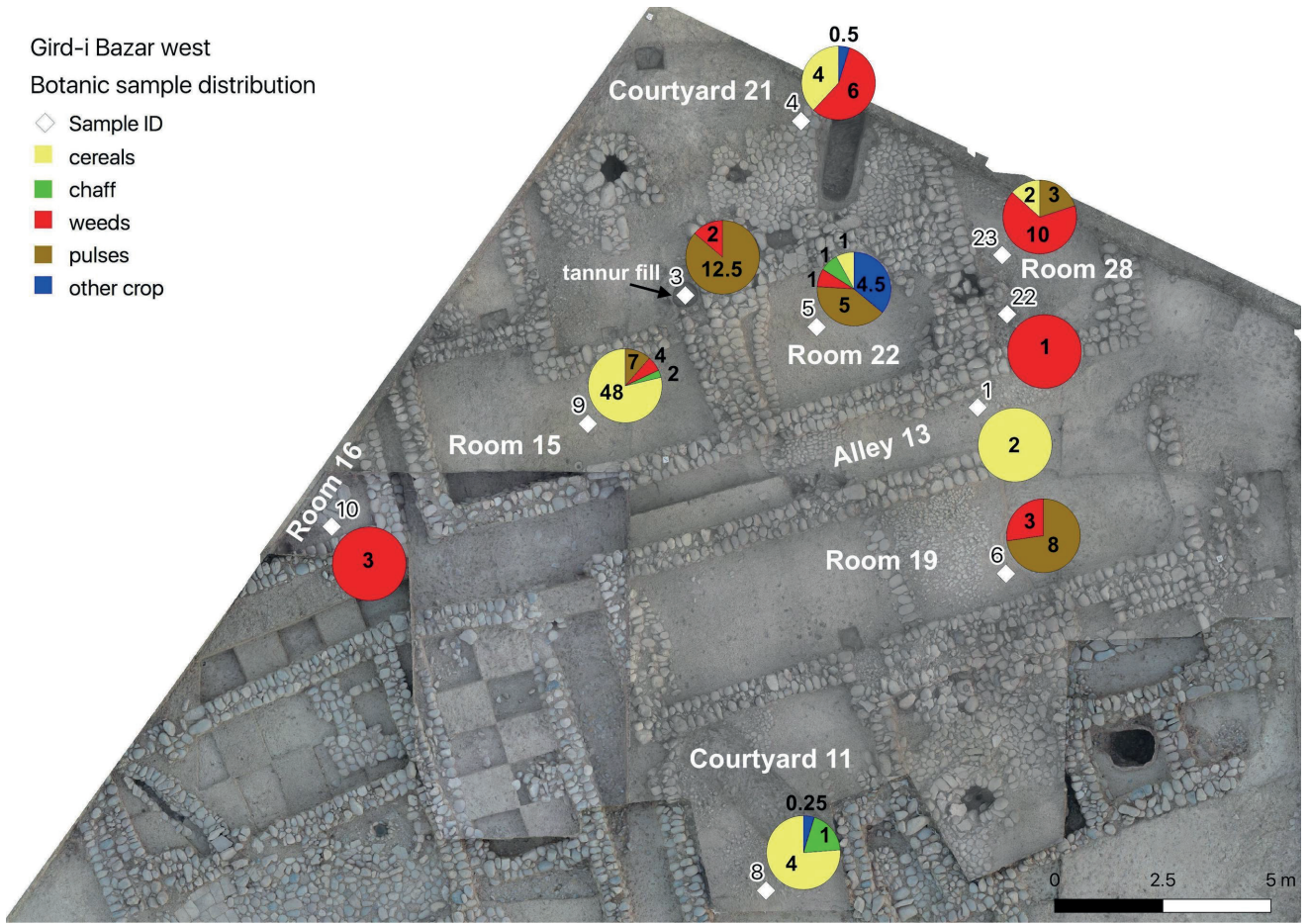


Fig. H12: Map of the plant composition of the samples from Gird-i Bazar West. Map created by Andrea Squitieri.

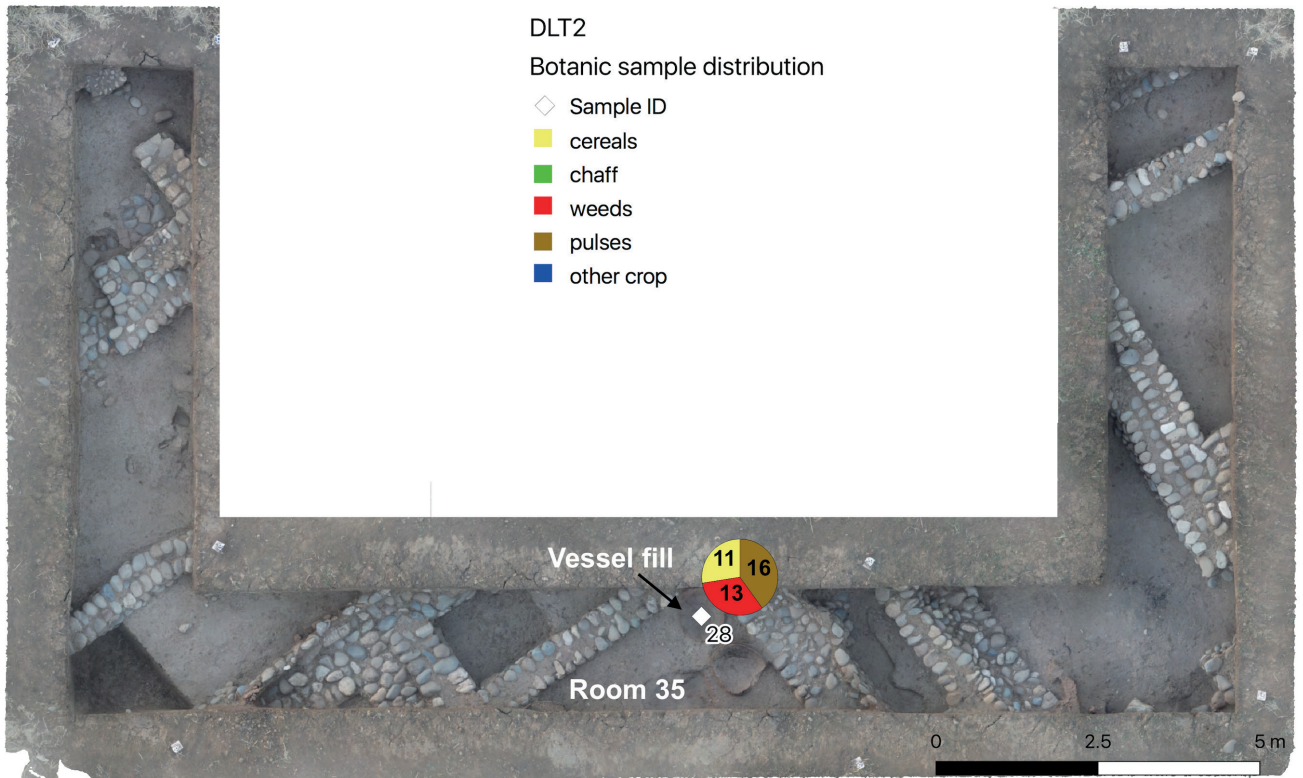


Fig. H13: Map of the plant composition of the samples from Dinka Lower Town 2 (DLT2). Map created by Andrea Squitieri.

DLT3

Botanic sample distribution

- ◇ Sample ID
- cereals
- chaff
- weeds
- pulses
- other crop



Fig. H14: Map of the plant composition of the samples from Dinka Lower Town 3 (DLT3). Map created by Andrea Squitieri.

barley and pulses could then be conducted through sieving and shaking techniques during processing³⁸⁰.

Dinka Lower Town 3 (DLT3) was only partially excavated by the Peshdar Plain Project's archaeological team. The limited exposure produced portions of buildings that contained pottery similar to the types recovered from Gird-i Bazar, suggesting contemporary occupation, along with evidence from radiocarbon dates. In this area, evidence for crop storage and consumption is scant (**Fig. H14**). The three floor samples from Room 64 (Samples 29, 30 and 32) are dominated by wild plants. Combined, the samples from Room 64 contain seeds of indeterminate cereals, wheat chaff (one spikelet fork and one glume base), and pedicles and fragments of grape. Sample 31 from the floor of Outdoor Area 63, however, contains a great variety of edible plants: wheat, barley, lathyrus, lentil, common vetch, and grape. There is only one chaff item in Sample 31, indeterminate cereal culm, even though Outdoor Area 63

is presumed to be a preferred location for crop processing, giving the spatial patterns in Gird-i Bazar East and West. Either crop processing was not conducted (only) in outdoor spaces in DLT3, or loci containing evidence for outdoor processing activities were not revealed in the opened DLT3 trenches. Interestingly, all four samples from DLT3 contained grape remains – not whole grape pips themselves, only pedicles and pip fragments. No other area in this dataset approaches the 100% ubiquity of grape remains found in DLT3. Although the sample size is too small to draw any conclusions, one possible interpretation is that these are the by-products of wine-pressing: the pomace of wine must contain pedicles and pip fragments that would have been sieved from the grape juice and reserved as fertilizer or fuel³⁸¹. To be clear, however, much greater quantities of grape pedicles, peduncles, and pip fragments would be expected of on-site wine-pressing practices.

380 Jones/Halstead 1995, 105.

381 Margaritis/Jones 2006, 799.

I. A Chalcolithic kiln in the Bora Plain

*Andrea Squitieri, Mark Altaweel, Silvia Amicone, Jean-Jacques Herr,
Sophie Pietsch & Jens Rohde*

This chapter outlines the results of the excavation of a Chalcolithic kiln found in the Bora Plain (UTM 38N 512258 E; 3999222 N), underneath the Iron Age structures of the Dinka Settlement Complex in operation DLT₃ (**Fig. A3**). The fieldwork was made possible by a Rust Family Foundation Archaeology Grant awarded to Andrea Squitieri and Mark Altaweel (UCL) and took place between 19 April and 5 May 2019.

1.1 The discovery of the kiln and the goals of the 2019 excavation

Andrea Squitieri & Mark Altaweel

In 2015, during the first fieldwork season of the Peshdar Plain Project whose excavation component targeted Gird-i Bazar, three geoarchaeological trenches (GA₄₀, GA₄₁, and GA₄₂) were opened between Gird-i Bazar and Qalat-i Dinka in order to investigate the geology of the Bora Plain³⁸². At that time, these trenches were deemed to be “off-site” as there was no evidence for the existence of archaeological features in the flat area in between Gird-i Bazar and Qalat-i Dinka; the settlement's full extent only became apparent in autumn 2016 after conducting an extensive magnetometer survey³⁸³.

The third of these trenches (GA₄₂) was opened about 400 m southwest of Gird-i Bazar. Excavated by backhoe, it measured about 3×8 m and reached a maximum depth of about 5 m. During its excavation, some archaeological features were intercepted, including a wide burnt area appearing in section, about 1.5-2 m below the surface, that was thought to possibly be a kiln³⁸⁴. In autumn 2018, because of the promising Iron Age ¹⁴C date retrieved from GA₄₂³⁸⁵, we resumed excavations in this location by opening a 8×10 m trench (dubbed DLT₃), designed to include

GA₄₂ (**Fig. 11**). Its archaeological excavation uncovered parts of three buildings (designated Q, R, and S) that are firmly dated to the Iron Age on the basis of pottery and radiocarbon datings³⁸⁶ (**SA**).

During the 2018 excavations, the GA₄₂ geoarchaeological trench was partially reopened, and the burnt area was re-exposed. We investigated this burnt area from the old 2015 section without removing the Iron Age wall above it. This new work confirmed that the structure was indeed a kiln, with a partially-exposed central column and fills on either side that contained burnt layers combined with collapsed architectural elements³⁸⁷ (**Figs. 12, 13**). It also became clear that the kiln partially cut into a layer of natural pebbles beneath it³⁸⁸. Based on preliminary observations made by Jean-Jacques Herr, the pottery collected from the kiln was dated to the Chalcolithic period³⁸⁹. Opposite the kiln, a portion of a floor (Locus:226922:055) was intercepted about 50 cm beneath the Iron Age floor of Building R's Room 64³⁹⁰ (**Fig. 14**). On the floor Locus:226922:055, some pottery was found that was also dated to the Chalcolithic period³⁹¹.

The pottery survey conducted by Jessica Giraud and her team in 2013 and 2015 had found Chalcolithic pottery throughout the Bora Plain³⁹²; however, no structures related to this period were exposed during our excavations at Gird-i Bazar, DLT₂, and the operations on the western slope of Qalat-i Dinka. The discovery of Chalcolithic features in DLT₃ in 2018 came as a complete surprise.

382 Altaweel/Marsh 2016.

383 Fassbinder/Ašandulesei/Scheiblecker 2017.

384 Altaweel/Marsh 2016, 27, Fig. B2.6.

385 Altaweel/Marsh 2016, 28, Fig. B2.7.

386 Radner/Kreppner/Squitieri (ed.) 2019, 68-93.

387 Palmisano 2019, 75, Fig. E9.

388 This layer had become already visible in 2015 in the section of the test trench GA₄₂ (Altaweel/Marsh 2016, Fig. B2.5), but it was then misinterpreted as a possible floor.

389 Palmisano 2019, 75; Herr 2019, 114.

390 Rohde 2019, 74-75.

391 Herr *et al.* 2019, 114. Initially, the pottery was preliminarily assigned to the Late Chalcolithic period; however, the 2019 excavations have permitted us to update the chronology (see the following discussion).

392 Giraud 2016.

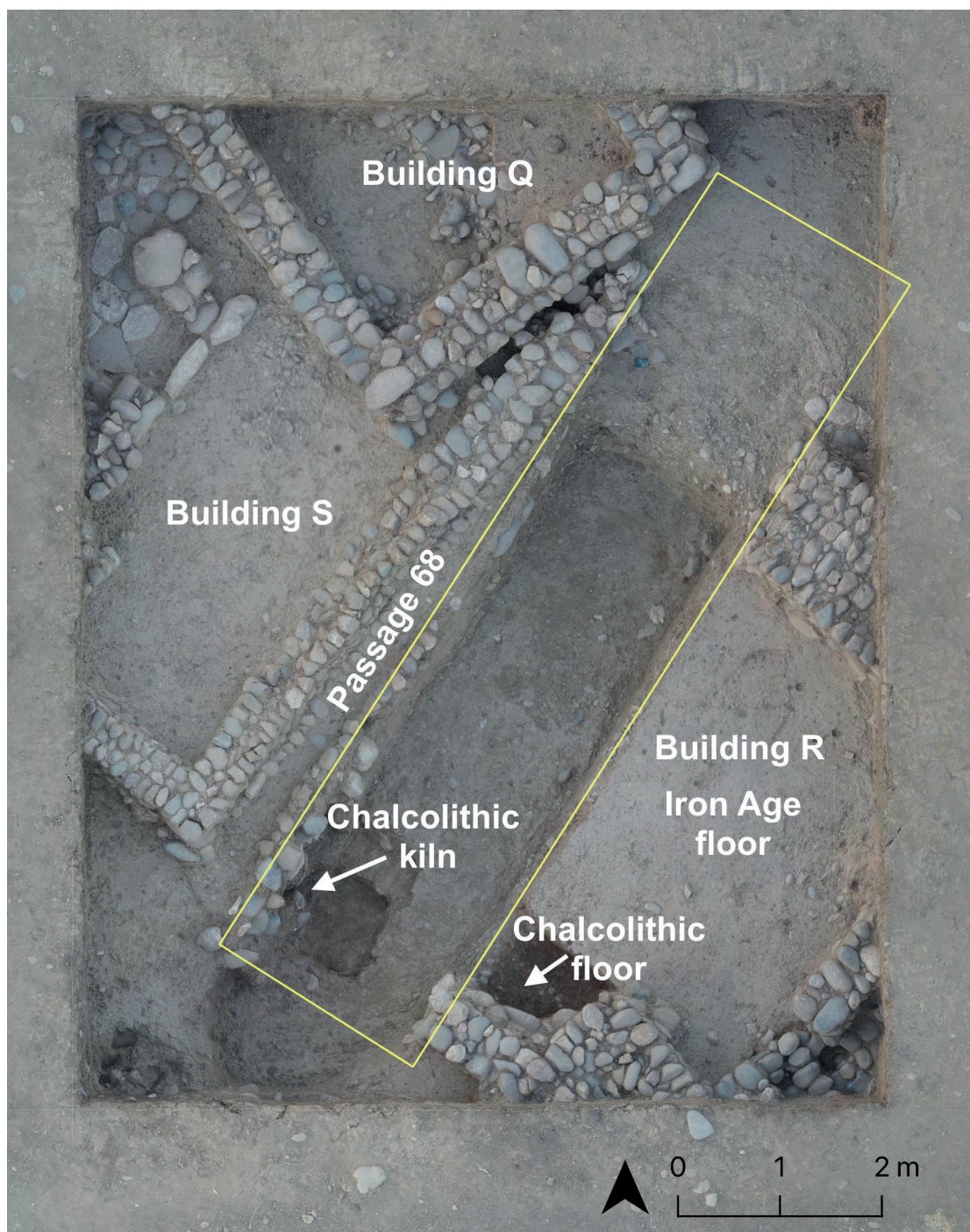


Fig. 11: Orthophoto of the excavation area DLT3 at the end of the 2018 excavations. It shows the Iron Age structures (Buildings Q, R, S and Passage 68), the limits (yellow line) of the 2015 geoarchaeological trench (GA42), and the Chalcolithic features found below the Iron Age remains. Prepared by Andrea Squitieri.

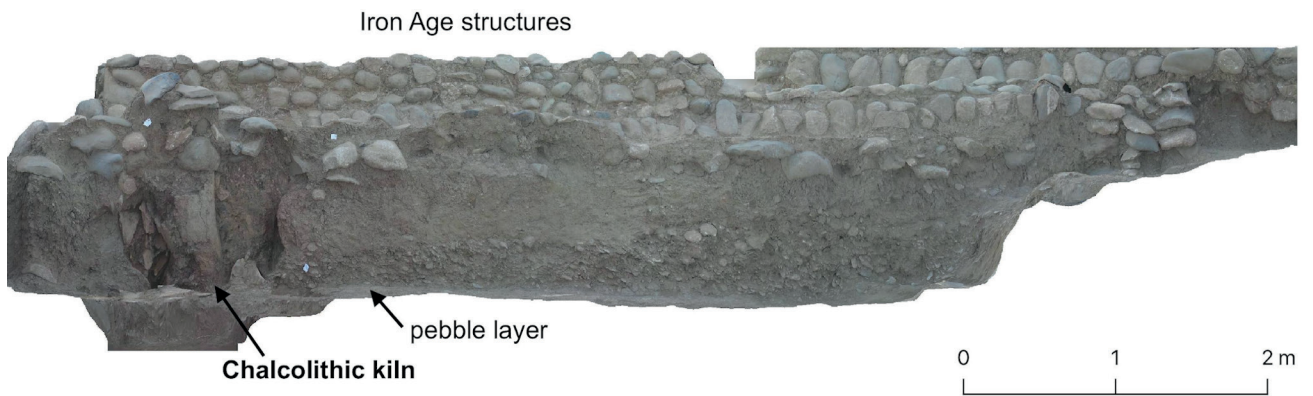


Fig. 12: Orthophoto of the northwestern section of the trench GA42 showing the Chalcolithic kiln at the end of the 2018 excavations, the Iron Age wall above it, and the natural pebble layer into which the kiln had been cut. Prepared by Andrea Squitieri.

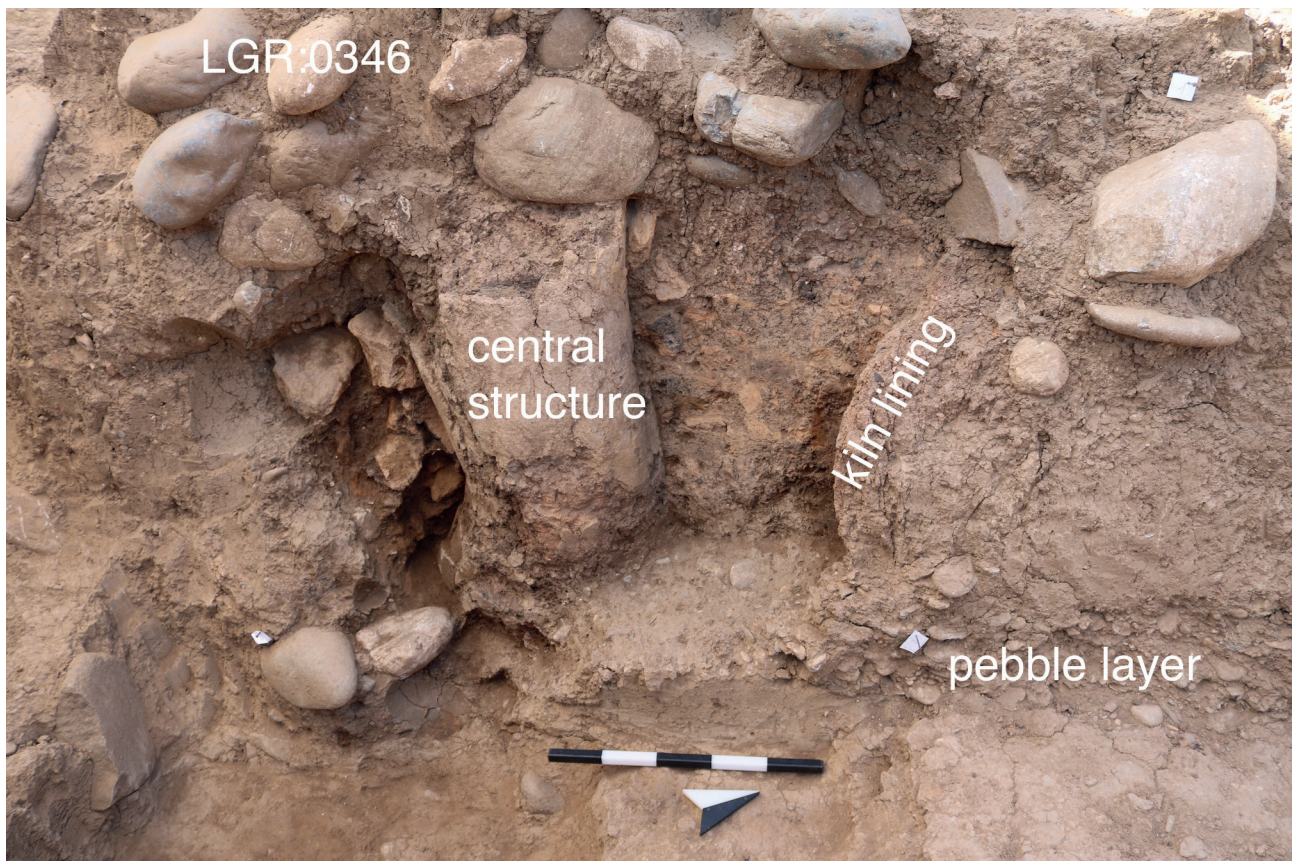


Fig. 13: The Chalcolithic kiln at the end of the 2018 excavations. Photo by Andrea Squitieri.



Fig. 14: The Chalcolithic floor under the Iron Age floor of Building R, at the end of the 2018 excavations. Photo by Jens Rohde.

Without the backhoe trench of GA42 and its exposure of archaeological layers, we would not have had any clue as to the existence of a Chalcolithic settlement in this area since they had been completely sealed by the Iron Age structures above, which were the focus of our 2018 excavation. The discovery of the kiln greatly contributes to our understanding of the Chalcolithic period in the Bora Plain, and more generally in the Peshdar Plain and the Zagros mountains that surround it, and this prompted us to seek further funding to continue the kiln's excavation in the spring of 2019 alongside the already scheduled geoarchaeological fieldwork campaign. The 2019 excavations of the Chalcolithic kiln had the following three goals:

- to excavate the pottery kiln in its entirety to uncover its structure;
- to analyse the pottery retrieved from a morphological and technological point of view through both macroscopic analysis and thin sections;
- to collect samples for radiocarbon dating, micromorphological analysis and archaeomagnetic analysis.

The excavation was continued according to the digital excavation methods established for the Peshdar Plain Project in 2015, entailing:

- the use of a MySQL-based database designed by Christoph Forster (Berlin, www.datalino.de);
- the use of a dGPS to allow 3D measurements of all stratigraphic units as well as relevant find spots (i.e.,

finds, samples), using the locus-collection registration system according to the Peshdar Plain Project protocol (as summarised in §C1);

- the creation of daily orthophotos and Digital Elevation Models by means of a DJI Phantom 4 Pro drone combined with the software Agisoft Metashape (an updated version of Agisoft PhotoScan);
- the creation of a 3D stratigraphy model through the visualisation of each stratigraphic unit (locus) within the Metashape-generated model by means of Autodesk AutoCAD 2018 software³⁹³.

The sections below present a first assessment of the results and the outcome of some of the analyses carried out on the pottery material. Further results of the ongoing pottery, micromorphology, and archaeomagnetism analyses will be published once they have been completed.

I.2 2019 excavation results

Jens Rohde & Sophie Pietsch

In order to proceed with the excavation of the kiln, it was necessary to remove the Iron Age wall that superimposed it, called LGR:0346. This was the south-eastern portion of the wall of Passage 68, a narrow passage between the Iron Age Buildings S and R³⁹⁴ (Figs. 11, 12, 13). Only about one third of the kiln is preserved, because it was destroyed in the south-west by the cut of the geoarchaeological trench GA42 while to the south it was damaged by an Iron Age disturbance (Fig. 15). The preserved structure of the kiln was given the locus number Locus:225922:056. Originally, the kiln consisted of two parts. The upper part was the firing chamber, which would have been above ground, while the lower part, comprising the combustion chamber, was recessed into the ground. The former, however, was not preserved. Only a few of its tumbled remains were found inside the kiln fill. The combustion chamber was dug into the ground from a floor or a surface destroyed by the Iron Age construction. Immediately below this structure, the highest parts of the combustion chamber could be observed. This chamber reaches down to the natural layer of pebbles called Locus:225922:089. Above this layer, there is a dark yellowish-brown soil with some pebbles into which the cut for the kiln, named Locus:225922:057, was dug.

The lining of the combustion chamber consists of heavily fired clay, grey-greenish in colour. At the rear of the

³⁹³ Squitieri/Rohde 2019.

³⁹⁴ Palmisano 2019, 75, Fig. E4.



Fig. 15: Orthophoto of the Chalcolithic kiln during the 2019 excavations. Grid with 50 cm spacing, annotated with UTM coordinates (North coordinates on the left, East coordinates on top). Photo by Jens Rohde. Prepared by Andrea Squitieri.

kiln, the lining has a reddish tinge, caused by the heat. The lining extends down almost vertically, only interrupted when it meets the bottom of the combustion chamber. The pebble layer, Locus: 225922:089, surfaces at the lowest part of the combustion chamber. A partially preserved column is found close to the center of the combustion chamber (**Figs. 16, 17**). This column has a diameter of about 30 cm and is made of a light-greyish, clayey material with a 3-4 cm thick lining. Its lower half is broken, and it now sits in a slightly slanted position because of destructive processes that occurred after the kiln ceased to be used.

The northwestern portion of the kiln was filled with a dark brown soil embedded with architectural elements from the uppermost construction, labelled LGR:0364 (made up of Locus:225922:049, Locus:225922:080, Locus:225922:082, Locus:225922:083 and Locus:225922:084) (**Fig. 18**). The architectural elements were gathered in several collections³⁹⁵. Among these, there were fragments with a plano-convex shape, which are part of the supporting structure located

between the kiln edge and the central column (**Fig. 19**). These fragments come in a variety of sizes. There were also fragments that are flat on one side and concave on the other, which probably helped to fix the plano-convex elements between the column and the kiln edge. Some curved fragments were possibly part of the perforated kiln floor (**Fig. 110**). Several thick pieces with a flattish shape probably belonged to the outer construction of the firing chamber. Overall, the kiln fill yielded various architectural fragments belonging to the intermediate zone between the two chambers as well as fragments belonging to the outer edge of the firing chamber. Several samples were taken from the kiln fill for an array of purposes, such as phytolith analysis, micro-debris flotation, pyrotechnology, and micromorphology. There were a few finds in this fill, namely some pottery sherds, and a few flint and obsidian fragments (PPP 225922:080:010, PPP 225922:083:003, PPP 225922:083:005 and PPP 225922:084:003).

Above the kiln, deposit LGR:0365 covered the preserved remains of the combustion chamber. This is a moist, clayey, greyish-brown soil containing a few pottery sherds (Locus:225922:071, Locus:225922:079, Locus:225922:081) representing an intermediate zone that post-dates the

³⁹⁵ Collections: PPP 225922:049:018, PPP 225922:080:004, 009, 011, 013, PPP 225922:082:004, 005, PPP 225922:083:004.



Fig. 16: The structure of the Chalcolithic kiln towards the end of the 2019 excavations, viewed from south. Photo by Jens Rohde.



Fig. 17: The structure of the Chalcolithic kiln towards the end of the 2019 excavations, viewed from east. Photo by Jens Rohde.



Fig. 18: Collapsed architectural elements in the kiln fill, belonging to the kiln's upper structure. Photo by Jens Rohde.



Fig. 19: Fragment of a plano-convex architectural element. Photo by Sophie Pietsch.



Fig. 110: Fragment of the kiln floor. Photo by Sophie Pietsch.

Late Chalcolithic and pre-dates the Iron Age. Pottery from both periods was found in this deposit. In the southernmost part of the kiln an Iron Age disturbance, excavated as LGR:0367 (Locus:225922:074, Locus:225922:085), is responsible for the partial destruction of the combustion chamber. It was filled with dark brown soil, some bones, baked bricks and pebbles. It contained both Chalcolithic and Iron Age pottery. It is possible that LGR:0367 is the fill of a pit that cuts into the combustion chamber. Inside LGR:0367, Locus:225922:087 cuts the debris sloping from the southeast.

In the area above the kiln structure and above the deposit LGR:0367, a cut, named Locus:225922:073, is visible. It was made for the construction pit of the Iron Age wall LGR:0346. Its fill, Locus:225922:072, is composed of a yellowish-brown, clayey soil and contained, in addition to some pottery sherds and charcoal, the cobbles of the Iron Age wall LGR:0346, which had not been uncovered in 2018 (Fig. 111). More cobbles from this wall were excavated further to the north, and assigned the label Locus:225922:078. Some of these cobbles were placed directly on top of the kiln structure. Hence, it seems that it was the construction of the Iron Age wall that affected the kiln structure and was responsible for its partial destruction.



Fig. 111: The fill Locus:225922:072 of the cut opened for the construction of the Iron Age wall above the Chalcolithic kiln. Photo by Jens Rohde.

I.3 The kiln's structure and its parallels

Sophie Pietsch

Based on its preserved structures, the kiln had a free-standing, double-chamber updraught construction, with an underground combustion chamber, a central column supporting the kiln floor, and holes positioned between the combustion chamber below and the firing chamber above. The closest match for this type of structure are the “development line V” kilns in Boroffka and Becker's typology³⁹⁶.

During excavations, the kiln entrance could not be identified. In structures where fire is employed, it is common to place the entrance in a direction that would be protected from disturbing agents such as winds. In the Bora Plain, winds normally blow in a northwesterly direction. Therefore, the kiln entrance is likely to have faced south or southwest, and this is precisely where the kiln structure has not been preserved.

Comparisons for this type of kiln are available at several Chalcolithic sites in Iraq and Iran. In Iraq, two-chamber kilns dated to the 5th millennium BC have been found in Tell Abada in the Hamrin basin. One of them (no. 11) is a close parallel to our kiln as it has a floor with holes supported by vertical structures and a central column; on the other hand, kiln no. 13 from the same site shows two lateral protrusions and a quasi-rectangular shape³⁹⁷.

In southwestern Iran, parallels to our kiln are known from Darre-ye Bolaghi in the province of Fars where several kilns dated to the late Fars Chalcolithic Period (ca. 5500-4300 BC) were found. Kiln 405 (Site 73) has a quasi-rounded shape like ours, although its middle wall supports the kiln floor rather than a central column. Our kiln more closely matches Kiln 504 (Site 131), which features a kiln floor formed by a platform with holes on the edges, connected to a central column³⁹⁸. In the published photograph of this kiln, some plano-convex architectural elements are visible that resemble those found in our kiln's fill. In Kiln 110 (Site 73), these elements form an intermediate floor, which then serves as a stacking platform, leaving gaps for holes. Above this, another clay layer was applied to insulate the construction thoroughly. This double-floor construction is another potential parallel for our kiln.

In central Iran, another close match for our kiln was discovered at the site of Arisman in the province of Isfa-

³⁹⁶ Boroffka/Becker 2004, 219.

³⁹⁷ Jasim 1985, Fig. 35a; Fig. 39.

³⁹⁸ Helwing/Seyedin 2016, 286.

han. There, the late 4th millennium BC levels have yielded a pottery kiln showing a central column connected to the kiln walls by a radial structure that supported the kiln floor³⁹⁹.

I.4 The Ubaid/LC1 pottery associated with the kiln

Jean-Jacques Herr & Silvia Amicone

Only very few pottery sherds were collected from the kiln fill (24 diagnostic sherds and 83 non-diagnostic sherds). Importantly, the pottery shapes matched those that had been found in 2018, allowing us to securely link the kiln's use with the floors found at the other side of the backhoe trench of GA42⁴⁰⁰.

The assemblage includes non-diagnostic sherds belonging to a pot with a flared rim, polished walls and faint traces of red painting (Figs. 112–113). The sherds are made of a fabric that, macroscopically, consists of 15–20 % large, shiny, reddish-grey, sub-angular, moderately-sorted inclusions (4.6–8.5 mm long, 2.5 mm wide), 10 % small, blue-grey, sub-angular, well-sorted inclusions, and 10 % tiny, shiny yellow inclusions. There is a small amount (5 %) of planar voids (8.2 mm long, 0.4 mm wide) probably left by the combustion of organic materials. The colour of the surface is heterogeneous, ranging from red to dark brown. The outside wall of this pot presents a shiny topography with almost no visible striations whereas large inclusions are embedded inside the wall of the vessel. This may indicate the use of a textile for polishing the surface in order to give the outside of the pot a hard leathery consistency⁴⁰¹. Moreover, faint traces of a very thin reddish layer have been found on both the outer and inner surfaces (Fig. 113.1–2). Parallels for this type of pot (sometimes described as “angle-neck jar”) can be found in the nearby site of Qalat Said Ahmadan (Ubaid layer 1 in Operation E)⁴⁰², and in the Shahrizor Plain at Gurga Chiya (Trench E)⁴⁰³. Further afield, such containers also occur at Tepe Gawra (Level XII A)⁴⁰⁴. Parallels for the surface treatment can also be found in the Iranian Zagros where the sites of

Hajji Firuz Tepe⁴⁰⁵ and Dalma Tepe⁴⁰⁶ both yielded painted and polished pottery.

Our kiln also contained round and thinned everted rim fragments, made of an orange-coloured fabric with plant tempering (probably chaff, as is also suggested by the results of the ongoing petrographic analysis). These rims most likely belong to deep bowls. Parallels are known from Tepe Gawra (Level XII), including a flared rim pot with plant tempering⁴⁰⁷.

Moreover, we found two fragments that together form the complete profile of a small conical bowl with a flat base (Fig. 112.2.a, Fig. 114.1–2). This vessel was built from four levels of coil segments. The wall was formed by compressing the coils and spreading the clay with an upward movement of the fingers, a technique that obliterated the coil joins. Fig. 114.2 clearly shows a preferential fracture following the coil joins at the end of the clay accumulation on the first layer of coil. Macroscopically, the fabric of this bowl is composed of 5–10 % large, grey, sub-angular inclusions, 5 % fine, white, sub-rounded, well-sorted inclusions, and 1 % tiny, shiny inclusions. The main temper consists of an abundance of fine plant material (4.3 mm long, 0.3 mm wide). The colour is mostly orange and the firing is semi-oxidizing. Morphological parallels are known from Tepe Marani⁴⁰⁸ and Gurga Chiya⁴⁰⁹ in the Shahrizor Plain and from Hajji Firuz Tepe in Iran, dating from the “Late Neolithic” to the end of the 6th millennium BC⁴¹⁰. The vessel from our kiln is not burnished, in contrast to the examples from Gurga Chiya and Hajji Firuz Tepe.

Overall, this preliminary assessment of our kiln's pottery and its known parallels suggest an Ubaid to Late Chalcolithic 1 date⁴¹¹, ranging from the late 6th millennium BC through the 5th millennium BC⁴¹².

A sample for petrographic analysis was taken from a flared rim pot (PPP 226922:057:001; Fig. 112.1) made from

399 Boroffka/Becker 2004, 220; Boroffka *et al.* 2011, 34.

400 Herr *et al.* 2019, 114

401 In an experimental and traceological study, Lepère 2014, 150–151 called this “furbishing”.

402 Tsuneki *et al.* 2016, 100, Fig. 2.10.1–2.

403 Wengrow *et al.* 2016, 267, Fig. 12.4–6.

404 Tobler 1950, pl. CXXXVIII, 291.

405 Voigt 1983, pl. 19 and pl. 21 (“red washed and burnished”).

406 Some sherds found in Kul Tepe VIII in northwestern Iran show a smoothed and reddish shiny surface designated as “Dalma red-slipped”. For comparisons, see Hamlin 1975, 117, Fig. 9.A–D; Abedi *et al.* 2015, 328, Fig. 5. In the material recovered from our kiln, however, no painted motifs (such as the inverse triangular motif or the zig zag pattern) have been observed.

407 Herr *et al.* 2019, 116, Fig. G1.9.1.

408 Wengrow 2016, 273, Fig. 19.1–6, where the description of the fabric is similar to PPP 225922:082:003:001 (Fig. 114).

409 Wengrow 2016 *et al.*, 267, Fig. 12.23.

410 Voigt 1983, 75.

411 For a synthesis of the Northern Ubaid–LC1 chronological framework, see Peyronel/Vacca 2015.

412 We would like to thank Johnny Samuele Baldi (Institut français du Proche-Orient, Beirut) for his help in identifying the pottery and indicating the parallels with Gurga Chiya and Tepe Marani.



Fig. I12. Chalcolithic period pottery: (1) from the fill Locus:226922:057 above the floor excavated in 2018, and (2) from the kiln fill Locus:225922:082 excavated in 2019: (a) diagnostic sherds from a small conical bowl (PPP 225922:082:003:001+002); (b) non-diagnostic bodysherds from a polished and painted pot similar to the specimen shown in (1). Prepared by Jean-Jacques Herr.

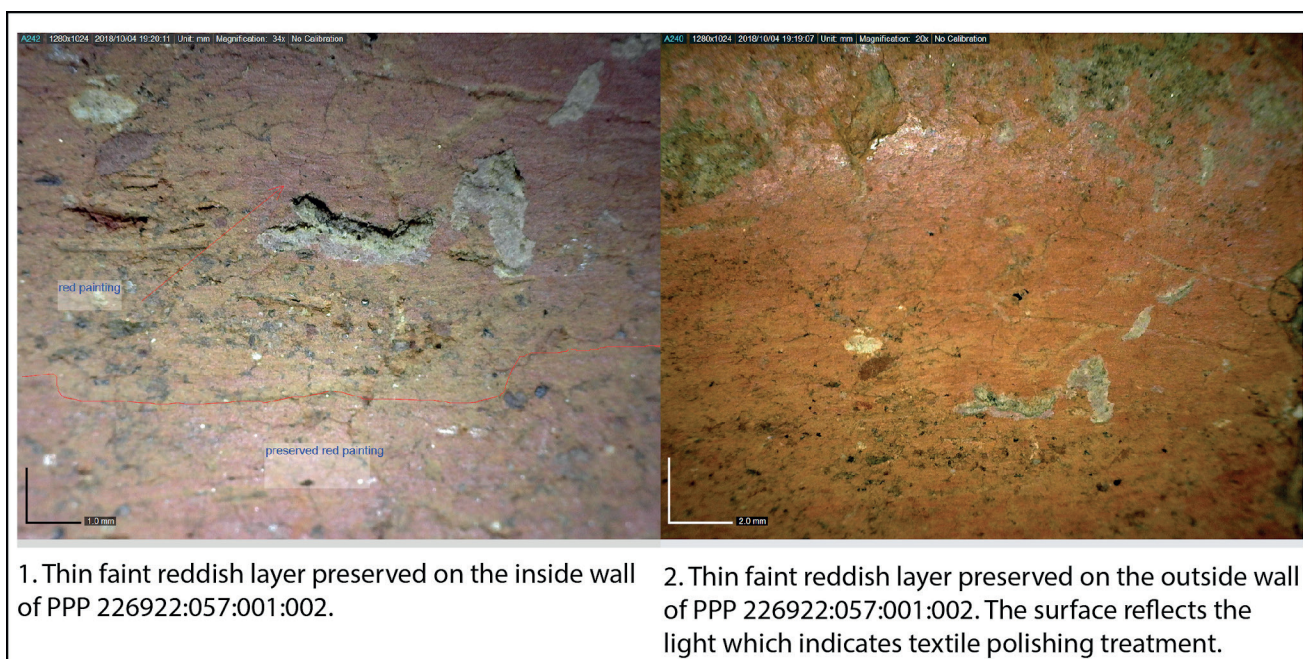


Fig. I13. Dino-Lite microscope images of a sherd belonging to the polished and painted pot of Fig. I12.1, showing the surface treatment on the inside (1) and the outside (2). Prepared by Jean-Jacques Herr.

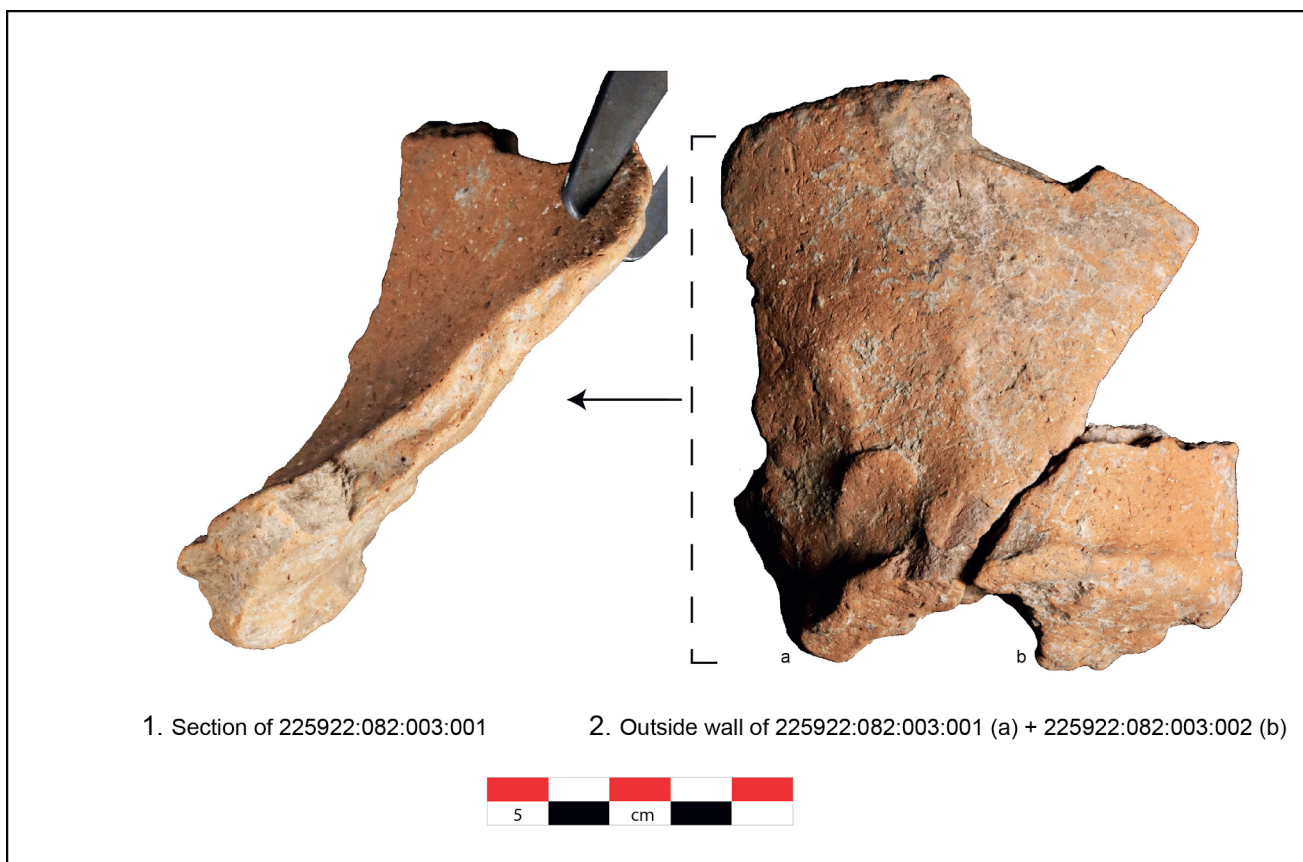


Fig. I14: Sherds PPP 225922:082:003:001 and PPP 225922:082:003:002 from the conical bowl found in the kiln fill: (1) section; (2) outside wall. Prepared by Jean-Jacques Herr.

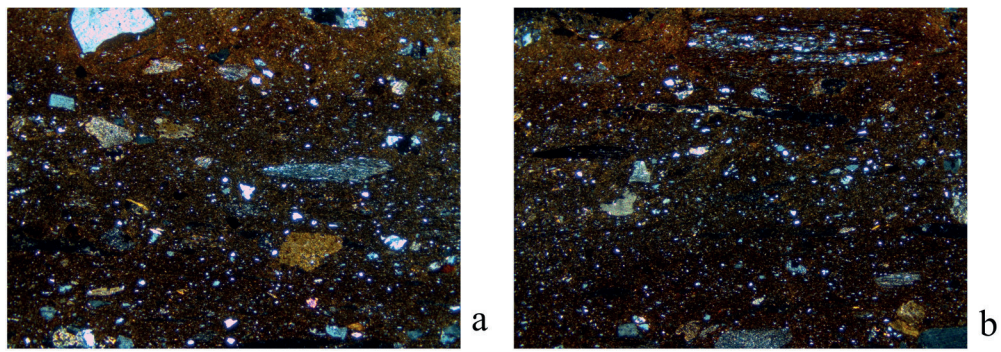


Fig. 115: Thin-section photomicrographs of sample PPP 226922:057:001:001 (= laboratory number PPP 110): (a) with metamorphic rocks and micrite XP; b) with foliated metamorphic rocks composed of quartz and biotite XP. Image width = 6 mm. Prepared by Silvia Amicone.

one of the most common fabrics encountered among the sherds of the Chalcolithic period associated with our kiln. The sample number PPP 226922:057:001:001 corresponds to the laboratory number PPP 110. The petrographic study showed that this sample's fabric features metamorphic inclusions and micritic calcite (**Fig. 115**) and is very similar to Fabric C₁, which is characteristic of the Iron Age pottery of the DSC⁴¹³. This suggests that the same local clay sources were in use during both the Chalcolithic period and the Iron Age.

Detailed petrographic description⁴¹⁴: Quartz (sa.-eq., max=0.30 mm, mode=0.08 mm) and fragments of foliated metamorphic rocks (sr.-el., max=2.8 mm, mode=0.80 mm) composed of quartz, muscovite and biotite are common. Micritic and sparry calcite (wr.-eq., max=2.5 mm, mode=0.85 mm). Few inclusions of plagioclase (sr.-eq., max=0.50 mm, mode=0.20 mm), biotite (sr.-el., max=0.35 mm, mode=0.20 mm), muscovite (sa.-el., max=0.30 mm, mode=0.20 mm) and clay pellets (wr.-eq., max=0.65 mm, mode=0.50 mm) were observed. Very rarely epidote (sa.-eq., max=0.35 mm, mode=0.30 mm). The grain size distribution is polymodal. Voids are vesicles and vughs, and they do not show any preferential orientation. The matrix is light brown in PPL and orange to brown in XP. The matrix is non-calcareous, and the sample exhibits low optical activity.

1.5 The kiln's radiocarbon dating and preliminary conclusions

Andrea Squitieri

A charcoal sample was collected from the kiln fill (sample PPP 225922:049:019) and analysed for ¹⁴C dating at the Curt-Engelhorn-Zentrum Archäometrie in Mannheim (Germany), producing a date range of 5218–5024 calBC (95.4% probability) (**Fig. 116**). This date roughly corresponds to Ubaid 3-4 in southern Mesopotamia and “Northern Ubaid” in northern Mesopotamia⁴¹⁵, hence confirming the results obtained from the pottery analysis and also matching the dates assigned to some of the structural comparisons identified for the kiln itself.

The 2019 fieldwork completed the excavation of a Chalcolithic pottery kiln, preserved underneath the Iron Age structures of the Dinka Settlement Complex in the area of the excavation area DLT₃. For the kiln's double-chamber structure with a central column supporting the kiln floor, architectural parallels can be found on the Iranian plateau, indicating close links between the Bora Plain and Iran at this time. Based on morphological comparisons, the pottery retrieved can be attributed to the Ubaid – Late Chalcolithic 1 period, and this dating fits well with the radiocarbon date obtained for the kiln fill, which falls into the late 6th millennium BC. Further analysis of the materials retrieved from the kiln is ongoing and will be published in the future.

⁴¹³ Amicone 2017a; 2018; 2019. See also §D2.

⁴¹⁴ For the abbreviations and terminology, see §D2.

⁴¹⁵ Stein/Alizadeh 2014, Table 1.

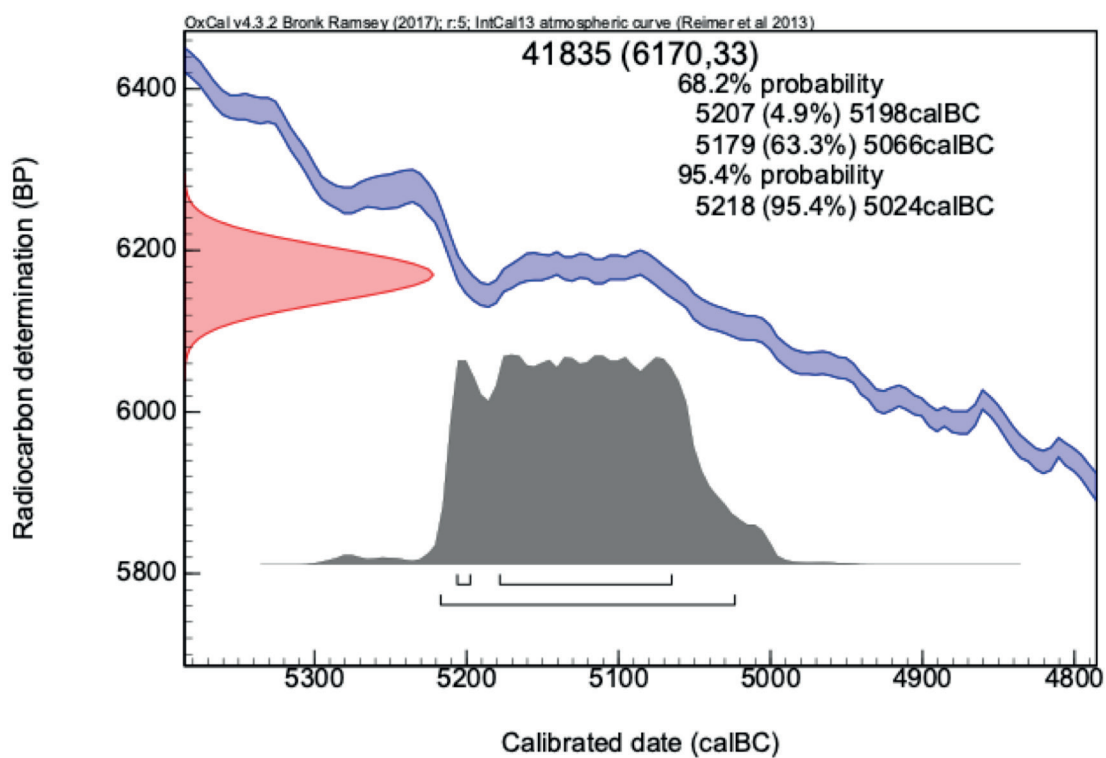


Fig. I16: Calibrated radiocarbon date for the charcoal sample from the Chalcolithic kiln (MAMS-41835). Calibration software OxCal v4.3.2.

J. Preliminary report on the archaeological survey of the Iron Age sites in the central part of the Sardasht district, Iran

Salahaddin Ebrahimipour, Kazem Mollazadeh & Ali Binandeh

The Iranian stretch of the river basin of the Lower Zab is a poorly known area. This area runs through the Sardasht district, the Piranshahr district, and a part of the Baneh district which geographically are located in the western strip of the Zagros mountains in northwestern Iran (**Fig. J1**). Politically, the area is situated in the south of West-Azərbayjan Province and in the northern area of the Kurdistan Province.⁴¹⁷ This area of the Zagros Mountains, based on its environmental and biological features, has been of interest to humans from prehistoric to contemporary times.⁴¹⁸ Its location in the Lower Zab River Basin, and its proximity to the Urmia Lake Basin in the north and Mesopotamia in the west, gives it great importance for archaeological studies.

Archaeological surveys of the central part of the Sardasht district in the southern area of the Lower Zab river basin were made in spring and summer 2018. Our surveys aimed to identify new Iron Age sites and to review known sites in the area based on the evidence from the site of Rabat. During our archaeological survey of the central Sardasht district, a significant number of archaeological sites, from the prehistoric to the Islamic periods, were identified and registered.

J1. The surveyed area

The Sardasht district, with an area of 1411 km², is located in the southern part of the West-Azərbayjan Province in Iran (**Fig. J2**). Most of the area is mountainous and con-

sists of deep folds and piedmont plains. The most notable mountains that embrace the area are the Nestan in the east, with a height of 2410 m, and the Bolfat in the west, with a height of 2399 m⁴¹⁹. The most notable plains include the Wazine Plain in the west, sitting at a height of 1700 m, and the Kallwe Plain, at a height of about 1000 m. The Kallwe Plain is located in the east, where the Lower Zab enters from the north and then passes to the west to enter the Peshdar Plain⁴²⁰.

Our surveyed area encompasses the Kallwe plain and a section of the western highlands of Sardasht towards the international border between Iran and Iraq (**Fig. J3**). The Kallwe is the largest plain found in the Sardasht, and it is also the home of the Rabat II site. In the course of our assessment, we surveyed approximately 546 km² of the Sardasht district.

J2. The history of the archaeological exploration of Sardasht

The earliest references to Sardasht's archaeological sites and artefacts go back to the 19th century. In the 1890s, Jacques de Morgan visited Sardasht and indicated various archaeological sites on the Zab river banks.⁴²¹ In 1968, Ralph Solecki visited the West-Azərbayjan Province but was unable to visit Sardasht.⁴²² Afterwards, in 1975, Wolfram Kleiss visited Rabat and reported some Iron Age grey and grooved pottery forms⁴²³. A few months after Kleiss' visit, Stephan Kroll studied the materials from his investigations⁴²⁴.

⁴¹⁶ We would like to sincerely thank Salah Salimi and Obeid Sorkhabi for their help during the field surveys and archaeological studies. Also, we would like to thank Salah Mohammadi, the ICHTO's chief executive in Sardasht. We are grateful to Karen Radner for the opportunity to include our report in this volume and thank F. Janoscha Kreppner and Jean-Jacques Herr for their help and guidance in preparing this paper.

⁴¹⁷ Hejebri Nobari *et al.* 2012, 28.

⁴¹⁸ Binandeh 2017, 118.

⁴¹⁹ Khezri 2000, 28-33.

⁴²⁰ Ebrahimi 2004, 18.

⁴²¹ de Morgan 1895, map: "Carte de la partie centrale du Kurdistan".

⁴²² Solecki 1999, 29.

⁴²³ Kleiss 1977, 141.

⁴²⁴ Kroll 2005, 71.

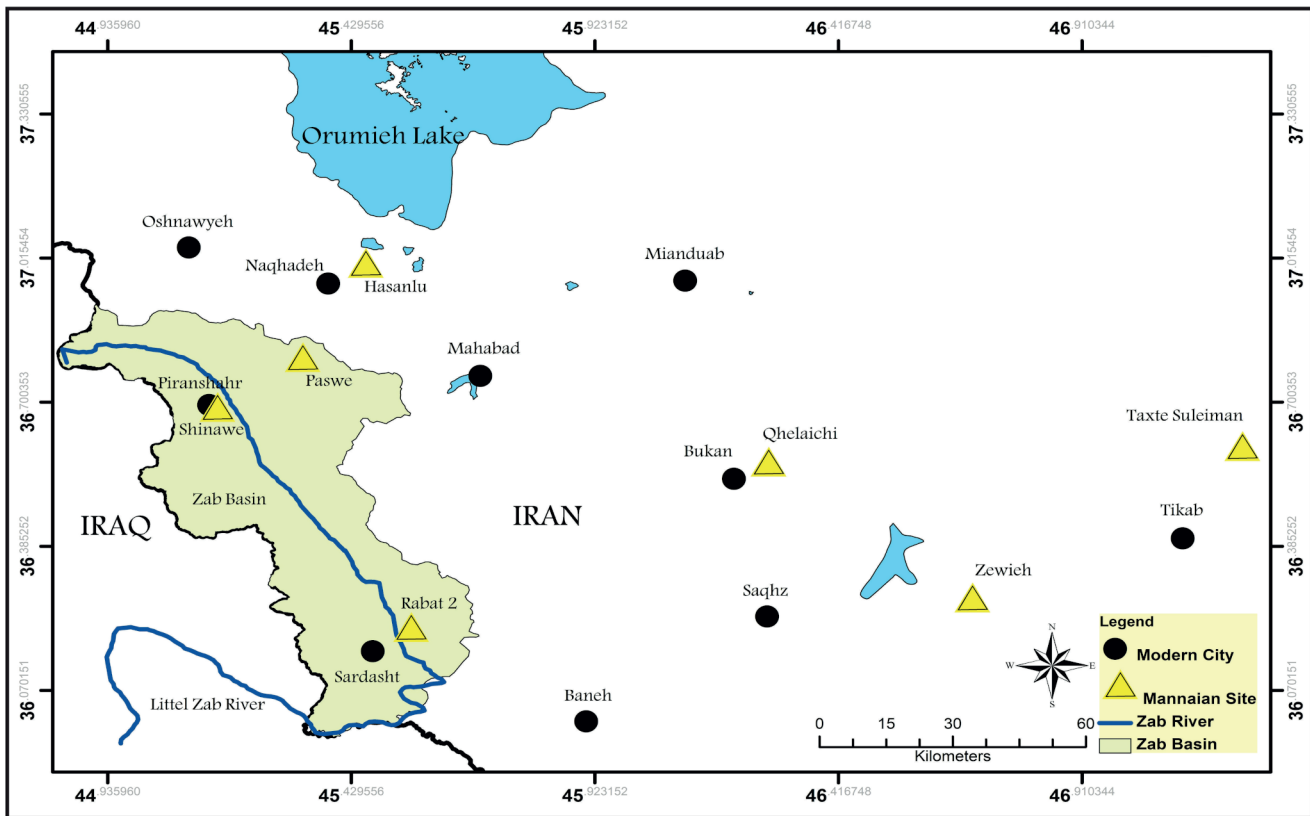


Fig. J1: The location of the Lower Zab River and its basin in Iran. From Salimi/Ebrahimipour/Sorkhabi 2019, 105.

More recently, Bahman Karegar and Reza Heidari excavated the Rabat II site for five seasons⁴²⁵. They referred to five Iron Age sites in their initial studies, but recent research has settled on only four sites with Iron Age indicators. In 2007, Ali Binandeh surveyed the river banks of the Lower Zab from Piranshahr to Sardasht, and he cited a number of archaeological sites ranging from the prehistoric period to the Islamic period⁴²⁶. Because of their interest in establishing dams in the region, the Iranian Ministry of Energy provided financial support for archaeological salvage projects in Sardasht in 2016. Apart from these studies, only sporadic surveys and studies have been conducted, and their results remain unpublished.

J3. Field survey methodology

Before beginning our field survey, we studied the geographical features to identify the obstacles we might face while conducting our surveys. Based on the geographical attributes, the area was divided into two categories: pied-

mont plain and mountainous areas. Our method was to first divide the area into hypothetical networks and then survey each block separately. Local guides, who contributed their navigation experience and knowledge of the area, were essential to our survey effort. Since sampling is an important part of every survey, we used a random sampling method to collect artefacts. For sampling, we divided the sites into northern, southern, western, and eastern sections, and pottery was collected randomly from each of these areas. When collecting pottery sherds, we particularly focused on rims and pieces from the main body of vessels. Once they were collected, the most suitable sherds were selected to be drawn.

J4. 2018 fieldwork and identified Iron Age sites

Our fieldwork during the spring and summer of 2018 resulted in the recording of 57 archaeological sites dating from the prehistoric to the Late Islamic periods (Fig. J4). The sites can be categorized into mounds and forts. The first group comprises the sites located on the plains; these archaeological mounds represented the majority of the sites we examined. The second group comprises forts, which are mostly located at high elevations, and most

425 Heidari 2010.

426 Binandeh 2008.

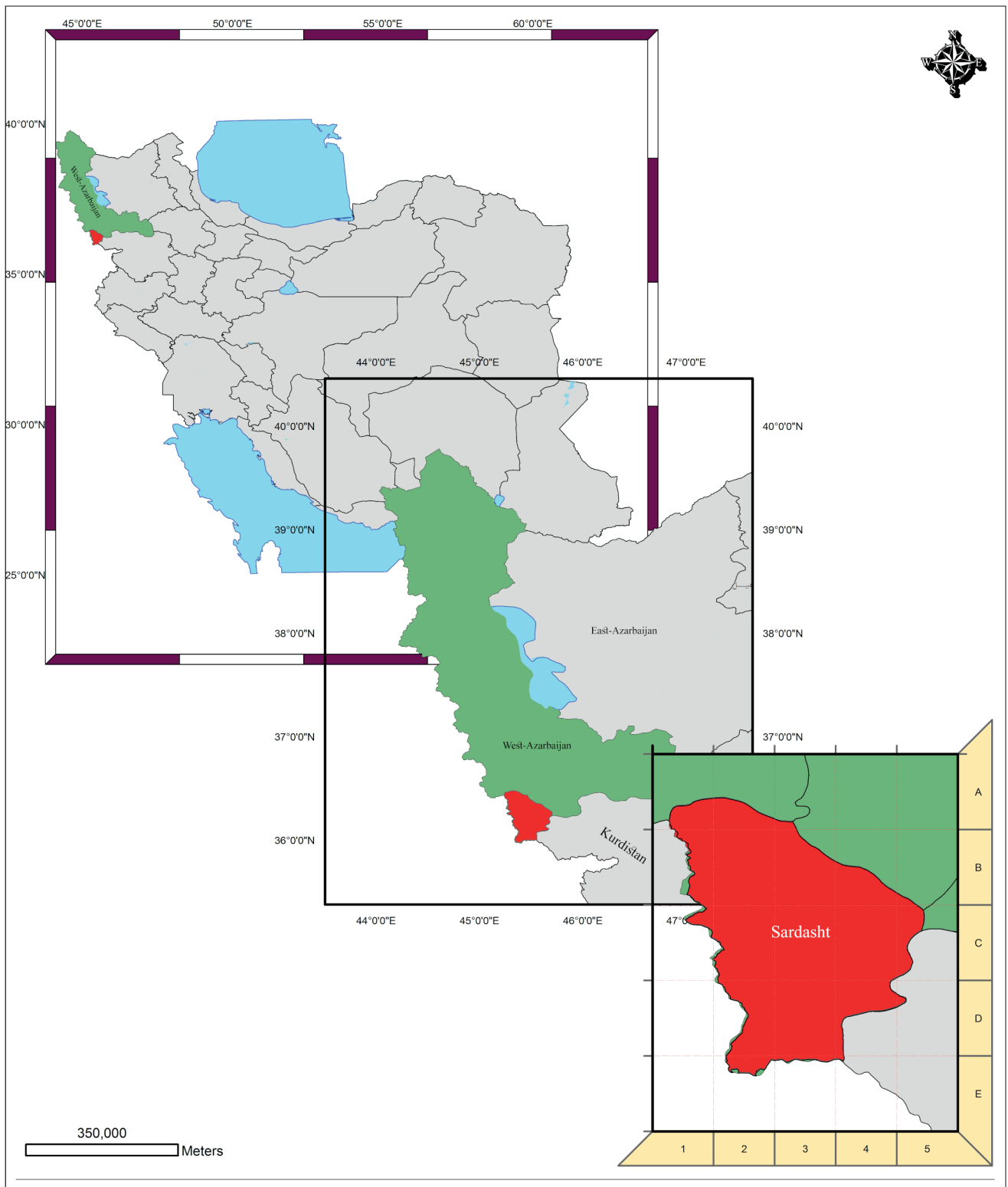


Fig. J2: Sardasht's location in Iran. Drawing by Salahaddin Ebrahimipour, 2019.

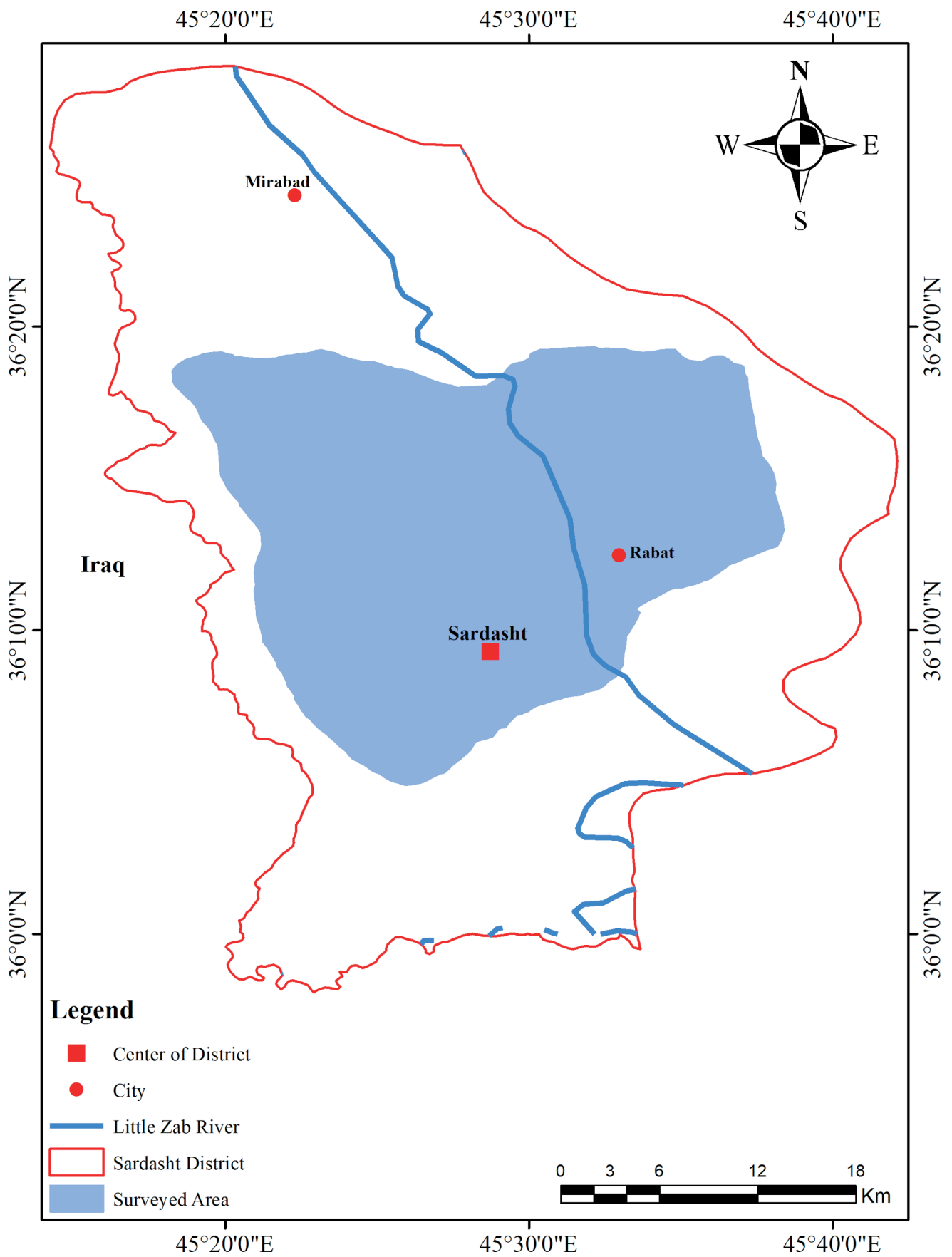


Fig. J3: Surveyed area. Drawing by Salahaddin Ebrahimipour, 2019.

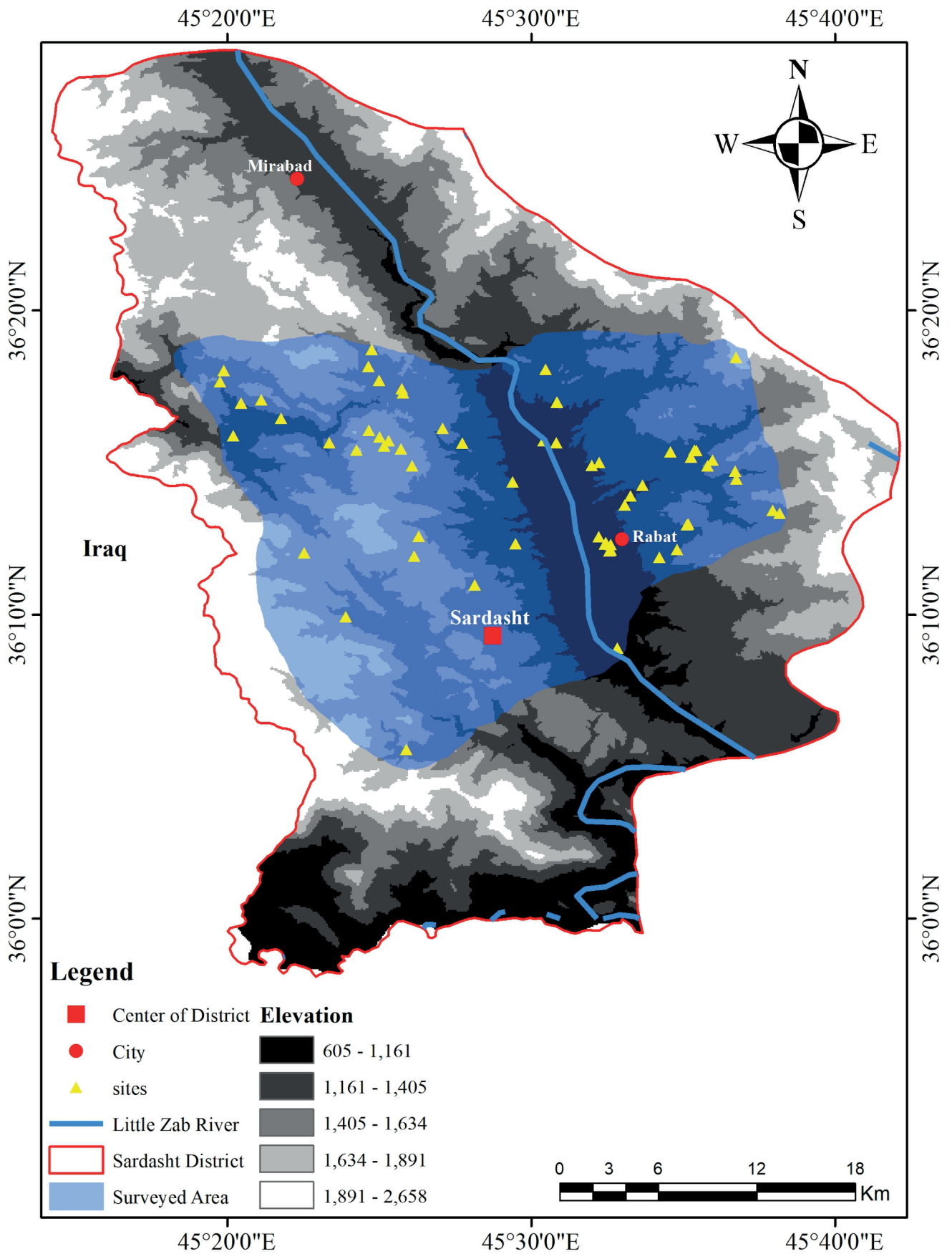


Fig. J4: Sites identified during the survey. Drawing by Salahaddin Ebrahimipour, 2019.

of which belong to the Parthian and late Islamic periods. Of these 57 archaeological sites, 33 were newly identified by our survey. The remaining 24 sites had been examined by previous surveys. Ten sites have evidence of Iron Age occupation (**Table J1**). Of these ten sites, only three had been identified by previous surveys. The vast Kallwe Plain lies east of the Lower Zab river, in Sardasht. Eight of the ten Iron Age sites are located on this plain. The other two sites are located to the west of the river, in the mountainous area of our survey.

Site Name	Longitude	Latitude	Altitude (m a.s.l.)
Rabat I	45°32'36"	36°12'17"	1131
Rabat II	45°32'24"	36°12'06"	1129
Rabat III	45°32'29"	36°12'22"	1139
Walliw I	45°30'52"	36°17'01"	1165
Walliw II	45°30'28"	36°18'03"	1357
Lilane I	45°34'44"	36°12'09"	1352
Lilane II	45°34'14"	36°11'52"	1245
Tappe Berisu	45°32'23"	36°09'03"	1013
Warshi-Qazyawe	45°29'34"	36°10'59"	1469
Hallishe	45°20'26"	36°17'59"	1592

Table J1: Coordinates of surveyed Iron Age sites.

Rabat II is a key Iron Age site in the Sardasht district and has been excavated for five seasons. During the survey, the Rabat II site was reviewed, although our focus mainly rested on the surrounding area, in order to study the connections and coherence between Rabat II and nearby sites (**Fig. J5**). Ceramics formed the bulk of the cultural material that we collected during this survey. The pottery is formed from common and fine wares, with brownish and buff colours. Golden and silver mica, lime, and fine sand were used in the clay fabric (**Fig. J6**). The most significant site close to Rabat II is Rabat I, which, as mentioned earlier, had been visited in the 1970s by Wolfram Kleiss (**Fig. J7**). Rabat I is a conical mound, located a few metres north-east of Rabat II, and it has been partly destroyed by modern inhabitants. In Rabat I, we found a variety of pottery types dating from the Chalcolithic to the Iron Age. The Iron Age pottery is composed of mostly fine and common wares in buff, brown, and greyish colours (**Fig. J8**). Their fabrics are the same as found in Rabat II site pottery. On the eastern side of the hill is a stone feature that appears to represent the remnants of a wall (**Fig. J9**). North of Rabat II lies a vast site that contains significant evidence of Iron Age pottery. This site is known as Rabat III (**Fig. J10**). The pottery is comparable to the other two Rabat sites and is similar in colour, slip, and fabric. It ranges in date from the

Late Chalcolithic⁴²⁷ to Iron Age III⁴²⁸. Additionally, during our surface survey of Rabat III, we discovered a grindstone on the southern slope (**Fig. J11** and **Fig. J12**).

Tappe Walliw (= Walliw I) is located in the northern part of the Kallwe Plain near a small village (**Fig. J13**). Although the mound has been disturbed by the cultivation of crops, it was possible to examine the surface where evidence from the Bronze Age to the Sasanian periods could still be found. The Iron Age pottery is wheel-thrown, and consists of common, coarse, and fine wares in brownish, buff, and greyish colours. Fine sand, lime, and silver mica have been used in the fabric (**Fig. J14**). Our survey identified another badly-damaged site about two kilometres northwest of Tappe Walliw. Therefore, it is called Walliw II (**Fig. J15**). The pottery comprises coarse and common wares in buff and light-brown colours (**Fig. J16**). Their forms appear to all be in local style, with the exception of one (**Fig. J16: n:3**) which is comparable to the Iron Age forms from Yanik Tepe⁴²⁹ in northwestern Iran.

Lilane I is situated about 2.5 kilometres east of the Rabat sites in the Lilane Village. This site is quite disturbed, and has been mostly ruined by the construction of buildings in the past few decades (**Fig. J17**). However, pottery evidence for an ancient settlement that dated from the Bronze Age to the early Islamic period can still be found there. The Iron Age pottery from this site consists of coarse ware, with mostly buff and partly brownish colours. Fine sand, and golden and silver mica were also used in the fabric (**Fig. J18**). One piece of buff ware (**Fig. J18: n:6**) from this site could be compared to sherds from Qalaichi.⁴³⁰ Since this site has endured so much destruction, it is not possible to gain much information about periods or pottery forms. Lilane I is located at a higher altitude than the other sites in the Kallwe Plain. Another site, Lilane II, sits about 600 m west of Lilane I, on the plain (**Fig. J19**). This site also produced evidence from the Chalcolithic to the Iron Age periods. The Iron Age pottery comprises coarse and common wares and the fabrics are the same as found at Lilane I, although here most of the pottery is buff-coloured (**Fig. J20**).

There is another Iron Age site located near the Berisu village on the southern part of the same plain (**Fig. J21**). This site contains evidence ranging from the Iron Age to the Parthian periods. This site was originally identified by Ali Binandeh and has since been partly destroyed by road construction. The pottery it yielded is wheel-thrown, in buff and brown colours. Common and coarse ware forms

427 Potts *et al.* 2019, 117, Fig. 36: j.

428 Mollazadeh 2008, 124, Fig. P1.10:17 & 26.

429 Summers/Burney 2012, 299, Fig. 12. n. 14 and Fig. 18. n. 4.

430 Mollazadeh 2008, Fig. P1.2.

are attested; the fabric includes fine sand and mica (**Fig. J22**: n:4, n:5, n:6, n:7).

Warshi-Qazyawe is situated close to the Rabat sites, but on the western side of the Lower Zab river, and at a much higher elevation (**Fig. J23**). It features stone structures, which we interpret as the remnants of an Iron Age fortress. From this location, the plain was perfectly visible and easily controlled. There are indications that this area had been damaged by military activity during the Iran-Iraq wars of the 1980s, and this might explain why we found no pottery sherds during our surface examination of the site. The stone structure is comparable to the Guringan fortress in the Piranshahr⁴³¹; both are almost identical in plan and architectural structure. The building is also very appropriately located for a fortress, and could have been used as a sentry fortress for observing the entire area around the Rabat complex during the Iron Age. Currently, traces of the limestone walls on both the northern and eastern fronts can be seen. The fortress is surrounded by a defensive wall, most of which is ruined. There are still remnants of this wall in the northern and eastern sides. The preserved height of the remaining walls on the northern side is 1.5 m (**Fig. J24**), and 0.4 m on the eastern side. The foundation was built with small, square stone and the outer walls were faced with stones that had been cut flat and made even.

Close to Savan village, in the highlands close to the Iran-Iraq frontier, there is a massive mound called Hallisha (**Fig. J25**). This is one of the major sites in the area, measuring approximately 130 m in length and 85 m in width. Pottery found at Hallisha is also wheel-thrown, with common and coarse ware in buff, brownish, and greyish colours (**Fig. J26**). Some of the pottery (**Fig. J26**: n:3, **Fig. J26**: n:5 and **Fig. J26**: n:6) is comparable to Iron Age pottery from Gird-i Bazar⁴³². There are some remains of a wall on top of the mound (**Fig. J27**). Around the foot of the mound, we found some ancient stones being reused in modern constructions.

J5. Spatial indicators

Analysis of the environmental and spatial indicators of settlements is a useful method for understanding settlement patterns. Therefore, we examined the Iron Age settlements for their proximity to water resources and their elevation.

J5.1 Spatial analysis of sites with access to the water resources

Accessing water resources is an essential consideration for site formation. To understand a site's accessibility to water resources (e.g., minor rivers and the Lower Zab river), we classified the sites into three groups. The first group consists of sites with an average distance from surface water of between 50 to 500 metres. This group consists of six sites. The second group consists of sites with an average distance from surface water of between 500 to 1000 metres. This category consists of two sites. The last category is sites with an average of 1000 to 1500 metres distance from water. This final category also comprises two sites. Accordingly, Rabat I, Rabat II, Rabat III, Tappe Berisu, Warshi-Qazyawe, and Hallishe lie in the first group. These are the closest sites to the water resources. Walliw I and Lilane I fall into the second group, at a middle distance to water. The final two sites, Walliw II and Lilane II, are in the third category; these two sites are the most distant from water resources (**Fig. J28**).

J5.2 Spatial analysis of sites according to the elevation

The lowest altitude in the study area is close to the Lower Zab river at 620 m and the highest elevation is 2683 m above sea level. Based on the importance of altitude to the distribution and formation of the settlements, we divided our surveyed sites into four categories, by elevation (**Fig. J29**). The first category consists of Rabat I, Rabat II, Rabat III, and Tappe Berisu: these sites were settled at elevations of 620 to 1150 m above sea level. The second group of sites are situated at a higher elevation. Lilane I, Lilane II, Warshi-Qazyawe, Walliw I, and Walliw II were all established at elevations between 1150 to 1500 m. The third category encompassed sites located at an elevation between 1500 to 2000 m above sea level. Hallishe is the only Iron Age site in this category, located at 1592 m above sea level. The fourth category includes no sites from the Iron Age.

J6. Conclusions

This chapter provides a brief outline of the Iron Age sites found in the surveyed area. Our aim was to focus on Iron Age sites along the central area of Sardasht, as the existence of Rabat II suggested that other sites were likely to exist within the unsurveyed areas. Most of the sites we discovered are located on the eastern banks of the Lower Zab river, in the Kallwe Plain. Out of the total ten sites,

⁴³¹ Salimi/Sorkhabi 2019, 210.

⁴³² Herr 2016, 96 (**Fig. D2.6**, 9-10); 2017, 122 (**Fig. E1.13**, 5); 2017, 124 (**Fig. F1.2**, 5).

eight are situated on this plain. Of this eight, three (Rabat I, II, and III) coexisted in a close relationship and perhaps should be considered a single settlement complex. Two sites were located on the western bank of the Lower Zab river. Warshi-Qazyawe was situated near the Rabat complex and may have served as a sentinel fortress. Only Hallishe is noticeably far from the other sites in our survey, and it was positioned especially high in the mountains. Therefore, Hallishe may have played a role in controlling the traffic on the main westward route across the Zagros mountain chain.

In terms of material culture, pottery could be categorised into common, coarse, and fine wares. Pottery colours ranged between brown, light brown, buff, and grey. Fabrics that included fine sand and mica were the most commonly used. Most of the sites are situated close to water resources and within the lower two elevation categories (up to 1400 metres a. s. l.). Only one settlement was located higher. This seems to have been as favourable to the peoples of the past as it is today: the altitude levels of the Iron Age sites correspond to the majority of settlements in use today.



Fig. J5: Rabat II, view from north. Photo by Salahaddin Ebrahimipour, 2018.

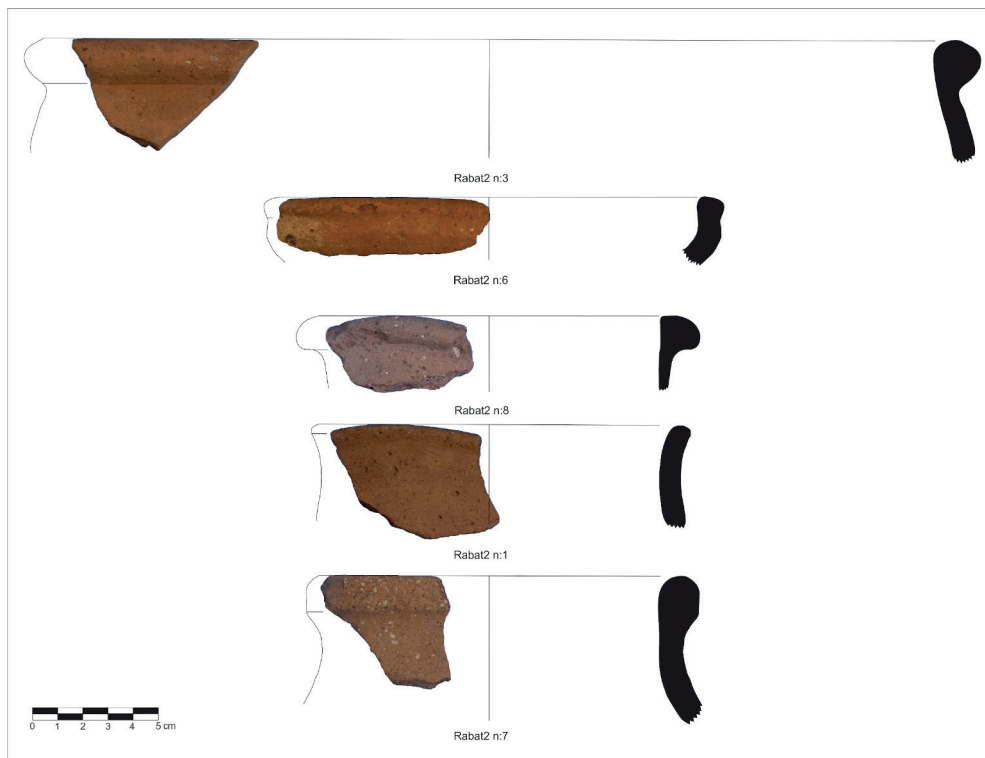


Fig. J6: Pottery from Rabat II. Drawing by Salah Salimi, 2018.



Fig. J7: Rabat I, view from west. Photo by Salahaddin Ebrahimipour, 2018.

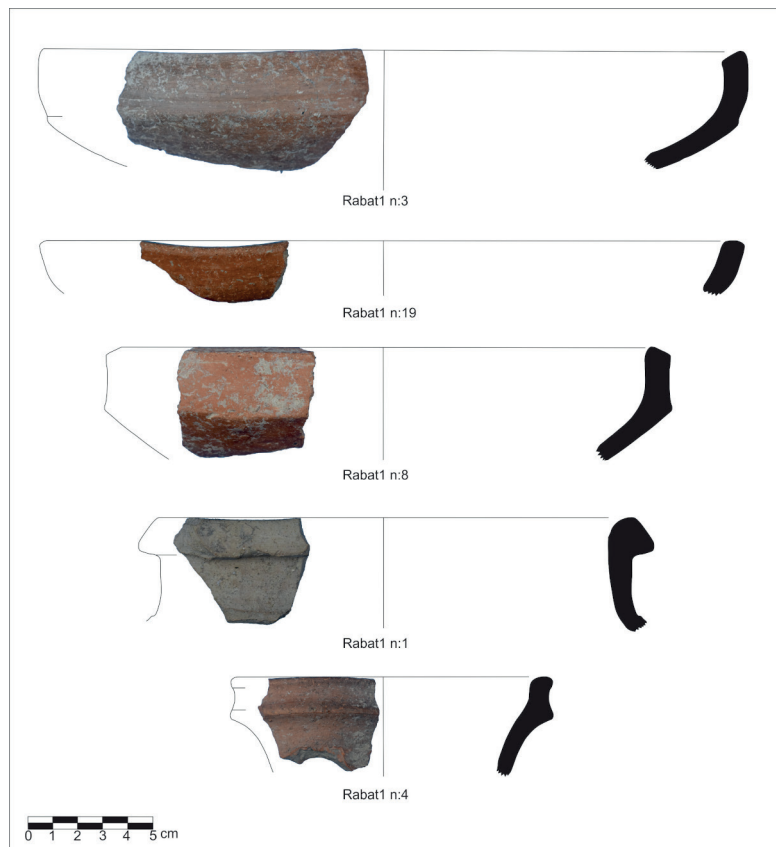


Fig. J8: Pottery from Rabat I. Drawing by Salah Salimi, 2018.



Fig. J9: Evidence of architectural structures on Rabat I. Photo by Salah Salimi, 2018.



Fig. J10: Rabat III, view from south. Photo by Salahaddin Ebrahimi, 2018.



Fig. J11: Groundstone tool found on Rabat III. Photo by Salah Salimi, 2019.



Fig. J12: Pottery from Rabat III. Drawing by Salah Salimi, 2018.



Fig. J13: Tappe Walliw (= Walliw I), view from east. Photo by Salahaddin Ebrahimipour, 2018.

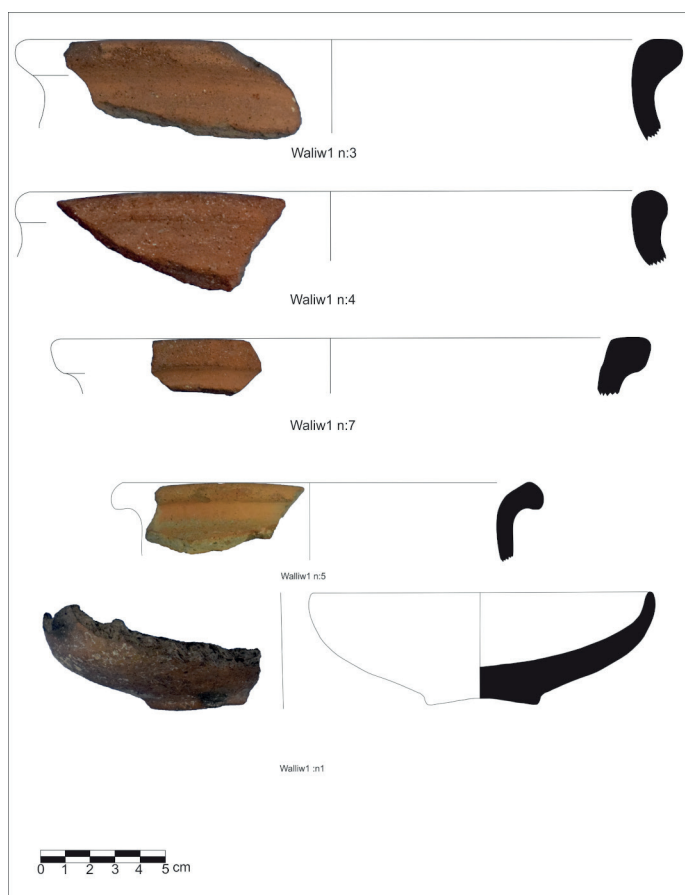


Fig. J14: Pottery from Walliw I. Photo by Salahaddin Ebrahimipour, 2018.



Fig. J15: Walliw II, view from east. Photo by Salahaddin Ebrahimipour, 2018.

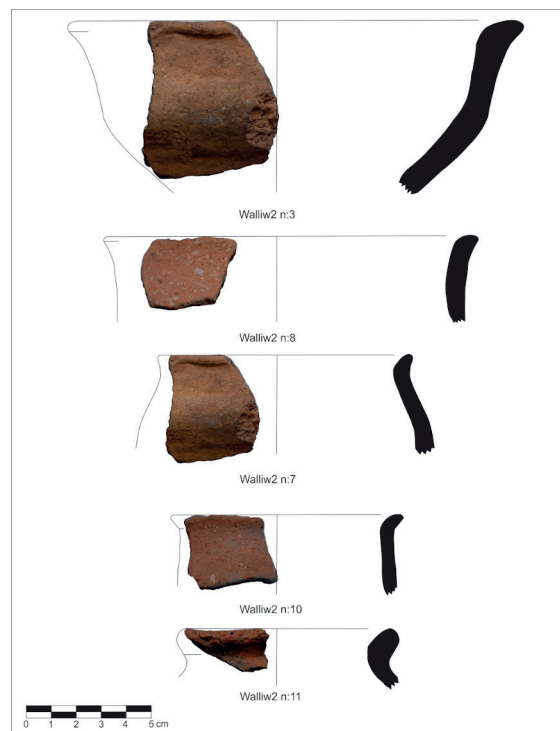


Fig. J16: Pottery from Walliw II. Drawing by Salah Salimi, 2018.



Fig. J17: Lilane I, view from north-east. Photo by Salahaddin Ebrahimipour, 2018.

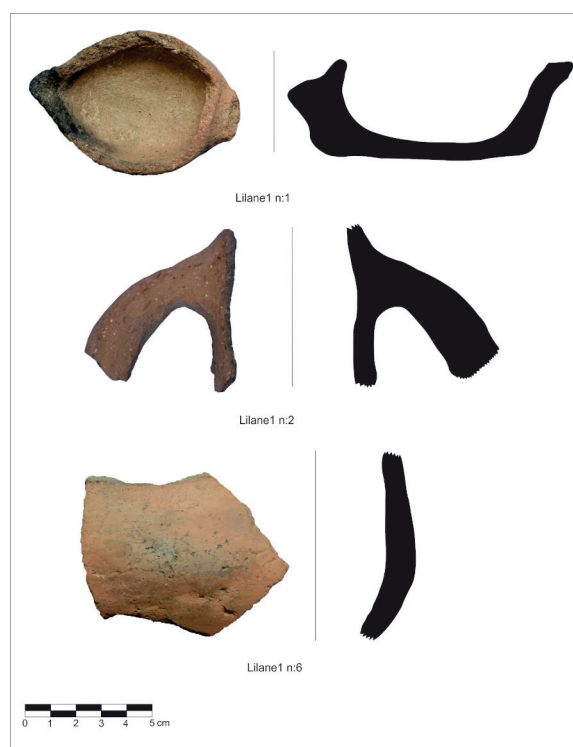


Fig. J18: Pottery from Lilane I, mostly local. Prepared by Salah Salimi, 2018.



Fig. J19: Lilane II, view from north-east. Photo by Salahaddin Ebrahimipour, 2018.

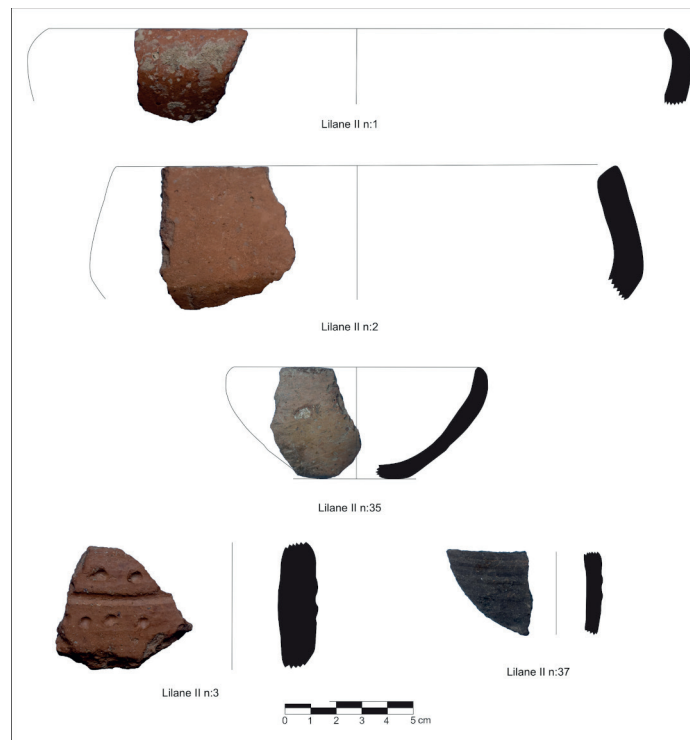


Fig. J20: Pottery from Lilane II. Drawing by Salah Salimi, 2018.



Fig. J21: Berisu and the section cut by the road, view from north. Photo by Ali Binandeh, 2008.



Fig. J22: Pottery from Berisu. Prepared by Ali Binandeh, 2008.



Fig. J23: The location of the Warshi-Qazyawe fortress, view from the west. Photo by Salahaddin Ebrahimipour, 2018.



Fig. J24: Remains of the walls at the Warshi-Qazyawe fortress. Photo by Salahaddin Ebrahimipour, 2018.



Fig. J25: Hallisha, view from west. Photo by Salahaddin Ebrahimipour, 2018.

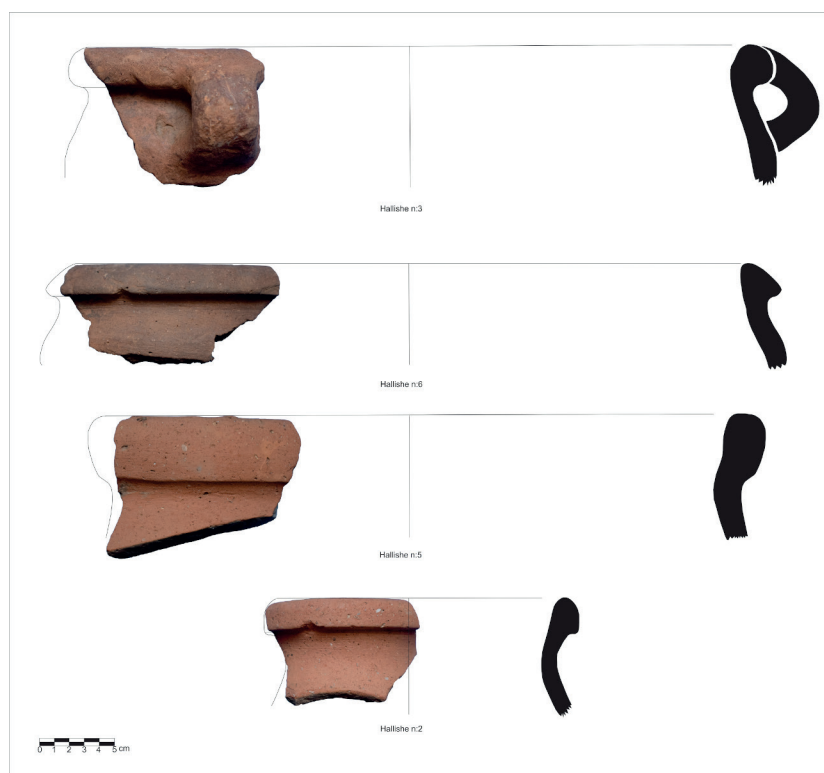


Fig. J26: Pottery from Hallisha. Drawing by Salah Salimi, 2018.



Fig. J27: Remains of a wall at Hallisha. Photo by Salahaddin Ebrahimipour, 2018.

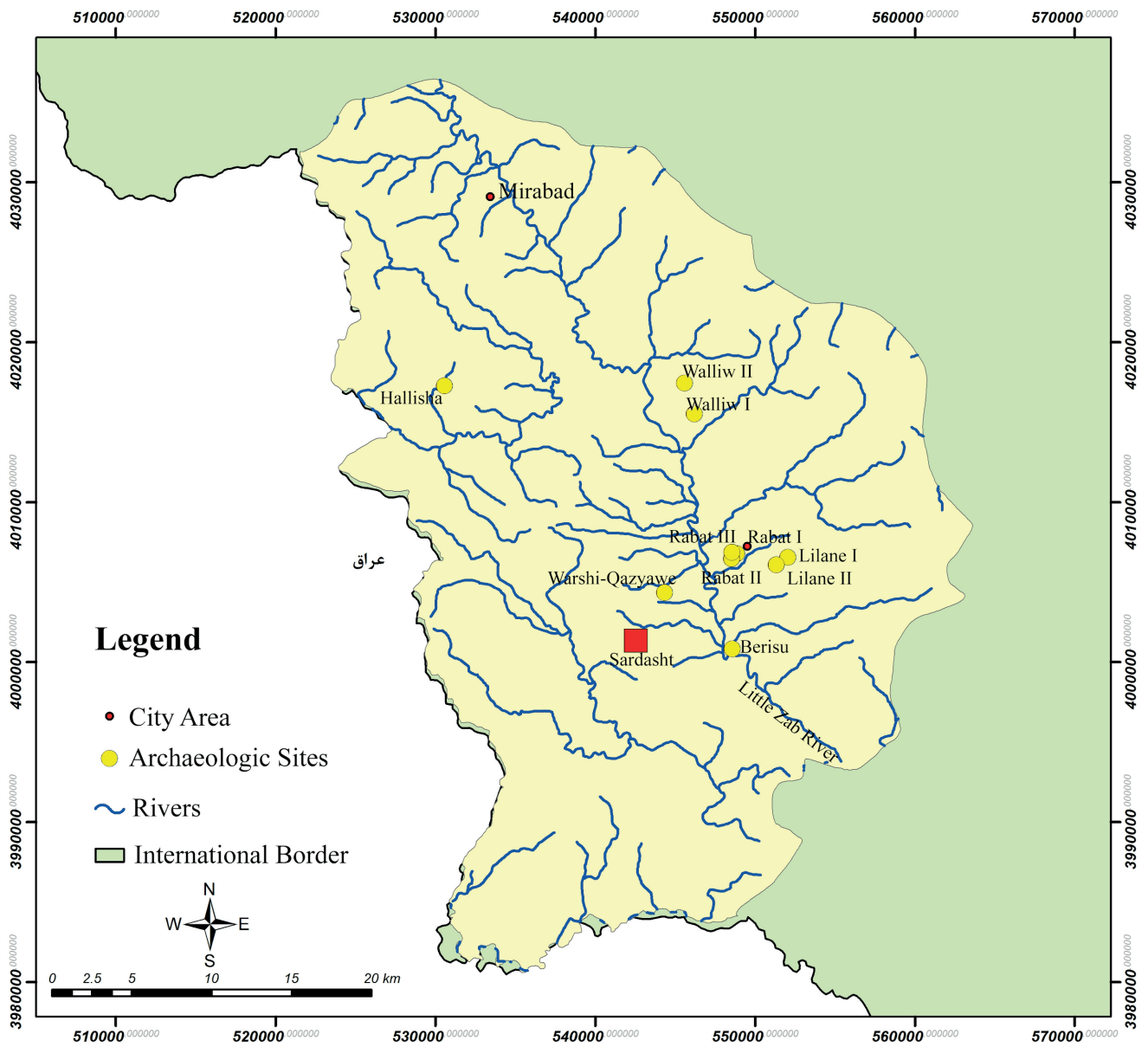


Fig. J28: Map showing the Iron Age sites and their vicinity to water resources. Prepared by Obeid Sorkhabi, 2018.

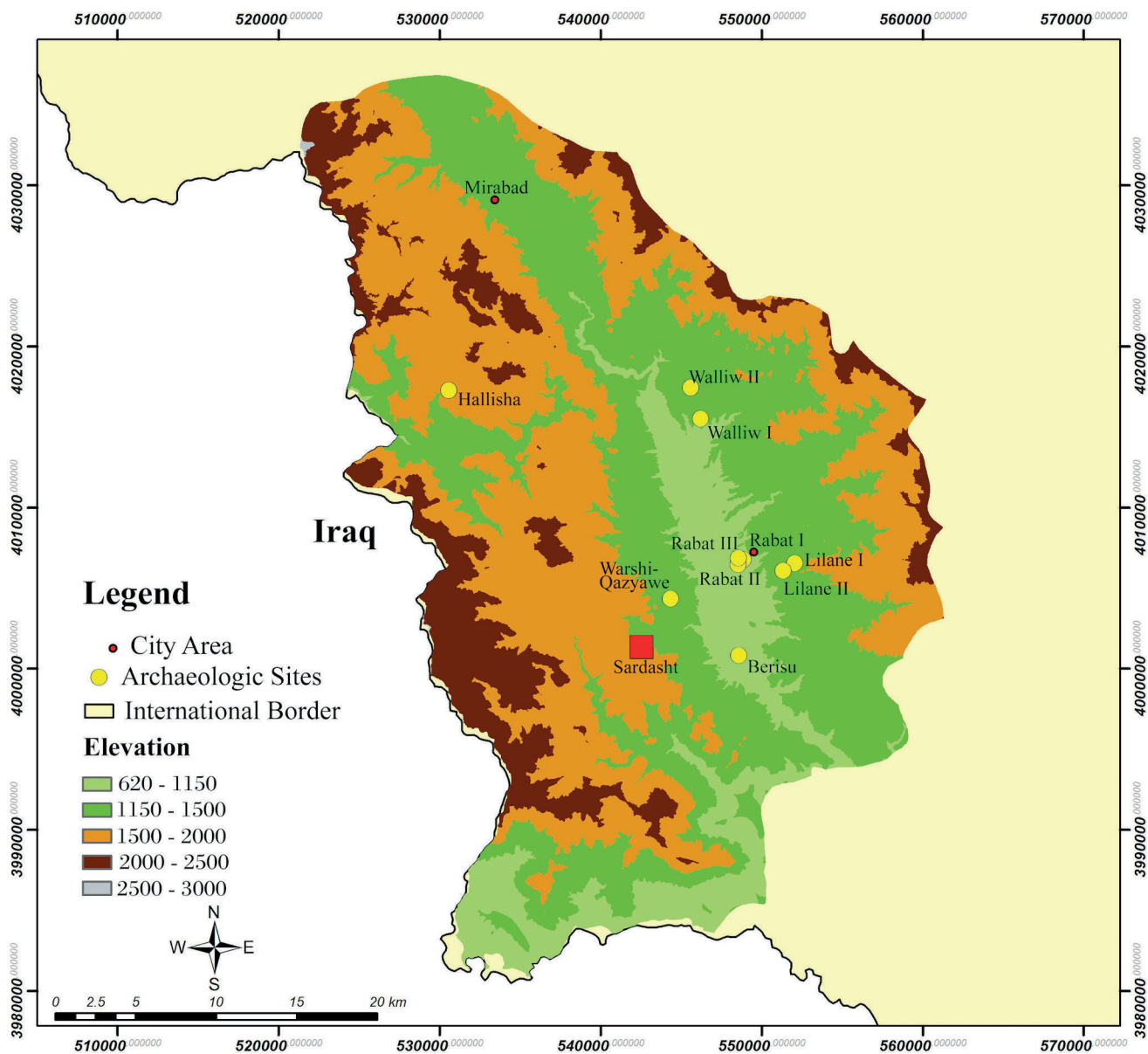


Fig. J29: Map showing the Iron Age sites and their elevations. Prepared by Obeid Sorkhabi, 2018.

K. Conclusions and perspectives

Karen Radner, F. Janoscha Kreppner and Andrea Squitieri

What have we learned about the Dinka Settlement Complex (DSC) in 2019? On the one hand, our fieldwork in that year – the last one chiefly funded by the Alexander von Humboldt Foundation as part of the creation of Karen Radner’s Alexander von Humboldt Chair for the Ancient History of the Near and Middle East at LMU Munich in 2015 – has greatly contributed to our understanding of the Iron Age settlement. This was achieved through the excavations and geophysical surveying on Qalat-i Dinka, which constitutes the Iron Age settlement’s Upper Town. Our work there continued to focus on completing the excavation of the monumental Iron Age Building P and also brought to light substantial evidence for cremation and inhumation burials around the building. Not only do these graves contribute important new data on the funerary practices in the western Zagros area during the first millennium BC, regionally they allow for a better comparison of the Dinka Settlement Complex with many sites in western Iran where excavations have mostly targeted cemeteries rather than settlements; the inventory includes diagnostic materials such as fibulae, cylinder seals and a bronze drinking vessel. Also on Qalat-i Dinka, the partially excavated fortifications first identified by magnetometer prospecting in 2015 were further investigated using Electrical Resistivity Tomography (ERT) surveying, which confirmed the previous interpretation of the structures as a combination of a glacis and a palisade wall. Down in the Lower Town and the surrounding Bora Plain, ERT prospecting and sediment coring were used to provide new data for our ever-increasing understanding of the *qanat* system and the ancient environment of the Dinka Settlement Complex, greatly aided by the ongoing analyses of soil samples as well as animal and plant remains (macro-botanical and phytoliths), on all of which reports are presented in this volume.

On the other hand, also other periods of the occupation of the Bora Plain have come into sharper focus, thanks to the unearthing of a Chalcolithic kiln under the Iron Age structures of the Lower Town excavation area DLT₃, and the discovery of Middle Islamic Pottery in the modern looting pits that had damaged Building P’s structures.

If we focus on the results from the excavation of Building P and its immediate surroundings, then the already

known fact that this area of the Dinka Settlement Complex, while sharing basic construction techniques, is very different from the architecture encountered in the Lower Town has again been confirmed by the additional evidence. Both the pottery and the radiocarbon dates indicate, however, that Building P and the Lower Town were occupied simultaneously. The Iron Age dating of Building P had already been confirmed in 2018 when a charcoal sample taken from the floor of Room 58 was radiocarbon dated to 1001–847 calBC (95.4% probability)⁴³³, a date which is consistent with those obtained from the Lower Town’s structures in Gird-i Bazar, DLT₂ and DLT₃ (cf. **Fig. A4-A6** and **Table A1** presented in **§A.1**). Architectural practices shared with the other structures of the Dinka Settlement Complex include the use of unworked river cobbles for the construction of the walls and the use of baked bricks to pave the floor.

The distinctive characteristics that set apart the monumental building on the western slope of Qalat-i Dinka from all the other Iron Age buildings known through excavation and magnetometer surveying are chiefly connected to its size, which dwarfs all buildings of the Lower Town: notably, its thick walls, large rooms, brick-paved indoor flooring, and the monumental gateway (of which the sizable threshold survives) that connects Room 58 with Room 59. Moreover, Room 58 features distinctive stone pilasters set against its northern and southern walls, into which also steps were built – all of these structures possibly form part of large-scale furniture elements that once may have covered these walls with paneling and built-in cupboards and whose wooden parts are now lost (except for perhaps some of the charcoal found on the floor and in the fills). The decorated ivory/bone inlays unearthed during the 2018 excavations may well have belonged to this furniture.

Because Building P was built against the natural slope running down to the bank of the Lower Zab, it has a stepped structure: the northern and southern walls of Room 58 meet the eastern wall of this room at a much lower level, and there is a difference in height of about

433 Radner/Squitieri 2019: 43 Fig. D5: A.

90 cm between the floors of Room 58 and Room 59. Building P's northeastern and southeastern corners are slightly asymmetric, with a wide, squarish shape and a rounded profile, respectively. During the 2019 campaign, it was established that the building was free-standing and situated in an open space that surrounded it in the north, east and south (designated as Outdoor Areas 60, 70, and 71). In this open space, the top layer of a thick package of pebbles and pottery sherds served as a walking surface.

Building P's primary function cannot be identified with certainty. However, the 2018 and 2019 results suggest that it was part of a larger citadel system comparable to that of Hasanlu, which consists of communal buildings of various functions, including defensive, representative, religious and economic (**Fig. K1**). The results of the 2015 magnetometer survey on the western slope of Qalat-i Dinka, of the 2018 excavations where a glacis structure was unearthed (trench QID2), and the already mentioned 2019 ERT survey in the area adjoining QID2 which confirmed the presence of a glacis flanked by a palisade wall, all document the defensive structures that guarded Building P towards the river, with a large gate (as indicated by two large river cobbles with a diameter of 1 m each that were made into door sockets⁴³⁴) providing access to the protected area from that direction (**Fig. K2**). That the defenses of this citadel were eventually tested, and were found wanting, is indicated by the presence of arrowheads in the fills of QID1 (**§E4**).

Several graves have been identified in the area around Building P, sadly generally in a poor state of preservation due to the modern looting activity that had targeted this area. We have been able to unearth the remains of six inhumation burials, namely four cist graves (Graves 102, 103, 105 and 107) and two simple pit graves (Graves 106 and 110), as well as two cremation burials (Graves 101 and 109). As the stratigraphy is badly disturbed by the looting pits, it does not help much in establishing conclusively whether these graves were contemporary or later than Building P.

The inhumation Grave 110 is the only one so far to yield a ¹⁴C date (**Fig. C4: d**) whose long time range of 767–488 calBC (due to the unfortunate Hallstatt radiocarbon calibration plateau of ca. 750–400 cal BC) includes the Late Iron Age horizon of the 7th century BC also suggested by

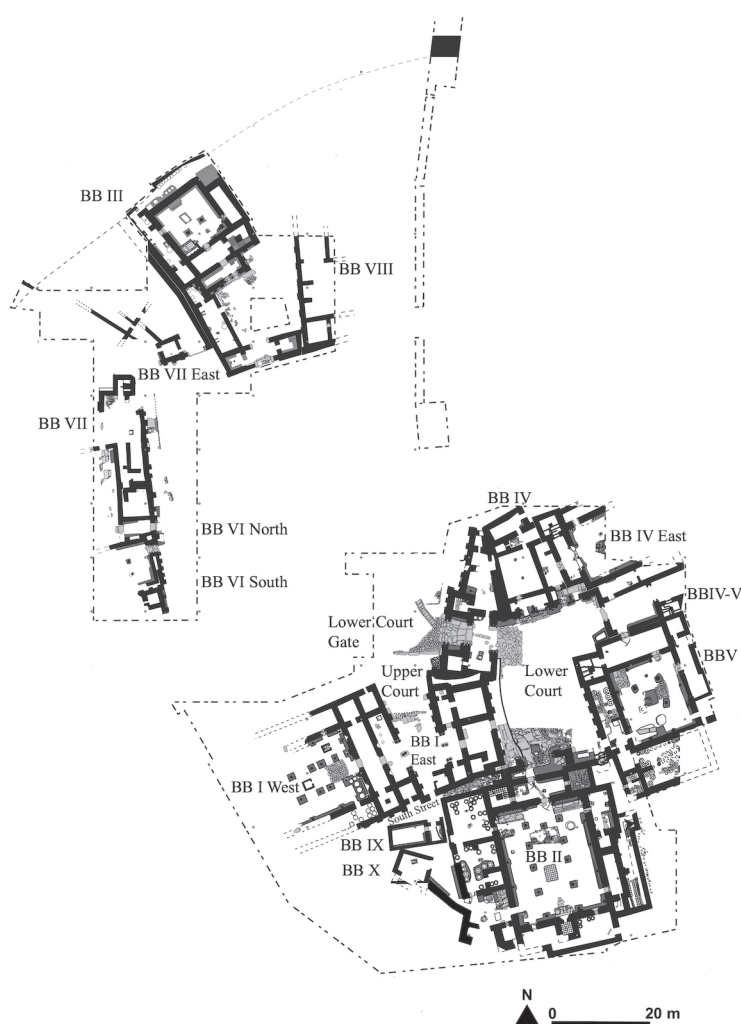


Fig. K1: The Iron Age II citadel of Hasanlu. Adapted from Danti/Cifarelli 2013, Fig. 1.6. Prepared by Andrea Squitieri.

the three bronze fibulae (**§E2.1**) and the cylinder seal in the “Provincial Assyrian Style” depicting an archer hunting a winged horse (**§E3.2**) found in that burial. While all this indicates that the individual buried in Grave 110 was deposited after the construction of Building P it is beyond our current knowledge whether the building was still in use at that time, or not.

Although the two cremation burials did not yield radiocarbon dates (because of the lack of collagen due to the exposure of the bones and teeth to heat during cremation), the items and the pottery retrieved from Grave 101 are consistent with a Late Iron Age or even Achaemenid-period date. Like Grave 110, the two cremation burials were cut into the pebble package surrounding Building P. We should therefore be open to the possibility that all three of these graves may be later in date than the usage phase of Building P.

On the other hand, the chronological relation of these burials with the cist graves (Graves 102, 103, 105 and 107)

434 Previously depicted in Fassbinder/Aşandulesei 2016, 42 Fig. B4.7a-b; see also **Fig. K2: A and B**.



Fig. K2: The occupation of the western slope of Qalat-i Dinka according to the results from excavations and geophysical prospecting, 2015-2019. The orthophoto is overlaid by the 2015 magnetogram, showing a possible fortification line (marked with white arrows). Inset images: (A) and (B): two large door socket stones, likely part of the gateway leading through the fortifications from the river (photos by Jörg Fassbinder); (C): orthophoto of Building P; (D): stone support structure for a now-lost wooden palisade (photo by Felix Wolter), with a possible reconstruction to the right; (E): glaciis (photo by Zahra Hashemi). Prepared by Andrea Squitieri.

is difficult to establish; because of their poor state of preservation, there were no human remains suitable for ^{14}C analysis. It is unclear whether they were constructed underneath the walking surface (which is entirely possible) or whether they were later cut into the pebble package. Because of their shared architecture, all four cist graves are likely to be largely contemporaneous with each other. Unlike the previously discussed burials, they may well be contemporaneous to Building P, although this is impossible to ascertain beyond any doubt. That this area of Qalat-i Dinka was used for burials from the late second until the late first millennium BC is beyond doubt because of the radiocarbon dates derived from the human remains of the 2018 campaign⁴³⁵.

If we attempt to put the construction of graves, which apparently no longer respected the architectural integrity of Building P and its surroundings, into the larger perspective of the Dinka Settlement Complex, it must be emphasised that the radiocarbon dating of Grave 110 is very close to the radiocarbon date range obtained from one of the human bodies found inside a well excavated in Building I of Gird-i Bazar in the Lower Town, dated to 748–409 calBC (95.4% probability; again affected by the Hallstatt radiocarbon calibration plateau)⁴³⁶. The presence of human skeletons inside this well, which could of course no longer be used after such contamination, is clearly connected to the end of the occupation of this part of the settlement. The chronological match with Grave 110 on

435 Radner/Squitieri 2019, 43 Fig. D5: C (tooth from Grave 99: 1259–1117 cal BC; 95.4% probability) and D (bone from Grave 98: 355–93 cal

BC; 95.4% probability).

436 Kreppner/Radner 2018, 56–57, Table D1: no. 8 and Fig. D5: d.

Qalat-i Dinka may point to a radical reorganisation of the architectural spaces and their functions across the entire Dinka Settlement Complex, affecting both the Lower and the Upper Towns. If contemporaneous, the dumping of bodies in the well of a now abandoned private house in the Lower Town and the cutting of new elite graves into the walking surface around the monumental building on Qalat-i Dinka may indicate profound social changes in the settlement. They are too late in date to be connected to the effects of the Assyrian annexation of the Peshdar Plain in the second half of the 9th century BC but they may be linked to the end of Assyrian rule in the area at some point in the 7th century BC – a subject to which we will return below.

The rich collection of items retrieved on the western slope of Qalat-i Dinka during the 2019 excavations represents an ensemble of very different object categories (**§E1**), from stone tools to arrowheads and jewellery, some of which can be assigned to the graves. Certain items, notably the decorated bone tubes and the fibulae, exhibit close stylistic links with objects excavated in the Levant. On the other hand, the three cylinder seals are a good match for the “Provincial Assyrian Style” as known from Hasanlu, where several close parallels can be identified. Other objects, such as the small pieces of jewellery found in the fill of modern looting pits that most likely come from the looted graves we excavated around Building P, are not closely associated with a specific area of the Middle East; nevertheless, close stylistic similarities can be observed with objects unearthed in graves from various western Iranian cemeteries dating to the Late Iron Age, thus matching the evidence of the pottery of the Dinka Settlement Complex that has long been understood to indicate close cultural connections with western Iran. It is tempting to suggest that those objects with connections to regions further afield, including the Levant, date to the period after the late 9th century BC when the Peshdar Plain and the Dinka Settlement Complex had been absorbed into the Assyrian Empire, as this state greatly facilitated the movement of goods and people across the wider region⁴³⁷.

Our 2019 fieldwork also took place in the Bora Plain that surrounds the Lower Town of the Dinka Settlement Complex, which we continued to investigate by means of sediment coring and ERT survey. Cores taken to the north, east and south of the Lower Town have allowed us to better define the limits of the settlement, which does indeed

not seem to extend much beyond the area covered by the available magnetograms. However, we still need to establish the extent of the settlement to the west, and this will be the subject of further research, scheduled for spring 2021. To the east of the Lower Town, only a few meters southwest of Gird-i Bazar, ERT surveys were conducted to test the presence of the *qanat* system that was first identified in 2015 and then further investigated by ERT in 2016 in the eastern part of the Bora Plain. The new ERT results showed the presence of features that may be interpreted as collapsed underground tunnels. Although the possibility that they are in fact collapsed palaeochannels cannot be entirely excluded, this new data makes it very likely that the *qanat* system was constructed to support the Iron Age Dinka Settlement Complex (as we assume due to the fact that while the Bora Plain was certainly occupied in the Chalcolithic period and the Sasanian period, no other suitable large-scale settlement structures have been identified so far). More ERT surveying is planned for 2021 in this area.

Additional investigations were conducted in 2019 across the Lower Town, in the area covered already by the magnetogram. The ERT survey showed the presence of artificial structures, possibly to be related to a building, underneath the structures that were made visible by the magnetometer survey and that are generally attributed to the Iron Age (as supported by the results of the subsequent excavations in DLT2 and DLT3). The underlying architecture now indicated by the new ERT data must therefore belong to a period prior to the Iron Age occupation. While we have at present no directly connected evidence for dating these older structures a charcoal sample isolated from Core 36 (C36), taken about 10 m south of the western extremity of the ERT profile (**Fig. B1.6**), can provide a possible suggestion for its date. This piece of charcoal was radiocarbon dated to 3329–2929 calBC (95.4% probability; see **Fig. B1.15**), and we presently assume that the deep-lying structures highlighted in the ERT profile could date to roughly the same time horizon.

The existence of archaeological occupation(s) considerably older than the Iron Age in the Bora Plain is also supported by the results of the pottery surface survey conducted in 2013 by a team headed by Jessica Giraud, which collected ceramics identified as Late Chalcolithic and Early Bronze Age pottery across the area of the Dinka Settlement Complex⁴³⁸. For the Chalcolithic period, this has now been confirmed by the discovery of a kiln with pottery inside and associated floors in the excavation area DLT3 (**§I**). The excavation of this kiln was begun in 2018

437 Cf. Radner/Amelirad/Azizi 2020 on the comparable situation with the Late Iron Age cemetery near Sanandaj, Kurdistan Province, Iran.

438 Giraud 2016, 33 Fig. B3.4.

(as an unexpected find in the course of the uncovering of the Iron Age layers in that area) and completed in spring 2019, made possible as a side mission of the PPP's environmental fieldwork campaign thanks to funding granted to Andrea Squitieri and Mark Altaweel by the Rust Family Foundation (Fairfield, Connecticut).

This kiln was revealed to be a double-chamber structure with a central column supporting a now-lost upper structure. A charcoal sample retrieved from the kiln's fill was radiocarbon dated to 5218–5024 calBC (**§I.16**), which corresponds to the Ubaid 3–4 period. Thin-section analysis on pottery demonstrated that the Chalcolithic and Iron Age pottery shared the same fabric (designated as Fabric C₁ for the latter⁴³⁹), made from a local source of clay. This therefore constitutes a clear case of long-term continuity of human-environment relations in the Bora Plain, but also highlights the potential dangers of dating pottery on the basis of fabric alone. Pyrotechnological and archaeomagnetic⁴⁴⁰ samples were taken from the Chalcolithic kiln by Silvia Amicone, Jörg Fassbinder and Cajetan Geiger; the analyses of these are ongoing, and their results will be published once they have become available. Further fieldwork is planned in spring 2021 in order to investigate the Chalcolithic occupation located below the Iron Age structures of the Lower Town by means of a combination of coring and ERT surveying, with new funding for this purpose recently awarded by the Gerda Henkel Foundation to Karen Radner, Jörg Fassbinder and Andrea Squitieri (AZ 42/V/20).

Our knowledge of the excavated areas of the Lower Town, namely Gird-i Bazar, DLT₂ and DLT₃, has also substantially grown due to the fresh results gained from studies on the animal and plant remains unearthed in the 2015–2019 campaigns. Anja Prust's analysis of all animal bones found in these three excavation areas of the Lower Town (**§F**) resulted in the observation of some patterns in the animal consumption behaviour of the inhabitants. Whereas wildlife plays a relatively minor role in local consumption, domestic animals were exploited as a major source of food; but while there were prepared cuts of mainly lower-value portions of meat present in all architectural units excavated so far, butchering clearly took place elsewhere. These results broadly match the interpretations of Gird-i Bazar as a workshop area mainly dedicated to pottery production, and of the buildings partially exposed in DLT₂ as dedicated to the storage and administration

of other types of food such as grain. Prust's study of the faunal remains found inside the large communal well located in the eastern part of Gird-i Bazar, which reached a depth of 7 m and yielded a large amount of well-preserved pottery sherds and animal bones, indicates that the well was not used continually as a waste pit over a long period of time but that the refuse material found therein was deposited there in the course of a few separate events. It is tempting to connect this with the abandonment of Gird-i Bazar when the already-mentioned human bodies were dumped in the private well of nearby Building I. Perhaps this coincided with the collection of various refuse materials in this part of the settlement, which were then thrown into the large well that was now no longer meant to be of use to the inhabitants.

Further information on the Dinka Settlement Complex was derived from the ongoing analysis of phytoliths by Fatemeh Ghaheri (**§G**) and macro plant remains by Melissa S. Rosenzweig and Anne Grasse (**§H**). The analysis of phytoliths indicates that the plant exploitation of the Iron Age took place in a marshy and wet environment (as expected due to the vicinity to the Lower Zab), in a relatively cool, temperate climate, and demonstrated the use of baskets and floor matting in the houses of the Lower Town. The ongoing study of the macro plant remains suggests distinctive room-by-room plant profiles for the buildings excavated in Gird-i Bazar, which points to specific practices being undertaken in specific spaces (**§H4**). Among all the excavation areas, DLT₃ is the only one that has hitherto produced evidence for grapes (and in all samples taken in this area), which points to wine-pressing activities in this part of the settlement.

The architecture excavated at DLT₃ exhibits also other peculiarities compared to the rest of the Lower Town. Most notably, DLT₃ has yielded a charcoal sample from a fill that was radiocarbon dated to 830–789 calBC (95.4% probability)⁴⁴¹, that is the period when the Dinka Settlement Complex, and the surrounding Peshdar Plain, were certainly under the control of the Neo-Assyrian Empire. This seems to go together with a change in the architectural organisation of the area, as Building Q was built over the extent of the earlier Building S, but with a different orientation in direction. Furthermore, this excavation area in the Lower Town is so far the only one to have yielded a text find (albeit certainly in secondary position): a brick fragment with a minuscule rest of a Neo-Assyrian cuneiform inscription, which can nevertheless be dated with some certainty to the time of Shalmaneser III of Assyria.

439 For the Iron Age Fabric C₁ at the Dinka Settlement Complex, see Herr 2017, 120; Amicone 2017a, 135–136.

440 Cf. Arneitz/Leonhardt 2019 for the results of a previous archaeometric study on a kiln from Gird-i Bazar.

441 Altaweel/Marsh 2016, 28 Fig. B2.7; Radner 2019a; and see **§A1** with **Table A1**.

ia (r. 859–824 BC)⁴⁴², during whose reign the Province of the Palace Herald was created in this part of the Zagros mountains.

In addition to the already-mentioned ongoing work on the plant remains, there are two further studies underway on the Iron Age materials from the Dinka Settlement Complex. Firstly, the production and consumption of the pottery assemblages, which the availability of absolute dates and its quantitative extent lends great importance for the wider Zagros region of northeastern Iraq and northwestern Iran, is currently being comprehensively studied, qualitatively and quantitatively analysed and prepared for publication by Jean-Jacques Herr in the course of a two-year LMU Incoming Research Fellowship (funded by LMUexcellent from 2019-2021). Secondly, Jana Richter is conducting a PhD dissertation project at WWU Münster devoted to the spatial analysis of the micro-refuse patterns at the Dinka Settlement Complex on the basis of the systematically sampled heavy fraction from all excavation areas.

When we commenced our excavations in the Bora Plain, we assumed that with the arrival of the Assyrians in the area, an infrastructure programme was implemented in whose context the extended Lower Town was created, as comparisons for this scenario upon the establishment of an Assyrian province are well known from sites in Syria and southeastern Turkey, e.g. Dur-Katlimmu (Tell Sheikh Hamad) or Tušhan (Ziyaret Tepe). However, the results of our investigations so far demonstrate that the large Lower Town existed already prior to the reign of Shalmaneser III of Assyria and thus before the integration of the Peshdar Plain into the Assyrian Empire. The architecture and finds of the Dinka Settlement Complex are particularly important as they elucidate the hitherto poorly-known local cultural traditions of the western Zagros region in the early first millennium BC.

It is remarkable, and certainly potentially instructive for the assessment of other regions, that the incorporation of the Dinka Settlement Complex into the Assyrian Empire in the second half of the 9th century BC has not left clearer material traces in its architecture and pottery – in the way we were initially led to expect from the northern provinces established on the Upper Tigris or from the western provinces created along and beyond the Euphrates. In the future, we hope to be able to resume the promising investigations of the Buildings K, L and M started with test trenches in 2017 in the excavation area DLT2. Gaining further insight into the largest buildings of the Lower Town of the Dinka Settlement Complex, which we assume to have fulfilled centralised administrative functions, would certainly allow us to refine, and possibly change, our assessment of the organisation of this intriguing Iron Age settlement on the upper reaches of the Lower Zab.

442 Radner 2019b.

Bibliography

Abedi et al. 2015

A. Abedi, O. Behrooz and K. Azam, "Fifth and fourth millennium BC in north-western Iran: Dalma and Pisdeli revisited." *Documenta Praehistorica* 42 (2015), pp. 321-338.

Al-Bahloul et al. 2005

K. Al-Bahloul, A. Barro and L. D'Alfonso, "Area H, the Iron Age cremation cemetery." In: L. Bachelot and F.M. Fales (eds.), *Tell Shiukh Fawqani, 1994-1998*, Padova 2005, pp. 997-1048.

Allen 2017

M.J. Allen, "Land snails in archaeology." In: M.J. Allen (ed.), *Molluscs in archaeology: methods, approaches and applications*, Oxford and Philadelphia 2017, pp. 6-29.

Altaweel 2017

M. Altaweel, "Electrical resistivity tomography investigations of the *qanat* system, 2016-2017." In: Radner/Kreppner/Squitieri 2017, pp. 33-43.

Altaweel/Eckmeier 2019

M. Altaweel and E. Eckmeier, "Geoarchaeological work at the Dinka Settlement Complex, 2018." In: Radner/Kreppner/Squitieri 2019, pp. 25-31.

Altaweel/Marsh 2016

M. Altaweel and A. Marsh, "Landscape and geoarchaeology of the Bora Plain." In: Radner/Kreppner/Squitieri 2016, pp. 23-28.

Amelirad/Azizi 2019

S. Amelirad and E. Azizi, "Kani Koter, Iron Age cemetery from Iranian Kurdistan." *Iran* (2019): DOI: 10.1080/05786967.2019.1633240.

Amelirad/Razmpoush 2015

S. Amelirad and A. Razmpoush, "A newly discovered Iron Age site at Sarrez, Iranian Kurdistan." *Ancient Near Eastern Studies* 52 (2015), pp. 207-215.

Amelirad et al. 2012

S. Amelirad, B. Overlaet and E. Haerinck, "The Iron Age 'Zagros Graveyard' near Sanandaj (Iranian Kurdistan): preliminary report on the first season." *Iranica Antiqua* 47 (2012), pp. 41-99.

Amelirad et al. 2017

S. Amelirad, A. Mohajerynezhad and M. Javidkhah, "A report on the excavation at the Mala Mcha graveyard, Kurdistan, Iran." *Iran* 55 (2017), pp. 171-207.

Amicone 2017a

S. Amicone, "Petrographic analysis of the 2015-2016 pottery from Gird-i Bazar." In: Radner/Kreppner/Squitieri 2017, pp. 128-138.

Amicone 2017b

S. Amicone, "The pottery kiln." In: Radner/Kreppner/Squitieri 2017, pp. 77-82.

Amicone 2018

S. Amicone, "Petrographic analysis on the DLT2 pottery." In: Radner/Kreppner/Squitieri 2018, pp. 134-139.

Amicone 2019

S. Amicone, "Petrographic analyses of selected 2018 pottery from Qalat-i Dinka." In: Radner/Kreppner/Squitieri 2019, p. 124.

Arneitz/Leonhardt 2019

P. Arneitz and R. Leonhardt, "An archaeometric study on a kiln from Gird-i Bazar." In: Radner/Kreppner/Squitieri 2019, pp. 150-155.

Ashkenazi et al. 2013

D. Ashkenazi, O. Golan and O. Tal, "An archaeometallurgical study of 13th-century arrowheads and bolts from the crusader castle of Arsuf/Arsur." *Archaeometry* 55 (2013), pp. 235-257.

Baitinger 2001

H. Baitinger, *Die Angriffswaffen aus Olympia*, Berlin and New York 2001.

Bartl 2014

P. Bartl, *Die Ritzverzierungen auf den Relieforthostaten Assurnaširpals II aus Kalḫu*, Darmstadt 2014.

Bartl 2018

P. Bartl, "Courtyard 18." In: Radner/Kreppner/Squitieri 2018, pp. 90-96.

Bar-Yosef Mayer 2005

D.E. Bar-Yosef Mayer, "The exploitation of shells as beads in the Palaeolithic and Neolithic of the Levant." *Paléorient* 31 (2005), pp. 176-185.

Bassampour 2014

F. Bassampour, "A study on metal objects of the Iron Age in Masjed-e-Kabud located in Tabriz." *European Online Journal of Natural and Social Sciences* 3 (2014), pp. 914-924.

Bendrey et al. 2016

R. Bendrey, J. Whitlam, S. Elliott, K. Rauf Aziz, R. Matthews and W. Matthews, "'Seasonal rhythms' of a rural Kurdish village: ethnozoarchaeological research in Bestansur, Iraq." In: L.G. Broderick (ed.), *People with animals: perspectives and studies in ethnozoarchaeology*, Oxford and Philadelphia 2016, pp. 42-56.

Bernbeck 2005

R. Bernbeck, "Material der seleukidischen bis römischen Zeit vom Tall Šeh Hamad I: die Grabungen von 1978 bis 1981 am Westhang der Zitadelle." In: H. Kühne, *Magdalu/Magdala. Tall Šeh Hamad von der postassyrischen Zeit bis zur römischen Kaiserzeit*, Berlin 2005, pp. 91-130.

Biel 1998

J. Biel, *Der Keltenfürst von Hochdorf*, Stuttgart 1998.

Bill 2003

A. Bill, *Studien zu den Gräbern des 6. bis 1. Jahrhunderts v. Chr. in Georgien unter besonderer Berücksichtigung der Beziehungen zu den Steppenvölkern*, Bonn 2003.

Binandeh 2008

A. Binandeh, *Archaeological survey of Little Zab river basin*. MA thesis, Tarbiat Modares University, Tehran 2008 (in Farsi).

Binandeh 2017

A. Binandeh, "The study and survey of the first millennium BC settlements in the Little Zab basin." *Pazhohesh-haye Bastanshenasi Iran* 7 (15) (2017), pp. 117-130 (in Farsi, with English abstract). DOI:10.22084/nbsh.2017.14909.1660.

Boehmer 1972

R.M. Boehmer, *Die Kleinfunde von Boğazköy aus den Grabungskampagnen 1931-1939 und 1952-1969*, Berlin 1972.

Boessneck et al. 1964

J. Boessneck, H. Müller and M. Teichert, "Osteologische Unterscheidungsmerkmale zwischen Schaf (*Ovis aries*

LINNÉ) und Ziege (*Capra hircus* LINNÉ)." *Kühn-Archiv* 78 (1964), pp. 1-129.

Boroffka/Becker 2004

N. Boroffka and J. Becker, "Töpferöfen in Arisman." In: T. Stöllner, R. Slotta and A. Vatandoust (eds.), *Persiens antike Pracht: Bergbau – Handwerk – Archäologie*, Bochum 2004, pp. 218-221.

Boroffka et al. 2011

N. Boroffka, N.N. Chegini and H. Parzinger, "Excavations at Arisman, Area B." In: A. Vatandoust, H. Parzinger and B. Helwing (eds.), *Early mining and metallurgy on the Central Iranian plateau: report of the first five years of research of the joint Iranian-German research project*, Mainz am Rhein 2011, pp. 28-39.

Braidwood et al. 1983

L.S. Braidwood, R.J. Braidwood, B. Howe, C.A. Reed and P.J. Watson (eds.), *Prehistoric archaeology along the Zagros flanks*, Chicago 1983.

Burney 1970

C. Burney, "Excavations at Haftavān Tepe, 1968: first preliminary report." *Iran* 8 (1970), pp. 157-171.

Burney 1972

C. Burney, "Excavations at Haftavān Tepe, 1969: second preliminary report." *Iran* 10 (1972), pp. 127-142.

Burney 1973

C. Burney, "Excavations at Haftavān Tepe, 1971: third preliminary report." *Iran* 11 (1973), pp. 153-172.

Burney 1975

C. Burney, "Excavations at Haftavān Tepe, 1973: fourth preliminary report." *Iran* 13 (1975), pp. 149-164.

Burton-Brown 1951

T. Burton-Brown, *Excavations in Azerbaijan, 1948*, London 1951.

Cifarelli 2018

M. Cifarelli, "Gender, personal adornment, and costly signaling in the Iron Age burials of Hasanlu, Iran." In: S. Svärd and A. Garcia-Ventura (eds.), *Studying gender in the Ancient Near East*, University Park 2018, pp. 73-108.

Cinquabre 1978

D. Cinquabre, "Les tombes de l'Age du Fer en Iran du Nord-Ouest." *Paléorient* 4 (1978), pp. 335-346.

Collon 2001

D. Collon, *Catalogue of the Western Asiatic seals in the British Museum: cylinder seals 5: Neo-Assyrian and Neo-Babylonian periods*, London 2001.

Curtis 2013

J. Curtis, *An examination of Late Assyrian metalwork*, Oxford 2013.

Danti 2014

M.D. Danti, "The Rowanduz Archaeological Program 2013: first report to the Kurdistan Regional Government." *Subartu* 8 (2014), pp. 50-72.

Danti/Cifarelli 2013

M.D. Danti and M. Cifarelli, *Hasanlu V: the Late Bronze and Iron I periods*, Philadelphia 2013.

Danti/Cifarelli 2015

M.D. Danti and M. Cifarelli, "Iron II warrior burials at Hasanlu Tepe, Iran." *Iranica Antiqua* 50 (2015), pp. 61-157.

Danti/Cifarelli 2016

M.D. Danti and M. Cifarelli, "Assyrianizing contexts at Hasanlu IVb? Materiality and identity in Iron II northwest Iran." In: J. MacGinnis, D. Wicke and T. Greenfield (eds.), *The provincial archaeology of the Assyrian Empire*, Cambridge 2016, pp. 357-369.

Derin/Muscarella 2001

Z. Derin and O.W. Muscarella, "Iron and bronze arrows." In: A. Çilingiroğlu and M. Salvini, *Ayanis I: ten years' excavation at Rusahinili Eiduru-kai, 1989-1998*, Rome 2001, pp. 189-217.

Dehpahlavan et al. 2019

M. Dehpahlavan, M. Jahed, A. Tazik and E. Farnam, "A newly found Iron II-II western graveyard of Qara-Tappeh, Sagzabad Mostafa." In: Y. Hassanzadeh, A.A. Vahdati and Z. Karimi (eds.), *Proceedings of the international conference on the Iron Age in Western Iran and neighbouring regions, vol. 1*, Tehran 2019, pp. 370-391.

Dezső 2017

T. Dezső, "The arrowheads from Grd-i Tle (Rania Plain, Iraqi Kurdistan)." *Dissertationes Archaeologicae* 3 (2017), pp. 97-112.

Dusinberre 1999

E.R.M. Dusinberre, "Satrapal Sardis: Achaemenid bowls in an Achaemenid capital." *American Journal of Archaeology* 103 (1999), pp. 73-102.

Dyson/Muscarella 1989

R.H. Dyson and O.W. Muscarella, "Constructing the chronology and historical implications of Hasanlu IV." *Iran* 27 (1989), pp. 1-27.

Ebrahimi 2004

N. Ebrahimi, *Assessing climate for tourism in the city of Sardasht*. MA thesis, Tehran University 2004 (in Farsi).

Eckmeier/Tolbas/Weidenhiller 2018

E. Eckmeier, H. Tolbas and M. Weidenhiller, "Soils and sediments in the Dinka Settlement Complex and the surrounding Bora Plain as indicator for landscape and site formation processes." In: Radner/Kreppner/Squitieri 2018, pp. 107-119.

Erzen 1988

A. Erzen, *Çavuştepe I: Urartian architectural monuments of the 7th and 6th centuries BC and the necropolis of the Middle Age*, Ankara 1988.

Fales 2010

F.M. Fales, "Production and consumption at Dür-Katlimmu: a survey of the evidence. The Middle Assyrian period." In: H. Kühne (ed.), *Dür-Katlimmu 2008 and beyond*, Wiesbaden 2010, pp. 67-86.

Fassbinder/Aşandulesei 2016

J. Fassbinder and A. Aşandulesei, "The magnetometer survey of Qalat-i Dinka and Gird-i Bazar, 2015." In: Radner/Kreppner/Squitieri 2016, pp. 36-42.

Fassbinder/Aşandulesei/Scheiblecker 2017

J. Fassbinder, A. Aşandulesei and M. Scheiblecker, "Magnetometer prospection at the Dinka Settlement Complex and Gawr Miran, 2016." In: Radner/Kreppner/Squitieri 2017, pp. 18-32.

Fassbinder/Aşandulesei/Scheiblecker 2018

J. Fassbinder, A. Aşandulesei and M. Scheiblecker, "The 2017 magnetometer survey of the Dinka Settlement Complex." In: Radner/Kreppner/Squitieri 2018, pp. 20-30.

Fechter/Falkner 1989

R. Fechter and G. Falkner, *Weichtiere*, München 1989.

Frahm/Tryon 2018

E. Frahm and C.A. Tryon, "Origins of Epipalaeolithic obsidian artifacts from Garrod's excavations at Zarzi cave in the Zagros foothills of Iraq." *Journal of Archaeological Science: Reports* 21 (2018), pp. 472-485.

Fügert 2015

A. Fügert, *Die neuassyrische und spätbabylonische Glyptik aus Tall Šēh Ḥamad*, Wiesbaden 2015.

Gaitzsch 2005

W. Gaitzsch, *Eisenfunde aus Pergamon: Geräte, Werkzeuge und Waffen*, Berlin and New York 2005.

Gaspa 2012

S. Gaspa, *Alimenti e pratiche alimentari in Assiria: le materie alimentari nel culto ufficiale dell'Assiria del primo millennio a.C.*, Padova 2012.

Genz 2003

H. Genz, *Ritzverzierte Knochenhülsen des dritten Jahrtausends im Ostmittelmeerraum: eine Studie zu den frühen Kulturverbindungen zwischen Levante und Ägäis*, Wiesbaden 2003.

Ghasimi et al. 2019

T. Ghasimi, M. Akbari, A. Ghasimi, M. Qadri, F. Bahrololoumi Shapurabadi, M. Azimi and E. Azizi, "Salvage excavation in an Iron Age tomb at Ruwar in the Sirwan river area, Hawraman, Kurdistan." In: Y. Hassanzadeh, A.A. Vahdati and Z. Karimi (eds.), *Proceedings of the international conference on the Iron Age in Western Iran and neighbouring regions, vol. 1*, Tehran 2019, pp. 50-63.

Ghazanfar/McDaniel 2016

S.A. Ghazanfar and T. McDaniel, "Floras of the Middle East: a quantitative analysis and biogeography of the flora of Iraq." *Edinburgh Journal of Botany* 73 (2016), pp. 1-24.

Ghirshman 1979

R. Ghirshman, *Tombe princière de Ziwiyé et le début de l'art animalier scythe*, Paris 1979.

Giraud 2016

J. Giraud, "Surface survey of the Dinka Settlement Complex, 2013-2015." In: Radner/Kreppner/Squitieri 2016, pp. 29-35.

Golani 2014

A. Golani, "Cowrie shells and their imitations as ornamental amulets in Egypt and the Near East." In: A. Golani and Z. Wygnańska (eds.), *Beyond ornamentation: jewelry as an aspect of material culture in the ancient Near East*, Warsaw 2014, pp. 71-94.

Gottlieb 2004

Y. Gottlieb, "The weaponry of the Assyrian attack, section A: the arrowheads and selected aspects of the siege battle."

In: D. Ussishkin (ed.), *The renewed archaeological excavations at Lachish (1973-1994)*, Tel Aviv 2004, pp. 1907-1969.

Gottlieb 2016

Y. Gottlieb, "Beer-Sheba under attack: a study of arrowheads and the story of destruction of the Iron Age settlement." In: Z. Herzog and L. Singer-Avitz (eds.), *Beer-Sheba III: the Early Iron IIA enclosed settlement and the Late Iron IIA-Iron IIB cities*, Tel Aviv 2016, pp. 1192-1228.

Grant 1982

A. Grant, "The use of tooth wear as a guide to the age of domestic ungulates." In: B. Wilson, C. Grigson and S. Payne (eds.), *Ageing and sexing animal bones from archaeological sites*, Oxford 1982, pp. 91-108.

Greenfield 2016

T. Greenfield, "The bioarchaeological sampling strategy." In: Radner/Kreppner/Squitieri 2016, pp. 77-80.

Greenfield 2017

T. Greenfield, "Bioarchaeological research at Gird-i Bazar, 2016." In: Radner/Kreppner/Squitieri 2017, pp. 168-175.

Greenfield 2019

T. Greenfield, "Analytical results from the zooarchaeological remains at Gird-i Bazar, 2015-16." In: Radner/Kreppner/Squitieri 2019, pp. 140-149.

Greenfield et al. 2013

T. Greenfield, D. Wicke and T. Matney, "Integration and interpretation of architectural and faunal evidence from Assyrian Tušhan, Turkey." *Bioarchaeology of the Near East* 7 (2013), pp. 47-75.

Guenther 2007

T. Guenther, "Roll-along inversion: a new approach for very long DC resistivity profiles." In: *Near Surface 2007: conference proceedings of the 13th EAGE European Meeting of Environmental and Engineering Geophysics*, Houten 2007. DOI:10.3997/2214-4609.20146557.

Guest/Al-Rawi 1966

E. Guest and A. Al-Rawi, *Flora of Iraq, vol. 1: introduction*, Ministry of Agriculture, Baghdad 1966.

Habermehl 1975

K.-H. Habermehl, *Die Altersbestimmung bei Haus- und Labortieren*, Berlin and Hamburg 1975.

Haerinck/Overlaet 1998

E. Haerinck and B. Overlaet, *Chamahzi Mumah: an Iron Age III graveyard*, Leuven 1998.

Haerinck/Overlaet 1999

E. Haerinck and B. Overlaet, *Djub-i Gauhar and Gul Khanan Murdah: Iron Age III graveyards in the Aivan Plain*, Leuven 1999.

Haerinck/Overlaet 2004a

E. Haerinck and B. Overlaet, *The Iron Age III graveyard at War Kabud, Pusht-i Kuh, Luristan*, Leuven 2004.

Haerinck/Overlaet 2004b

E. Haerinck and B. Overlaet, "The chronology of the Pusht-i Kuh, Luristan: results of the Belgian archaeological expedition in Iran." In: K. von Folsach, H. Thrane and I. Thuesen (eds.), *From handaxe to Khan: essays presented to Peder Mortensen on the occasion of his 70th birthday*, Aarhus 2004, pp. 119-135.

Haller 1954

A. Haller, *Die Gräber und Gräfte von Assur*, Berlin 1954.

Hamlin 1975

C. Hamlin, "Dalma Tepe." *Iran* 13 (1975), pp. 111-127.

Hasanpur et al. 2015

A. Hasanpur, Z. Hashemi and B. Overlaet, "The Baba Jilan graveyard near Nurabad, Pish-i Kuh, Luristan: a preliminary report." *Iranica Antiqua* 50 (2015), pp. 171-212.

Hashemi 2019

Z. Hashemi, "The excavations in QID2." In: Radner/Krep-
pner/Squitieri 2019, pp. 59-62.

Hassanzadeh 2016

Y. Hassanzadeh, "A survey on an 'Assyrian' glazed pottery type in the Zagros Mountains." In: J. MacGinnis, D. Wicke and T. Greenfield (eds.), *The provincial archaeology of the Assyrian Empire*, Cambridge 2016, pp. 371-383.

Hauser 2012

S.R. Hauser, *Status, Tod und Ritual: Stadt- und Sozialstruktur Assurs in neuassyrischer Zeit*, Wiesbaden 2012.

Heidari 2010

R. Heidari, "Hidden aspects of the Mannean rule in northwestern Iran." *Aramazd* 5 (2010), pp. 147-151.

Hejebri Nobari et al. 2012

A. Hejebri Nobari, A. Binandeh, J. Neyestani and H.V.

Nasab, "A new archaeological research in northwestern Iran: prehistoric settlements of Little Zab river basin." *International Journal of Humanities* 19 (2) (2012), pp. 27-42.

Helbaek 1966

H. Helbaek, "Appendix I: the plant remains from Nimrud." In: M. Mallowan (ed.), *Nimrud and its remains*, London 1966, pp. 613-620

Hellmuth 2007

A. Hellmuth, "Neues zum 'Bogenschützengrab' aus Libna." In: M. Blečić, M. Črešnar, B. Hänsel, A. Hellmuth, E. Kaiser and C. Metzner-Nebelsick (eds.), *Scripta praehistorica in honorem Biba Teržan*, Ljubljana 2007, pp. 465-475.

Hellmuth Kramberger 2016

A. Hellmuth Kramberger, *Die Pfeilspitzen aus Tall Šēh Hamad/Dūr-Katlimmu von der mittelassyrischen bis zur parthisch-römischen Zeit in ihrem westasiatischen und eurasischen Kontext*, Wiesbaden 2016.

Hellmuth Kramberger 2017

A. Hellmuth Kramberger, "Archäologische Hinweise zu kriegerischen Auseinandersetzungen mit reiternomadischen Gruppen im östlichen Mitteleuropa und im Vorderen Orient." In: E. Miroššayova, C. Pare and S. Stegmann-Rajtár (eds.), *Das nördliche Karpatenbecken in der Hallstattzeit: Wirtschaft, Handel und Kommunikation in früheisenzeitlichen Gesellschaften zwischen Ostalpen und Westpannonien*, Budapest 2017, pp. 571-590.

Helwing/Seyedin 2016

B. Helwing and M. Seyedin, "Bakun-Period sites in Darre-Ye Bolaghi, Fars." In: R.A. Carter and G. Philip (eds.), *Beyond the Ubaid: transformation and integration in the Late Prehistoric societies of the Middle East*, Chicago 2016, pp. 277-292.

Herles 2011

M. Herles, "Überlegung zur Sitte der Kremation bei den Urartäern." *Aramazd* 6 (2011), pp. 60-90.

Herr 2016

J.-J. Herr, "The pottery of Gird-i Bazar, 2015: a preliminary study." In: Radner/Krep-
pner/Squitieri 2016, pp. 80-99.

Herr 2017

J.-J. Herr, "The 2016 season pottery and a first catalogue of the chaînes opératoires at Gird-i Bazar." In: Radner/Krep-
pner/Squitieri 2017, pp. 104-127.

Herr 2019

J.-J. Herr, "The excavations in QID1." In: Radner/Kreppner/Squitieri 2019, pp. 44-58.

Herr et al. 2018

J.-J. Herr, A.B. Othman and H.S. Ahmed, "A first assessment of the 2017 pottery from DLT2." In: Radner/Kreppner/Squitieri 2018, pp. 120-133.

Herr et al. 2019

J.-J. Herr, A. B. Othman and H.S. Ahmed, "The 2018 pottery from the Dinka Settlement Complex." In: Radner/Kreppner/Squitier 2019, pp. 99-123.

Howes Smith 1986

P.H.G. Howes Smith, "A study of 9th-7th century metal bowls from Western Asia." *Iranica Antiqua* 21 (1986), pp. 1-88.

Ilan 2014

D. Ilan, "The crescent-lunate motif in the jewellery of the Bronze and Iron Ages in the Ancient Near East." In: R.A. Stucky, O. Kaelin and H.-P. Mathys (eds.), *Proceedings of the 9th international congress on the archaeology of the ancient Near East, vol. 1*, Wiesbaden 2014, pp. 137-150.

Ishida et al. 2014

K. Ishida, M. Tsumura and H. Tsumoto, *Excavations at Tell Al-Hajj, Rumeilah: a Bronze-Iron Age settlement on Syrian Euphrates*, Tokyo 2014.

Iversen 2015

I. Iversen, "The molluscs of Bestansur, Iraqi Kurdistan: a case study of Early Holocene *Helix salomonica* exploitation in the Zagros." *Environmental Archaeology* 20 (2015), pp. 239-250.

James/Taylor 1994

S.T. James and J.H. Taylor, "Parts of Roman artillery projectiles from Qasr Ibrim, Egypt." *Saalburg Jahrbuch* 47 (1994), pp. 93-98.

Jancović 2004

B. Jancović, *Vogelzucht und Vogelfang in Sippar im 1. Jahrtausend v. Chr.*, Münster 2004.

Jasim 1985

S.A. Jasim, *The Ubaid period in Iraq: recent excavations in the Hamrin region*, Oxford 1985.

Johns 1933

C.N. Johns, "Excavations at 'Atlit (1930-1): the south-east-

ern cemetery." *The Quarterly of the Department of Antiquities in Palestine* 2 (1933), pp. 41-104.

Jones/Halstead 1995

G. Jones and P. Halstead, "Maslins, mixtures and monocrops: on the interpretation of archaeobotanical crop samples of heterogeneous composition." *Journal of Archaeological Science* 22 (1995), pp. 103-114.

Kalla/Dezső 2019

G. Kalla and T. Dezső, "Hungarian archaeological expedition in the mountains of Iraqi Kurdistan: excavations undertaken by the Faculty of Humanities, Eötvös Loránd University, at Grd-i Tle (Rania Plain)." *Hungarian Archaeology* 8 (4) (2019), pp. 1-12.

Kerney/Cameron/Jungbluth 1983

M.P. Kerney, R.A.D. Cameron and J.H. Jungbluth, *Die Landschnecken Nord- und Mitteleuropas*, Hamburg and Berlin 1983.

Khezri 2000

S. Khezri, *Natural geography of Kurdistan Moukrian with emphasis on the Zab basin*, Tehran 2000.

Kleiss 1977

W. Kleiss, "Alte Wegen in West-Iran." *Archäologische Mitteilungen aus Iran* 10 (1977), pp. 137-151.

Klengel-Brandt et al. 2005

E. Klengel-Brandt, S. Kulemann-Ossen and L. Martin, *Tall Knēdiğ: die Ergebnisse der Ausgrabungen des Vorderasiatischen Museums Berlin in Nordost-Syrien von 1993 bis 1998*, Berlin 2005.

König/Liebich 2001

H.E. König and H.-G. Liebich, *Anatomie der Haussäugetiere, Band 1: Bewegungsapparat*, Stuttgart and New York 2001.

Kreppner 2014

F.J. Kreppner, "The new primary cremation custom of Iron Age Tell Sheikh Hamad/Dur-Katlimmu (north-eastern Syria)." In: P. Pfälzner, H. Niehr, E. Pernicka and S. Lange (eds.), *Contextualising grave inventories in the ancient Near East*, Wiesbaden 2014, pp. 171-186.

Kreppner/Radner 2018

F.J. Kreppner and K. Radner, "The results of the ¹⁴C analysis and their discussion." In: Radner/Kreppner/Squitieri 2018, pp. 56-58.

Kreppner/Schmid 2013

F. J. Kreppner and J. Schmid, *Stratigraphie und Architektur des «Roten Hauses» von Tall Šēḫ Ḥamad/Dūr-Katlimmu*, Berlin 2013.

Kreppner/Squitieri 2017a

F.J. Kreppner and A. Squitieri, "Excavating Qalat-i Dinka: the 2016 season." In: Radner/Kreppner/Squitieri 2017, pp. 44-56.

Kreppner/Squitieri 2017b

F.J. Kreppner and A. Squitieri, "The excavation methodology." In: Radner/Kreppner/Squitieri 2017, pp. 57-59.

Kreppner/Squitieri 2018

F.J. Kreppner and A. Squitieri, "Excavation overview and method." In: Radner/Kreppner/Squitieri 2018, p. 31.

Kreppner/Forster/Squitieri 2016

F.J. Kreppner, C. Forster and A. Squitieri, "Introducing the excavation methodology." In: Radner/Kreppner/Squitieri 2016, pp. 43-52.

Kroll 1976

S. Kroll, *Keramik urartäischer Festungen in Iran: ein Beitrag zur Expansion Urartus in Iranisch-Azarbaidjan*, Berlin 1976.

Kroll 1979

S. Kroll, "Die Kleinfunde." In: W. Kleiss, *Bastam I: Ausgrabungen in den urartäischen Anlagen 1972-1975*, Berlin 1979, pp. 151-182.

Kroll 1988

S. Kroll, "Die Kleinfunde." In: W. Kleiss, *Bastam II: Ausgrabungen in den urartäischen Anlagen 1972-1975*, Berlin 1988, pp. 155-164.

Kroll 2005

S. Kroll, "The southern Urmia Basin in the early Iron Age." *Iranica Antiqua* 40 (2005), pp. 65-85.

Kroll et al. 2012

S. Kroll, C. Gruber, U. Hellwag, M. Roaf and P. Zimansky, "Introduction." In: S. Kroll, C. Gruber, U. Hellwag, M. Roaf and P. Zimansky (eds.), *Biainili-Urartu: the proceedings of the symposium held in Munich 12-14 October 2007*, Leuven 2012, pp. 1-38.

Kubiak-Martens 2015

L. Kubiak-Martens, "Plant remains from Tell Ashara (Terqa) and Tell Masaikh in the Middle Euphrates, south-eastern Syrian: archaeobotanical report (field seasons 2006

and 2007)." In: J. Margueron, O. Rouault, P. Butterlin and P. Lombard (eds.), *Akh Purattim* 3, Lyon 2015, pp. 423-442.

Kühne 2006-2008

H. Kühne, "Šaiḫ Ḥamad, Tall. B. Archäologisch." *Realexikon der Assyriologie und Vorderasiatischen Archäologie* 11 (2006-2008), pp. 543-551.

Layard 1853

A.H. Layard, *Discoveries in the ruins of Nineveh and Babylon*, London 1853.

Lamon/Shipton 1938

R. Lamon and G. Shipton, *Megiddo I: seasons of 1925-34, strata I-V*, Chicago 1938.

Lepère 2014

C. Lepère, "Experimental and traceological approach for a technical interpretation of ceramic polished surfaces." *Journal of Archaeological Science* 46 (2014), pp. 144-155.

Lightfoot 1996

D.R. Lightfoot, "Syrian qanat Romani: history, ecology, abandonment." *Journal of Arid Environments* 33 (1996), pp. 321-336.

Loke et al. 2013

M.H. Loke, J.E. Chambers, D.F. Rucker, O. Kurasan and P.B. Wilkinson, "Recent developments in the direct-current geoelectrical imaging method." *Journal of Applied Geophysics* 95 (2013), pp. 135-156.

Loud 1948

G. Loud, *Megiddo II: seasons of 1935-39*, Chicago 1948.

Luschan 1943

F. von Luschan, *Die Kleinfunde von Sendschirli*, Berlin 1943.

Luschey 1939

H. Luschey, *Die Phiale*, Bleicherode am Harz 1939.

Magee 2008

P. Magee, "Deconstructing the destruction of Hasanlu: archaeology, imperialism and the chronology of the Iranian Iron Age." *Iranica Antiqua* 43 (2008), pp. 89-106.

Mallowan 1966

M.E.L. Mallowan, *Nimrud and its remains*, London 1966.

Marcus 1996

M.I. Marcus, *Emblems of identity and prestige: the seals and sealings from Hasanlu, Iran*, Philadelphia 1996.

Margaritis/Jones 2006

E. Margaritis and M. Jones, "Beyond cereals: crop processing and *Vitis vinifera* L.: ethnography, experiment and charred grape remains from Hellenistic Greece." *Journal of Archaeological Science* 33 (2006), pp. 784-805.

Matermawi 2005

M. Matermawi, "Tell Afis (Siria), 2002-2004: Area A3." *Egitto e Vicino Oriente* 28 (2005), pp. 30-31.

Matney et al. 2017

T. Matney, J. MacGinnis, D. Wicke and K. Koroğlu, *Ziyaret Tepe: exploring the Anatolian frontier of the Assyrian Empire*, Istanbul 2017.

McCown et al. 1978

D.E. McCown, R.C. Haines and R.D. Biggs, *Nippur II: the North Temple sounding E*, Chicago 1978.

Medvedskaya 1988

I. Medvedskaya, "Who destroyed Hasanlu IV?" *Iran* 26 (1988), pp. 1-15.

Miglus et al. 2016

P.A. Miglus, K. Radner and F.M. Stępniewski, *Ausgrabungen in Assur: Wohnquartiere in der Weststadt, Teil I*, Wiesbaden 2016.

Miller 1984

N.F. Miller, "The use of dung as fuel: an ethnographic example and an archaeological application." *Paléorient* 10 (1984), pp. 71-79.

Mollazadeh 2008

K. Mollazadeh, "The pottery from the Mannean site of Qalaichi, Bukan (NW-Iran)." *Iranica Antiqua* 43 (2008), pp. 107-125.

Moorey 1980

P.R.S. Moorey, *Cemeteries of the first millennium B.C. at Deve Hüyük, near Carchemish, salvaged by T. E. Lawrence and C. L. Woolley in 1913 (with a catalogue raisonné of the objects in Berlin, Cambridge, Liverpool, London, and Oxford)*, Oxford 1980.

Moortgat 1940

A. Moortgat, *Vorderasiatische Rollsiegel: ein Beitrag zur Geschichte der Steinschneidekunst*, Berlin 1940.

Morandi Bonacossi et al. 2018

D. Morandi Bonacossi, H.A. Qasim, C. Coppini, K. Gavnin, E. Giroto, M. Iamoni and C. Tonghini, "The Irani-

an-Kurdish excavations at Gir-e Gomel in the Kurdistan Region of Iraq. Preliminary report on the 2017 and 2018 field seasons." *Mesopotamia* 53 (2018), pp. 67-162.

de Morgan 1895

J. de Morgan, *Mission scientifique en Perse: cartes des rives méridionales de la mer Caspienne, du Kurdistan, du Moukri et de l'Elam*, Paris 1895.

Muscarella 1966

O.W. Muscarella, "Hasanlu 1964." *Bulletin of the Metropolitan Museum of Art* 25 (1966), pp. 121-136.

Muscarella 1973

O.W. Muscarella, "Excavations at Agrab Tepe, Iran." *Metropolitan Museum Journal* 8 (1973), pp. 47-76.

Muscarella 1974

O.W. Muscarella, "The Iron Age at Dinkha Tepe, Iran." *Metropolitan Museum Journal* 9 (1974), pp. 35-90.

Muscarella 1981

O.W. Muscarella, "Surkh Dum at the Metropolitan Museum of Art: a mini-report." *Journal of Field Archaeology* 8 (1981), pp. 327-359.

Muscarella 1988

O.W. Muscarella, *Bronze and Iron: ancient Near Eastern artifacts in the Metropolitan Museum of Art*, New York 1988.

Naegele 1899

G. Naegele 1899, "Eine neue Pomatia aus Persien." *Nachrichtsblatt der Deutschen Malakozoologischen Gesellschaft* 31 (1899), pp. 28-29.

Neubert 2014

E. Neubert, "Revision of *Helix LINNAEUS*, 1758 in its eastern Mediterranean distribution area, and reassignment of *Helix godetiana* KOBELT, 1878 to *Maltzanella* HESSE, 1917 (Gastropoda, Pulmonata, Helicidae)." *Contributions to Natural History* 26 (2014), pp. 1-200.

Novák/Ghafour 2009

M. Novák and S.A. Ghafour, "Grabungen im Nordost-Palast." In: A. Baghdo, L. Martin, M. Novák and W. Orthmann (eds.), *Vorbericht über die erste und zweite syrisch-deutsche Grabungskampagne auf dem Tell Halaf*, Wiesbaden 2009, pp. 41-60.

Overlaet 2005

B. Overlaet, "The chronology of the Iron Age in the Pusht-i Kuh, Luristan." *Iranica Antiqua* 40 (2005), pp. 1-33.

Palmisano 2019

A. Palmisano, "The Late Chalcolithic kiln." In: Radner/Kreppner/Squitieri 2019, p. 75.

Parsi et al. 2019

M. Parsi, J.W.E. Fassbinder, N. Papadopoulos, M. Scheiblecker and S. Ostner, "Revealing the hidden structure of the ancient city Ur (Iraq) with electrical resistivity tomography." In: J. Bonsall (ed.), *New global perspectives on archaeological prospection*, Oxford 2019, pp. 206-208.

Payne 1973

S. Payne, "Kill-off patterns in sheep and goats: the mandibles from Aşvan Kale." *Anatolian Studies* 23 (1973), pp. 281-303.

Pedde 2000

F. Pedde, *Vorderasiatische Fibeln von der Levante bis Iran*, Saarbrücken 2000.

Pedde 2001

F. Pedde, "Development and extension of Near Eastern fibulae in the Iron Age." In: R. Eichmann and H. Parzinger (eds.), *Migration und Kulturtransfer: der Wandel vorder- und zentralasiatischer Kulturen im Umbruch vom 2. zum 1. vorchristlichen Jahrtausend*, Berlin 2001, pp. 485-496

Pedde 2018

F. Pedde, "Fibulae in Neo-Assyrian burials." In: E. Simpson (ed.), *The adventure of the illustrious scholar: papers presented to Oscar White Muscarella*, Leiden and Boston 2018, pp. 351-359.

Peyronel/Vacca 2015

L. Peyronel and A. Vacca, "Northern Ubaid and Late Chalcolithic 1-3 periods in the Erbil Plain: new insights from recent research at Helawa, Iraqi Kurdistan." *Origini* 37 (2015), pp. 89-127.

Poppa 1978

R. Poppa, *Kamid el-Loz 2: der eisenzeitliche Friedhof: Befunde und Funde*, Bonn 1978.

Potts 1998

D.T. Potts 1998, "Some issues in the study of the pre-Islamic weaponry of southeastern Arabia." *Arabian Archaeology and Epigraphy* 9 (1998), pp. 182-208.

Potts et al. 2019

D.T. Potts, K. Radner, A. Squitieri, A. Ameen, J. Rohde, P. Yawar, J.-J. Herr, H. Salih, F. Petchey, A. Hogg, B. Gratuze, K.R. Raheem and H.B. Potts, "Gird-i Rostam 2018: preliminary

report on the first season of excavations by the joint Kurdish-German-American team." *Jaarbericht "Ex Oriente Lux"* 47 (2019), pp. 91-128.

Radner 2015

K. Radner, "A Neo-Assyrian slave sale contract of 725 BC from the Peshdar Plain and the location of the Palace Herald's Province." *Zeitschrift für Assyriologie und Vorderasiatische Archäologie* 105 (2015), pp. 192-197.

Radner 2016

K. Radner, "The Peshdar Plain in the Neo-Assyrian period: the border march of the Palace Herald." In: Radner/Kreppner/Squitieri 2016, pp. 17-22.

Radner 2018

K. Radner, "The first ¹⁴C dates from DLT2 and their preliminary interpretation." In: Radner/Kreppner/Squitieri 2018, pp. 31-33.

Radner 2019a

K. Radner, "Selecting the excavation area DLT3." In: Radner/Kreppner/Squitieri 2019, p. 68.

Radner 2019b

K. Radner, "A fragmentary brick with a Neo-Assyrian cuneiform inscription from DLT3." In: Radner/Kreppner/Squitieri 2019, pp. 137-139.

Radner 2019c

K. Radner, "The Peshdar Plain Project in its fourth year: the 2018 work programme." In: Radner/Kreppner/Squitieri 2019, pp. 13-20.

Radner/Amelirad/Azizi 2020

K. Radner, S. Amelirad and E. Azizi, "A first radiocarbon date for the Iron Age cemetery of Sanandaj: Dating an elite burial in the Assyrian province of Parsua." In: S. Hasegawa and K. Radner (eds.), *The reach of the Assyrian and Babylonian empires: case studies in eastern and western peripheries*, Wiesbaden 2020, pp. 95-109.

Radner/Kreppner 2019

K. Radner and F.J. Kreppner, "Conclusions and perspectives." In: Radner/Kreppner/Squitieri 2019, pp. 156-159.

Radner/Kreppner/Squitieri 2016

K. Radner, F.J. Kreppner and A. Squitieri (eds.), *Exploring the Neo-Assyrian frontier with Western Iran: the 2015 Season at Gird-i Bazar and Qalat-i Dinka* (Peshdar Plain Project Publications 1), Gladbeck 2016. Online: <https://epub.ub.uni-muenchen.de/29236/>.

Radner/Kreppner/Squitieri 2017

K. Radner, F.J. Kreppner and A. Squitieri (eds.), *Unearthing the Dinka Settlement Complex: the 2016 seasons at Gird-i Bazar and Qalat-i Dinka* (Peshdar Plain Project Publications 2), Gladbeck 2017. Online: <https://epub.unimuenchen.de/40252/>.

Radner/Kreppner/Squitieri 2017a

K. Radner, F.J. Kreppner and A. Squitieri, "Conclusions and future lines of research." In Radner/Kreppner/Squitieri 2017, pp. 176-180.

Radner/Kreppner/Squitieri 2018

K. Radner, F.J. Kreppner and A. Squitieri (eds.), *The Dinka Settlement Complex 2017: the final season at Gird-i Bazar and first work in the Lower Town* (Peshdar Plain Project Publications 3), Gladbeck 2018. Online: <https://epub.uni-muenchen.de/57255/>.

Radner/Kreppner/Squitieri 2019

K. Radner, F.J. Kreppner and A. Squitieri (eds.), *The Dinka Settlement Complex 2018: continuing the excavations at Qalat-i Dinka and the Lower Town* (Peshdar Plain Project Publications 4), Gladbeck 2019. Online: <https://epub.unimuenchen.de/68561/>.

Radner/Kreppner/Squitieri 2019a

K. Radner, F.J. Kreppner and A. Squitieri, "The Iron Age Dinka Settlement Complex near Qaladze (Peshdar Plain): archaeological exploration, 2015-2018." *Sumer* 65 (2019), pp. 165-174.

Radner/Kreppner/Squitieri 2019b

K. Radner, F.J. Kreppner and A. Squitieri, "The Iron Age Dinka Settlement Complex in the Peshdar Plain: archaeological exploration, 2015-2018." In Y. Hassanzadeh, A.A. Vahdati and Z. Karimi (eds.), *Proceedings of the international conference on the Iron Age in Western Iran and Neighbouring Regions, vol. 2*, Tehran 2019, pp. 243-257.

Radner/Squitieri 2019

K. Radner and A. Squitieri, "The first ¹⁴C dates." In: Radner/Kreppner/Squitieri 2019, pp. 41-43.

Ramsey/Rosen 2016

M.N. Ramsey and A.M. Rosen, "Wedded to wetlands: exploring Late Pleistocene plant-use in the eastern Levant." *Quaternary International* 396 (2016), pp. 5-19.

Reese 1991

D.S. Reese, "The trade of Indo-Pacific shells into the Med-

iterranean basin and Europe." *Oxford Journal of Archaeology* 10 (1991), pp. 159-196.

Rezvani/Roustaei 2007

H. Rezvani and K. Roustaei, "A preliminary report on two seasons of excavations at Kul Tarike cemetery, Kurdistan, Iran." *Iranica Antiqua* 42 (2007), pp. 139-184.

Rohde 2018

J. Rohde, "Outdoor Area 7." In: Radner/Kreppner/Squitieri 2018, pp. 70-73.

Rohde 2019

J. Rohde, "The Late Chalcolithic floor under Building R." In: Radner/Kreppner/Squitieri 2019, pp. 74-75.

Rosen 1999

A.M. Rosen, *Phytolith analysis in Near Eastern archaeology*, London 1999.

Rosen/Weiner 1994

A.M. Rosen and S. Weiner, "Identifying ancient irrigation: a new method using opaline phytoliths from emmer wheat." *Journal of Archaeological Science* 21 (1994), pp. 125-132.

Rosenzweig 2018

M.S. Rosenzweig, "Assessing the politics of Neo-Assyrian agriculture." *Archeological Papers of the American Anthropological Association* 29 (2018), pp. 30-50.

Salimi/Sorkhabi 2019

S. Salimi and O. Sorkhabi, "Guringan: new evidence of Iron Age in the plain of Piranshahr." In: Y. Hassanzadeh, A.A. Vahdati and Z. Karimi (eds.), *Proceedings of the international conference on the Iron Age in Western Iran and neighboring regions, vol. 1*, Tehran 2019, pp. 208-227.

Salimi/Ebrahimipour/Sorkhabi 2019

S. Salimi, S. Ebrahimipour and O. Sorkhabi, "Some Mannean glazed bricks from the Little Zab river basin, north-western Iran." *Aramazd* 8 (2019), pp. 101-110.

Salvemini et al. 2014

F. Salvemini, F. Grazzi, I. Angelini, P. Vontobel, A. Vigoni, G. Artioli and M. Zoppi, "Morphological reconstruction of Roman arrowheads from *Iulia Concordia*, Italy." *Applied Physics A* 117 (2014), pp. 1227-1240.

Schmidt 1929

E.F. Schmidt, "Test excavations in the city on Kerkenes Dagh." *The American Journal of Semitic Languages and Literatures* 45 (1929), pp. 221-274.

Schmidt 1933

E.F. Schmidt, *The Alishar Hüyük: seasons of 1928 and 1929, part II*, Chicago 1933.

Schmidt 1957

E.F. Schmidt, *Persepolis II: contents of the treasury and other discoveries*, Chicago 1957.

Schmidt 1970

E.F. Schmidt, *Persepolis III: the royal tombs and other monuments*, Chicago 1970.

Schmidt 2013

A. Schmidt, *Earth resistance for archaeologists*, Lanham 2013.

Schütt 2010

H. Schütt, *Turkish land snails*, Solingen 2010.

Shillito 2013

L.-M. Shillito, "Molluscs from Sheikh-e Abad and Jani." In: R. Matthews, W. Matthews and Y. Mohammadifar (eds.), *The earliest Neolithic of Iran: 2008 excavations at Sheikh-e Abad and Jani*, Oxford 2013, pp. 201-205.

Solecki 1999

R.S. Solecki, "An archaeological survey in western Azarbaijan, Iran." In: A. Alizadeh, Y. Madjidzadeh and S. Malek Shahmirzadi (eds.), *The Iranian world: essay on Iranian art and archaeology, presented to Ezat O. Negahban*, Tehran 1999, pp. 28-43.

Squitieri 2017

A. Squitieri, "Neo-Assyrian period small finds of Gird-i Bazar, 2016." In: Radner/Kreppner/Squitieri 2017, pp. 155-167.

Squitieri 2018

A. Squitieri, "The Iron Age small finds of the 2017 campaigns at DLT2 and Gird-i Bazar." In: Radner/Kreppner/Squitieri 2018, pp. 146-172.

Squitieri 2019

A. Squitieri, "The 2018 small finds from Qalat-i Dinka and DLT3." In: Radner/Kreppner/Squitieri 2019, pp. 126-136.

Squitieri 2020

A. Squitieri, "The Sasanian cemetery of Gird-i Bazar in the Peshdar Plain (Iraqi Kurdistan)." *Iran* 58 (2020). DOI: 10.1080/05786967.2020.1749008.

Squitieri/Rohde 2019

A. Squitieri and J. Rohde, "The grid, the registration sys-

tem and the new 3D documentation." In: Radner/Kreppner/Squitieri 2019, pp. 68-69.

Stein/Alizadeh 2014

G. Stein and A. Alizadeh, "Excavation at Surezha (Erbil Plain, Kurdistan region, Iraq)." *Oriental Institute Annual Report 2013-2014* (2014), pp. 138-151.

Stone 2016

A. Stone, "The connecting trench." In: Radner/Kreppner/Squitieri 2016, pp. 62-70.

Stronach 1958

D. Stronach, "Metal objects from the 1957 excavations at Nimrud." *Iraq* 20 (1958), pp. 169-179.

Stronach 1959

D. Stronach, "The development of the fibula in the Near East." *Iraq* 21 (1959), pp. 181-206.

Summers/Burney 2012

G.D. Summers and C.A. Burney, "Late Iron Age pottery from northwestern Iran: the evidence from Yanik Tepe." In: A. Çilingiroğlu and A. Sagona (eds.), *Anatolian Iron Ages 7*, Leuven 2012, pp. 269-315.

Szudy 2015

M.J. Szudy, *Archery equipment in the Neo-Assyrian period*. PhD dissertation, Universität Wien 2015. Available online at: <http://othes.univie.ac.at/38210/>.

Tabbagh 2017

A. Tabbagh, "Electrical resistivity and electromagnetism." In: A.S. Gilbert, P. Goldberg, V.T. Holliday, R.D. Mandel and R.S. Sternberg (eds.), *Encyclopedia of geoarchaeology*, Dordrecht 2017, pp. 211-219.

Taylor/Bell 2017

V.K. Taylor and M. Bell, "Land mollusc middens." In: M.J. Allen (ed.), *Molluscs in archaeology: methods, approaches and applications*, Oxford and Philadelphia 2017, pp. 195-212.

Tenu 2005

A. Tenu, "La pratique de la crémation en Syrie: un usage marginal?" *Ktema* 30 (2005), pp. 37-46.

Thareani 2011

Y. Thareani, *Tel 'Aroer: the Iron Age II caravan town and the Hellenistic-Early Roman settlement – the Avraham Biran (1975-1982) and Rudolph Cohen (1975-1976) excavations*, Jerusalem 2011.

Thornton/Pigott 2011

C.P. Thornton and V.C. Pigott, "Blade-type weaponry of Hasanlu period IVB." In: M. de Schauensee (ed.), *Peoples and crafts in period IVB at Hasanlu, Iran*, Philadelphia 2011, pp. 135-182.

Thureau-Dangin/Dunand 1936

F. Thureau-Dangin and M. Dunand, *Til-Barsip*, Paris 1936.

Tobler 1950

A.J. Tobler, *Excavations at Tepe Gawra, levels IX-XX*, Philadelphia 1950.

Tsuneki et al. 2016

A. Tsuneki, K. Rasheed, S.A. Saber, S. Nishiyama, N. Watanabe, T. Greenfield, B.B. Ismail, Y. Tatsumi and M. Minami, "Excavations at Qalat Said Ahmadian, Qaladizah, Iraq-Kurdistan: second interim report (2015 season)." *Al-Rafidan* 37 (2016), pp. 89-140.

Turnbull 1983

P.F. Turnbull, "The faunal remains from M'lefaat." In: L.S. Braidwood, R.J. Braidwood, B. Howe, C.A. Reed and P.J. Watson (eds.), *Prehistoric archeology along the Zagros flanks*, Chicago 1983, pp. 693-695.

Ullrich/Günther/Rücker 2008

B. Ullrich, T. Günther and C. Rücker, "Electrical resistivity tomography methods for archaeological prospection." In: A. Posluschny, K. Lambers and I. Herzog (eds.), *Layers of perception*, Bonn 2008, pp. 1-7.

Vanden Berghe 1978

L. Vanden Berghe, "Les fibules provenant des fouilles au Pusht-i Kuh, Luristan." *Iranica Antiqua* 13 (1978), pp. 35-74.

van Ess/Pedde 1992

M. van Ess and F. Pedde, *Uruk, Kleinfunde II: Metall und Asphalt, Farbreste, Fritte/Fayence, Glas, Holz, Knochen/Elfenbein, Leder, Muschel/Perlmutter, Schnecke, Schilf, Textilien*, Mainz 1992.

van Ess et al. 2012

M. van Ess, A. Hausleiter, H.H. Hussein, N.B. Mohammed, E. Petiti and F. Tourtet, "Excavations in the city of Arbil, 2009-2011: the Neo-Assyrian tomb." *Zeitschrift für Orient-Archäologie* 5 (2012), pp. 104-165.

Voigt 1983

M. Voigt, *Hajji Firuz Tepe, Iran: the Neolithic settlement*, Philadelphia 1983.

von den Driesch 1976

A. von den Driesch, *A guide to the measurement of animal bones from archaeological sites*, Cambridge 1976.

von der Osten 1937

H.H. von der Osten, *The Alishar Hüyük seasons of 1930-1932, part 1*, Chicago 1937.

von der Osten 1957

H.H. von der Osten, *Altorientalische Siegelsteine der Sammlung Hans Silvius von Aulock*, Uppsala 1957.

Wartke 1990

R.-B. Wartke, *Toprakkale: Untersuchungen zu den Metallobjekten im Vorderasiatischen Museum zu Berlin*, Berlin 1990.

Wartke 1993

R.-B. Wartke, *Urartu: das Reich am Ararat*, Mainz am Rhein 1993.

Wengrow et al. 2016

D. Wengrow, R. Carter, G. Brereton, M. Shepperson, S.J. Hamarashi, S.A. Saber, A. Bevan, D. Fuller, H. Himmler, H. Sosnowska and L.G. Carretero, "Gurga Chiya and Tepe Marani: new excavations in the Shahrizor Plain, Iraq Kurdistan." *Iraq* 78 (2016), pp. 253-284.

Wicke 2008

D. Wicke, *Vorderasiatische Pyxiden der Spätbronzezeit und der Früheisenzeit*, Münster 2008.

Wicke 2011

D. Wicke, *Kleinfunde aus Elfenbein und Knochen aus Assur*, Wiesbaden 2011.

Wicks 2018

Y. Wicks, *Profiling death: Neo-Elamite mortuary practices, afterlife beliefs, and entanglements with ancestors*, Leiden and Boston 2018.

Wilkinson/ Squitieri/ Hashemi 2016

E.B. Wilkinson, A. Squitieri and Z. Hashemi, "The small finds." In: Radner/Kreppner/Squitieri 2016, pp. 100-108.

Wolter 2019

F. Wolter, "The excavations in QID3." In: Radner/Kreppner/Squitieri 2019, pp. 63-66.

Woolley 1921

C.L. Woolley, *Carchemish, part II: the town defences*, London 1921.

Woolley 1939

C.L. Woolley, "The Iron Age graves of Carchemish." *Annals of Archaeology and Anthropology* 26 (1939), pp. 9-37.

Yalçıklı 2006

D. Yalçıklı, *Eisenzeitliche Pfeilspitzen aus Anatolien*, Bonn 2006.

Zeder 2006

M.A. Zeder, "Reconciling rates of long bone fusion and tooth eruption and wear in sheep (*Ovis*) and goat (*Capra*)." In: D. Ruscillo (ed.), *Recent advances in ageing and sexing animal bones*, Oxford 2006, pp. 87-118.

Zeder/Lapham 2010

M.A. Zeder and H.A. Lapham, "Assessing the reliability of criteria used to identify postcranial bones in sheep, *Ovis*, and goats, *Capra*." *Journal of Archaeological Science* 37 (2010), pp. 2887-2905.

Zeder/Pilaar 2010

M.A. Zeder and S.E. Pilaar, "Assessing the reliability of criteria used to identify mandibles and mandibular teeth in sheep, *Ovis*, and goats, *Capra*." *Journal of Archaeological Science* 37 (2010), pp. 225-242.